

CHEMICAL CONSTITUENTS AND ANTIOXIDANT ACTIVITY OF *Croton megalocarpoides* FRIIS & GILBERT AND *Physalis angulata* LINN.

BY

BABATOPE OLUSEUN ODUSINA

B.Sc. (OGUN), M.Sc. ORGANIC CHEM (IBADAN)

MATRIC NO: 119929

A Thesis in the Department of Chemistry

Submitted to the Faculty of Science

In partial fulfillment of the requirements for the

Degree of

DOCTOR OF PHILOSOPHY

Of the

UNIVERSITY OF IBADAN

March, 2019.

ABSTRACT

Available drugs used in the treatment of wounds, diabetes, whooping cough, jaundice and ear aches have side effects. *Croton megalocarpoides* and *Physalis angulata* are used in ethno-medicine for treatment of these diseases with no scientific proof and there is thus a need to provide scientific based evidence to support the ethno-medicinal uses of these plants. The aim of this study was to isolate and identify phytochemicals responsible for the ethno-medicinal uses of *Croton megalocarpoides* and *Physalis angulata*.

C. megalocarpoides and *P. angulata* were collected, identified and authenticated at the herbaria, in the School of Biological Sciences, University of Nairobi, Kenya B/N 2009/08 and Forestry Research Institute of Nigeria, Ibadan FHI 109674, respectively. Pulverised samples of stem bark of *C. megalocarpoides* and whole plant of *P. angulata* were macerated with dichloromethane and methanol, respectively. Extracts were screened for the presence of phytochemicals using standard methods. The extracts were further purified using column and flash chromatography. Purified compounds were characterised spectroscopically with Infra-Red (IR), Nuclear Magnetic Resonance (NMR), and Mass Spectroscopic (MS). Extracts and purified compounds were investigated for antioxidant and radical scavenging activities using 2,2-diphenyl-1-picrylhydrazyl (DPPH) at concentration of 1.00-0.06 mg/mL. Data were analysed using descriptive statistics.

Dichloromethane extract (7.4 %) of *C. megalocarpoides* and methanol extract (4.0 %) of *P. angulata* were obtained. Flavonoid, saponin, terpenoid and tannin were detected in the extract of *C. megalocarpoides* while alkaloid, saponin, flavonoid, terpenoid and steroid were found to be present in extract of *P. angulata*. Two new compounds (12-*epi*-Croton zambefuran A and 1-(*p*-hydroxy coumaric acid) – geranyl geran-1-ol) and six known compounds (lupeol, 15,16-epoxy-3,13(16),14-clerodatriene-20,12-olide-18,19-dioic acid dimethyl ester, 18,19-dimethoxy-carbonyl-3-acetoxy,4 β -hydroxy-15,16-epoxy-clerodane-7,13(16),14-triene-

12,20-olide, 1,2-dehydrocrotonylifuran-2-one, 7,8-dehydrocrotonylifuran and lignoceryl-trans-ferulate) were isolated from the extract of *C. megalocarpoides*. The 12-*epi*-Croton zambefuran A showed IR absorption band typical of lactone at 1760 cm⁻¹ while the NMR analysis revealed three olefinic signals δ_H at 6.40, 7.47 and 7.49 ppm and four sp² carbons at δ_C 108.4, 125.6, 139.5 and 144.4 ppm. The MS displayed M⁺ peak at m/z 423.7 corresponding to the molecular formula C₂₂H₂₄O₇. A new squalene derivative (1-hydroxy-squalene) and three known compounds (phytol, squalene and α -tocopherol) were isolated from methanol extract of *P. angulata*. *Croton megalocarpoides* and *P. angulata* extracts exhibited the highest percentage radical scavenging activity at 58.0 and 73.0, respectively. The extracts of *C. megalocarpoides* and *P. angulata* showed antioxidant activity with IC₅₀ of 0.79 and 0.06 mg/mL, respectively. The new isolates from both plants showed antioxidant activity with IC₅₀ values ranging from 0.72 to 0.76 mg/mL.

Both plants contain phytochemicals that showed antioxidant activity that could be responsible for their ethno-medicinal uses.

Keywords: *Croton megalocarpoides*, *Physalis angulata*, Antioxidant properties, 1-hydroxy-squalene

Word count: 428

ACKNOWLEDGEMENT

I will like to first and foremost acknowledge the efforts and contributions of my supervisor, Prof. Patricia .A. Onocha to this study. She has been a true mother to me. My appreciation also goes to my wife, Ifedayo, my sons, Oluwademilade and Oluwafemi, my parents, Mr. and Mrs. S.A. Odusina, my Siblings Dr. Lekan Odusina (M.D) and Dr. Niyi Odusina (Ph.D) and Mrs. Dele Osiyemi. I love you all.

My fatherly Head of Department Prof. T. I Odiaka, who is so caring, is also acknowledged and appreciated at this juncture. All members of staff of the Department of Chemistry, University of Ibadan, Ibadan especially Dr. Sheriffat A. Aboaba, Dr. I.A. Oladosu, Prof. O. O. Sonibare, Prof. Olapeju O. Aiyelaagbe, Dr. Ganiyat K. Oloyede are also hereby acknowledged. I also thank Mr. Charles Nwabueze. You are all wonderful.

I am grateful to Prof. Dulcie Mulholland (University of Surrey-UK) for making her research laboratory available for my research work. I would also like to thank Dr. Moses Langat, (University of Surrey-UK) for sharing his knowledge and wisdom with me.

DEDICATION

This project is dedicated to God Almighty.

CERTIFICATION

I hereby certify that this work was carried out by BABATOPE OLUSEUN ODUSINA in the Department of Chemistry, University of Ibadan, Ibadan.

.....

Supervisor

Prof. Patricia A. Onocha FRSC, MICCON

B.Sc., M.Sc. PhD (Ibadan)

Department of Chemistry,

University of Ibadan,

Ibadan.

TABLE OF CONTENTS

Title Page	i
Abstract	ii
Acknowledgement	iv
Dedication	v
Certification	vi
Table of content	vii
List of Appendices	xii
List of tables	xv
List of figures	xvi
List of abbreviations and acronyms	xx
CHAPTER ONE	
1.0 Introduction	1
1.1 Background Information	1
1.2 Justification of the Study	3
1.3 Aim of Study	4
1.4 Specific Objectives of Study	4
CHAPTER TWO	
2.0 Literature Review	5
2.1 <i>Croton megalocarpoides</i>	5
2.1.1 Traditional uses of <i>Croton megalocarpoides</i>	5
2.1.2 Review on <i>Croton megalocarpoides</i>	5
2.2 <i>Physalis angulata</i>	6
2.2.1 Traditional uses of <i>Physalis angulata</i>	6
2.2.2 Review on <i>Physalis angulata</i>	7
2.3 Natural Product	8

2.3.1	Flavonoids	8
2.3.2	Anthocyanin	10
2.3.3	Alkaloids	11
2.3.4	Saponins	14
2.3.5	Terpenoids and essential oil	15
2.3.6	Cardiac glycosides	16
2.3.7	Steroids	17
2.4	Extraction	19
2.4.1	Soxhlet Extraction	19
2.4.2	Cold pressing	19
2.4.3	Maceration	19
2.5	Purification of natural products	20
2.5.1	Gas chromatography	20
2.5.2	Column chromatography	21
2.5.3	Thin layer chromatography	22
2.5.4	High performance chromatography	22
2.6	Analysis of natural products	23
2.6.1	Ultra violet spectroscopy	23
2.6.2	Infra red spectroscopy	24
2.6.3	Mass spectroscopy	24
2.6.4	Nuclear magnetic spectroscopy	25
2.6.5	Antioxidant assay	26
CHAPTER THREE		
3.1	Collection and preparation of the plants	28
3.1.1	<i>Croton megalocarpoides</i>	28
3.1.2	Extraction	28

3.1.3	<i>Physalis angulata</i>	28
3.1.4	Extraction	28
3.2	Preliminary phytochemical screening tests on <i>Croton megalocarpoides</i> and <i>Physalis angulata</i>	30
3.2.1	Test for Saponins	30
3.2.2	Test for alkaloids	30
3.2.3	Test for steroids	30
3.2.4	Test for tannins	30
3.2.5	Test for reducing sugar	30
3.2.6	Test for anthroquinone	31
3.2.7	Test for flavonoids	31
3.3	Column chromatography of DCM extract of <i>Croton megalocarpoides</i> and methanol extract of <i>Physalis angulata</i>	31
3.4	Antioxidant activity of extracts and isolated chemical compounds <i>Croton megalocarpoides</i> and <i>Physalis angulata</i>	35
CHAPTER FOUR		
4.0	Results and Discussion	36
4.1	Phytochemical screening	36
4.2	Isolation and characterization of CMD-A-H	37
4.2.1	Isolation and Characterization of CMD-A	37
4.2.2	Structural elucidation of compound CMD-B	52
4.2.3	Structural elucidation of compound CMD-C	63
4.2.4	Structural elucidation of compound CMD-D	73
4.2.5	Structural elucidation of compound CMD-E	84
4.2.6	Structural elucidation of compound CMD-F	94
4.2.7	Structural elucidation of compound CMD-G	108

4.2.8	Structural elucidation of compound CMD-H	121
4.3.1	Structural elucidation of compound PA-A	133
4.3.2	Structural elucidation of compound PA-B	144
4.3.3	Structural elucidation of compound PA-C	153
4.3.4	Structural elucidation of compound PA-D	164
4.4	Result of antioxidant analysis (scavenging effect of DPPH) on dichloromethane extract of <i>Croton megalocarpoides</i> and methanol extract of <i>Physalis angulata</i>	174
4.5	Result of antioxidant analysis (scavenging effect of DPPH) of isolated compounds from <i>Croton megalocarpoides</i> and <i>Physalis angulata</i>	177
CHAPTER FIVE		
5.0	Conclusion	182
	References	184

LIST OF APPENDICES

Appendix 1:	IR spectrum of CMD-A in CDCl ₃	189
Appendix 2:	¹ H NMR (500MHz) spectrum of CMD-A in CDCl ₃	190
Appendix 3:	¹³ C NMR (125MHz) spectrum of CMD-A in CDCl ₃	191
Appendix 4:	¹³ C NMR (125MHz) spectrum of CMD-A in CDCl ₃	192
Appendix 5:	DEPT spectrum of CMD-A in CDCl ₃	193
Appendix 6:	HSQC DEPT spectrum of CMD-A in CDCl ₃	194
Appendix 7:	HSQC DEPT spectrum of CMD-A in CDCl ₃	195
Appendix 8:	HMBC spectrum of CMD-A in CDCl ₃ (expanded)	196
Appendix 9:	COSY spectrum of CMD-A in CDCl ₃	197
Appendix 10:	NOESY spectrum of CMD-A in CDCl ₃	198
Appendix 11:	NOESY spectrum of CMD-A in CDCl ₃	199
Appendix 12:	¹ H NMR (500MHz) spectrum of CMD-B in CDCl ₃	200
Appendix 13:	¹³ C NMR (125MHz) spectrum of CMD-B in CDCl ₃	201
Appendix 14:	DEPT spectrum of CMD-B in CDCl ₃	202
Appendix 15:	HSQC DEPT spectrum of CMD-B in CDCl ₃	203
Appendix 16:	HMBC spectrum of CMD-B in CDCl ₃	204
Appendix 17:	COSY spectrum of CMD-B in CDCl ₃	205
Appendix 18:	NOESY spectrum of CMD-B in CDCl ₃	206
Appendix 19:	¹ H NMR (500MHz) spectrum of CMD-C in CDCl ₃	207
Appendix 20:	¹³ C NMR (125 MHz) spectrum of CMD-C in CDCl ₃	208
Appendix 21:	DEPT spectrum of CMD-C in CDCl ₃	209
Appendix 22:	HSQC DEPT spectrum of CMD-C in CDCl ₃	210
Appendix 23:	HMBC spectrum of CMD-C in CDCl ₃	211
Appendix 24:	COSY spectrum of CMD-C in CDCl ₃ (expanded)	212
Appendix 25:	NOESY spectrum of CMD-C in CDCl ₃ (expanded)	213
Appendix 27:	¹ H NMR (500MHz) spectrum of CMD-D in CDCl ₃	215
Appendix 28:	¹³ C NMR (125MHz) spectrum of CMD-D in CDCl ₃	216
Appendix 29:	DEPT spectrum of CMD-D in CDCl ₃	217
Appendix 30:	HSQC DEPT spectrum of CMD-D in CDCl ₃	218
Appendix 31:	HMBC spectrum of CMD-D in CDCl ₃	219

Appendix 32:	COSY spectrum of CMD-D in CDCl ₃ (expanded)	220
Appendix 33:	NOESY spectrum of CMD-D in CDCl ₃ (expanded)	221
Appendix 34:	¹ H NMR (500MHz) spectrum of CMD-E in CDCl ₃	222
Appendix 35:	¹³ C NMR (125MHz) spectrum of CMD-E in CDCl ₃	223
Appendix 36:	DEPT spectrum of CMD-E in CDCl ₃	224
Appendix 37:	HSQC DEPT spectrum of CMD-E in CDCl ₃	225
Appendix 38:	HMBC spectrum of CMD-E in CDCl ₃	226
Appendix 39:	COSY spectrum of CMD-E in CDCl ₃ (expanded)	227
Appendix 40:	NOESY spectrum of CMD-E in CDCl ₃ (expanded)	228
Appendix 42:	¹ H NMR (500MHz) spectrum of CMD-F in CDCl ₃	230
Appendix 43:	¹³ C NMR (125MHz) spectrum of CMD-F in CDCl ₃	231
Appendix 44:	DEPT spectrum of CMD-F in CDCl ₃	232
Appendix 45:	HSQC DEPT spectrum of CMD-F in CDCl ₃	233
Appendix 46:	HMBC spectrum of CMD-F in CDCl ₃	234
Appendix 47:	COSY spectrum of CMD-F in CDCl ₃ (expanded)	235
Appendix 48:	NOESY spectrum of CMD-F in CDCl ₃ (expanded)	236
Appendix 49:	MS spectrum of CMD-F CDCl ₃ (expanded)	237
Appendix 50:	¹ H NMR (500MHz) spectrum of CMD-G in CDCl ₃	238
Appendix 51:	¹³ C NMR (125MHz) spectrum of CMD-G in CDCl ₃	239
Appendix 52:	¹³ C NMR (125MHz) spectrum of CMD-G in CDCl ₃	240
Appendix 53:	DEPT spectrum of CMD-G in CDCl ₃	241
Appendix 54:	HSQC DEPT spectrum of CMD-G in CDCl ₃	242
Appendix 56:	HMBC spectrum of CMD-G in CDCl ₃	244
Appendix 57:	COSY spectrum of CMD-G in CDCl ₃ (expanded)	245
Appendix 58:	NOESY spectrum of CMD-G in CDCl ₃ (expanded)	246
Appendix 60:	¹ H NMR (500MHz) spectrum of CMD-H in CDCl ₃	247
Appendix 61:	¹³ C NMR (125MHz) spectrum of CMD-H in CDCl ₃	248
Appendix 62:	DEPT spectrum of CMD-H in CDCl ₃	249
Appendix 63:	HSQC DEPT spectrum of CMD-H in CDCl ₃	250
Appendix 64:	HSQC DEPT spectrum of CMD-H in CDCl ₃	251
Appendix 65:	HMBC spectrum of CMD-H in CDCl ₃	252

Appendix 66:	COSY spectrum of CMD-H in CDCl ₃ (expanded)	253
Appendix 67:	NOESY spectrum of CMD-H in CDCl ₃ (expanded)	254
Appendix 68:	IR spectrum of PA-A in CDCl ₃ (expanded)	255
Appendix 69:	¹ H NMR (500MHz) spectrum of PA-A in CDCl ₃	256
Appendix 70:	¹³ C NMR (500MHz) spectrum of PA-A in CDCl ₃	257
Appendix 71:	¹³ C NMR (500MHz) spectrum of PA-A in CDCl ₃	258
Appendix 72:	DEPT (500MHz) spectrum of PA-A in CDCl ₃	259
Appendix 73:	HSQC DEPT (500MHz) spectrum of PA-A in CDCl ₃	260
Appendix 74:	HMBC (500MHz) spectrum of PA-A in CDCl ₃	261
Appendix 75:	HMBC (500MHz) spectrum of PA-A in CDCl ₃ (expanded)	262
Appendix 76:	¹ H NMR (500MHz) spectrum of PA-B in CDCl ₃	263
Appendix 77:	¹³ C NMR (125MHz) spectrum of PA-B in CDCl ₃	264
Appendix 78:	DEPT spectrum of PA-B in CDCl ₃	265
Appendix 79:	HSQC DEPT spectrum of PA-B in CDCl ₃	266
Appendix 80:	HMBC spectrum of PA-B in CDCl ₃	267
Appendix 81:	IR spectrum of PA-B in CDCl ₃	268
Appendix 82:	IR spectrum of PA-B in CDCl ₃	269
Appendix 83:	¹ H NMR (500MHz) spectrum of PA-C in CDCl ₃	270
Appendix 84:	¹³ C NMR (500MHz) spectrum of PA-C in CDCl ₃	271
Appendix 85:	DEPT (500MHz) spectrum of PA-C in CDCl ₃	272
Appendix 86:	HSQC DEPT (500MHz) spectrum of PA-C in CDCl ₃	273
Appendix 87:	HSQC DEPT (500MHz) spectrum of PA-C in CDCl ₃	274
Appendix 88:	HMBC (500MHz) spectrum of PA-C in CDCl ₃	275
Appendix 89:	HMBC (500MHz) spectrum of PA-C in CDCl ₃ (expanded)	276
Appendix 90:	¹ H NMR (500MHz) spectrum of PA-D in CDCl ₃	277
Appendix 91:	¹³ C NMR (500MHz) spectrum of PA-D in CDCl ₃	278
Appendix 92:	DEPT (500MHz) spectrum of PA-D in CDCl ₃	279
Appendix 93:	HSQC DEPT (500MHz) spectrum of PA-D in CDCl ₃	280
Appendix 94:	HMBC (500MHz) spectrum of PA-D in CDCl ₃	290

LIST OF TABLES		Pg
Table 1	Correlation table for compound CMD-A: Lupeol in CDCl ₃	40
Table 2	Correlation table for compound CMD-B: crotochryliferan in CDCl ₃	54
Table 3	Correlation table for compound CMD-C: 18,19-dimethoxycarbonyl-3 α -acetoxy,4 β -hydroxy-15,16-epoxy- clerodane-7,13(16),14-triene-12,20-olide in CDCl ₃	65
Table 4	Correlation table for compound CMD-D 1,2-dehydrocrotochryliferan-2-one in CDCl ₃	75
Table 5	Correlation table for compound CMD-E: 7,8-dehydrocrotochryliferan in CDCl ₃	86
Table 6	Correlation table for compound CMD-B: 12 epi-Croton zambefuran A in CDCl ₃	98
Table 7	Correlation table for compound CMD-G: I-(p-hydroxy coumaric acid) – geranyl geran-1-ol in CDCl ₃	111
Table 8	Correlation table for compound CMD-H: lignoceryl-trans-ferulate in CDCl ₃	123
Table 9	Correlation table for compound PA-A: Phytol in CDCl ₃	135
Table 10	Correlation table for compound PA-B: Squalene in CDCl ₃	146
Table 11	Correlation table for compound PA-C: α -tocopherol in CDCl ₃	155
Table 12	Table for compound PA-D: 1-hydroxy-squalene in CDCl ₃	166
Table 13	Result of antioxidant analysis (scavenging effect of DPPH) on dichloromethane extract of <i>Croton megalocarpoides</i>	175
Table 14	Result of antioxidant analysis on methanol extract of <i>Physalis angulata</i>	176
Table 15	Result of antioxidant analysis (scavenging effect of DPPH) of isolated compounds from <i>Croton megalocarpoides</i> and <i>Physalis angulata</i>	178

LIST OF FIGURES

Fig 4.1:	IR spectrum of CMD-A in CDCl ₃	41
Fig 4.2:	¹ H NMR (500MHz) spectrum of CMD-A in CDCl ₃	42
Fig 4.3:	¹³ C NMR (125MHz) spectrum of CMD-A in CDCl ₃	43
Fig 4.4:	¹³ C NMR (125MHz) spectrum of CMD-A in CDCl ₃	44
Fig 4.5:	DEPT spectrum of CMD-A in CDCl ₃	45
Fig 4.6:	HSQC DEPT spectrum of CMD-A in CDCl ₃	46
Fig 4.7:	HSQC DEPT spectrum of CMD-A in CDCl ₃	47
Fig 4.8:	HMBC spectrum of CMD-A in CDCl ₃ (expanded)	48
Fig 4.9:	HMBC spectrum of CMD-A in CDCl ₃	49
Fig 4.10:	NOESY spectrum of CMD-A in CDCl ₃	50
Fig 4.11:	NOESY spectrum of CMD-A in CDCl ₃	55
Fig 4.12:	¹ H NMR (500MHz) spectrum of CMD-B in CDCl ₃	56
Fig 4.13a:	¹³ C NMR (125MHz) spectrum of CMD-B in CDCl ₃	57
Fig 4.13b:	¹³ C NMR (125MHz) spectrum of CMD-B in CDCl ₃	58
Fig 4.14:	DEPT spectrum of CMD-B in CDCl ₃	59
Fig 4.15:	HSQC DEPT spectrum of CMD-B in CDCl ₃	60
Fig 4.16:	NOESY spectrum of CMD-B in CDCl ₃	61
Fig 4.17:	COSY spectrum of CMD-B in CDCl ₃	62
Fig 4.18:	HMBC spectrum of CMD-B in CDCl ₃	63
Fig 4.19:	¹ H NMR (500MHz) spectrum of CMD-C in CDCl ₃	66
Fig 4.20:	¹³ C NMR (125 MHz) spectrum of CMD-C in CDCl ₃	67
Fig 4.21:	DEPT spectrum of CMD-C in CDCl ₃	68
Fig 4.22:	HSQC DEPT spectrum of CMD-C in CDCl ₃	69
Fig 4. 23:	HMBC spectrum of CMD-C in CDCl ₃	70
Fig 4.24:	COSY spectrum of CMD-C in CDCl ₃ (expanded)	71
Fig 4.25:	NOESY spectrum of CMD-C in CDCl ₃ (expanded)	72
Fig 4.26:	IR spectrum of CMD-D in CDCl ₃ (expanded)	73
Fig 4.27:	¹ H NMR (500MHz) spectrum of CMD-D in CDCl ₃	77
Fig 4.28:	¹³ C NMR (125MHz) spectrum of CMD-D in CDCl ₃	78
Fig 4.29:	DEPT spectrum of CMD-D in CDCl ₃	79

Fig 4.30:	HSQC DEPT spectrum of CMD-D in CDCl ₃	80
Fig 4.31:	HMBC spectrum of CMD-D in CDCl ₃	81
Fig 4.32:	COSY spectrum of CMD-D in CDCl ₃ (expanded)	82
Fig 4.33:	NOESY spectrum of CMD-D in CDCl ₃ (expanded)	83
Fig 4.34:	¹ H NMR (500MHz) spectrum of CMD-E in CDCl ₃	87
Fig 4.35:	¹³ C NMR (125MHz) spectrum of CMD-E in CDCl ₃	88
Fig 4.36:	DEPT spectrum of CMD-E in CDCl ₃	89
Fig 4.37:	HSQC DEPT spectrum of CMD-E in CDCl ₃	90
Fig 4.38:	HMBC spectrum of CMD-E in CDCl ₃	91
Fig 4.39:	COSY spectrum of CMD-E in CDCl ₃ (expanded)	92
Fig 4.40:	NOESY spectrum of CMD-E in CDCl ₃ (expanded)	93
Fig 4.41:	MS spectrum of CMD-F in CDCl ₃	99
Fig 4.42:	IR spectrum of CMD-F in CDCl ₃ (expanded)	100
Fig 4.43:	¹ H NMR (500MHz) spectrum of CMD-F in CDCl ₃	101
Fig 4.44:	¹³ C NMR (125MHz) spectrum of CMD-F in CDCl ₃	102
Fig 4.45:	DEPT spectrum of CMD-F in CDCl ₃	103
Fig 4.46:	HSQC DEPT spectrum of CMD-F in CDCl ₃	104
Fig 4.47:	HMBC spectrum of CMD-F in CDCl ₃	105
Fig 4.48:	COSY spectrum of CMD-F in CDCl ₃ (expanded)	106
Fig 4.49:	NOESY spectrum of CMD-F in CDCl ₃ (expanded)	107
Fig 4.50:	MS spectrum of CMD-G in CDCl ₃	113
Fig 4.51:	IR spectrum of CMD-G in CDCl ₃	114
Fig 4.52:	¹ H NMR (500MHz) spectrum of CMD-G in CDCl ₃	115
Fig 4.53:	¹³ C NMR (125MHz) spectrum of CMD-G in CDCl ₃	116
Fig 4.54:	DEPT spectrum of CMD-G in CDCl ₃	117
Fig 4.55:	HSQC DEPT spectrum of CMD-G in CDCl ₃	118
Fig 4.56:	HMBC spectrum of CMD-G in CDCl ₃	119
Fig 4.57:	COSY spectrum of CMD-G in CDCl ₃ (expanded)	120
Fig 4.58:	NOESY spectrum of CMD-G in CDCl ₃ (expanded)	121
Fig 4.59:	IR spectrum of CMD-H in CDCl ₃	124
Fig 4.60:	¹ H NMR (500MHz) spectrum of CMD-H in CDCl ₃	125
Fig 4.61:	¹³ C NMR (125MHz) spectrum of CMD-H in CDCl ₃	126

Fig 4.62:	DEPT spectrum of CMD-H in CDCl ₃	127
Fig 4.63:	HSQC DEPT spectrum of CMD-H in CDCl ₃	128
Fig 4.64:	HSQC DEPT spectrum of CMD-H in CDCl ₃	129
Fig 4.65:	HMBC spectrum of CMD-H in CDCl ₃	130
Fig 4.66:	COSY spectrum of CMD-H in CDCl ₃ (expanded)	131
Fig 4.67:	NOESY spectrum of CMD-H in CDCl ₃ (expanded)	132
Fig 4.68:	IR spectrum of PA-A in CDCl ₃ (expanded)	136
Fig 4.69:	¹ H NMR (500MHz) spectrum of PA-A in CDCl ₃	137
Fig 4.70:	¹³ C NMR (125MHz) spectrum of PA-A in CDCl ₃	138
Fig 4.71:	¹³ C NMR (125MHz) spectrum of PA-A in CDCl ₃	139
Fig 4.72:	DEPT (500MHz) spectrum of PA-A in CDCl ₃	140
Fig 4.73:	HSQC DEPT (500MHz) spectrum of PA-A in CDCl ₃	141
Fig 4.74:	HMBC (500MHz) spectrum of PA-A in CDCl ₃	142
Fig 4.75:	HMBC (500MHz) spectrum of PA-A in CDCl ₃ (expanded)	143
Fig 4.76:	¹ H NMR (500MHz) spectrum of PA-B in CDCl ₃	147
Fig 4.77:	¹³ C NMR (125MHz) spectrum of PA-B in CDCl ₃	148
Fig 4.78:	DEPT spectrum of PA-B in CDCl ₃	149
Fig 4.79:	HSQC DEPT spectrum of PA-B in CDCl ₃	150
Fig 4.80:	HMBC spectrum of PA-B in CDCl ₃	151
Fig 4.81:	IR spectrum of PA-B in CDCl ₃	152
Fig 4.82:	IR spectrum of PA-C in CDCl ₃	156
Fig 4.83:	¹ H NMR (500MHz) spectrum of PA-C in CDCl ₃	157
Fig 4.84:	¹³ C NMR (125MHz) spectrum of PA-C in CDCl ₃	158
Fig 4.85:	DEPT spectrum of PA-C in CDCl ₃	159
Fig 4.86:	HSQC DEPT (500MHz) spectrum of PA-C in CDCl ₃	160
Fig 4.87:	HSQC DEPT (500MHz) spectrum of PA-C in CDCl ₃	161
Fig 4.88:	HMBC (500MHz) spectrum of PA-C in CDCl ₃	162
Fig 4.89:	HMBC (500MHz) spectrum of PA-C in CDCl ₃ (expanded)	163
Fig 4.90:	MS spectrum of PA-D in CDCl ₃	167
Fig 4.91:	IR spectrum of PA-D in CDCl ₃	168
Fig 4.92:	¹ H NMR (500MHz) spectrum of PA-D in CDCl ₃	169

Fig 4.93:	^{13}C NMR (125MHz) spectrum of PA-D in CDCl_3	170
Fig 4.94:	DEPT spectrum of PA-D in CDCl_3	171
Fig 4.95:	HSQC DEPT (500MHz) spectrum of PA-D in CDCl_3	172
Fig 4.96:	HMBC (500MHz) spectrum of PA-D in CDCl_3	173

LIST OF ABBREVIATIONS & ACRONYMS

^{13}C NMR	-	Carbon -13 nuclear magnetic resonance
Brs	-	Broad Singlet
CC	-	Column chromatography
COSY	-	correlated spectroscopy coupling constant
DD	-	doublet of doublet
DEPT	-	Distortionless enhancement by polarization transfer
DNP	-	Dictionary of natural products
EIMS	-	Electron impact mass spectroscopy
FTIR	-	Fourier transform infra red spectroscopy
HMBC	-	Heteronuclear multiple bond coherence
HSQC	-	Heteronuclear single quantum coherence
Hz	-	Hertz
MHz	-	Mega Hertz
IC₅₀	-	Half maximal inhibitory concentration
LR-EIMS	-	Low resolution electron impact mass spectrometry
MS	-	Mass spectrometry
NMR	-	Nuclear magnetic resonance
NOESY	-	Nuclear Overhauser effect spectroscopy
TLC	-	Thin layer chromatography
UV/VIS	-	Ultra violet/visible spectroscopy
δC	-	Carbon chemical shift in the carbon NMR spectra
δH	-	Proton chemical shift in the proton NMR spectra

CHAPTER ONE

1.0

INTRODUCTION

1.1 Background information

Plants are nature's gift to mankind. They are extraordinary "biochemical laboratories". They synthesize lipids, glycosides, tannin and other active compound (Padhee, 2001). Plants are used directly for medicinal purposes by a majority of cultures around the world. Many food crops have medicinal effects and medicinal plants are resources of new drugs (Motaleb, 2011). Greater importance is now being attached to the use of locally available medicines as a means of reducing reliance on expensive imported drugs (Sofowora, 1993).

Phytochemistry is a developed discipline, though closely related but somewhere in between natural product, organic chemistry and plant biochemistry. It is concerned with the enormous variety of organic substances that are accumulated by plants and deals with the isolation, purification, identification and chemical structure of the large number of secondary metabolic compounds found in plants. Literature and ethnobotanical records suggest that plants are the sleeping giants of pharmaceutical industry. They may provide natural source of antimicrobial drugs or novel compounds that could be employed in controlling some infections globally (Motaleb, 2011).

Medicinal plants are plants that have some active organic compounds which when taken into the body, change the condition of the body system. The World Health Organization (WHO) define medicinal plants as plants in which one or more of its organs/parts contain substances that can be used for therapeutic purposes or as a precursor for synthesis of useful drugs (Harbone,1993).

It is now a generally accepted fact that plants possess bioactive substances that can be used to serve the need of human beings. The properties of some medicinal plants were discovered

accidentally while investigating them for other usage, which the traditional healers have claimed for the plant (Sofowora, 1993).

Medicinal plants have been used for treatment of illness and diseases, since the dawn of time. Indigenous cultures (e.g. African and Native America) used herbs in their healing ritual while others developed traditional medical systems (e.g. Ayurvedic and traditional Chinese medicine) in which herbal therapies were used. Researchers have found that people in different parts of the world tend to use the same or similar plants for treating the same ailment (Burkill, 1985).

In Germany about 600-700 plant based medicines are available and are prescribed by some 70% of German physicians. In the last 20 years in the United States, public dissatisfaction with the cost of prescription medications, combined with an interest in returning to natural or organic remedies has led to an increase in use of herbal medicine (Motaleb, 2011).

A medicinal herb is different from the botanic term “herbs”. It refers to any plant used for medicinal purposes. For example a medicinal herb can be a real herbal plant, a shrub, other woody plant, or a fungus. The used part may be the seeds, berries, leaves, barks, roots, fruits or other parts of a plants or mushroom, which may be considered “herbs” in medicinal or spiritual use. While a herb is a plant that does not form a woody stem and in temperate climates usually dies, either completely (annual herb) or back to the roots (perennial herb) by the end of the growing season (Motaleb, 2011).The existence of traditional medicine, depends on plant species diversity and the related knowledge of their use as herbal medicine. Both plant species and traditional knowledge are important to the herbal medicine trade and the

pharmaceutical industry where plants provide raw materials and the traditional prerequisite information (Tabuti *et al.*, 2003). Many drugs listed as conventional medications were originally derived from plants. Compounds derived from the plants remain the basis for a large proportion of the commercial medications used today for the treatment of heart diseases, high blood pressure, pain, asthma, cancer and other diseases (Manuchair, 2002).

Plants have proven to be the richest source of medicinal compounds. Screening of plants is conducted either to discover a new drug or a lead structure. A lead structure is a prototype compound for a given biological activity e.g for anti-tumour activity, a natural product lead structure is subjected to chemical modification or scaffolds to arrive at the therapeutically important molecular fragment, the pharmacophore. Few natural products are directly used as drugs, but in many cases the chemical scaffolds of the lead structure give a more potent synthetic or semi synthetic analogs (Manuchair, 2002).

1.2 JUSTIFICATION FOR THE STUDY

Interest in traditional medicine in the African health care system can be justified because a large number of people in Africa cannot afford modern health care. Also in medical treatment of ailments, most microorganisms and parasites have developed resistance to available drugs partly due to drug abuse by users and there is need for discovery of more potent drugs. Many Africans use herbal based drugs but these folk medicine need to be scientifically validated to ensure their efficacy, safety of therapy and raw materials and interaction with other drugs. (Pharmacological – Toxicological profile). The world health organization has reported that infections and parasitic

diseases are the cause of 26.2% of deaths worldwide. In 2008, malaria caused nearly one million death, mostly among African children.

1.3 AIM OF THE STUDY

The aim of this study is to carry out isolation and characterization of chemical compounds present in the stem bark extract of *Croton megalocarpoides* and the whole plant extract of *Physalis angulata*. To investigate the extracts and isolated chemical compounds from *Croton megalocarpoides* and *Physalis angulata* for antioxidant activities.

1.4 SPECIFIC OBJECTIVES OF THE STUDY

1. To screen the extracts of *Croton megalocarpoides* and *Physalis angulata* plants for antioxidant activities
2. To isolate chemical compounds from stem bark extract of *Croton megalocarpoides* and whole plant extract of *Physalis angulata*
3. To characterize the isolated chemical compounds.
4. To screen the isolated compounds from *Croton megalocarpoides* and *Physalis angulata* for antioxidant activities.

CHAPTER TWO

2.0 LITERATURE REVIEW

2.1 *Croton megalocarpoides*

Croton megalocarpoides is a monoecious shrub or tree, growing up to 8 meters tall in rocky places and is restricted to semi evergreen coastal bush lands or forestry's of East Africa and South Somalia. *Croton megalocarpoides* is one of the fifteen *Croton* Species that occur in Kenya (Beentje, 1994). *Croton megalocarpoides* belongs to the family *Euphorbiaceae*. This plant is listed by International Union of Conservation of Nature (IUCN) among plant species that are threatened by extinction (IUCN, 1993). Its taxonomic relationship with other African *Croton* species is demonstrated by its semblance to *Croton mayumbensis* by possession of grey scaly bark, silvery beneath leaves and *tri*-lobed fruits (Beentje, 1994).

2.1.1 Traditional uses of *Croton megalocarpoides*

The root and stem bark of *Croton megalocarpoides* are used to treat microbial infections and human parasitic diseases. The leaf sap used topically to treat bleeding wounds and the leaf is also used in the treatment of whooping cough (Beentje, 1994).

2.1.2 Review on *Croton megalocarpoides*

The roots of *Croton megalocarpoides* is a rich source of clerodane and abietane diterpenoids. The roots and stem bark of *C. megalocarpoides* showed significant antimicrobial activities (Beth *et al.*, 2016).



Fig 2.1: *Croton megalocarpoides*
(<http://www.plantzafrica.com/planted/crotonmegalocarpoides.htm>)

2.2 *PHYSALIS ANGULATA*

Physalis angulata belongs to the family *Solanaceae* and is found in the tropics including Africa, Asia and America. It produces small, light yellowish orange fruit. It is propagated easily from the seeds in the fruit (Feka, 2013). It is distributed as a weed in gardens, waste lands in the forest and in cultivated fields. The fruit is about the size of a tomatoe and contains many tiny edible seeds inside (Shivi, 1980).

2.2.1 TRADITIONAL USES OF *Physalis angulata*

Indigenous people in the Brazilian Amazon use the sap of the plant for earaches and the roots for jaundice. In the Solomon Island, the fruit of the plant is taken internally to promote fertility. Some Colombian tribes believe the fruits and leaves have anti inflammatory activities and can be used as a disinfectant for skin diseases (Grubben, 2005).

P. angulata is used in the treatment of various human ailments like malaria, asthma and dermatitis. It is also considered as antinociceptive, antipyretic and anti inflammatory for hepatitis and cervicitis. *P. angulata* leaves and whole plant are used to reduce spleen, liver and bladder inflammations and in baths for inflammatory processes like rheumatism respectively. In amazon valley, the plant juice is used as sedative. The aerial parts and fruits of the plant are used in the treatment of boils, sores or wounds, constipation and digestive problems (Lawal *et al.*, 2010).

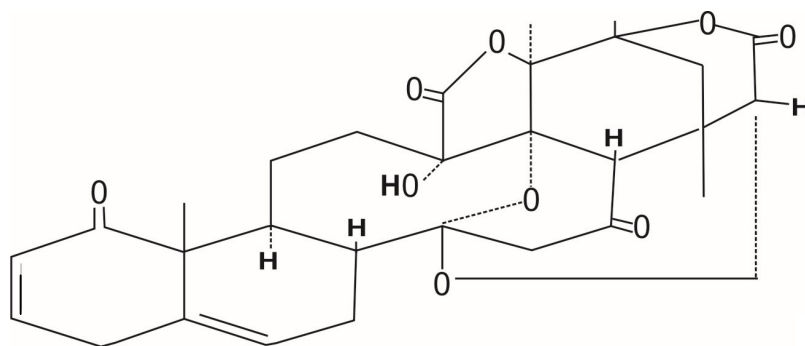


Fig 2.2: *Physalis angulata*

<http://www.ethnopharmacologia.org/phototheque/Physalisangulata1.jpg>

2.2.2 REVIEW ON *Physalis angulata*

Physalins [**1**] have been isolated from the leaves of *Physalis angulata*. It has been shown to have antimicrobial properties (Feka, 2013) and an effective immune stimulant, toxic to numerous types of cancer and leukemia cells (Shivi, 1980). Physalin [**1**] has a broad spectrum of biological activities which include anti-bacterial, abortifacient, molluscidal, anti-protozoal, anti-cancer, anti-septic, cytotoxic and immunomodulatory activities (Lawal *et al.*, 2010).



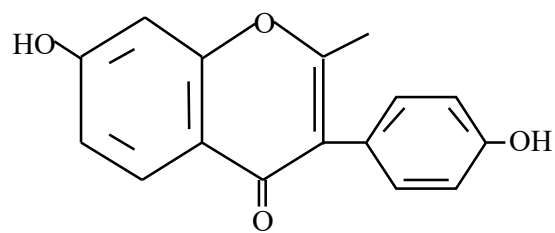
1

2.3 NATURAL PRODUCT

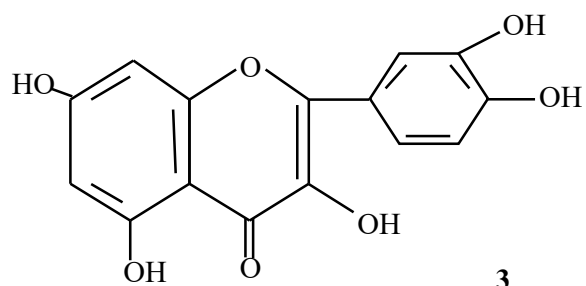
A natural product is a chemical compound or substance produced by a living organism. The cells of living organisms – plant, fungi, bacteria, insects and other animals are the site of intricate and complex synthetic activities that result in the formation of a variety of compounds, many of which are of great importance to man (Finar, 1973). Metabolites are intermediates in metabolic processes in nature and are usually small molecules. A primary metabolite is directly involved in normal growth, development and reproduction e.g fermentation products (acetic acid, lactic acid) and cell constituents (lipids, vitamins). A secondary metabolite is not directly involved in these processes and may not be important or useful to the organism e.g antibiotics, pigments and carotenoids (Cooper, 2013). Examples of natural products include flavonoids, anthocyanins, alkaloids, saponins, terpenoids and essential oils, cardiac glycosides and steroids.

2.3.1 FLAVONOIDS

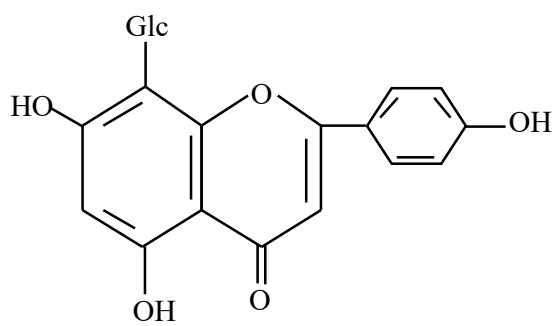
Flavonoids are characteristically plant products found in all groups except algae, bacteria and fungi. Flavonoids are pharmacologically active, largely through their inhibitory effects on many mammalian enzymes or cellular systems. Flavonoids occur in all parts of plants, including the fruits, pollen and roots. Flavonoids have been found in vitro to be effective antimicrobial substances against a wide array of micro organism (Harbone, 2000). An example is the flavonoid glycoside rutin, an anti-inflammatory used medically to prevent capillary fragility. Other examples include Daidzen [2], quercetin [3], vitexin [4] and isovitexin [5]. Flavonoids are most commonly known for their antioxidant activity (Kiritikar, 1997). The term flavonoid is used to embrace all compounds whose structure is based on flavone. The anthocyanins are one group of flavonoid compounds. The fundamental nucleus in anthocyanidin is benzopyrilium chloride but the parent compound is benzopyrilium chloride or flavylum chloride (Harbone, 2000).



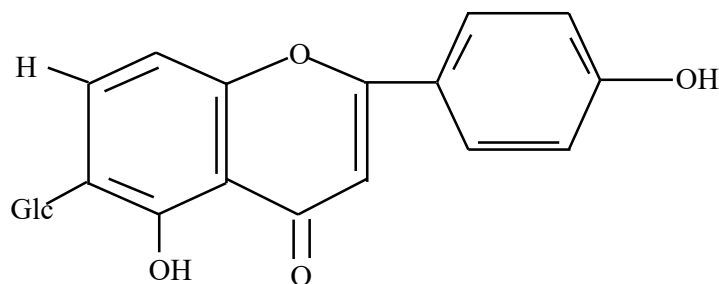
2



3



4



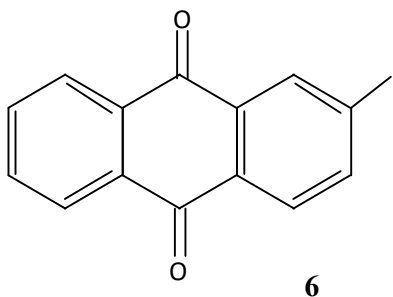
5

Glc = glucose

2.3.2 ANTHOCYANINS

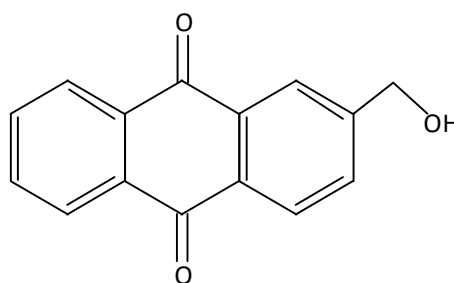
Anthocyanins are natural plant pigments. They are glycosides and their aglycons i.e the sugar free pigments are known as the anthocyanidins. The anthocyanins, which are water soluble pigments, generally occur in the aqueous cell sap, and are responsible for the large variety of colours in flowers. The various shades of colour exhibited by all flowers are due to a very small number of different compounds.

Furthermore, these different compounds were shown to contain the same carbon skeleton, and differed only in the nature of the substituent group. The anthocyanin pigments are amphoteric, their acid salts are usually red and their metallic salts usually blue. In neutral solution, the anthocyanins are violet. Examples include: Tectoquinone [6] and 2- hydroxymethyl – anthraquinone [7] (Harbone, 2000).



6

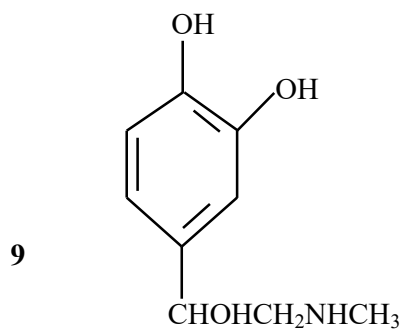
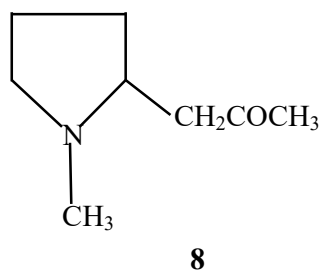
10

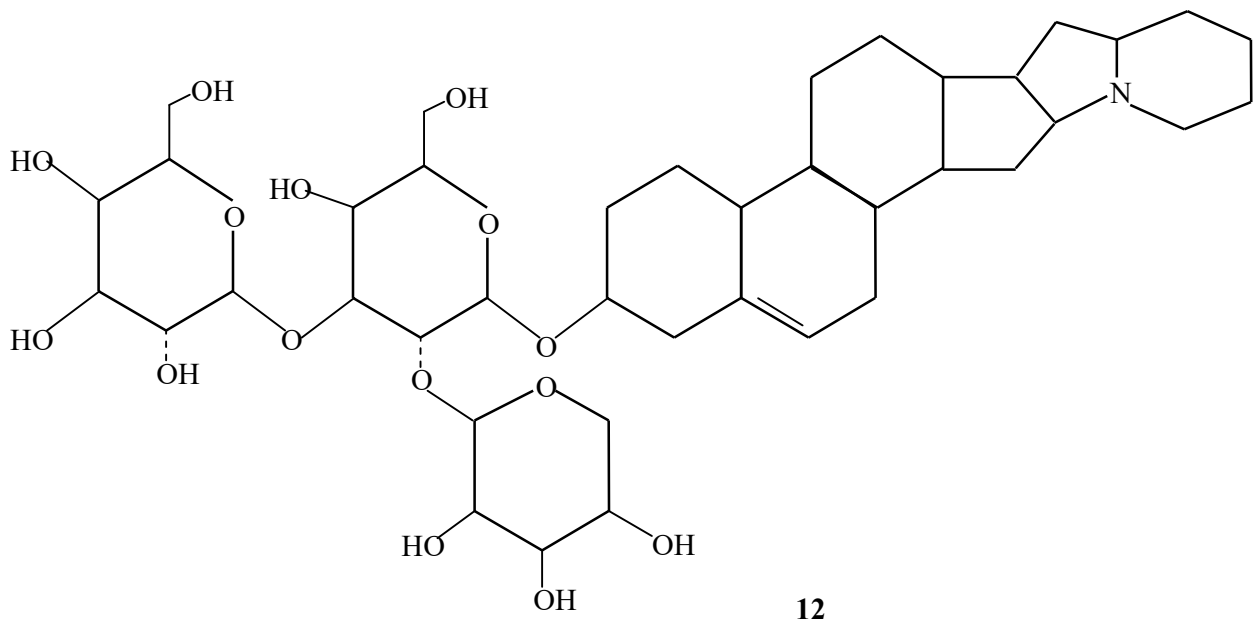
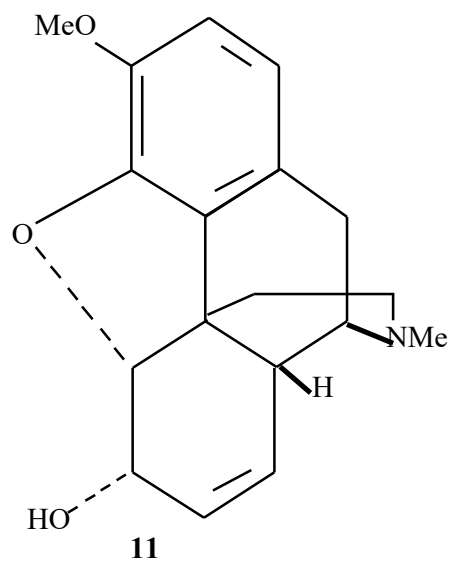
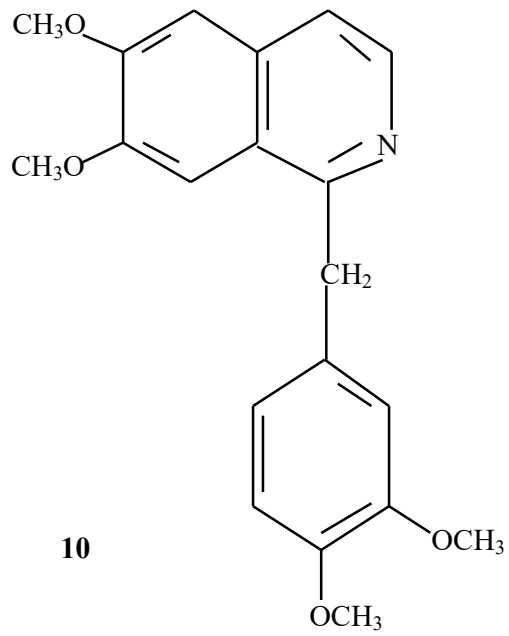


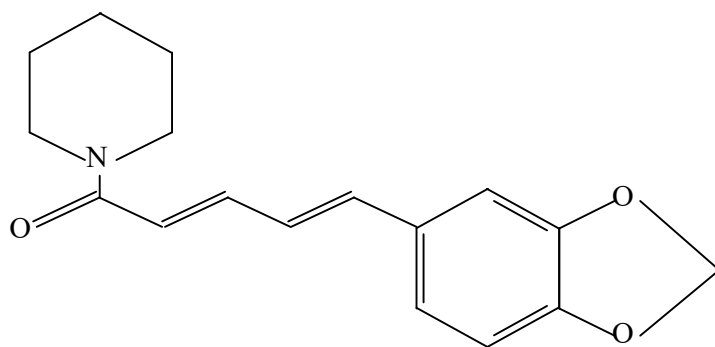
7

2.3.3 ALKALOIDS

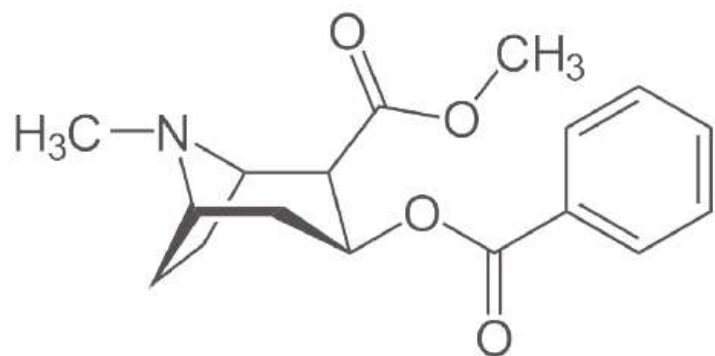
Alkaloids are generally defined as a group of organic compounds of plant origin that contain nitrogen (except proteins, peptides, amino acids and vitamin B). All organic compounds containing nitrogen from natural sources can be regarded as alkaloids. Alkaloids were some of the first natural products to be isolated from medicinal plants. Most alkaloids are colorless, crystalline compound, with bitter tastes. Quite a number of alkaloids possess curative properties for example morphine has narcotic action; reserpine acts as tranquilize while atropine has an antispasmodic action. Examples of alkaloids include Hygrine [8], adrenaline [9], papaverine [10] and codeine [11]. Some alkaloids are present in plants in combination with sugars e.g solanine [12] while others occur as acid amides e.g Piperine [13] or esters.e.g cocaine [14] (Chapman,1997).







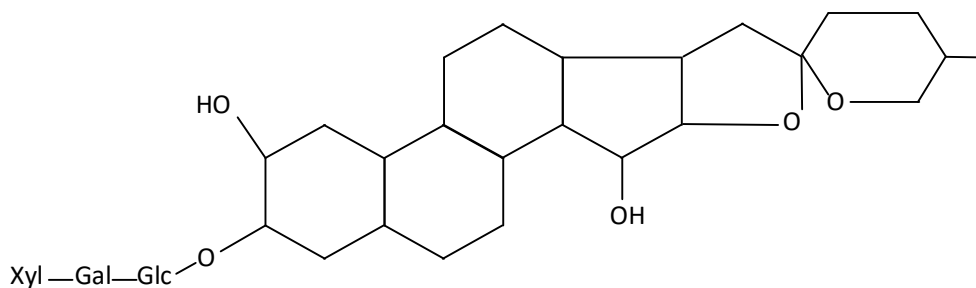
13



2.3.4 SAPONINS

Saponins are generally known as non-volatile, surface-active compounds that are widely distributed in nature, occurring primarily in the plant kingdom. The name “saponin” is derived from the Latin word *sapo*, which means “soap”, because saponin molecules form soap-like foams when shaken with water. They are structurally diverse molecules that are chemically referred to as triterpene and steroid glycosides. They consist of non-polar aglycones coupled with one or more monosaccharide moieties. This combination of polar and non-polar structural elements in their molecules explains their soap-like behaviour in aqueous solutions.

Saponins are very powerful emulsifiers, from pharmacological point of view. They have been shown to modify permeability of small intestine which may help the absorption of specific drugs. Saponins are historically understood to be plant derived but they have also been isolated from marine organisms. Example is digitonin [15] (Finar, 1973).



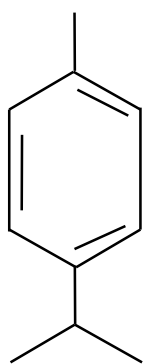
Gal = Galactose
Glc = Glucose
Xyl = Xylose

15

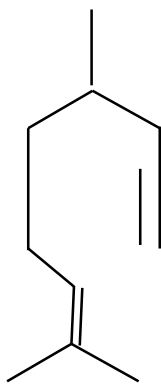
2.3.5 TERPENOIDS AND ESSENTIAL OILS.

Compounds with basic skeletons derived from mevalonic acid or closely related precursors are termed terpenoids. They are considered to be built up of isoprene units linked together in various ways, with different modes of ring closure, unsaturation and different functional groups. Classes of terpenoids include hemiterpenoids, monoterpenoids, sesquiterpenoids, diterpenoids, sesterterpenoids, tetraterpenoids and polyterpenoids.

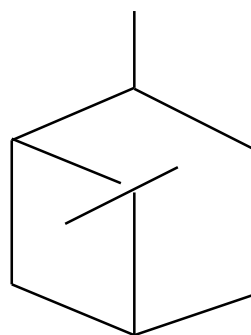
The simpler mono and sesquiterpenoids are chief constituents of essential oils, which are the volatile oils obtained from the sap and tissues of certain plants and trees. The di and triterpenoids which are not steam volatile are obtained from plant tree gums and resins. The essential oil fraction is responsible for the fragrance of plants. It has been reported that 60% of essential oil derivatives examined to date were inhibitory to fungi and 30% to bacteria (Chapman, 1997). Examples include P- cymene [16], Myrcene [17], Pinane [18], geraniol [19], γ - bisabolene [20] (Edeoga *et al.*, 2005).



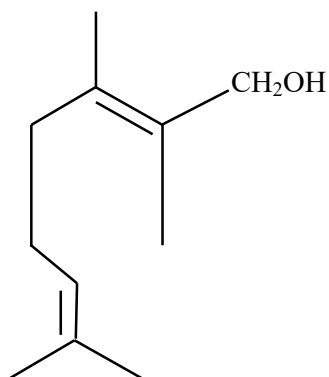
16



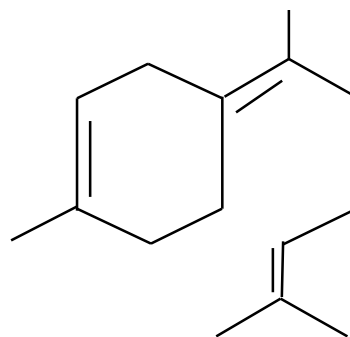
17



18



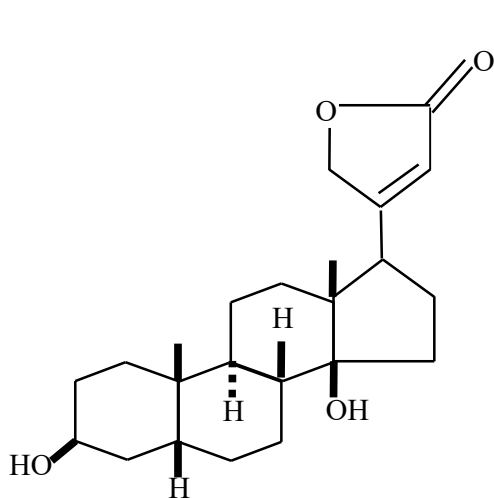
19



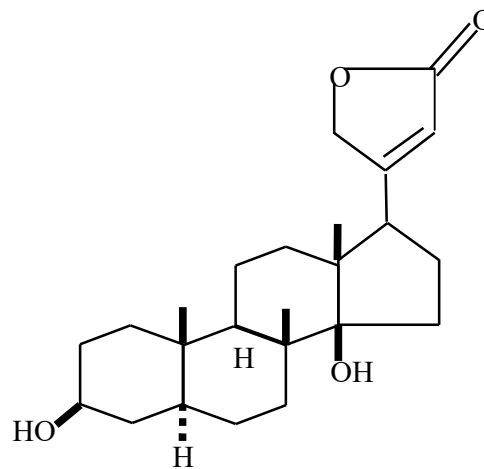
20

2.3.6 CARDIAC GLYCOSIDES

These are plant steroids which occur as glycosides and have the property of stimulating heart muscles. In some cases, a dehydration product of the aglycon is produced. These aglycons are of two types: the more common type contains α , β – unsaturated γ -lactone ring which are known as the cardenolides. The less common type contains a δ – ring which has a conjugated diene system and are known as the bufadienolides. The bufadienolides occur as glycosides in plants of the squill family and as esters of suberyl arginine in the venom from the skin secretions of poisonous toads (e.g. bufotoxin.) (Edeoga *et al.*, 2005). Examples of cardenolides include digitoxigenin [21], uzarigenin [22], strophanthidin [23]. An example of bufadienolides is scillaren A [24].

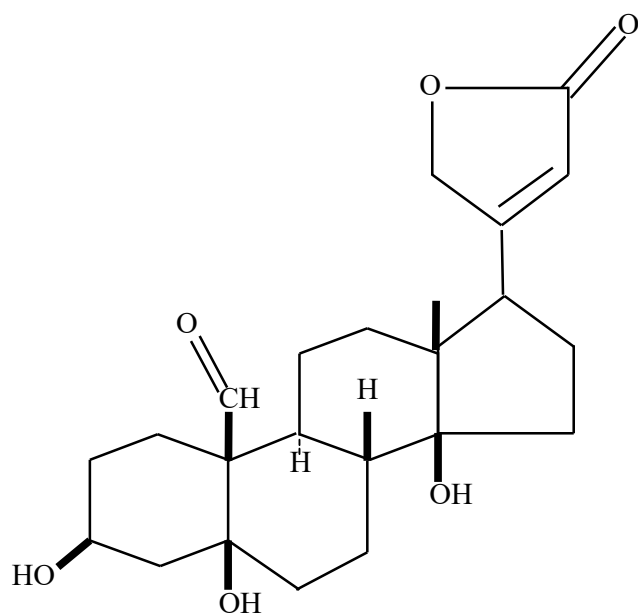


21

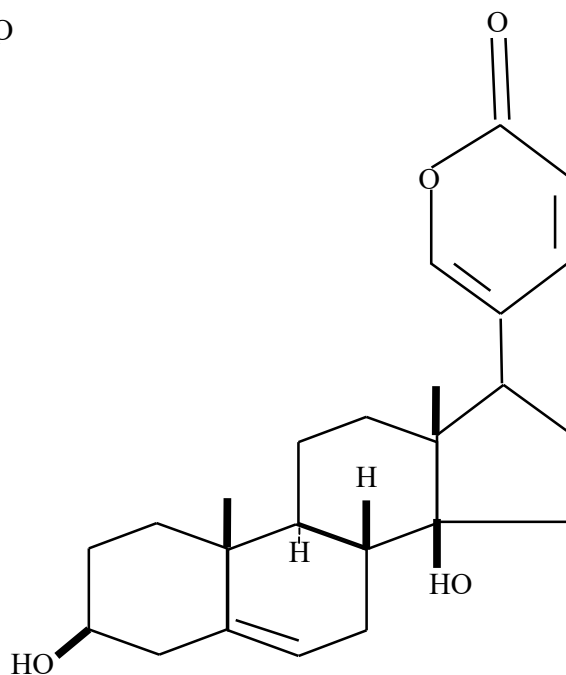


16

22



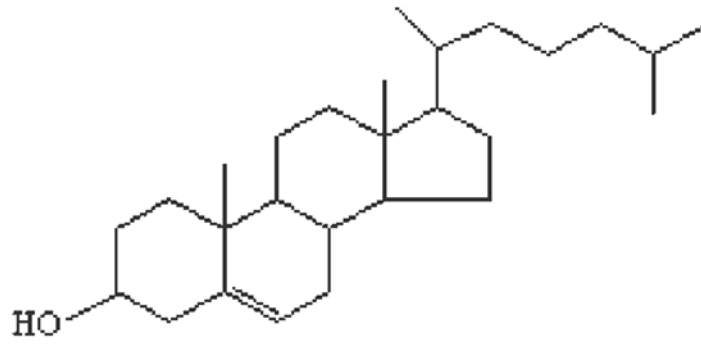
23



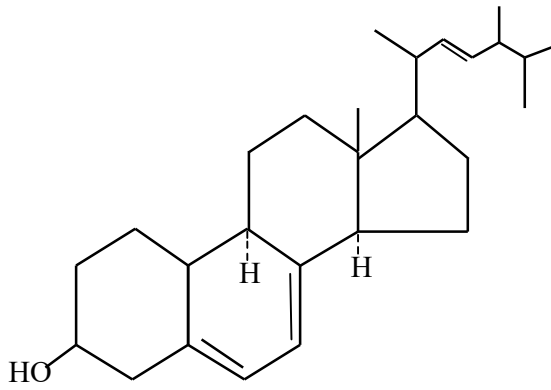
24

2.3.7 STEROIDS

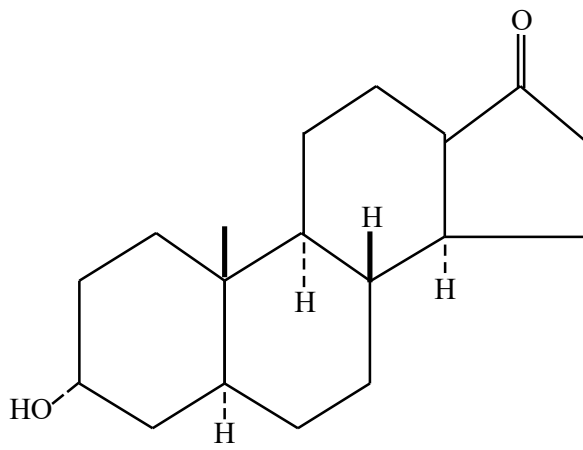
Steroids are found both in the free and combined states as esters or glycosides. Very often, they occur in the form of complex mixtures, the components of which are difficult to separate. Cholesterol, [25] one of the most abundant compounds is present in vertebrates, invertebrates and plants. All the steroids give, among other products, Diels hydrocarbon on dehydrogenation with Selenium at 360° C. In fact, a steroid could be defined as any product which gives Diels hydrocarbon when distilled with Selenium. The structures of steroids are based on the 1, 2-cyclopentenophenanthrene skeleton. Certain steroids exert a specific and powerful effect on the cardiac muscles and thus are called cardiac active steroids (Raphael, 1991). Examples include ergosterol [26], androsterone [27], ergocalciferol [28] (Chapman, 1997).



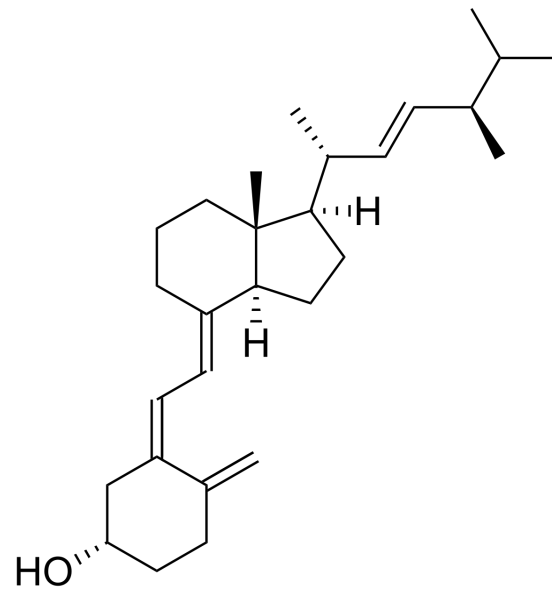
25



26



27



28

2.4 EXTRACTION METHODS

2.4.1 SOXHLET EXTRACTION

In soxhlet extraction, oil and fat from solid materials are extracted by repeated percolation with an organic solvent usually hexane or petroleum ether under reflux in a special glassware (soxhlet extractor). In this method, the sample is dried, ground into small particles and placed in a porous cellulose thimble. The thimble is placed in an extraction chamber, which is suspended above a flask containing the solvent and below a condenser. The flask is heated and the solvent evaporates and move into the condenser where it is converted into a liquid that trickles into the extraction chamber containing the sample (Harbone, 1993).

2.4.2 COLD PRESSING

This method is used to extract the essential oil from citrus fruits such as orange, lemon, grape fruits. The citrus rinds are separated from the fruit ground or chopped and then pressed. The result is a watery mixture of essential oil and liquid which will separate out over a given time. It is important to note that oils extracted using this method have a relatively short shelf life (Harbone, 1993).

2.4.3 MACERATION

This is also known as batch process, and it involves macerating the tissue with appropriate solvent in a Waring Blender, soaking for a short time, filtering through suitable size of Buchner funnel and then returning the residue to fresh solvent for further extraction. The combined solvent extracts are then evaporated, usually under reduced pressure and the residue submitted to appropriate fractionation procedures (Harbone, 1993).

2.5 PURIFICATION OF NATURAL PRODUCTS

2.5.1 GAS LIQUID CHROMATOGRAPHY (GLC)

Gas chromatography is one of the chromatographic techniques employed for purification of natural products. The principle involves separation of components of the sample under test due to partition in between gaseous mobile phase and stationary liquid phase. The components partitioned into gas come out first while the other components come out later. Stationary phase is a liquid layer supported over a stationary phase while mobile phase is an inert and stable gas. Gas chromatography separates a mixture into its constituent by passing a moving gas phase over a stationary phase. It is similar to liquid –liquid chromatography except that the mobile liquid phase is replaced by a moving gas. The apparatus required for gas liquid chromatography is sophisticated and expensive, relative to that required for paper chromatography or thin layer chromatography.

Apparatus for gas liquid chromatography has four main components: The column, heater, gas flow and a detective device. The main variables in GLC are the stationary phase of the column and the temperature of operation. These are varied according to the polarity and volatility of the compounds being separated. Many classes of substances are routinely converted to derivatives before being subjected to GLC, since these allow their separation at a lower temperature.

Most frequently, GLC is automatically linked to mass spectrometry (MS) and the combined Gas chromatography mass spectrometry (GCMS) apparatus has emerged in recent years as one of the most important of all techniques for phytochemical analysis. This type of chromatography is important in industry, biomedical analysis, and research because it is an extremely sensitive technique. The stationary phase is a liquid mixed with a solid packed into a long glass column with a small diameter. The moving phase is a fairly inert gas like helium

or nitrogen, referred to as the carrier gas, and heated to vaporize where necessary and passed through the column where separation occurs (Philip, 1996).

2.5.2 COLUMN CHROMATOGRAPHY

Column chromatography is suitable for the separation of gram quantities of sample. A solvent acts as the mobile phase while a finely divided solid surface acts as the stationary phase. The stationary phase will absorb the components of the mixture to varying degrees. As the solution containing the sample passes over the adsorbent, the components are distributed between the solvents and the adsorbent surface. The solvent and sample compete for positions in the solid adsorbent, the solvent displacing the sample reversibly and continuously in the direction of the solvent flow. Consequently a weakly adsorbed compound will spend less time in the adsorbent and will therefore be eluted first (Gelosa *et al.*, 2009). Compounds that have a high affinity for the solvent are carried along as it moves past the stationary support. Compounds that have a higher affinity for the solid move more slowly and get eluted out last.

This technique involves filling a glass column with a solid support, applying up to several grams of the sample to the top of the column and then eluates are collected slowly from the column. The mixture of mobile phase and sample to be separated are introduced from top of the column, the individual components of mixture move with different rates.

The stationary phase is in form of a packed column through which the mobile phase is allowed to flow. A clean dry, long, narrow tube is clamped and filled with glass wool. Slurry of silica gel is prepared, poured into the column and allowed to settle under gravity. The sample is introduced into the column either as a liquid or as a dry sample and acidified sand added to cover sample layer (Harbone, 1993).

2.5.3 THIN LAYER CHROMATOGRAPHY (TLC)

In thin layer chromatography, a solid adsorbent is coated onto a solid support as thin layer (0.25 mm thick) .The sample to be separated is dissolved in a suitable solvent and the resulting solution is spotted on the thin layer plate. The adsorbent will absorb a certain fraction of each component of the mixture and the remainder will be in solution. A compound that is strongly adsorbed will have a greater fraction of its molecule adsorbed and will spend more time on the adsorbent while a weakly adsorbed compound will spend less time on the adsorbent (Gelosa *et al.*, 2009). Solute and solvent molecule compete for “sites” in the adsorbent, to be adsorbed; the solute molecule must first displace a solvent molecule. Molecules with polar functional groups or those capable of hydrogen bonding will have a strong affinity for the adsorbent surface and will be strongly retained. The adsorbent surface consists of discrete adsorption sites. It employs a thin layer of microgranular adsorbent (silica gel/alumina) supported on a glass plate. Silica gel and alumina are the two most common adsorbents for thin layer chromatography. Slurry of micro granular adsorbent with water is spread as evenly as possible on a plate by means of special applicator. The application of the sample is called spotting usually with a capillary tube. Development of the chromatography can be by ascending or descending. Development usually discontinued when the solvent front has advanced 75% toward the end of plate (Ksumoto, 1993).

2.5.4 HIGH PERFORMANCE LIQUID CHROMATOGRAPHY (HPLC)

High performance liquid chromatography is a chromatographic separation technique in which the separation is accomplished by partitioning the solute between mobile solvent and a stationary column packing material of small, uniform particles size. The separation of compounds is achieved by their relative differences in movement through the column on application of pressure exerted through mobile phase or carrying liquid. The compounds of

the mixture travel with different rates due to their relative affinities with the solvent and stationary phase in high performance liquid chromatography. Separation is achieved by greater surface area as a result of the very small particle size of stationary phase. The small size of the particles gives very high column efficiency, but also result in large pressure drops across the column such that high pressure (>500 psi) is required to achieve reasonable flow rates.

A HPLC instrument consists of solvent supply system feeding a pumping device which is coupled to a column through a sample introduction system. The eluate from the column then passes through a detector and the response of the detector is measured by a digital output devices. The mobile phase consists of pure organic solvent in mixtures with aqueous solutions of salts or buffers. The column is made up of stainless steel tubes with internal diameters of 2 – 4.6 mm and lengths of 10 to 100 cm. High performance liquid chromatography allows researchers to study molecule that are difficult to separate by other means, particularly biomolecular compounds (Bohm, 1994).

2.6 TECHNIQUES USED IN ANALYSIS OF NATURAL PRODUCTS

2.6.1 ULTRA VIOLET SPECTROSCOPY

Ultraviolet spectroscopy refers to absorption spectroscopy in the Ultraviolet visible spectra of electromagnetic region. This means it absorbs light in the visible and adjacent (near ultraviolet and near infrared) region. In this region of the electromagnetic spectrum, molecules undergo electronic transitions. Ultraviolet visible spectroscopy is routinely used in the quantitative determination of solutions of transition metal ions and highly conjugated organic compound. Since most organic compounds are colorless, the visible region of the spectrum (400 - 700 nm) is of limited value. The ultra violet region, especially the wavelengths from 200 - 400 nm is very helpful as guide to the presence of certain functional

groups, particularly the unsaturated ones. The photons in ultraviolet light have the energy to raise the electrons to higher energy levels than they normally occupy in their ground state. When a photon excites an electron from its ground state to an excited state, the process is called electron excitation. Groups that cause light to be absorbed are called chromophores (Morrison, 2004).

2.6.2 INFRARED SPECTROSCOPY

The infrared spectrum is used for identification of functional groups present in compounds. In addition, it can be used to establish the identity of two compounds. A particular group of atoms gives rise to characteristic bands, that is to say a particular group absorbs light of certain frequencies that are much the same from compound to compound. On absorption of a photon of infrared radiation, a molecule is excited to a higher energy level in which vibrational transitions are more energetic. Some transitions are relatively localized, involving mainly two or, at the most, a few atoms. As a result, some structural features lead to infrared absorptions that appear in a narrow frequency range, regardless of the structure of the remainder of the molecule. For a vibration to result in absorption, it must change the dipole moment of the molecule (Harbone, 1993).

2.6.3 MASS SPECTROSCOPY (MS)

By mass spectral analysis, it is possible to determine the molecular weight and molecular formula of a compound. The structure of the compound is determined by breaking the molecule into smaller, identifiable fragments and then piecing them back together. Mass spectral analysis is initiated by bombarding a vaporized sample with an electron beam. This can cause an electron to be dislodged from the molecule, producing a positive molecular ion. The most intense peak in the mass spectrum is called the base peak and is assigned a value of 100%. The peak formed by the loss of one electron from the molecule results in the

molecular ion, M^+ and the corresponding peak as molecular ion peak. Any peak of less mass than the molecular ion is called fragment peak. Analysis of the masses of the fragment gives the molecular weight, possibly the molecular formula and clues to functional groups and the structure. Less than a milligram of the sample is destroyed in this analysis. The molecules are broken up into many fragments some of which are positive ions. Each of the ions has a particular ratio of mass to charge value.

Mass spectral analysis can be used to identify compounds and to help establish the structure of a new compound by giving the exact molecular weight and molecular formula (Dudley, 1980).

2.6.4 NUCLEAR MAGNETIC RESONANCE SPECTROSCOPY (NMR)

Nuclear magnetic resonance spectroscopy measures the energy absorbed when certain nuclei undergo nuclear spin transitions. These transitions involve photons of much less energy than those associated with electronic or vibrational transitions. Photons in the radio frequency region of the spectrum have the precise energy but only for selected nuclei. Nuclear magnetic resonance is concerned with the nucleus of H-atoms (the proton) or the nucleus of carbon atoms (^{13}C). With the proton nuclear magnetic resonance, information on many different kinds of hydrogen environment in the molecule is obtained.

Depending on the local chemical environment different protons in a molecule resonate at slightly different frequencies. Since both this frequency shift and the fundamental resonance frequency are directly proportional to the strength of the magnetic field, the shift is converted into a field-independent parameter known as the chemical shift. The chemical shift is expressed as fraction of the operating frequency of the NMR spectrometer. An atomic nucleus in a molecule are like tiny magnets, each with its own small magnetic field. There are also negatively charged electrons in the vicinity of each nucleus and these have magnetic

moments too. Therefore what any nucleus feels in an external magnetic field is affected by the small local fields of other nuclei and electrons near it. Some of the small local fields near a nucleus slightly increase the effect of the external field but others decrease it. The difference in frequency units between the sharp tetramethylsilane TMS peak and the absorption signal of another proton is called the chemical shift (Dudley, 1980).

2.6.5 Antioxidant Assay

Antioxidant chemistry is a major research focus of many scientists in recent times due to the fact that antioxidants inhibit oxidation reactions; a chemical reaction that transfers electrons from a substance to an oxidizing agent producing free radicals. Free radicals start chain reactions that damage living cells, degrade minerals and spoil food. Oxidation has therefore been implicated in many diseases. Substances containing atoms with an unpaired electron in the outer orbit are free radicals while reactive oxygen species (ROS) are free radicals involving oxygen molecules (Onocha *et al.*, 2016).

Antioxidants are agents that neutralizes harmful compounds called free radicals. Antioxidants can take the form of drugs, enzymes in the body, vitamin supplements or industrial additives. They are routinely added to metals, oils, foodstuffs and other materials to prevent free radical damage. Free radicals also play very important roles in human health and are beneficial in combating several diseases. However, excess formation is harmful to the body organs. Any molecule can become a free radical by either losing or gaining an electron. Once initiated these free radicals get involved in chain reaction with stable types. The compounds thus formed have longer stability in the body and increase the potential for cellular damage. Free radicals damage the cell at the site of their operation causing serious health disorders (Onocha *et al.*, 2011).

Natural antioxidants have gained increasing interest among the scientific community because epidemiological studies have shown that frequent consumption of natural antioxidants is associated with a lower risk of cardiovascular diseases and cancer (Renaud *et al.*, 1998, Temple, 2000). Several assays have been frequently used to estimate antioxidant capacities in plants. Examples include 2,2 diphenyl -1-picrylhydrazyl (DPPH), (Sleet and Brandel, 1983) and oxygen radical absorption capacity (ORAC) (Cao *et al.*, 1993, Prior *et al.*, 2003). Natural antioxidants occur in all parts of plants. These antioxidants include carotenoids, vitamins, phenols, flavonoids, dietary glutathione, and endogenous metabolites. Plant-derived antioxidants have been shown to function as singlet and triplet oxygen quenchers, free radical scavengers, peroxide decomposers, enzyme inhibitors, and synergists. The most current research on antioxidant action focuses on phenolic compounds, such as flavonoids. Fruits and vegetables contain different antioxidant compounds such as vitamin C, vitamin E and carotenoids, whose activities have been established in recent years.

Antioxidants are believed to play a very important role in the body defense system against reactive oxygen species (ROS), which are the harmful byproducts generated during normal cell aerobic respiration. Increasing intake of dietary antioxidants may help to maintain an adequate antioxidant status and, therefore, the normal physiological function of a living system is achieved (Sleet and Brandel, 1983).

CHAPTER THREE

3.0 MATERIAL AND METHODS

3.1 COLLECTION AND PREPARATION OF THE PLANTS

3.1.1 *Croton megalocarpoides*

The stem bark of *Croton megalocarpoides* was collected from Mombasa, Kenya in August, 2013. The plant was authenticated at the University of Nairobi Herbarium in the school of Biological science and a voucher specimen BN 2009/8 deposited.

3.1.2 EXTRACTION

The stem bark of *C. megalocarpoides* was air dried in the shade for 4 weeks and was ground into a coarse powder. The powder was extracted by cold extraction at room temperature with n- hexane, dichloromethane and methanol successively (2L each, 24 h each).The extracts were concentrated using a rotary evaporator, combined and dried, yielding 13 g n- hexane, 37 g dichloromethane and 20 g methanol extracts.

3.1.3 *Physalis angulata*

The whole plant material of *Physalis angulata* was collected from Ijagun area in Ijebu-Ode, Ogun State, Nigeria. They were authenticated at FRIN (Forestry Research Institute of Nigeria) with herbarium file FHI No109674. The entire plant (leaves, stem and roots) of *Physalis angulata* was dried and pulverized before extraction.

3.1.4 EXTRACTION

The dried plant sample of *Physalis angulata* was ground and 2 kg of sample obtained. 1.5 kg of the plant sample was carefully poured into an aspirator bottle and soaked with n-hexane

for 4 days. The same process was repeated with ethyl acetate and methanol. After 4 days, the mixtures were decanted and the extracts were recovered by rotary distillation process.

The two-dimensional proton NMR spectra were recorded in deuterated solvents on a Bruker AVANCE NMR spectrometer at the Department of Chemistry, University of Surrey, Guildford, UK. The spectra were recorded in deuterated chloroform (CDCl_3), and the chemical shifts were recorded in ppm (parts per million) relative to the standard. The deuterated chloroform was referenced at $\delta_{\text{H}} 7.26$ in the ^1H NMR spectrum and the central line at $\delta_{\text{C}} 77.23$ in the ^{13}C NMR spectrum.

Infrared spectra were recorded using a Perkin-Elmer (2000 FTIR) spectrometer. The liquid samples were sandwiched between NaCl plates at the Department of Chemistry, University of Surrey, Guildford, UK. Low resolution electron impact mass spectra were acquired by using a Hewlett Packard G1800A GCD system at Department of Chemistry, University of Surrey, Guildford, UK.

Laboratory grade solvents were used (Sigma – Aldrich, Germany). Silica gel 60 (Sigma Aldrich) and SephadexTM LH – 20 (GE Health Care Bio-sciences AB, Sweden) were used for column chromatography. Flash chromatography was performed on (Reveleris^{Grace}, silica 40 μm , 120 g Belgium) while thin layer chromatography was performed on DC – Fertigfolien ALUGRAM[®] SIL G/UV₂₅₄, layer – 0.20 mm silica gel 60 with fluorescent indicator UV₂₅₄, Germany. Detection of spots was carried out with by UV absorption and P-anisaldehyde in concentrated H_2SO_4 using sigma gun spray.

3.2 PHYTOCHEMICAL SCREENING TESTS ON *Croton megalocarpoides* AND *Physalis angulata*

3.2.1 TESTS FOR SAPONINS

Methanol extract (0.5 g) was shaken with water in a test tube. Observation of frothing is indicative of the presence of saponins (Kumar *et al.*, 2009)

3.2.2 TEST FOR ALKALOIDS

Methanol extract (0.5 g) was stirred with 5 mL of 1% aqueous hydrochloric acid on a steam bath. 1 mL of the filtrate was treated with a few drops of Dragendoff reagent. Observation of a precipitate is indicative of presence of alkaloid (Harborne, 1984; Evans, 1989).

3.2.3 TEST FOR STEROIDS

Methanol extract (0.5 g) was dissolved in 2 mL of chloroform. H₂SO₄ was carefully added. The formation of a reddish brown colour interphase is a positive test for steroids.

3.2.4 TEST FOR TANNINS

Methanol extract (0.5 g) was stirred with 10 mL of distilled water, warmed and filtered. Ferric chloride reagent was added to the filtrate. The formation of blue black precipitate is indicative of the presence of tannins (Savithamma *et al.*, 2011).

3.2.5 TEST FOR REDUCING SUGAR

A small portion of extract was dissolved in distilled water and warmed with Fehlings solutions A and B. Observation of brick red precipitate is a positive test for reducing sugar

3.2.6 TEST FOR ANTHRAQUINONES

Methanol extract (2 g) was shaken with 5 mL benzene, filtered and 10 mL aqueous H₂SO₄ was added to the filtrate. The mixture was shaken. Observation of pink, red, or violet colour is indicative of anthraquinone.

3.2.7 TEST FOR FLAVONOIDS

Dilute ammonia solution (5 mL) were added to a portion of the aqueous filtrate of test extracts followed by addition of concentrated H₂SO₄. A yellow colouration observed in each extract indicated the presence of flavonoids. The yellow colouration may disappear on standing (Edeoga *et al.*, 2005)

3.3 COLUMN CHROMATOGRAPHY OF THE DICHLOROMETHANE EXTRACT OF *Croton megalocarpoides* AND METHANOL EXTRACT OF *Physalis angulata*

The column was packed by introducing glass wool into a clean column clamped vertically. The slurry of the silica gel in hexane was poured down the column through a funnel. Acid washed sand was poured at the top of the column to prevent disturbance of the surface during loading.

Extract (15 g) was loaded on to the column. Different fractions were eluted using different solvent mixtures from 100% hexane to 100% ethyl acetate and from 100% ethyl acetate to 50% methanol.

Eluent (50 mL) was collected in each case as fraction and these individual fractions distilled and collected. The separation was monitored using thin layer chromatography. TLC analysis was carried out on 0.2 mm silica gel, aluminium-backed plates (Merck Art. 5554). Then, the

plates were analyzed using a UV-lamp at 254 nm and developed using anisaldehyde spray reagent (1 anisaldehyde: 2 sulphuric acid: 97 methanol) with subsequent heating.

Each fraction was spotted using thin layer chromatography (TLC) to determine fractions of similar components which were then combined based on their R_f values. Fractions were further packed on smaller column. Elution was done with hexane, followed with gradient of 5%, 10%, 15%, 20%, 30%, 40%, 50%, 60%, 70%, 80%, 90%, 100% ethyl acetate in hexane. The isolation scheme of dichloromethane extract of *C. megalocarpoides* (CMD) and methanol extract of *P. angulata* (PAM) are illustrated in Fig 3.1 and 3.2.

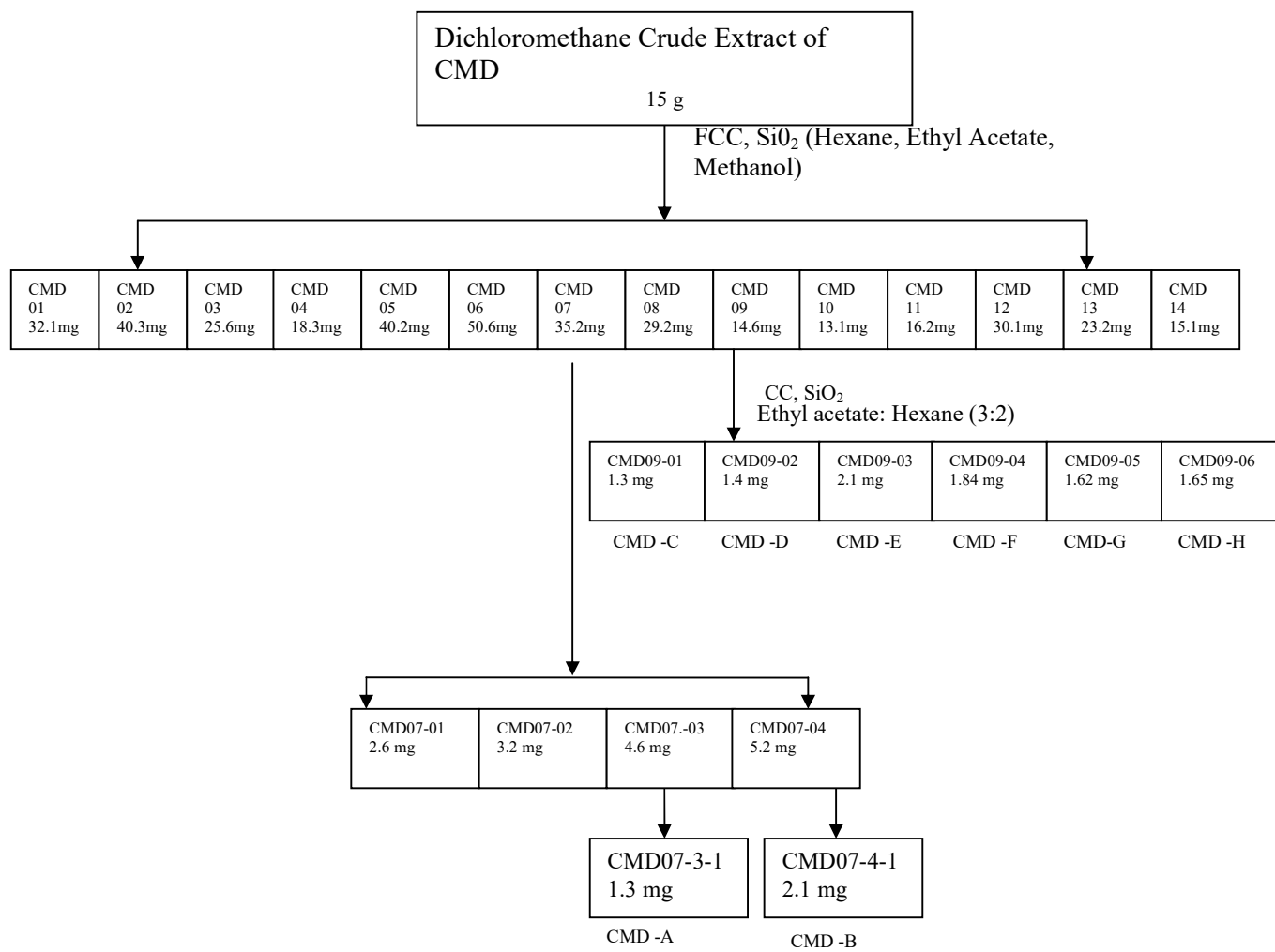


Fig.3.1: Isolation scheme of CMD-A to CMD-H

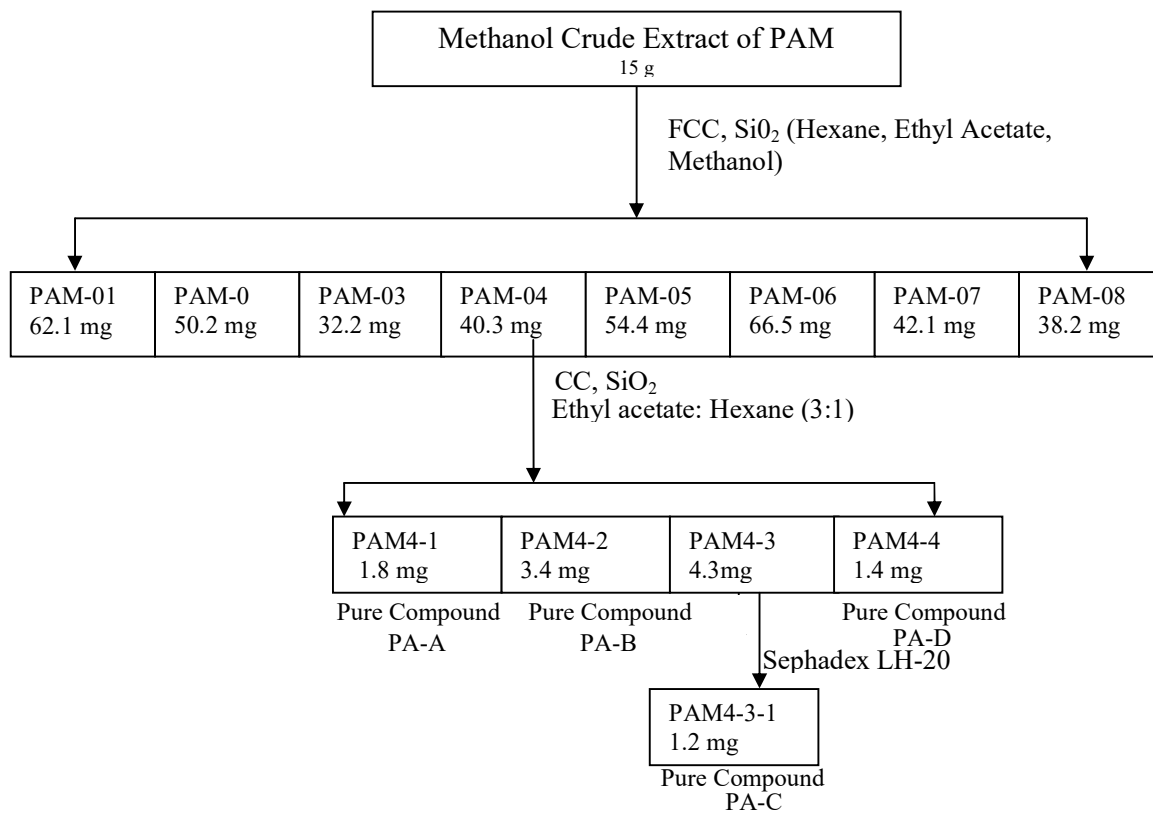


Fig. 3.2: Isolation scheme of PA-A to PA-D

3.4 ANTIOXIDANT ACTIVITY OF EXTRACTS AND ISOLATED CHEMICAL COMPOUNDS FROM *Croton megalocarpoides* AND *Physalis angulata*

The antioxidant activity of the crude methanol extracts of *Croton megalocarpoides* and *Physalis angulata* were determined using the DPPH free-radical scavenging activity.

A stable radical: 2, 2-diphenyl-1-picrylhydrazyl radical (DPPH) (3.94 mg), was dissolved in 100 mL methanol to give 100 ppm solution. Methanol solution of DPPH (3.0 mL) was added to 0.5 mL of the methanol extract taken from the stock solution.

The stock solution was prepared by dissolving 3.0 mg of the crude extract in 3 mL methanol. The mixture was shaken well and left to stand for 10 minutes, after which the decrease in absorption at 517 nm of DPPH was measured. The actual decrease in absorbance induced by the test compound was calculated by subtracting that of the control. Other concentrations (1.0, 0.5, 0.25, 0.125, 0.0625 mg/mL) of methanol extracts were prepared from the stock solution by serial dilution. Each of the concentrations was analyzed in the same way as the stock solution was analyzed. Ascorbic acid was used as a standard.

All the tests were carried out in triplicates and the results obtained were averaged. IC₅₀ values were calculated using Graph Pad prism statistical software.

CHAPTER FOUR

4.0 RESULTS AND DISCUSSION

4.1 Phytochemical Screening

The Phytochemical screening tests on Dichloromethane extract of stem bark of *Croton megalocarpoides* revealed the presence of alkaloids, tannins, saponins, flavonoids and steroids while phytochemical screening tests carried out on methanol extract of whole plant of *Physalis angulata* revealed the presence of flavonoid, saponins and tannins. Flavonoids have been reported to exert multiple biological effects including antioxidant and anti-inflammatory activities. Flavonoid administration significantly decreases oxidative damage in the liver in obstructive jaundice (Talha *et al.*, 2013). The presence of flavonoid in *Croton megalocarpoides* could be responsible for the medicinal uses of this plant in the treatment of jaundice. Flavonoids nowadays are being used in different formulations and wound healing dresses (Talha *et al.*, 2013). Most wound healing medicinal plants possess multiple flavonoids. Saponins have also been reported to show antioxidant activity (Talha *et al.*, 2013). The presence of flavonoid and saponins in *Physalis angulata* could be responsible for the medicinal uses of this plant in the treatment of wound.

4.2 ISOLATION AND CHARACTERIZATION OF CMD-A-H FROM *Croton megalocarpoides*

The dichloromethane extract of the stem bark of *C. megalocarpoides* was subjected to flash chromatography using various mixtures of hexane and ethyl acetate as solvents and it yielded 185 fractions. Similar fractions were pulled together based on their R_f values on thin layer chromatography (TLC) to give 14 fractions CMD-01 to CMD -14. Fraction CMD-07 (60 % hexane and 40% ethyl acetate) which contained solids was packed in a column (5 mm x 35 cm) and elution carried out, starting with the solvent mixture of 60 % hexane and 40% ethyl acetate. Thirty fractions were collected and pulled together to give four fractions- CMD07-01 to CMD07-04. **CMD-A** (1.3 mg) and **CMD-B** (2.1 mg) were purified from fractions CMD07-03 and CMD 07-04 respectively. Fraction CMD-09 (50 % hexane and 50% ethyl acetate) which contained solids was also packed in a column (5 mm x 35 cm) and elution was carried out, starting with the solvent mixture of 50 % hexane and 50% ethyl acetate. Eighty fractions were collected and pulled together based on the TLC to give six fractions-CMD09-01, CMD09-02, CMD09-03, CMD09-04, CMD09-05 and CMD09-06. Isolated compounds **CMD-C** (1.3 mg) , **CMD-D**(1.4 mg), **CMD-E** (2.1 mg), **CMD-F** (1.84 mg), **CMD-G** (1.6 mg) and **CMD-H** (1.6 mg) were purified from CMD09-01, CMD09-02,CMD09-03, CMD09-04, CMD09-05 and CMD09-06 respectively.

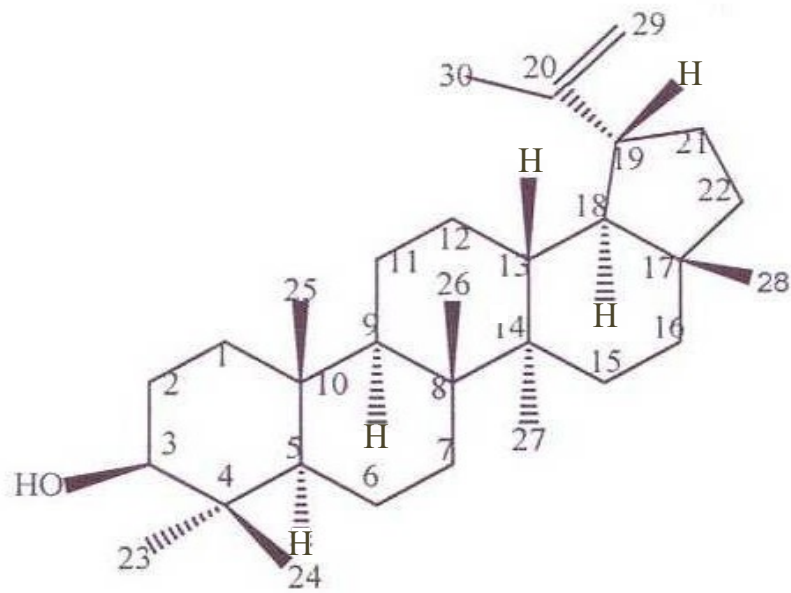
4.2.1 STRUCTURAL ELUCIDATION OF COMPOUND CMD-A

Compound **CMD-A** was isolated as a white solid from the DCM extract of stem bark of *Croton megalocarpoides*. The FTIR spectrum (Fig. 4.1) showed an absorption band 3393 cm^{-1} that was attributed to a hydroxyl group stretch.

The ^1H NMR spectrum (Fig 4.2) of compound **CMD-A** showed the presence of seven tertiary methyl proton resonances at δ_{H} 0.97 s, 0.78 s, 0.83 s, 1.02 s, 0.98 s, 0.79 s and 1.68 s

which corresponded to the carbon resonance spectrum at δ_C 28.2 , 15.6 , 16.3 ,16.2 , 14.7, 18.2 and 19.5 in the ^{13}C NMR spectrum (Fig 4.3) and HSQC spectrum (Fig 4.7). A multiplet of one proton at δ_H 2.38 corresponding to 19 β -H is characteristics of lupeol. A proton resonance at δ_H 3.18 (1H, dd, $J=11.35$, $J=4.85$ Hz) in the ^1H NMR spectrum (Fig 4.2) was seen to correspond to a carbon resonance at δ_C 79.2 in the HSQC spectrum (Fig 4.7). The deshielded signal at δ_C 79.2 was due to the presence of hydroxyl group at C-3. Correlations were observed between δ_{H-3} 3.18 with δ_{C-4} 38.9, $\delta_{H-23,24}$ 0.97, 0.78 with δ_{C-4} 38.9, δ_{H-19} 2.38 with δ_{C-20} 151.2 in the HMBC spectrum (Fig 4.8). A correlation between the downfield methyl group resonance at δ_H 1.68 and the two non-equivalent methylene proton resonances at δ_H 4.68 and 4.56 in the NOESY spectrum (Fig 4.11) were ascribed to H-29A and H-29B.

Comparison of the ^{13}C NMR and ^1H NMR spectrum signals with those reported in the literature (Gongalez, 1987) confirmed that **CMD-A** is identical to 3 β -hydroxylup-20(29)-ene[**29**], commonly known as lupeol, which has been evaluated for its anti-inflammatory and anti-angiogenic activities (Tolstiva *et al.*, 2006). It has been previously isolated from the root of *Croton megalocarpoides* (Beth *et al.*, 2016).



29

Table 1: Correlation Table of ^1H (500 MHz) and ^{13}C (125 MHz) NMR Data^a for compound CMD-A: Lupeol and Literature^b in CDCl_3

No	^{13}C NMR ^a (125 MHz) CDCl_3	^{13}C NMR ^b (125 MHz) CDCl_3	^1H NMR ^a (500 MHz) CDCl_3	^1H NMR ^b (500 MHz) CDCl_3
1 α	38.9 CH_2	38.7 CH_2	1.65 m	1.67 t
1b			0.94 m	0.90 d
2a	27.6 CH_2	27.4 CH_2	1.65 m	1.60 d
2b			1.57 m	1.56 q
3	79.2 CH	79.0 CH	3.18 dd	3.19 dd
4	38.9 C	38.8 C	-	-
5	55.5 CH	55.3 CH	0.67 d	0.68 d
6a	18.5 CH_2	18.3 CH_2	1.57 m	1.51 d
6b			1.39	1.39 m
7a	34.5 CH_2	34.3 CH_2	1.38	1.39 m
7b			1.38	1.39 m
8	40.2 C	40.8 C	-	-
9	50.7 CH	50.4 CH	1.28 m	1.27 d
10	37.4 C	37.2 C	-	-
11a	21.2 CH_2	20.9 CH_2	1.41 m	1.41 d
11b			1.22 m	1.21 q
12a	25.4 CH_2	25.2 CH_2	1.06 m	1.06 q
12b			1.67	1.67 d
13	38.3 CH	38.1 CH	1.65	1.66 t
14	43.1 C	42.9 C	-	-
15a	27.6 CH_2	27.5 CH	1.01 m	1.00 d
15b			1.67	1.68 t
16a	35.8 CH_2	35.6 CH	1.38	1.37 t
16b			1.41 m	1.47 m
17	43.2 C	43.0 C	-	-
18	48.5 CH	48.0 CH_2	1.36	1.36 t
19	48.2 CH	47.9 CH	2.38 m	2.39 m
20	151.2 C	151.0 C	-	-
21a	30.0 CH_2	29.9 CH_2	1.33	1.32 m
21b			1.92 m	1.92 m
22a	40.2 CH_2	40.0 CH_2	1.19 m	1.19 m
22b			1.38	1.38 m
23	28.2 CH_3	28.0 CH_2	0.97 s	0.97 s
24	15.6 CH_3	15.4 CH_2	0.78 s	0.77 s
25	16.3 CH_3	16.1 CH_2	0.83 s	0.83 s
26	16.2 CH_3	16.0 CH_2	1.02 s	1.02 s
27	14.7 CH_3	14.76 CH_2	0.98 s	0.98 s
28	18.2 CH_3	18.0 CH_2	0.79 s	0.79 s
29a	109.5 CH_2	109.3 CH_2	4.56 brs	4.56 m
29b			4.68 brs	4.68 m
30	19.5 CH_3	19.3 CH_2	1.68 s	1.68 s

^a Assignment aided by HMQC and HMBC experiments

^b Literature data of lupeol (Gongalez,1987)

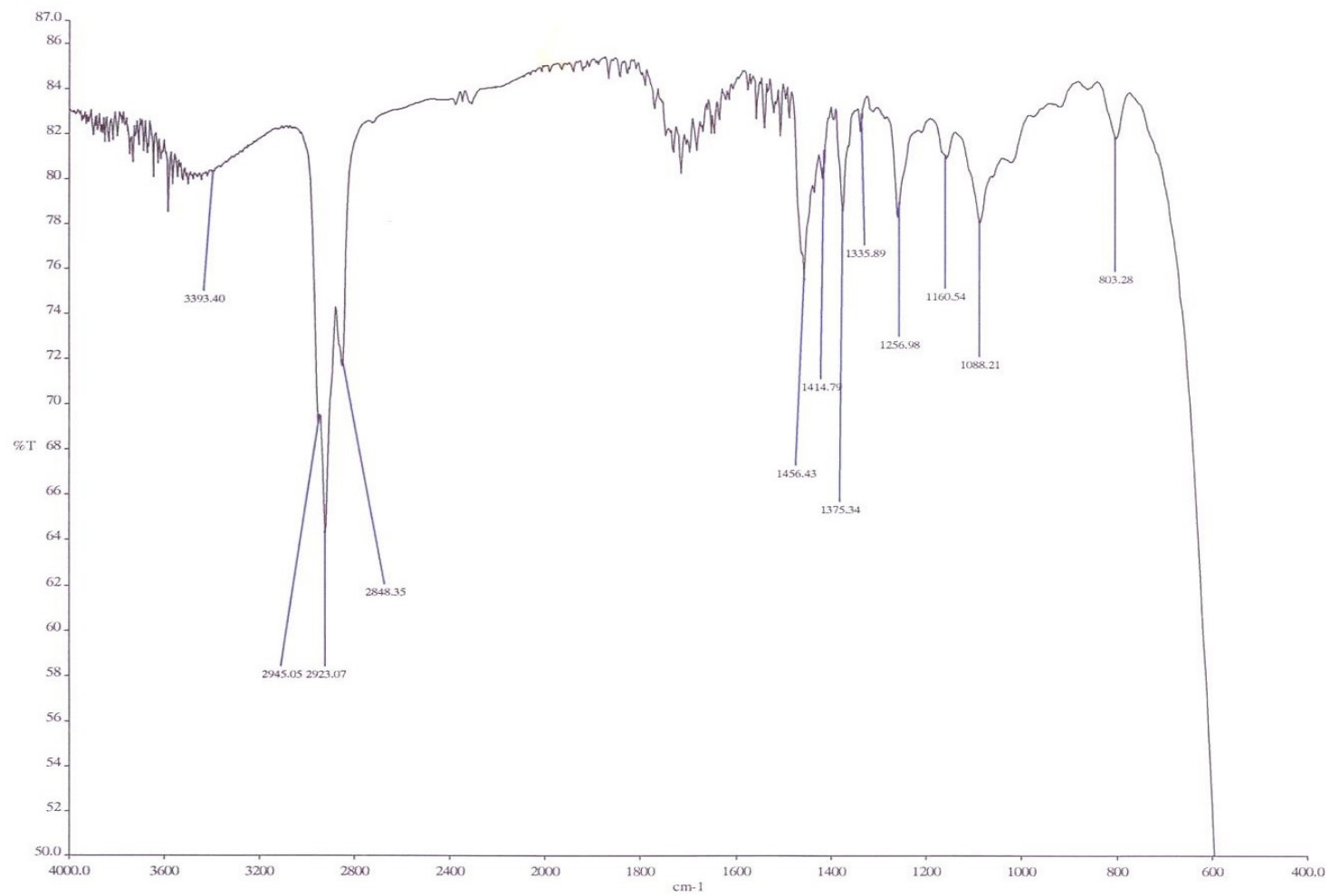


Fig. 4.1: IR spectrum of CMD-A in CDCl₃

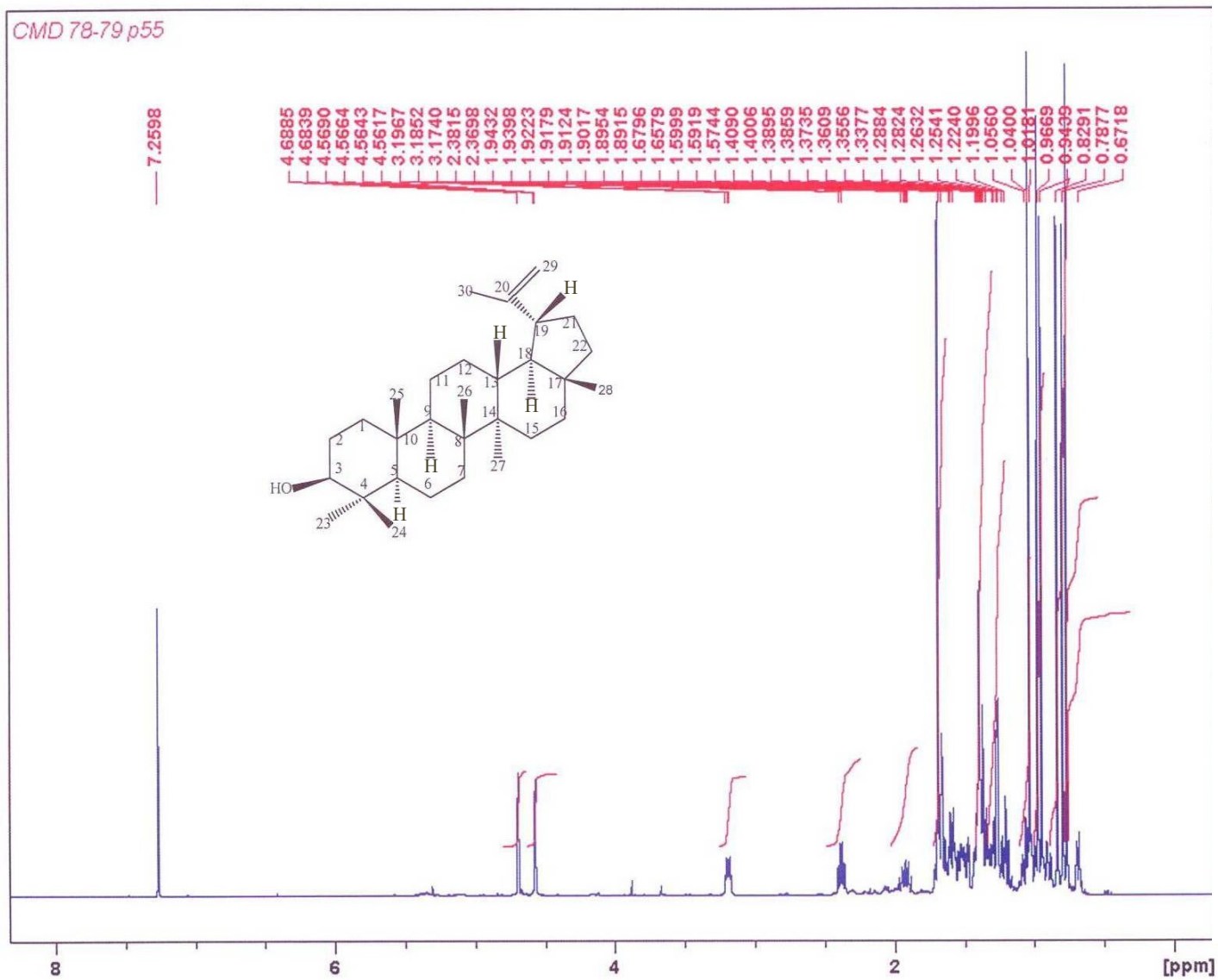


Fig. 4.2: $^1\text{H-NMR}$ (500MHz) spectrum of CMD-A in CDCl_3

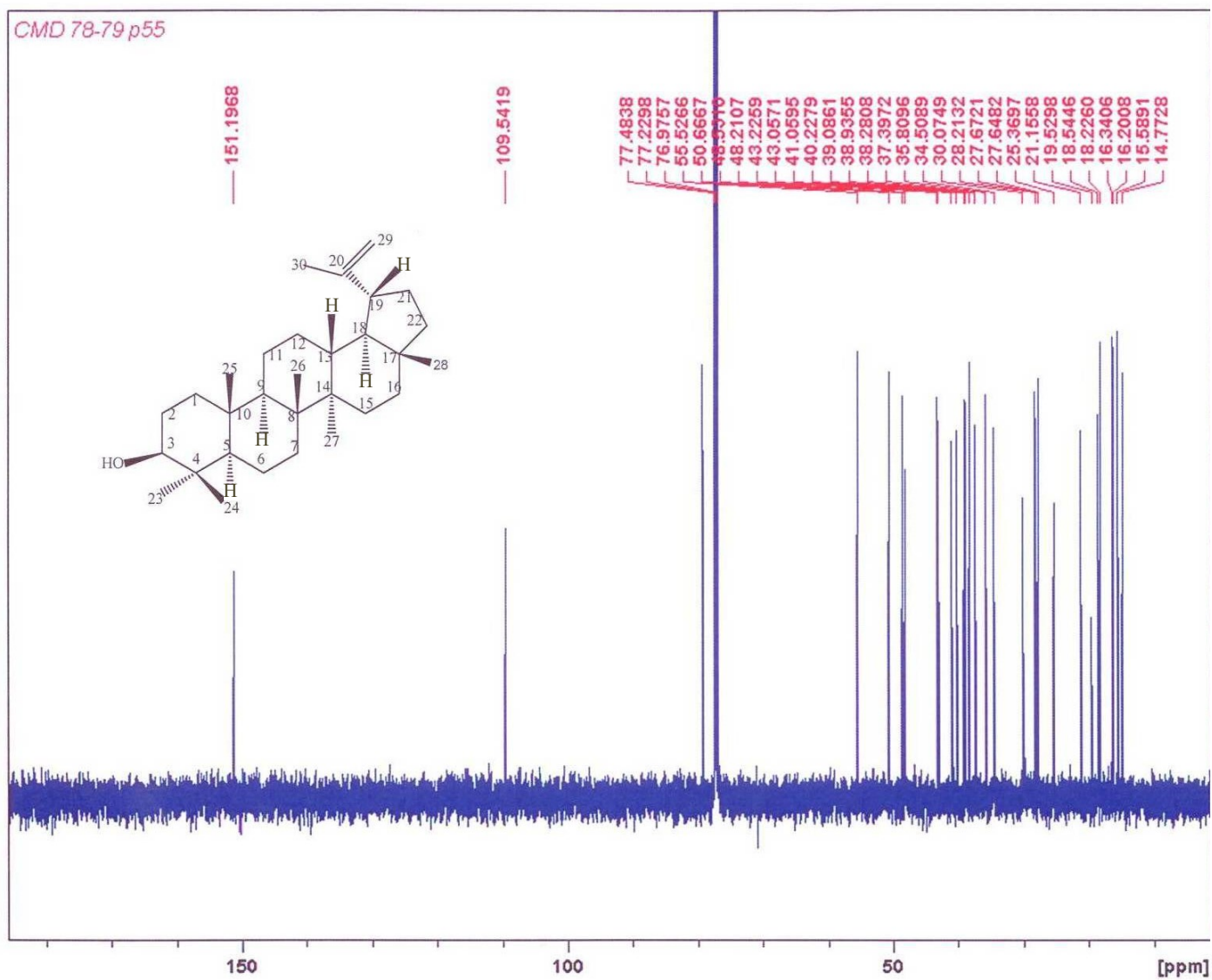


Fig. 4.3: ^{13}C -NMR (125 MHz) spectrum of CMD-A in CDCl_3

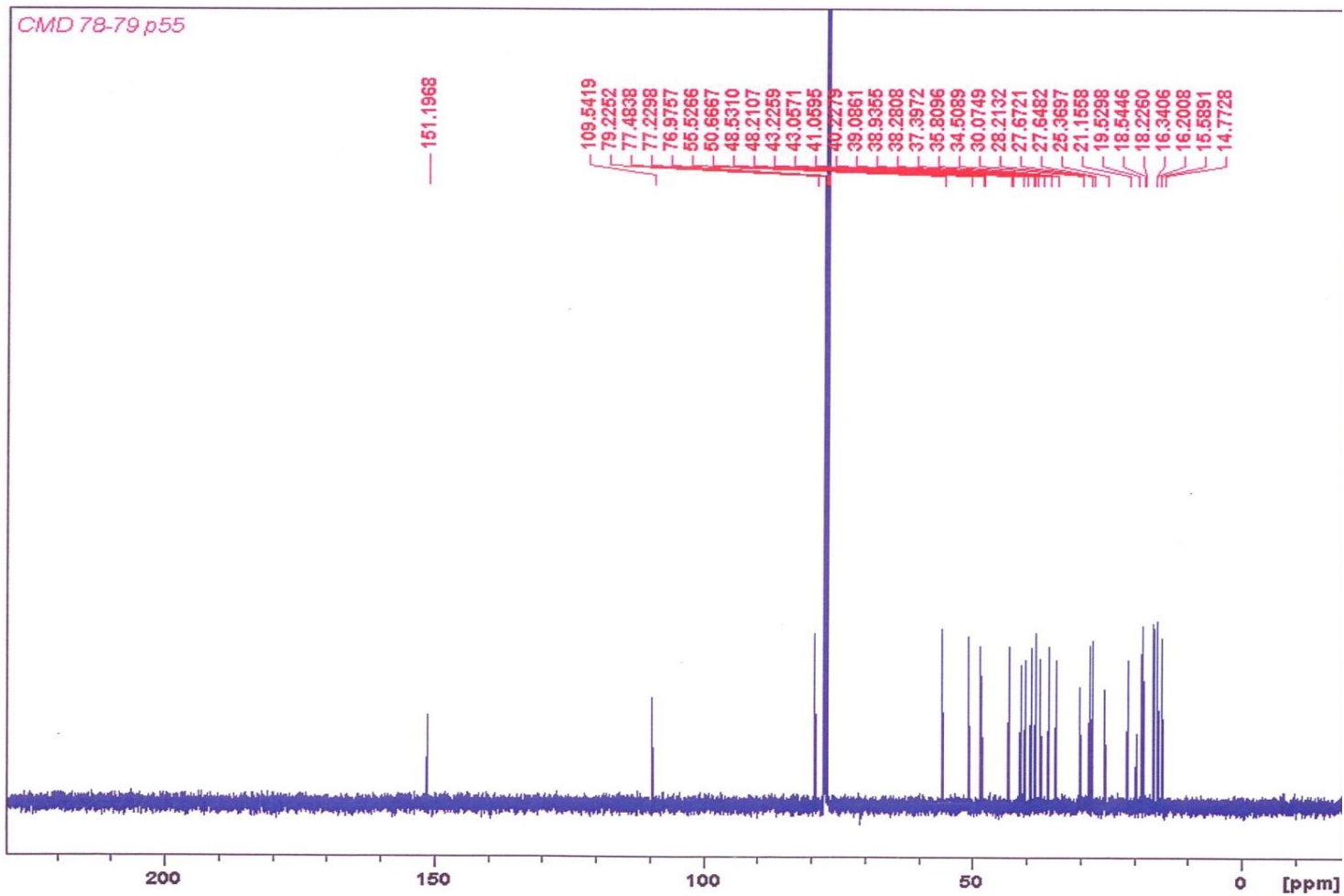


Fig. 4.4 : ^{13}C -NMR (125 MHz) spectrum of CMD-A in CDCl_3

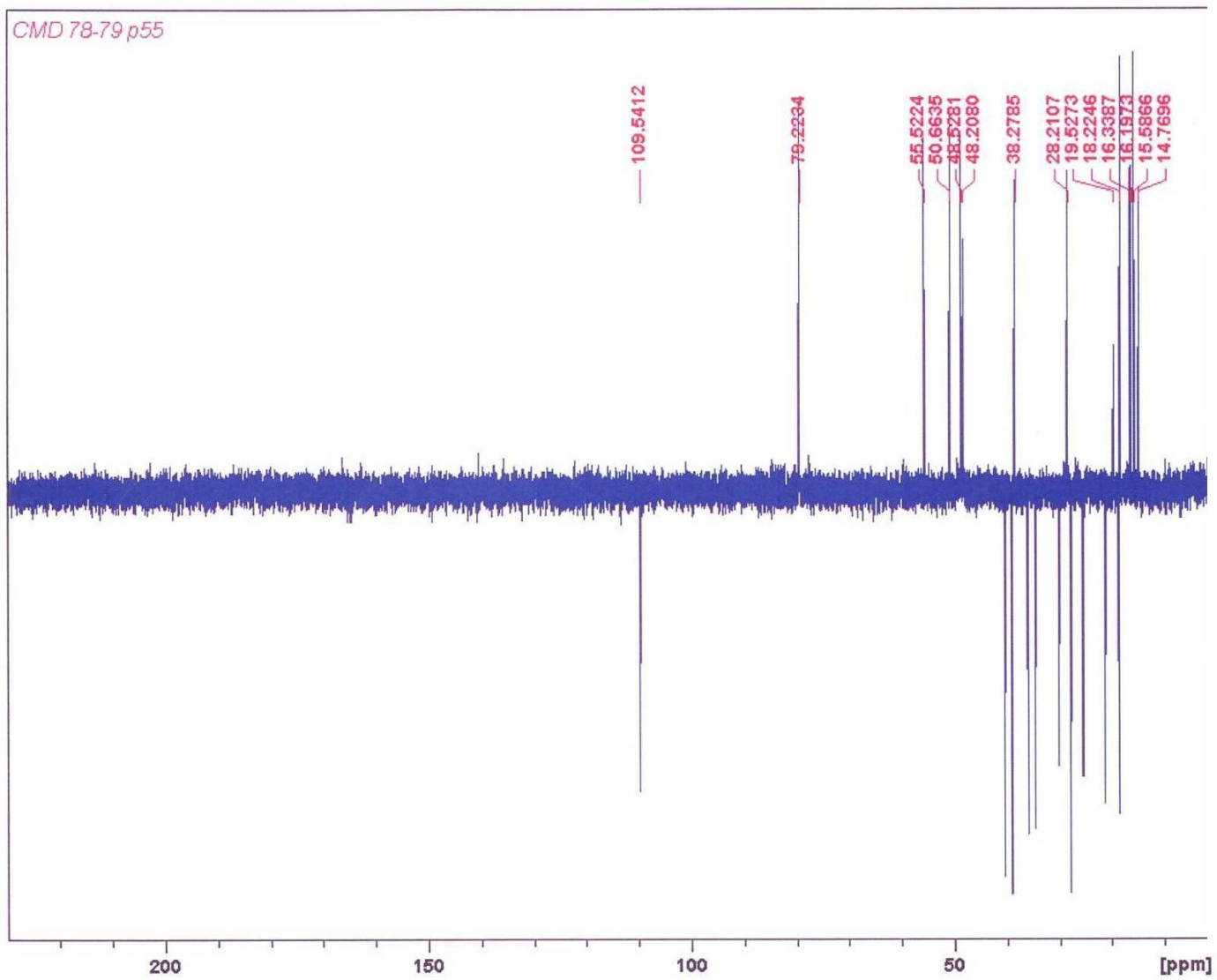


Fig. 4.5 : DEPT spectrum of CMD-A in CDCl_3

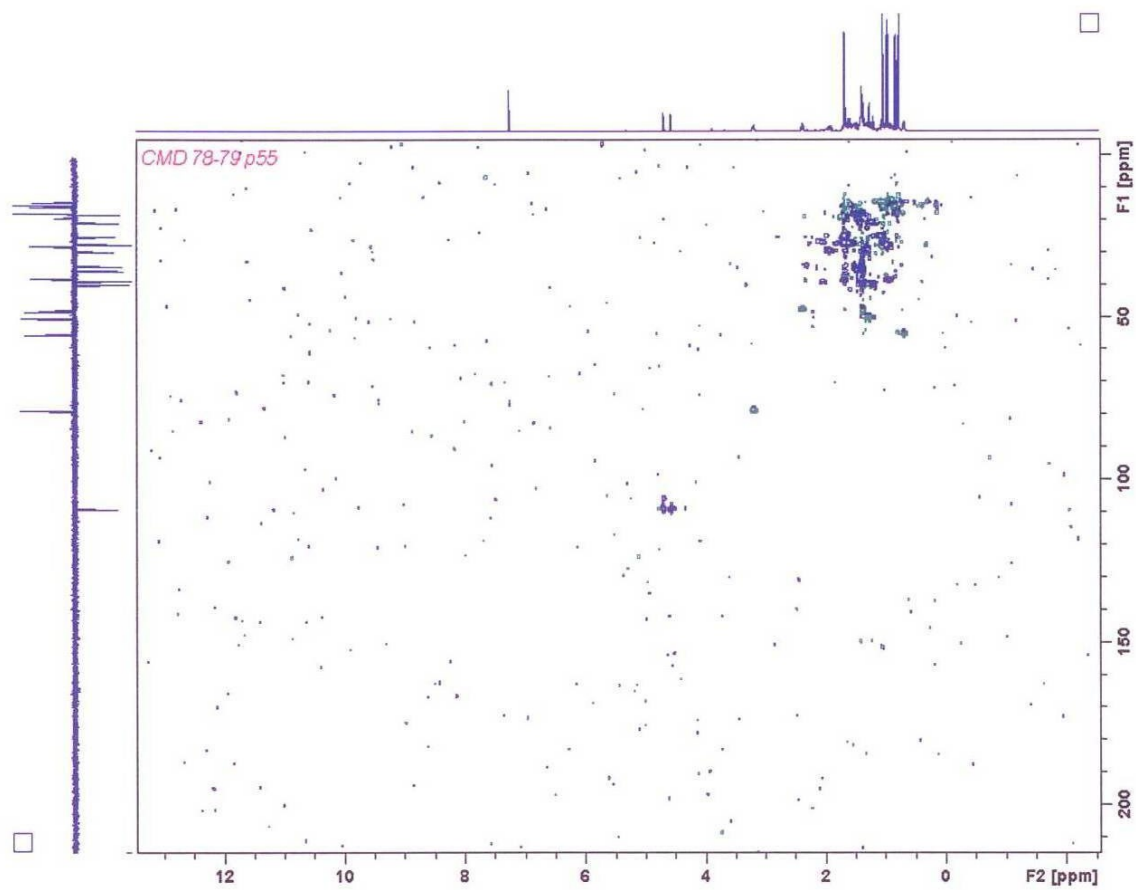


Fig. 4.6: HSQC DEPT spectrum of CMD-A in CDCl_3

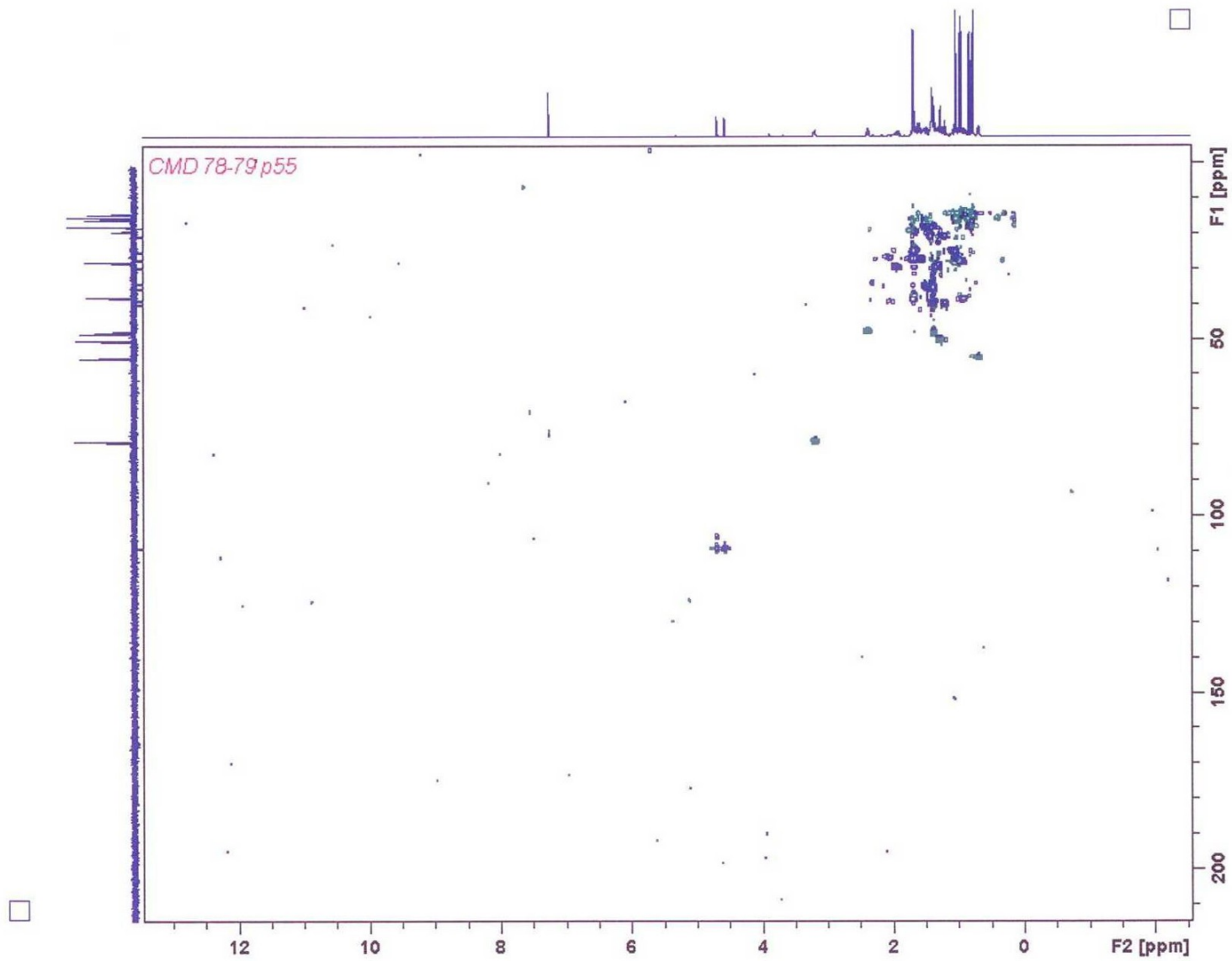


Fig. 4.7: HSQC DEPT spectrum of CMD-A in CDCl_3 (expanded)

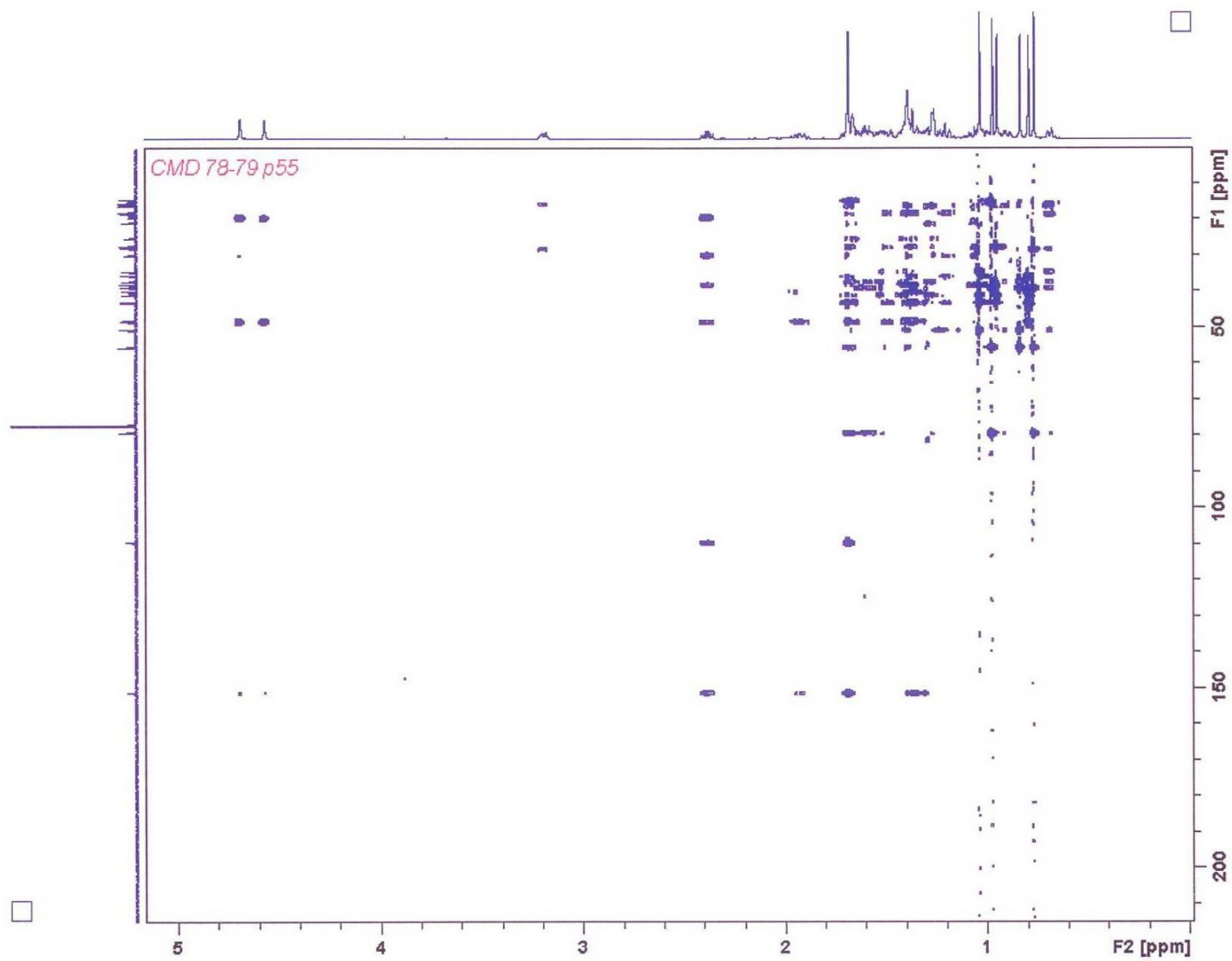


Fig. 4.8 : HMBC spectrum of CMD-A in CDCl₃

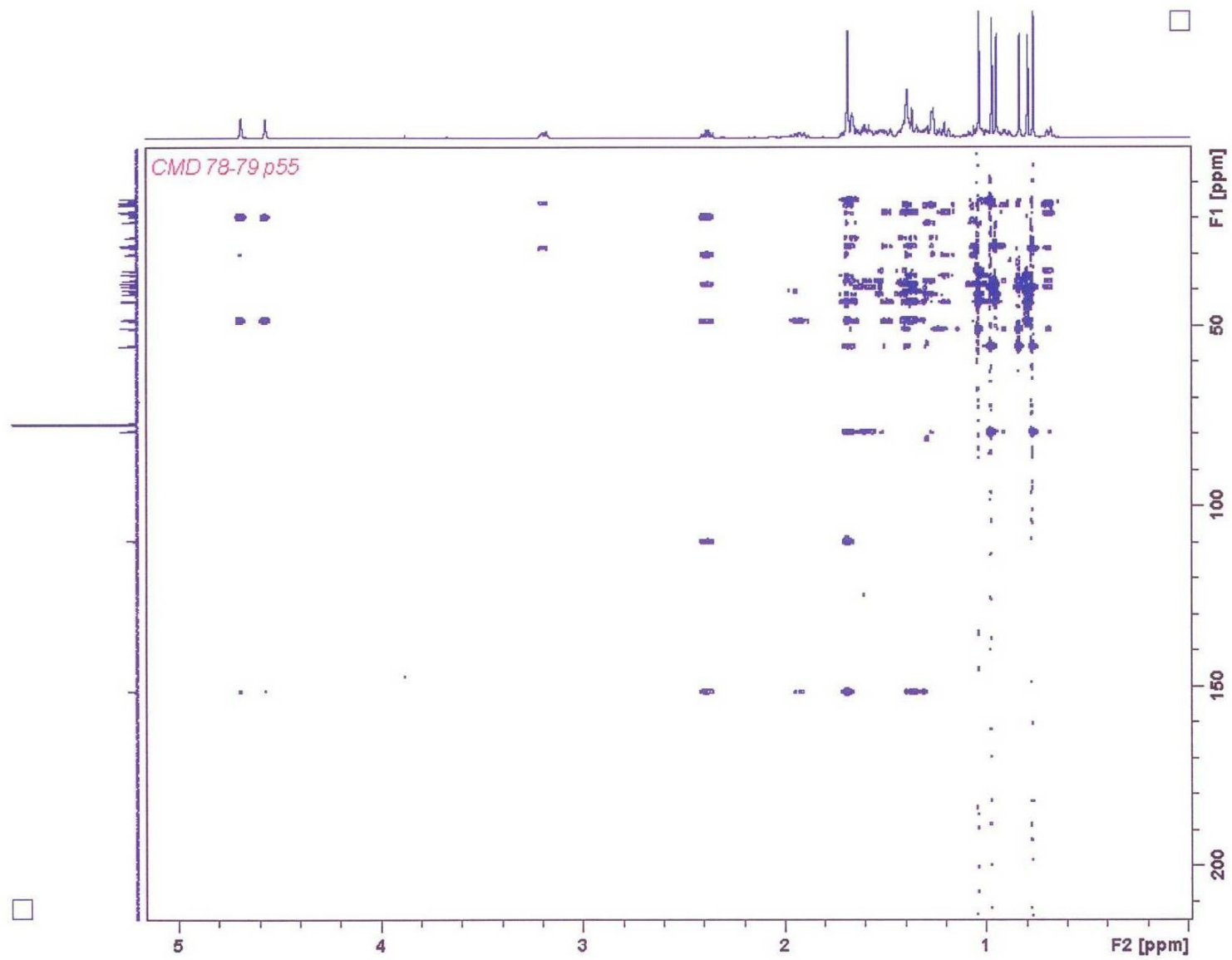


Fig. 4.9: HMBC spectrum of CMD-A in CDCl_3

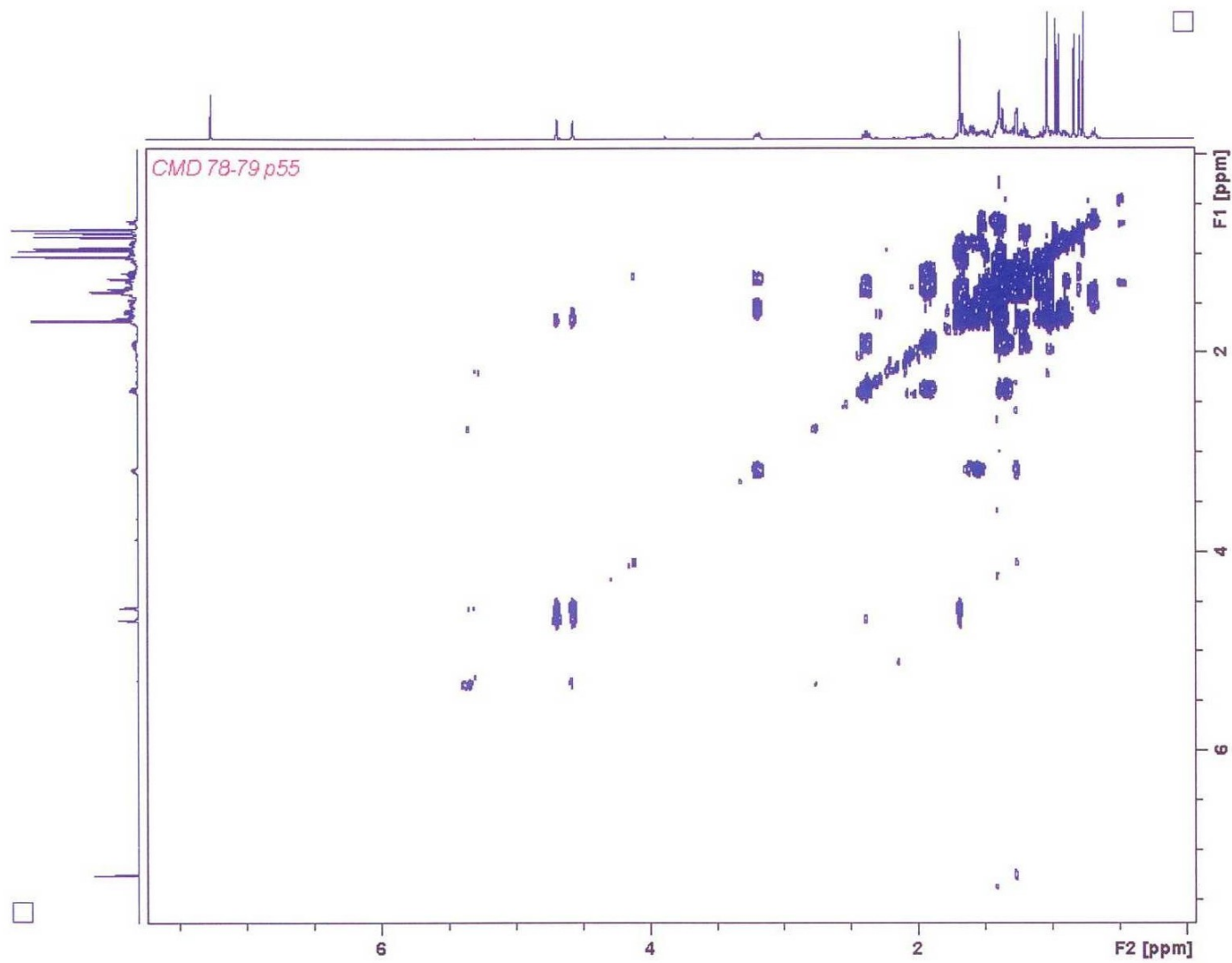


Fig. 4.10: NOESY spectrum of CMD-A in CDCl₃

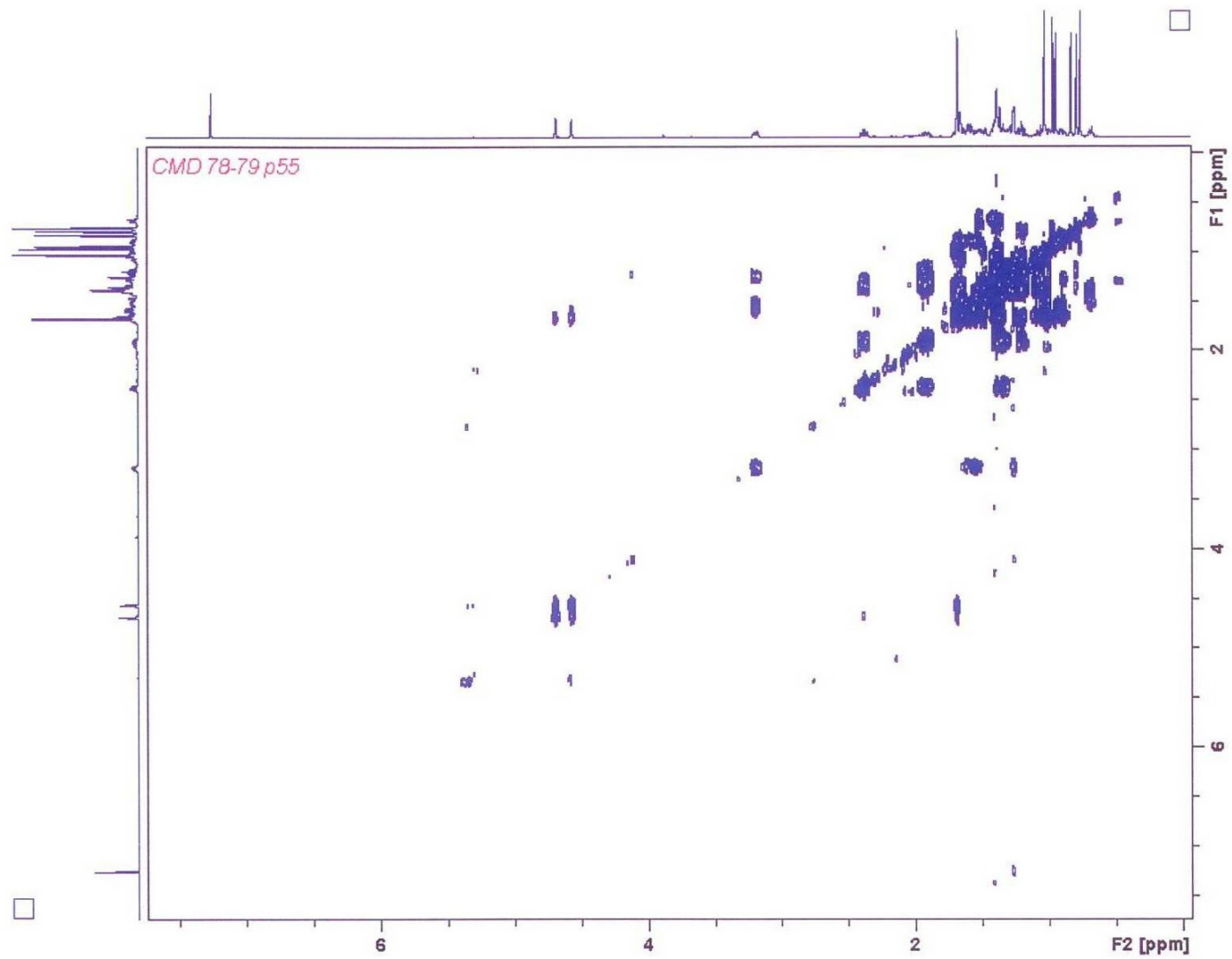


Fig. 4.11: NOESY spectrum of CMD-A in CDCl₃(expanded)

4.2.2 Structural elucidation of compound CMD-B

Compound **CMD-B** was isolated as a white solid. Four olefinic proton resonances were observed in the ^1H NMR spectrum (Fig 4.12), three of them characteristic of a β -substituted furanyl ring at δ_{H} 6.37 *s*, 7.43 *d* and 7.44 *s* (Tchissambou *et al.*, 1990). The fourth olefinic proton at δ_{H} 6.79 *s* was taken to be of a tri-substituted carbon-carbon double bond. A doublet at δ_{H} 1.01 indicated the presence of a secondary methyl group. Resonances of three-proton singlets were observed at δ_{H} 3.70 *s* and 3.75 *s* and were taken to be of two ester methyl groups. An oxymethine proton resonance was also observed at δ_{H} 5.39. The ^{13}C NMR spectrum (Fig 4.13) showed resonances of 22 carbons associated with a diterpenoid. Included were resonances of four sp^2 carbons of a β -substituted furanyl ring, three of them methine carbons at δ_{C} 108.1, 144.0, 139.4 and a fully substituted carbon at δ_{C} 125.5. Resonances of two sp^2 carbons associated with a tri-substituted double bond were observed (one fully substituted at δ_{C} 137.0 and a methine one at δ_{C} 139.8). In addition, three carbonyl carbons resonances at δ_{C} 166.7, 172.8 and 176.0; an oxymethine carbon at δ_{C} 71.8; five methylene carbons (δ_{C} 19.1, 42.3, 32.2, 27.9, 26.3), two methine carbons (δ_{C} 51.5, 40.0) and one methyl carbon (δ_{C} 17.0) carbons were also observed.

Correlations between $\delta_{\text{H-8}}$ 1.56 with $\delta_{\text{C-20}}$ 176.0 and an oxymethine proton resonance at $\delta_{\text{H-12}}$ 5.39 with $\delta_{\text{C-13}}$ 125.5 were observed in the HMBC spectrum (Fig 4.18). The relative configuration for the compound and correlations between $\delta_{\text{H-1a}}$ 1.89 *m* with $\delta_{\text{H-12}}$ 5.39 *t*, $\delta_{\text{H-10}}$ 1.76 *dd* with $\delta_{\text{H-11b}}$ 2.30 *m*; $\delta_{\text{H-10}}$ 1.76 *dd* with $\delta_{\text{H-8}}$ 1.56 *m*; $\delta_{\text{H-14}}$ 6.37 *s* with $\delta_{\text{H-17}}$ 1.01 *d* and $\delta_{\text{H-16}}$ 7.44 *s* with $\delta_{\text{H-17}}$ 1.01 *d*, confirmed that H-12 was α -configured based on observation from the NOESY spectrum (Fig 4.16). The ^1H NMR and ^{13}C NMR of **CMD-B** were compared with reported literature (Beth *et al.*, 2016) and was found to be similar to the known *Crotocorylifuran* (15, 16-epoxy-3, 13(16), 14-clerodatriene-20, 12-olide-18, 19-dioic acid dimethylester) [**30**] isolated previously from *C. zambesicus* (Ngadjui *et al.*, 2002), *C.*

hammanianus (Tchissambou *et al.*, 1990) and the roots of *Croton megalocarpoides* (Beth *et al.*, 2016).

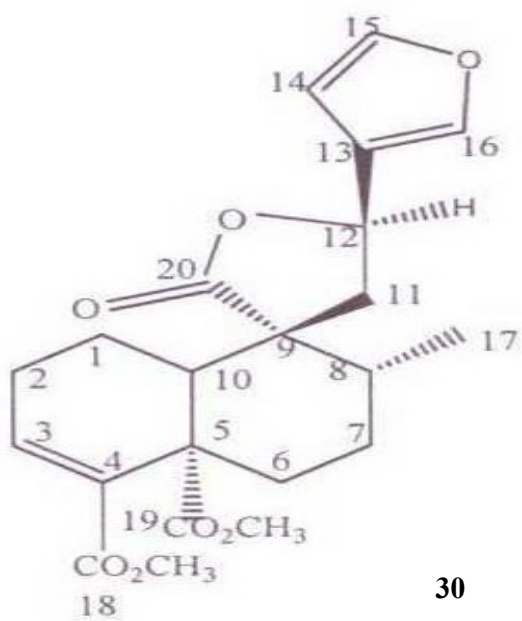


Table 2: Correlation Table of ^1H (500 MHz) and ^{13}C (125 MHz) NMR Data^a for compound CMD-B: Crotoerylifuran (15, 16-epoxy-3,13(16),14-clerodatriene-20,12-olide-18,19-dioic acid dimethylester) in CDCl_3

No	^{13}C NMR ^a (125 MHz) CDCl_3	^{13}C NMR ^b (125 MHz) CDCl_3	^1H NMR ^a (500 MHz) CDCl_3	^1H NMR ^b (500MHz) CDCl_3
1	19.1	19.2	1.89-1.93 <i>m</i> 2.50-2.60 <i>m</i>	1.89-1.93 <i>m</i> 2.50-2.60 <i>m</i>
2	42.3	42.6	2.50-2.60 <i>m</i> 2.30-2.45 <i>m</i>	2.50-2.60 <i>m</i> 2.30-2.45 <i>m</i>
3	139.8	140.6	6.79 <i>t</i>	6.80 <i>t</i>
4	137.0	136.5		
5	51.7	51.7		
6	32.2	32.3	1.08 <i>m</i> 2.94 <i>dt</i> ,	1.08 <i>m</i> 2.94 <i>d</i>
7	27.9	28.0	2.30-2.45 <i>m</i> 1.56-1.60 <i>m</i>	2.30-2.45 <i>m</i> 1.56-1.60 <i>m</i>
8	40.0	40.2	1.56-1.60 <i>m</i>	1.56-1.60 <i>m</i>
9	46.3	46.4		
10	51.5	52.1	1.76 <i>dd</i> ,	1.76 <i>dd</i> ,
11	26.3	26.9	2.30-2.45 <i>m</i>	2.30-2.45 <i>m</i>
12	71.8	72.0	5.39 <i>t</i>	5.39 <i>t</i>
13	125.5	125.9		
14	108.1	108.2	6.37 <i>s</i>	6.37 <i>s</i>
15	144.0	144.3	7.43 <i>d</i>	7.43 <i>d</i>
16	139.4	139.3	7.44 <i>s</i>	7.45 <i>s</i>
17	17.0	17.5	1.01 <i>d</i>	1.01 <i>d</i>
18	166.7	167.0		
19	172.8	173.3		
20	176.0	176.4		
18- acetoxy	51.3	51.7	3.70 <i>s</i>	3.70 <i>s</i>
19- acetoxy	51.4	51.8	3.75 <i>s</i>	3.75 <i>s</i>

^a Assignment aided by HMQC and HMBC experiments

^b Literature data of Crotoerylifuran (Beth *et al.*,2016)

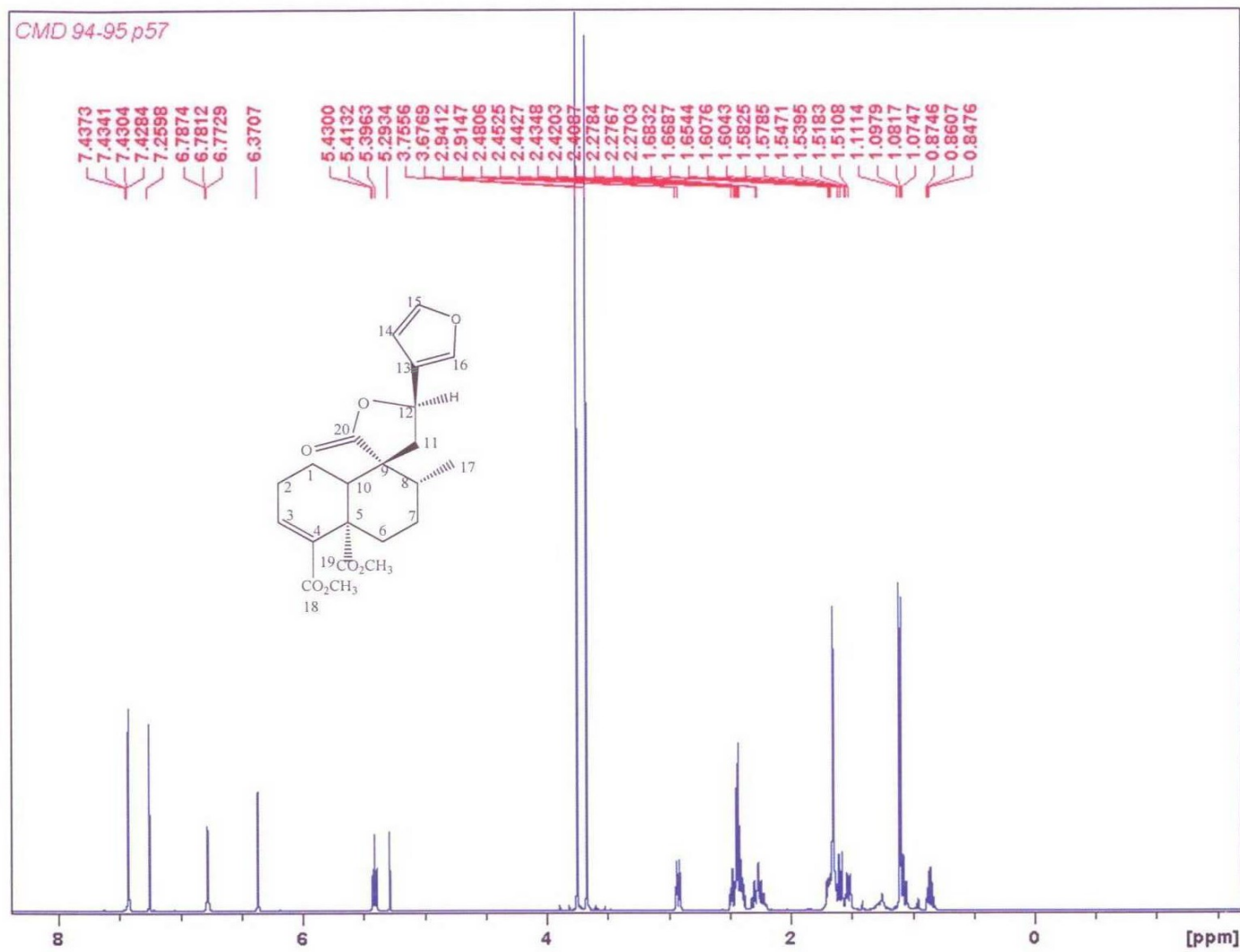


Fig. 4.12: ^1H NMR (500MHz) spectrum of CMD-B in CDCl_3

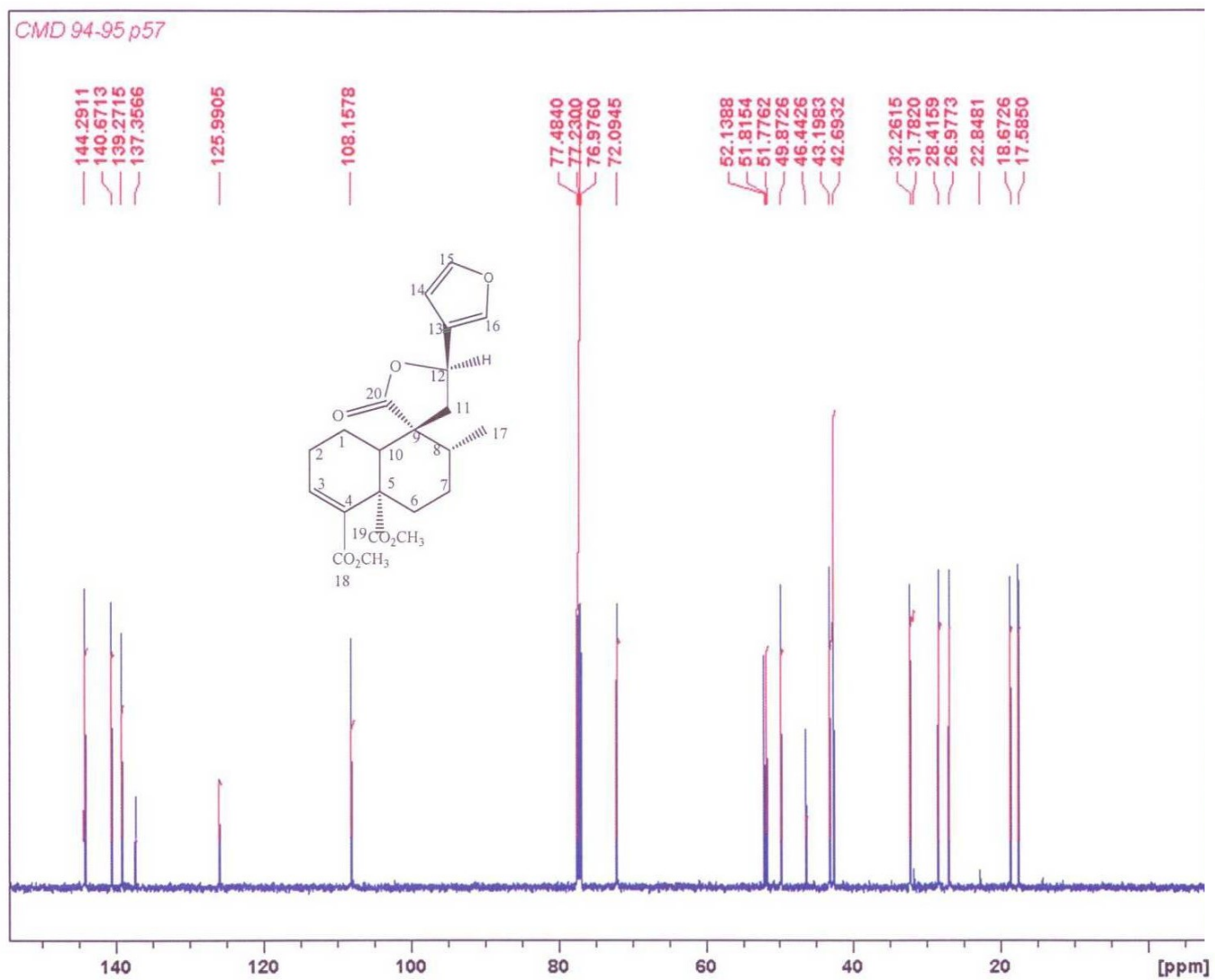


Fig. 4.13a: ^{13}C -NMR (125 MHz) spectrum of CMD-B in CDCl_3 (expanded)

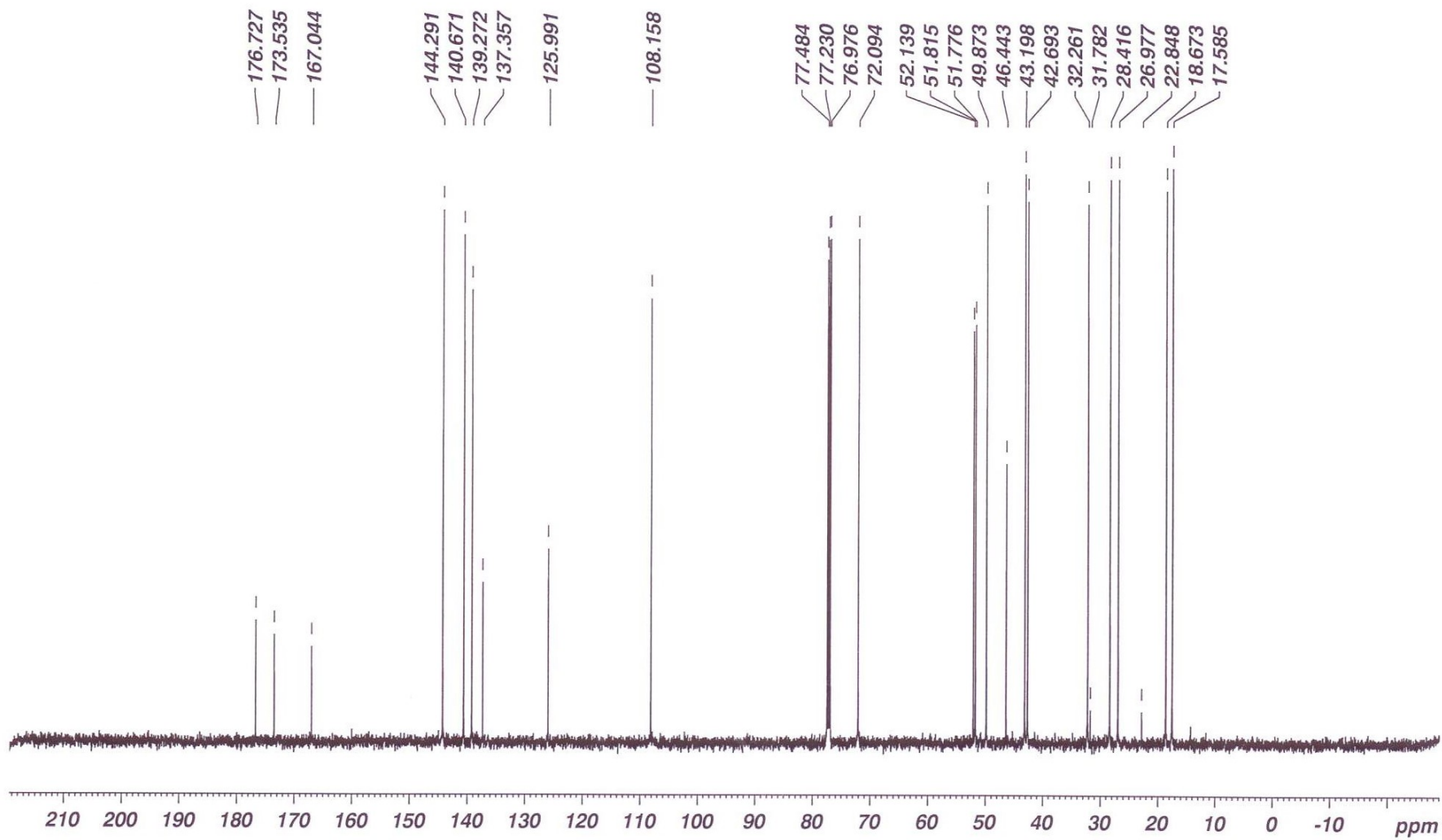


Fig. 4.13b: ^{13}C -NMR (125 MHz) spectrum of CMD-B in CDCl_3

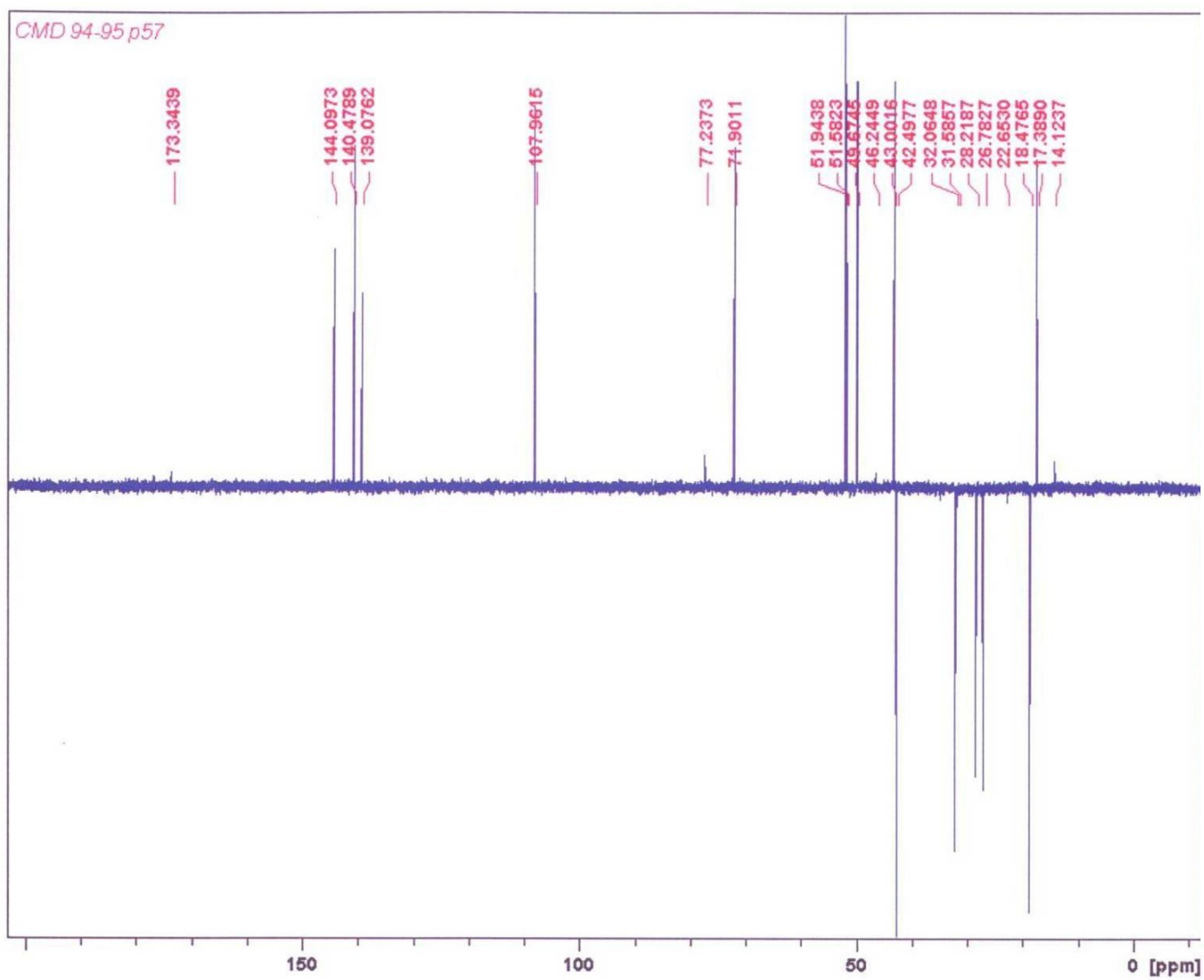


Fig. 4.14: DEPT spectrum of CMD-B in CDCl_3

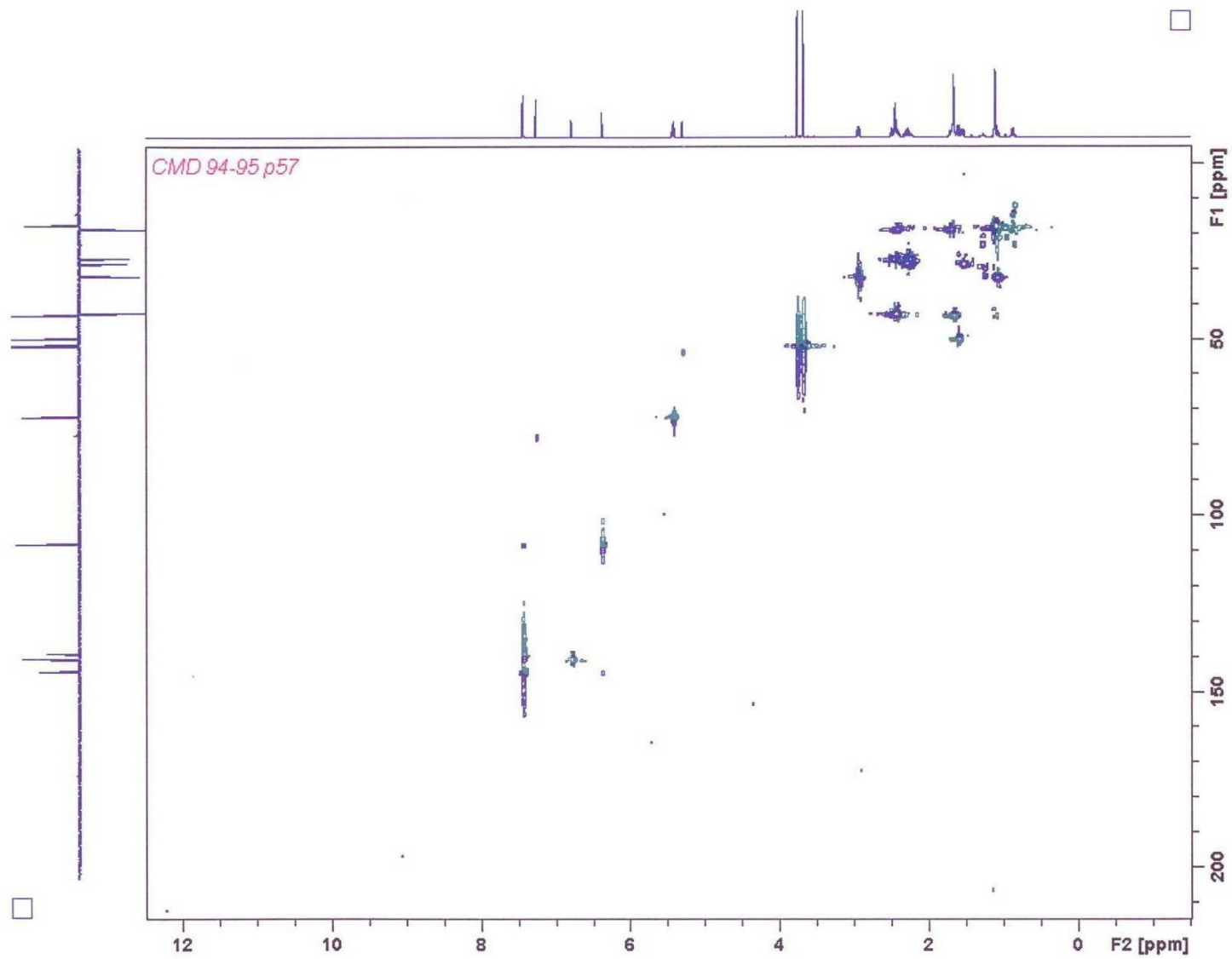


Fig. 4.15: HSQC DEPT spectrum of CMD-B in CDCl_3

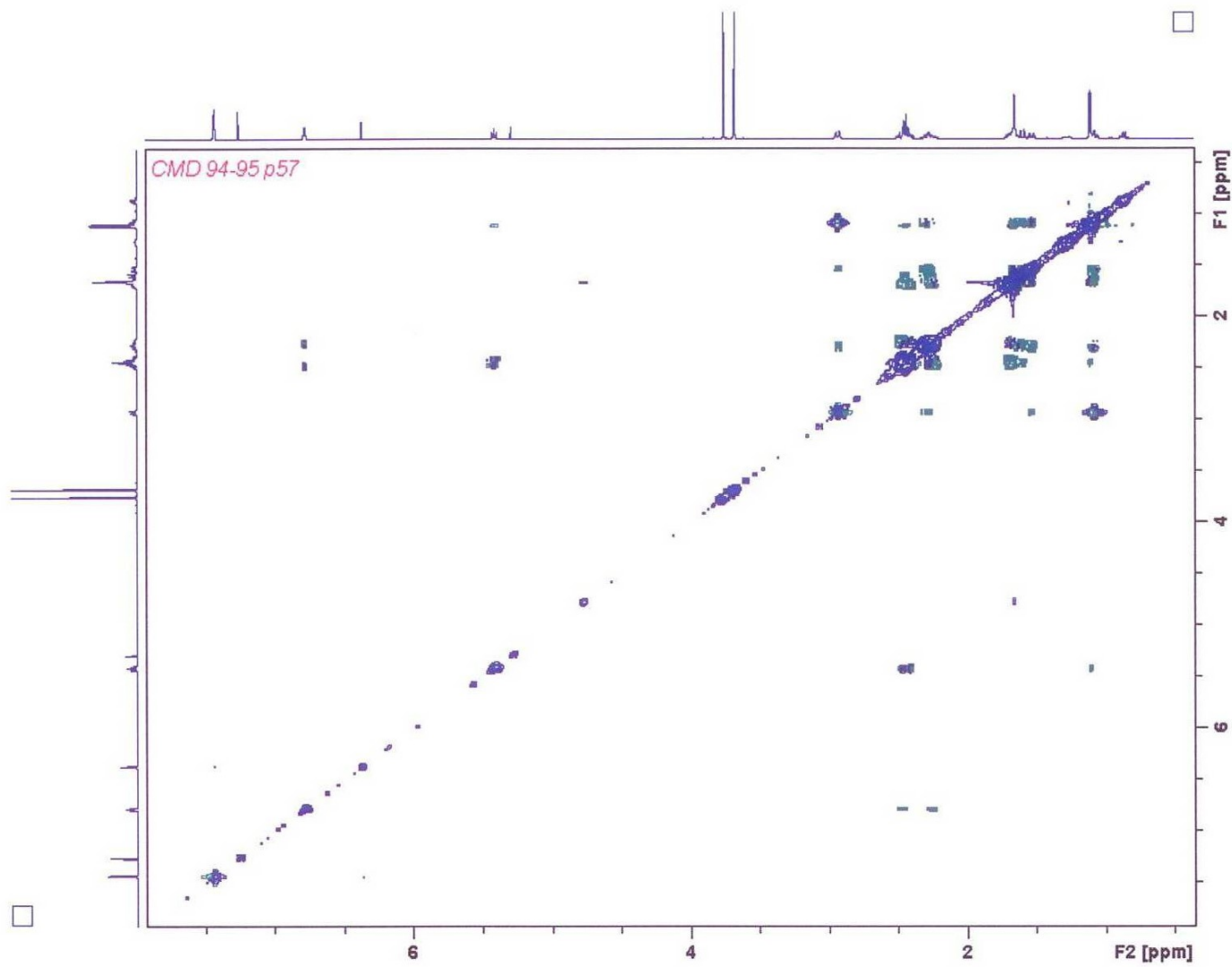


Fig. 4.16: NOESY spectrum of CMD-B in CDCl₃

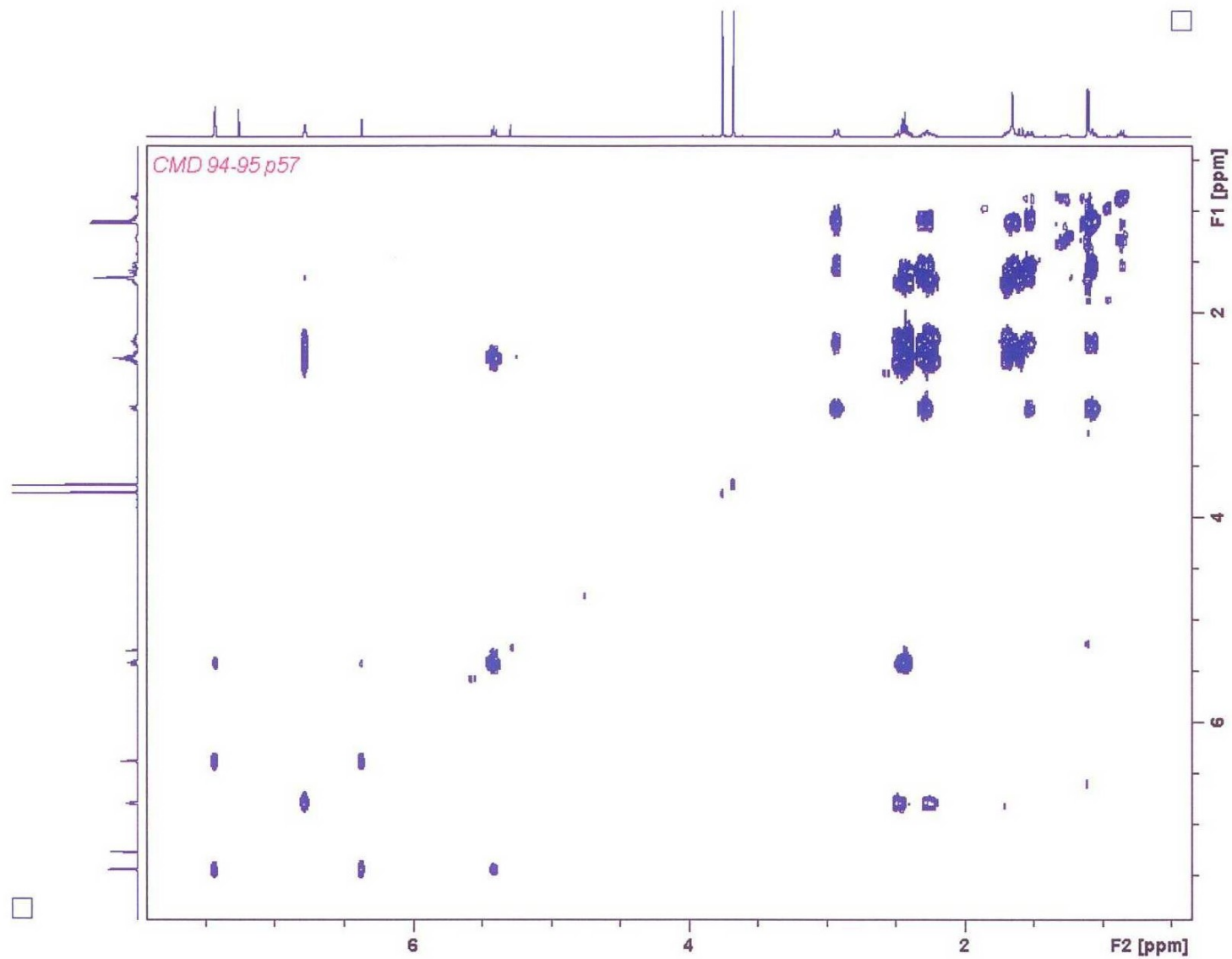


Fig. 4.17: COSY spectrum of CMD-B in CDCl₃

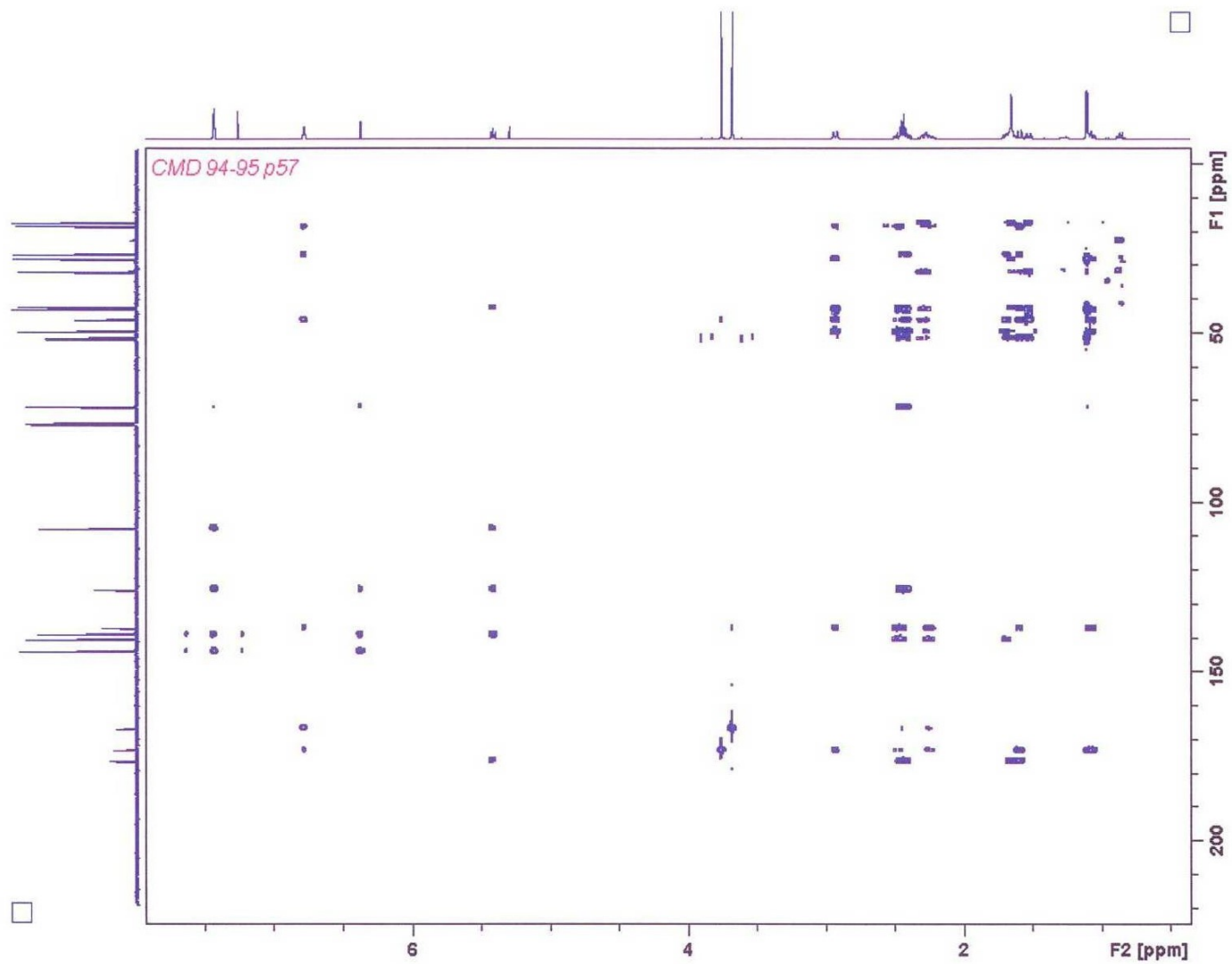
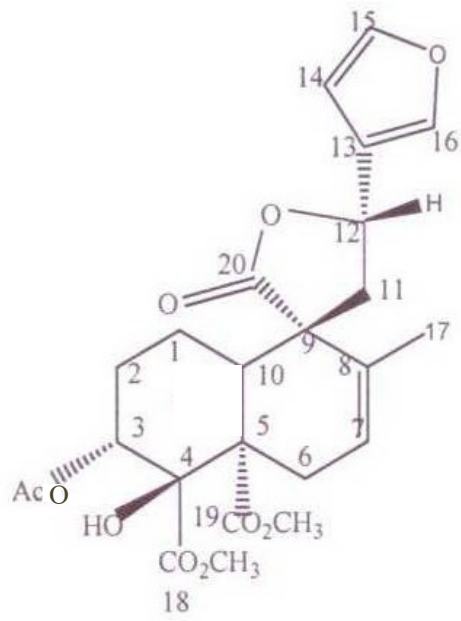


Fig. 4.18: HMBC spectrum of CMD-B in CDCl_3

4.2.3 Structural elucidation of compound CMD-C

Compound **CMD-C** was isolated as a white solid. In the ^1H NMR spectrum (Fig 4.19), four olefinic protons resonances were observed, three of them characteristic of a β -substituted furanyl ring at δ_{H} 6.40 s , 7.42 s and 7.46 s (Tchissambou *et al.*, 1990) and a doublet of an olefinic proton at δ_{H} 5.67 was assigned to H-7. Resonances of three-proton singlets at δ_{H} 3.73 s and 3.74 s taken to be of two ester methyl groups were observed. An oxymethine proton resonance was observed at δ_{H} 5.45. The ^{13}C NMR spectrum (Fig 4.20) showed resonances of four sp^2 carbons of a β -substituted furanyl ring, three of them methine carbons at δ_{C} 108.1, 144.2, 139.7 and a fully substituted carbon at δ_{C} 125.2. Three carbonyl carbons resonances at δ_{C} 173.0, 170.1 and 175.6 were also observed. Carbon resonances at δ_{C} 125.2 and 132.2 were observed in the ^{13}C NMR spectrum (Fig 4.20) and were assigned to C-7 and C-8 respectively. Resonances of an oxymethine at C-3 (δ_{H} 5.10 *br s*; δ_{C} 70.3) was also observed. An oxygenated quaternary sp^3 carbon was observed at δ_{C} 76.0 and was placed at position 4. In addition, resonances ascribed to an acetate methyl group substituent ($-\text{OOCCH}_3$; δ_{H} 2.01 s; δ_{C} 171.0 and 21.2) were observed and placed at position 3.

Correlations were observed at $\delta_{\text{H}-3}$ 5.10 with $\delta_{\text{C}-4,5,18}$, 76.0, 52.6, 173.0; $\delta_{\text{H}-7}$ with $\delta_{\text{C}-5, 9}$, 52.6, 53.2; the three proton singlets at δ_{H} 3.73 with the carbonyl at $\delta_{\text{C}-19}$ 170.1 and δ_{H} 3.73 with the carbonyl $\delta_{\text{C}-18}$ at 173.0; methylene protons at $\delta_{\text{H}-2\alpha,\beta}$ 2.60, 2.01 with $\delta_{\text{C}-4}$, 76.0 and the hydroxyl proton at $\delta_{\text{H}4-\text{OH}}$ 5.00 with $\delta_{\text{C}-4}$ 76.0 in the HMBC spectrum (Fig 4.23) which helped to confirm the proposed structure. The ^1H NMR and ^{13}C NMR of this compound were compared with reported literature (Beth *et al.*, 2016) and was found to be similar to megalocarpodolide H (18, 19, - dimethoxycarbonyl - 3 α acetoxy, 4 β - hydroxyl - 15, 16 - epoxy - clerodane-7, 13 (16), 14 - triene - 12, 20 - olide) [**31**]. It has been previously isolated from the roots of *Croton megalocarpoides* (Beth *et al.*, 2016).



31

Table 3: Correlation Table of ^1H (500 MHz) and ^{13}C (125 MHz) NMR Data^a for compound CMD-C:18,19,-dimethoxycarbonyl-3 α acetoxy,4 β -hydroxy-15,16-epoxy-clerodane-7,13(16),14-triene-12,20-olide in CDCl_3

No	^{13}C NMR ^a (125 MHz) CDCl_3	^{13}C NMR ^b (125 MHz) CDCl_3	^1H NMR ^a (500 MHz) CDCl_3	^1H NMR ^b (500MHz) CDCl_3
1	27.1	27.2	2.22 <i>m</i>	2.22 <i>m</i>
2	21.1	21.3	2.60 <i>m</i> 2.01 <i>br s</i>	2.60 <i>m</i> 2.01 <i>br s</i>
3	70.3	70.3	5.10 <i>br s</i>	5.10 <i>br</i>
4	76.0	76.0	5.00 <i>br s</i>	5.00 <i>br</i>
5	52.6	52.6		
6	29.8	29.8	2.35 <i>m</i> 1.26 <i>m</i>	2.35 <i>m</i> 1.26 <i>m</i>
7	125.2	125.3	5.67 <i>d</i>	5.67 <i>d</i>
8	132.2	132.1		
9	53.2	53.2		
10	46.1	46.2	2.68 <i>m</i>	2.68 <i>m</i>
11	45.0	45.1	2.50 <i>m</i> 2.52 <i>m</i>	2.50 <i>m</i> 2.52 <i>m</i>
12	71.7	71.9	5.45 <i>t</i>	5.45 <i>t</i>
13	125.2	125.4		
14	108.1	108.2	6.40 <i>s</i>	6.40 <i>s</i>
15	144.2	144.2	7.42 <i>d</i>	7.42 <i>d</i>
16	139.7	139.8	7.46 <i>s</i>	7.46 <i>s</i>
17	19.8	19.8	1.69 <i>s</i>	1.68 <i>s</i>
18	173.0	173.0		
19	170.1	170.2		
20	175.6	175.6		
18-acetoxy	53.2	53.2	3.73 <i>s</i>	3.73 <i>s</i>
19-acetoxy	53.6	53.6	3.74 <i>s</i>	3.74 <i>s</i>
3-OOCCH ₃	171.0	171.0		
3-OOCCH ₃	21.2	21.2	2.01 <i>s</i>	2.01 <i>s</i>

^a Assignment aided by HMQC and HMBC experiments

^b Literature on Megacarpodolide H (Beth *et al.*, 2016)

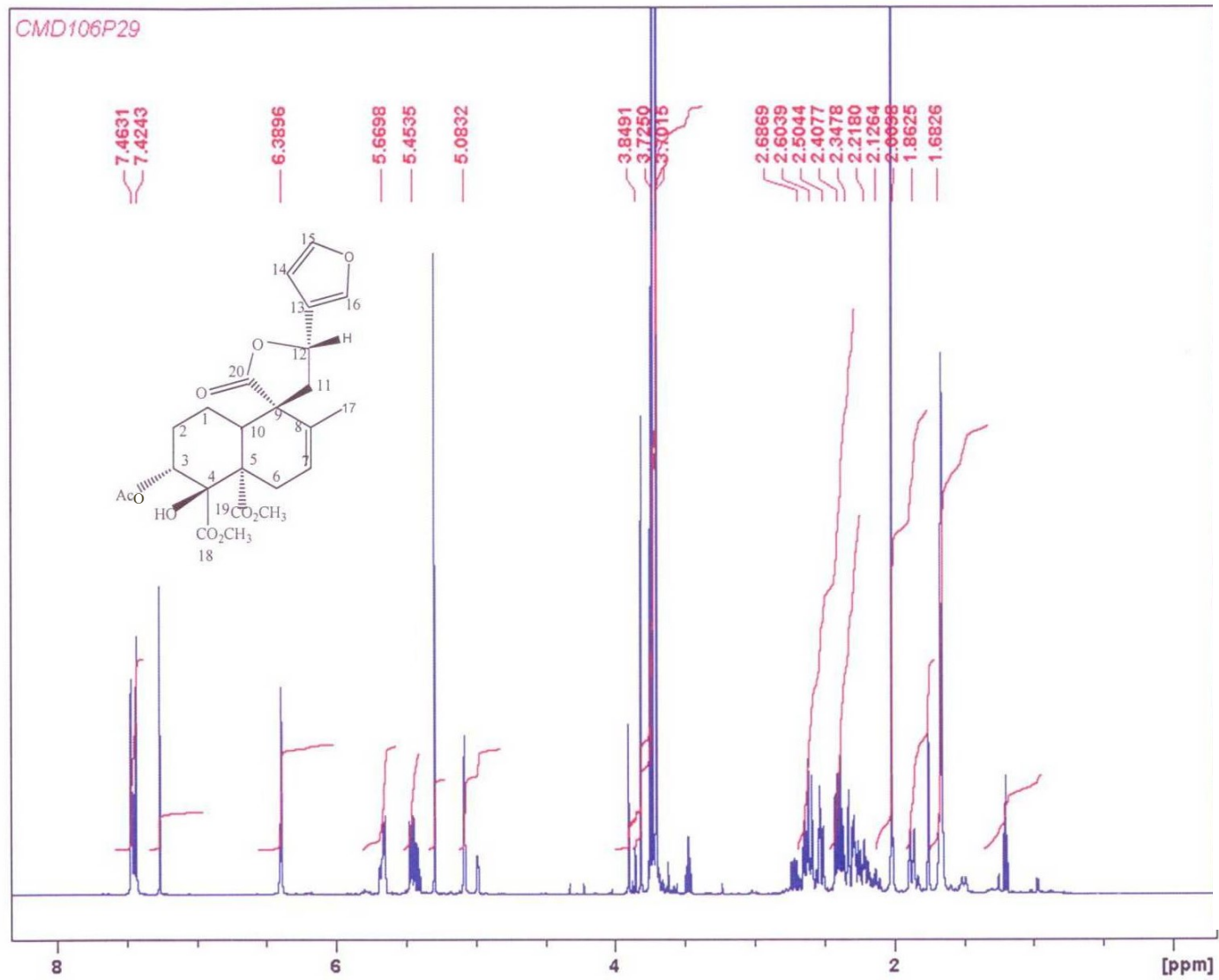


Fig. 4.19: ¹HNMR (500MHz) spectrum of CMD-C in CDCl₃

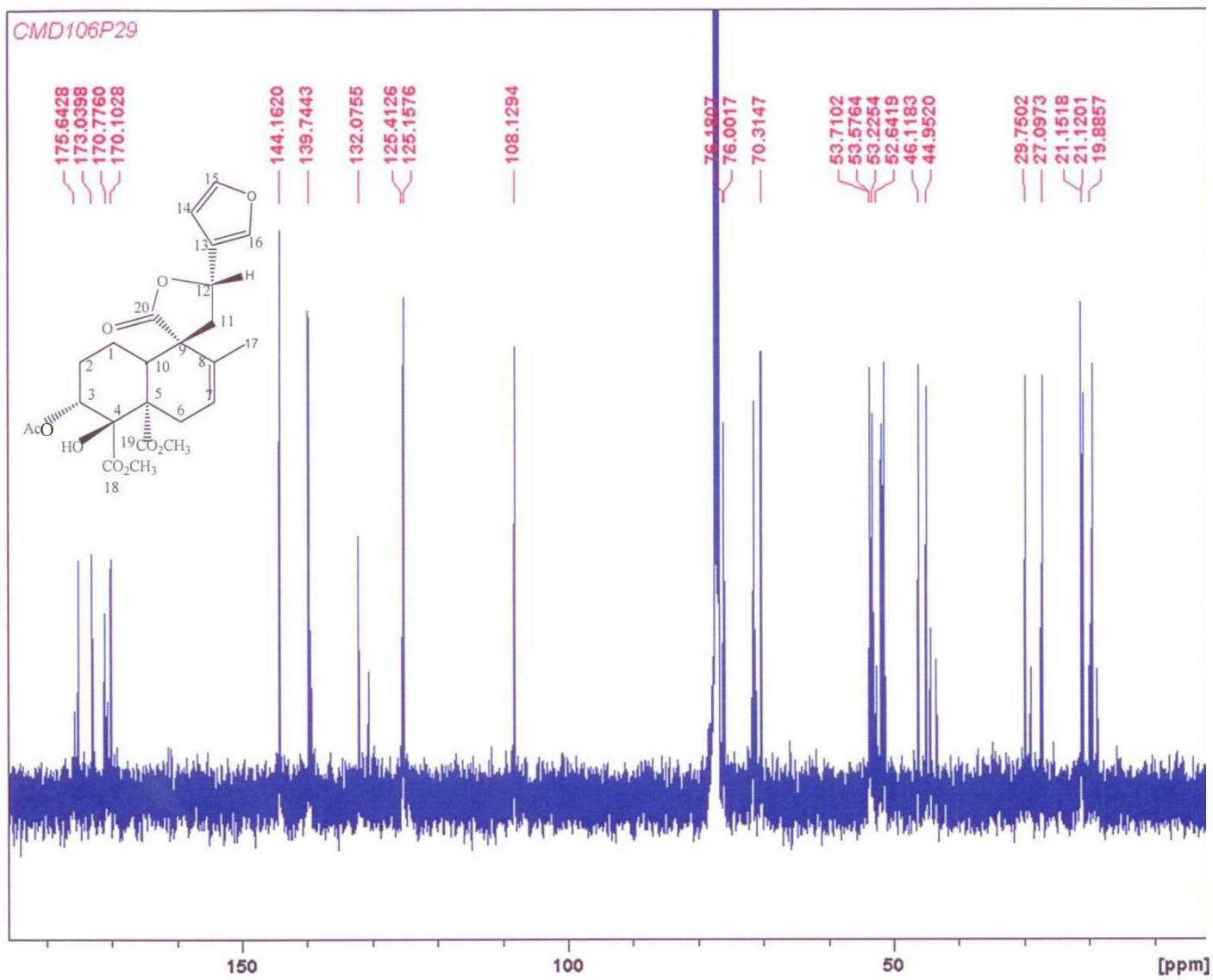


Fig. 4.20: ¹³CNMR (125 MHz) spectrum of CMD-C in CDCl₃

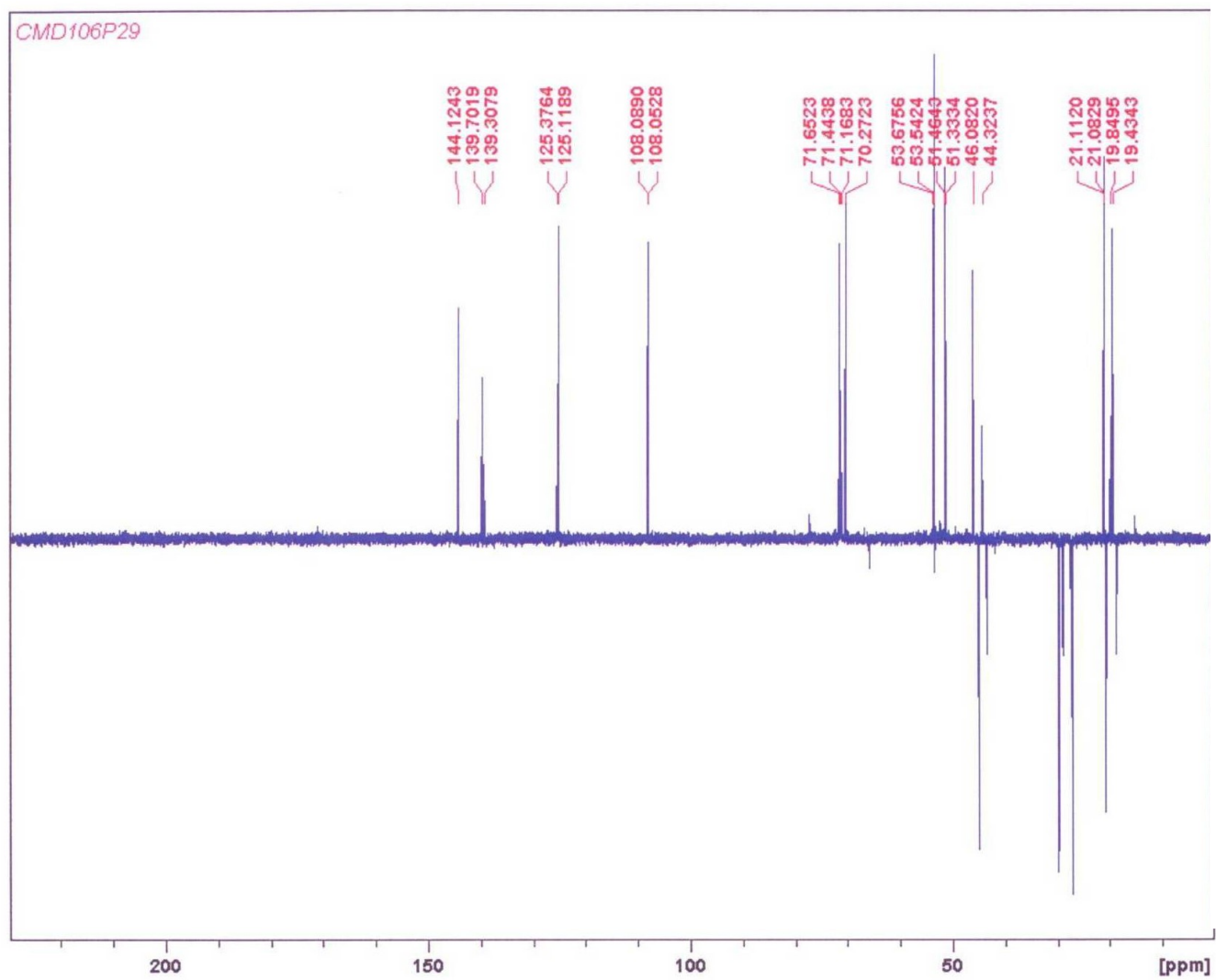


Fig. 4.21: DEPT spectrum of CMD-C in CDCl_3

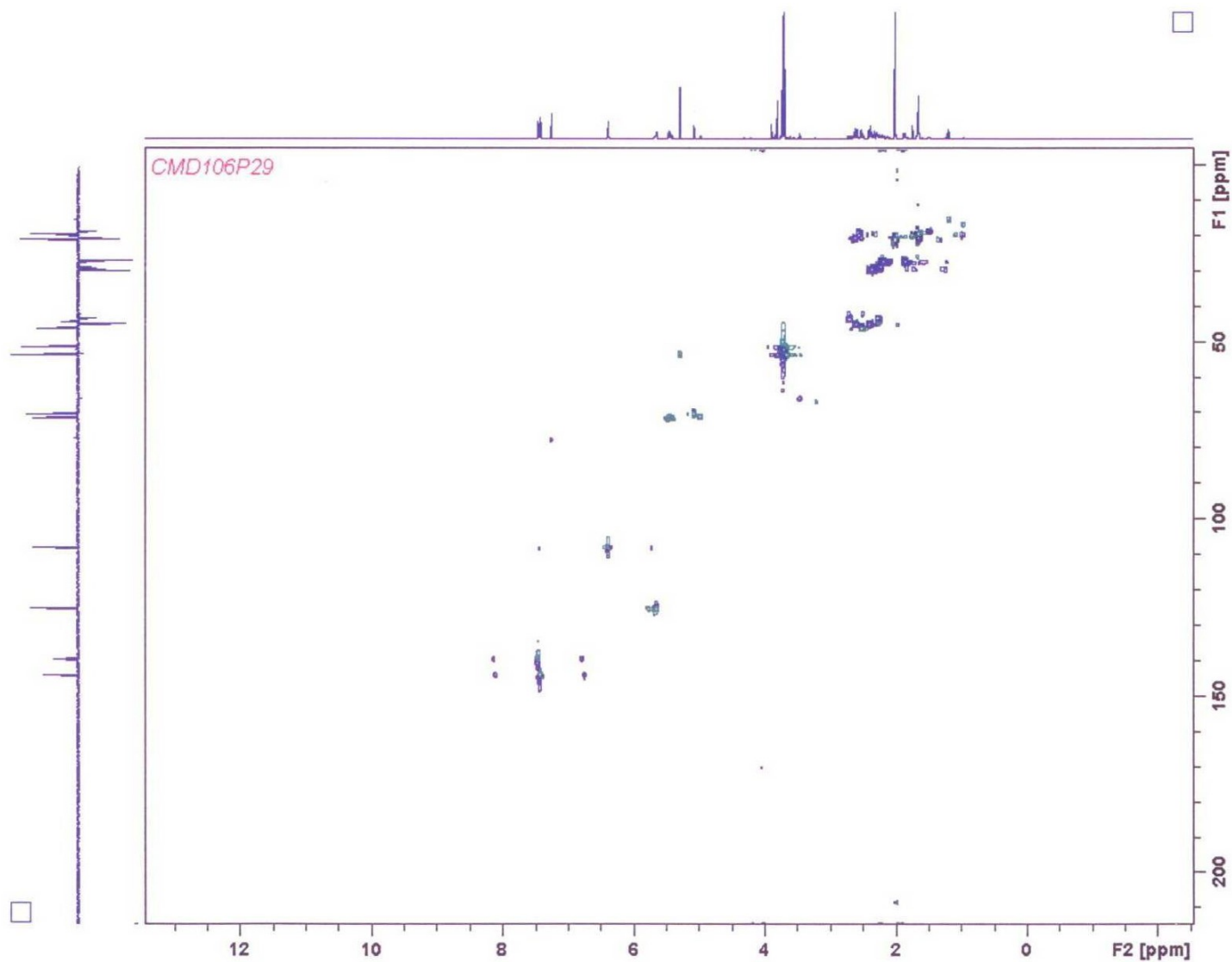


Fig. 4.22: HSQC DEPT spectrum of CMD-C in CDCl_3

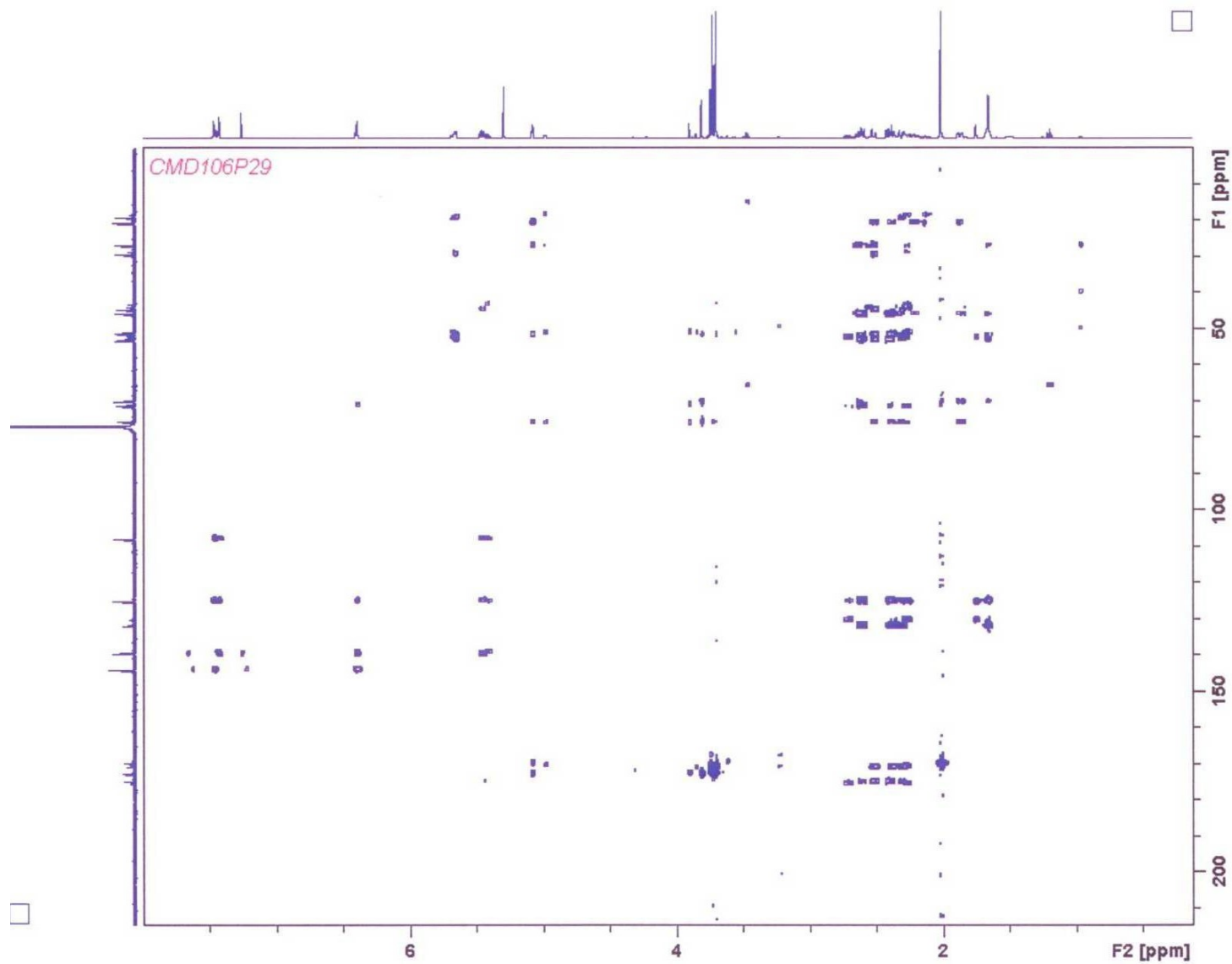


Fig. 4.23: HMBC spectrum of CMD-C in CDCl_3

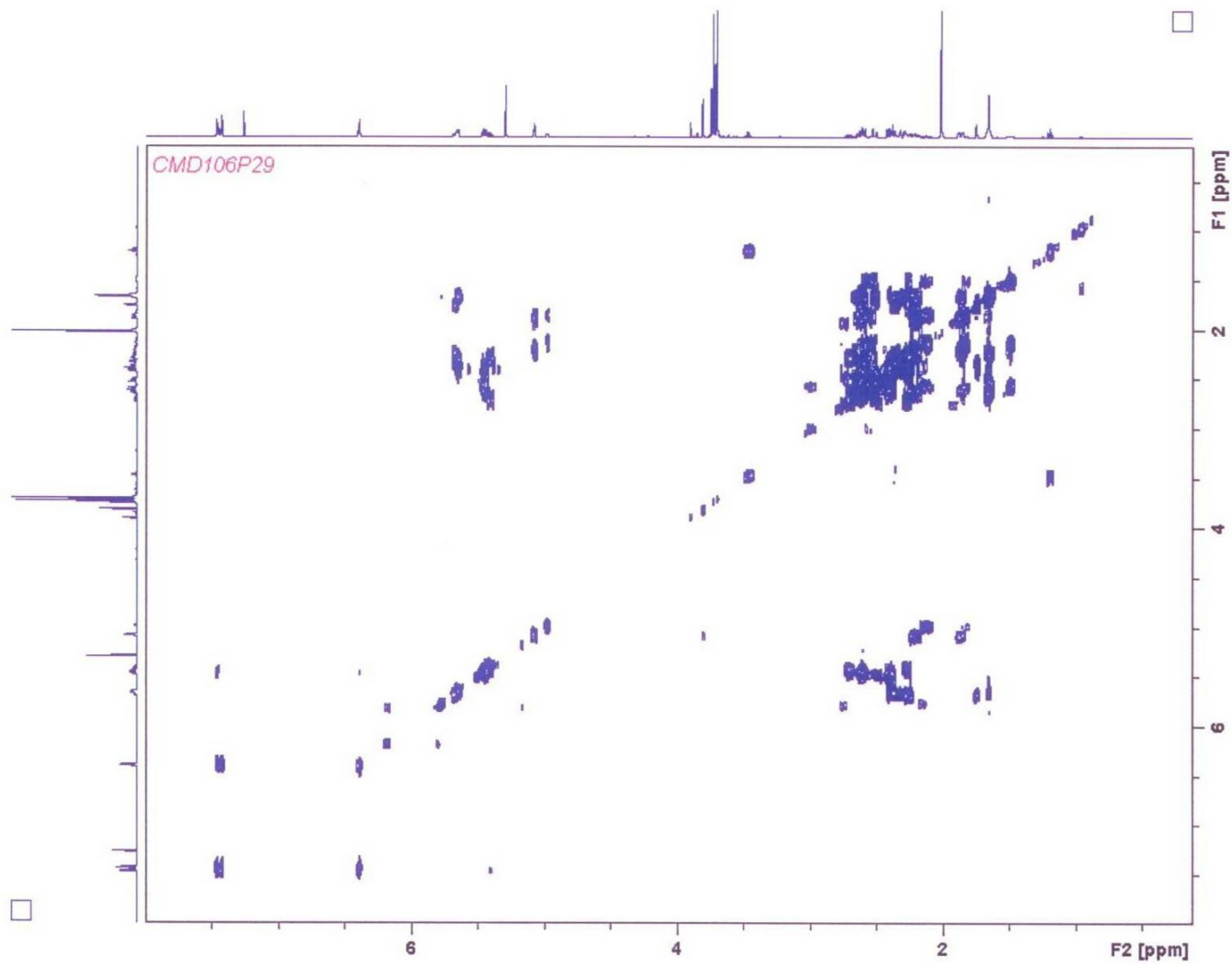


Fig. 4.24: COSY spectrum of CMD-C in CDCl_3

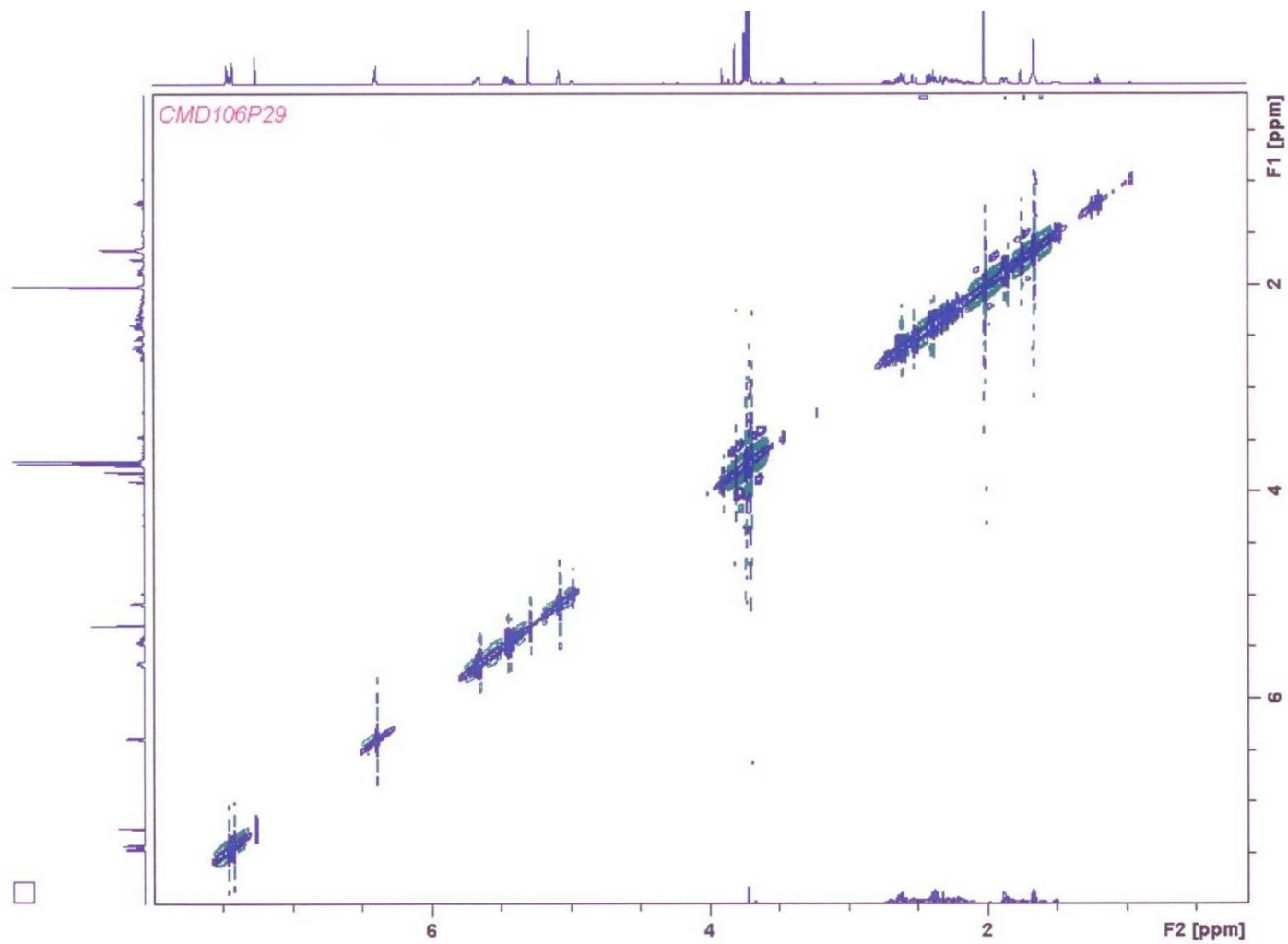
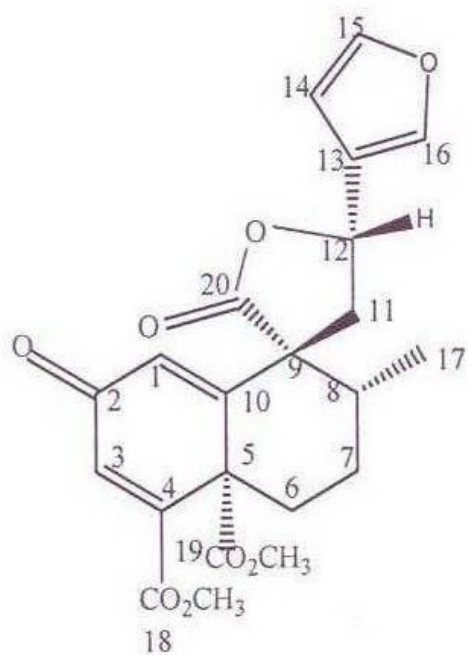


Fig. 4.25: NOESY spectrum of CMD-C in CDCl_3

4.2.4 Structural elucidation of compound CMD-D

Compound **CMD-D** was isolated as a white solid. The FTIR spectrum (Fig. 4.26) showed an absorption band at 1730, 1699, cm^{-1} for ester and ketone functional group. Resonances showing olefinic protons resonances at δ_{H} 6.43 s, 7.46 s and 7.53 s (Tchissambou *et al.*, 1990), which are characteristic of a β -substituted furanyl ring were observed in the ^1H NMR spectrum (Fig 4.27). Resonances showing singlets of olefinic protons at δ_{H} 6.75 and δ_{H} 6.86 assigned to H-1 and H-3 respectively were observed. Resonances of three-proton singlets were also observed at δ_{H} 3.83 s and 3.64 s and were taken to be of two ester methyl groups. An oxymethine proton resonance was observed at δ_{H} 5.55. The ^{13}C NMR spectrum (Fig 4.28) showed resonances of four sp^2 carbons of a β -substituted furanyl ring, three of them methine carbons at δ_{C} 108.2, 144.5, 140.6 and a fully substituted carbon at δ_{C} 123.6. Carbon resonances at δ_{C} 127.9, 131.6, 150.7 and 155.5 were assigned to C-1, C-3, C-4 and C-10 respectively. A resonance of a carbonyl carbon was observed at δ_{C} 185.9 and assigned to C-2. In addition, three carbonyl carbons resonances at δ_{C} 165.4, 166.4, 172.4 and an oxymethine carbon at δ_{C} 71.4 were observed.

^1H - ^{13}C crosspeaks at $\delta_{\text{H-1}}$ 6.75 with $\delta_{\text{C-9}}$ 55.1 and $\delta_{\text{H-3}}$ 6.86 with $\delta_{\text{C-5,18}}$ 53.6, 165.4 were observed in the HMBC spectrum (Fig 4.31), further supporting the proposed chemical structure. The ^1H NMR and ^{13}C NMR of **CMD-D** were compared with reported literature (Beth *et al.*, 2016) and was found to be similar to 1,2-dehydrocrotonylfuran-2-one [**32**] which has been previously isolated from the roots of *Croton megalocarpoides* (Beth *et al.*, 2016).



32

Table 4: Correlation Table of ^1H (500 MHz) and ^{13}C (125 MHz) NMR Data^a for compound CMD-D: 1,2-dehydrocrotoylifuran-2-one in CDCl_3

No	^{13}C NMR ^a (125 MHz) CDCl_3	^{13}C NMR ^b (125 MHz) CDCl_3	^1H NMR ^a (500 MHz) CDCl_3	^1H NMR ^a (500 MHz) CDCl_3
1	127.9	128.0	6.75 s	6.75 s
2	185.9	185.9		
3	131.6	131.6	6.86 s	6.86 s
4	150.7	150.8		
5	53.6	53.6		
6	33.2	33.2	1.43 d 3.12 dd	1.43 d 3.12 dd
7	26.6	26.7	2.63 d 2.80 d	2.63 d 2.80 d
8	39.4	39.5	1.71 m	1.71 m
9	55.1	55.1		
10	155.5	155.7		
11	39.1	39.2	2.77 d 2.63 s	2.77 d 2.63 s
12	71.4	71.4	5.55 dd	5.55 dd
13	123.6	123.6		
14	108.2	108.2	6.43 s	6.43s
15	144.5	144.6	7.46 s	7.46 s
16	140.6	140.6	7.53 s	7.53 s
17	17.1	17.1	1.17 d	1.17d
18	165.4	165.5		
19	166.4	166.4		
20	172.4	172.5		
18-acetox y	53.1	53.2	3.83 s	3.83 s
19-acetox y	53.3	53.4	3.64 s	3.64 s

^a Assignment aided by HMQC and HMBC experiments

^b Literature data of 1,2-dehydrocrotoylifuran-2-one (Beth *et al.*, 2016)

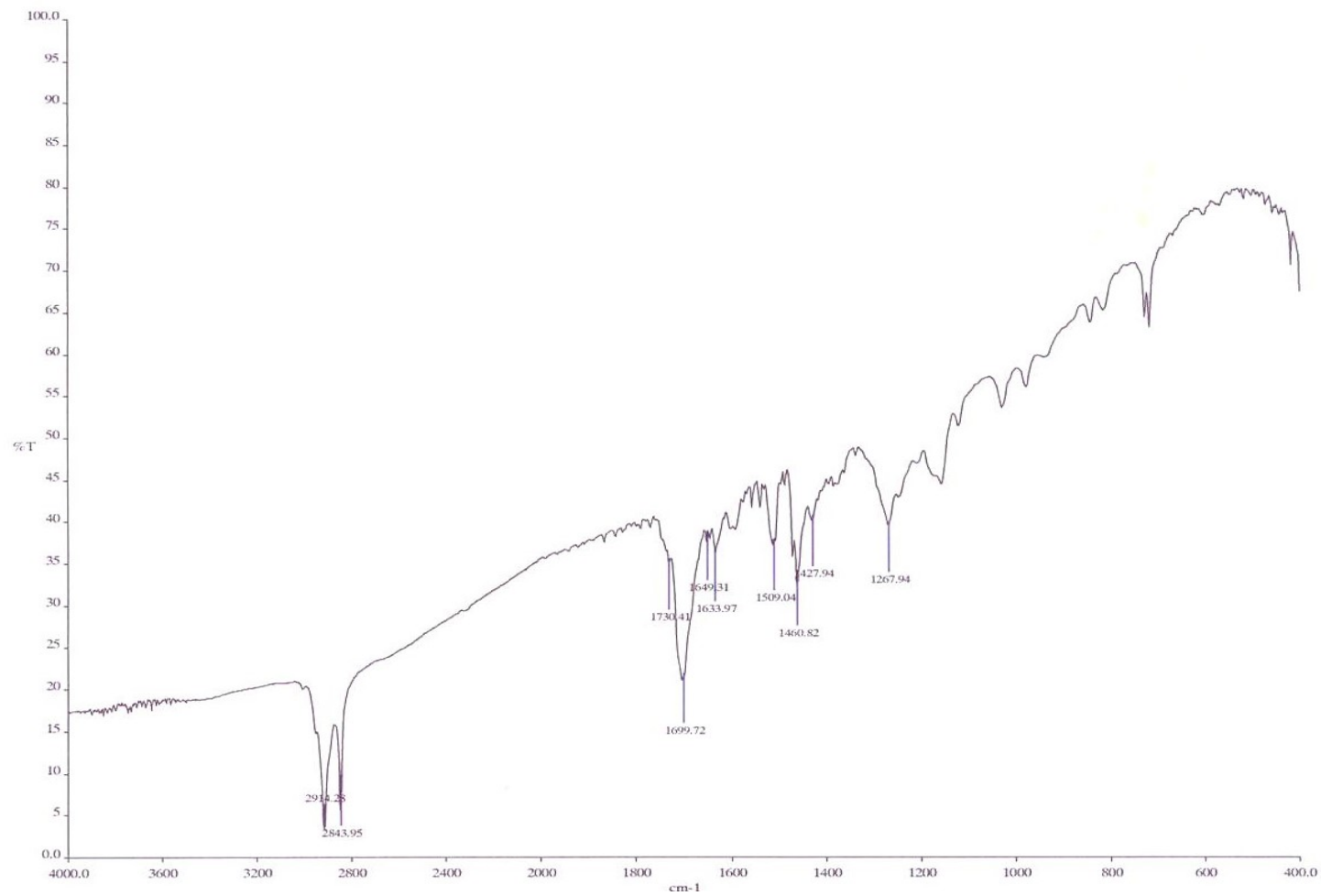


Fig. 4.26: IR spectrum of CMD-D in CDCl₃

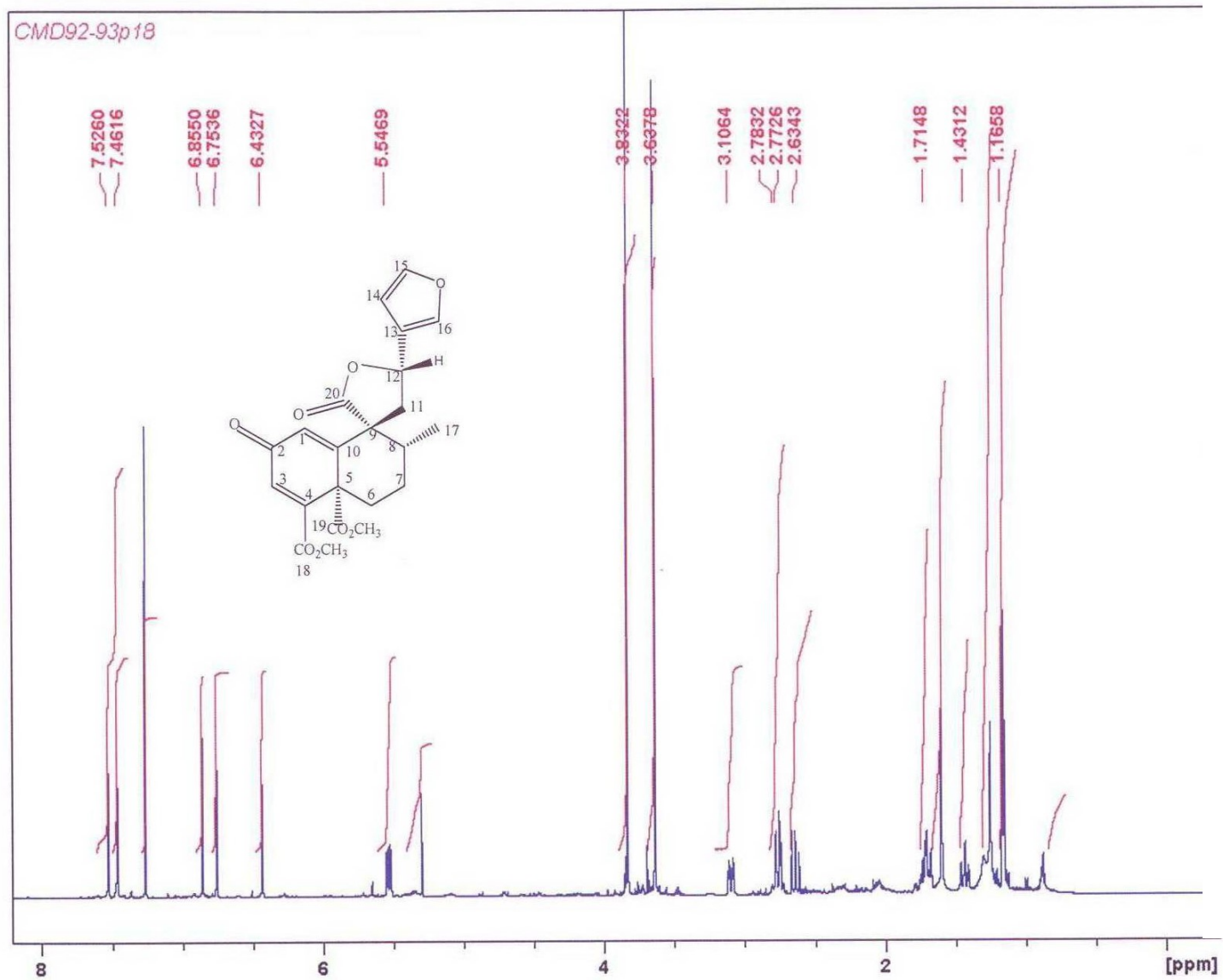


Fig. 4.27: ^1H NMR(500MHz) spectrum of CMD-D in CDCl_3

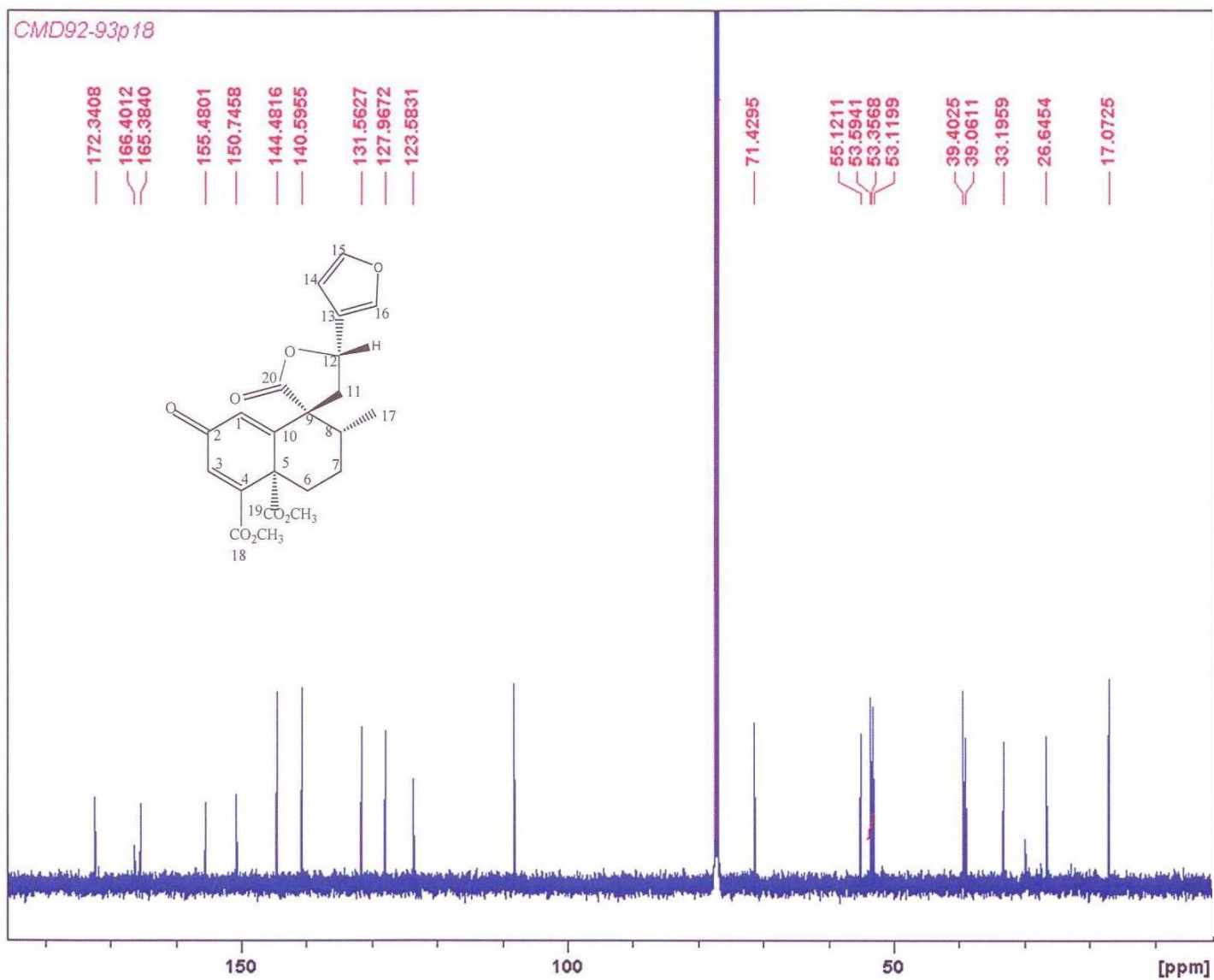


Fig. 4.28: ^{13}C NMR (125 MHz) spectrum of CMD-D in CDCl_3

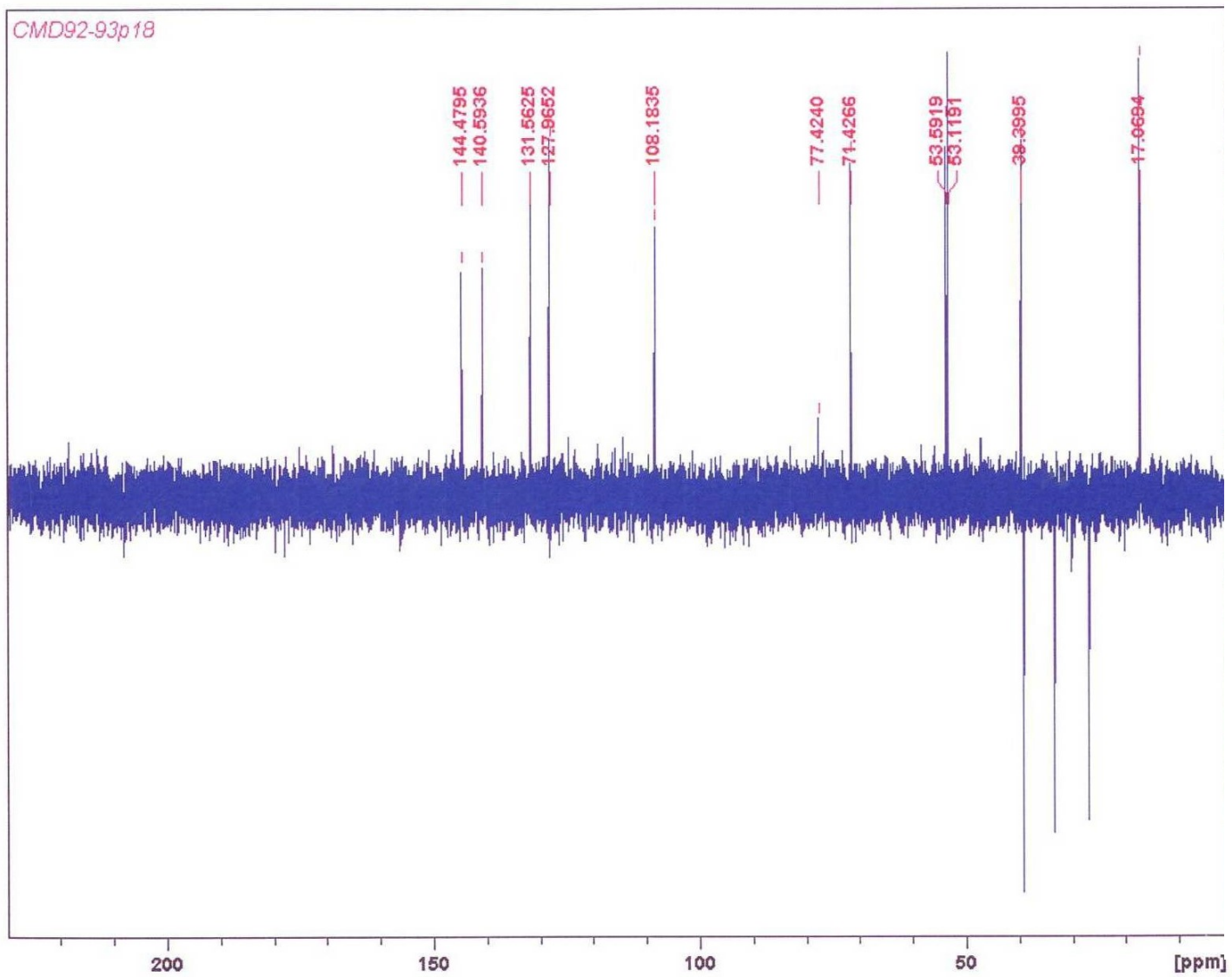


Fig. 4.29: DEPT spectrum of CMD-D in CDCl_3

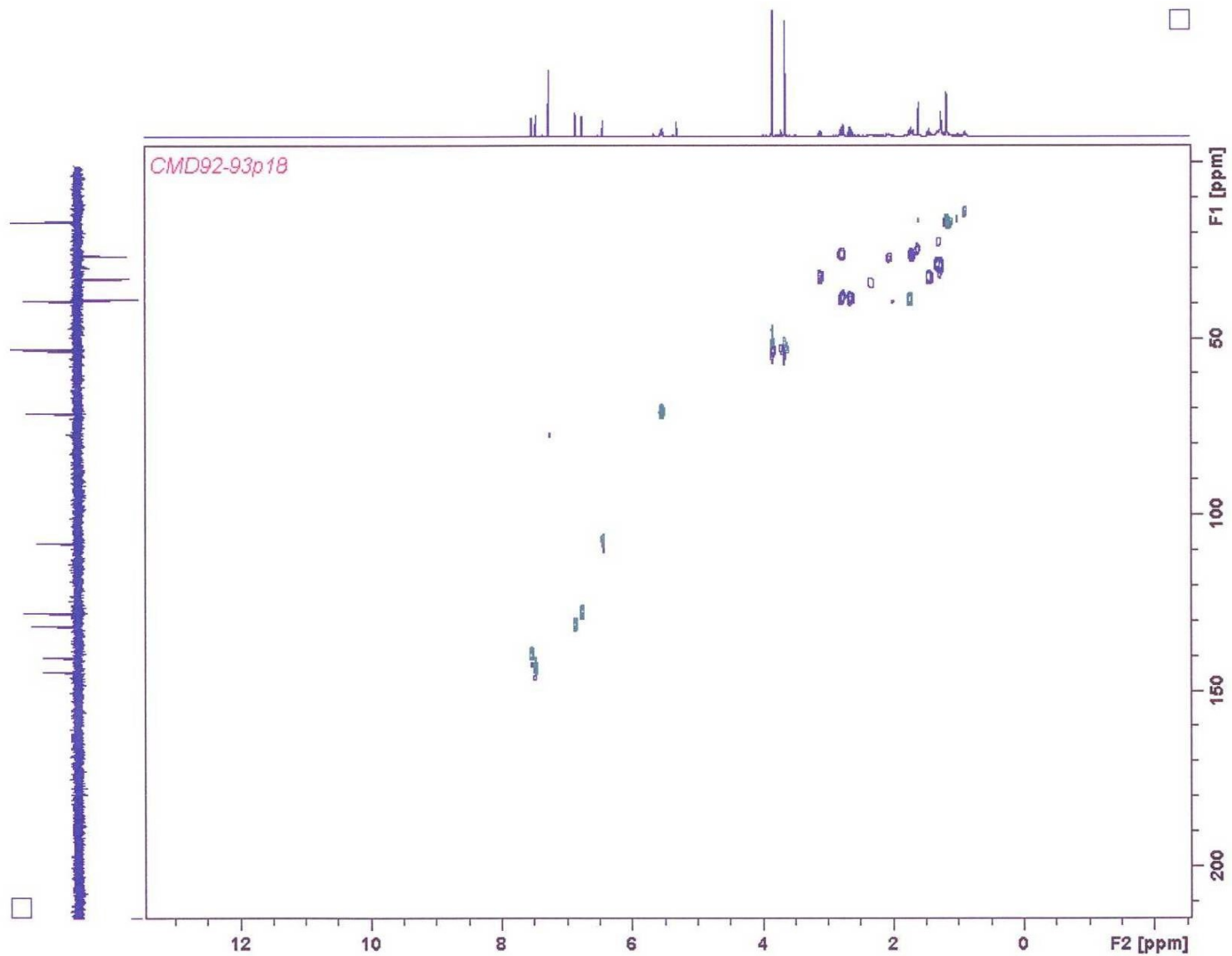


Fig. 4.30: HSQC DEPT spectrum of CMD-D in CDCl_3

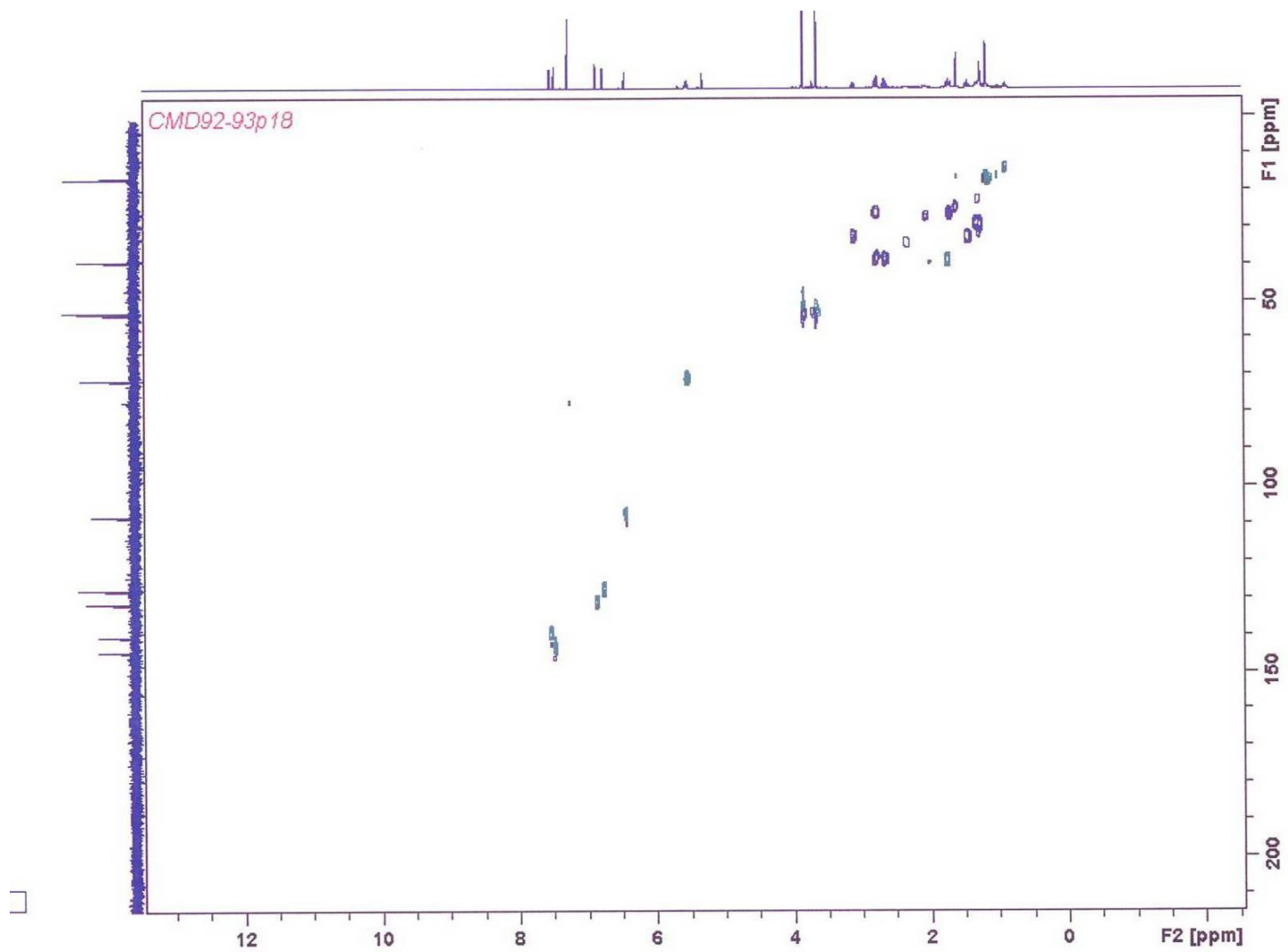


Fig. 4.31: HMBC spectrum of CMD-D in CDCl₃

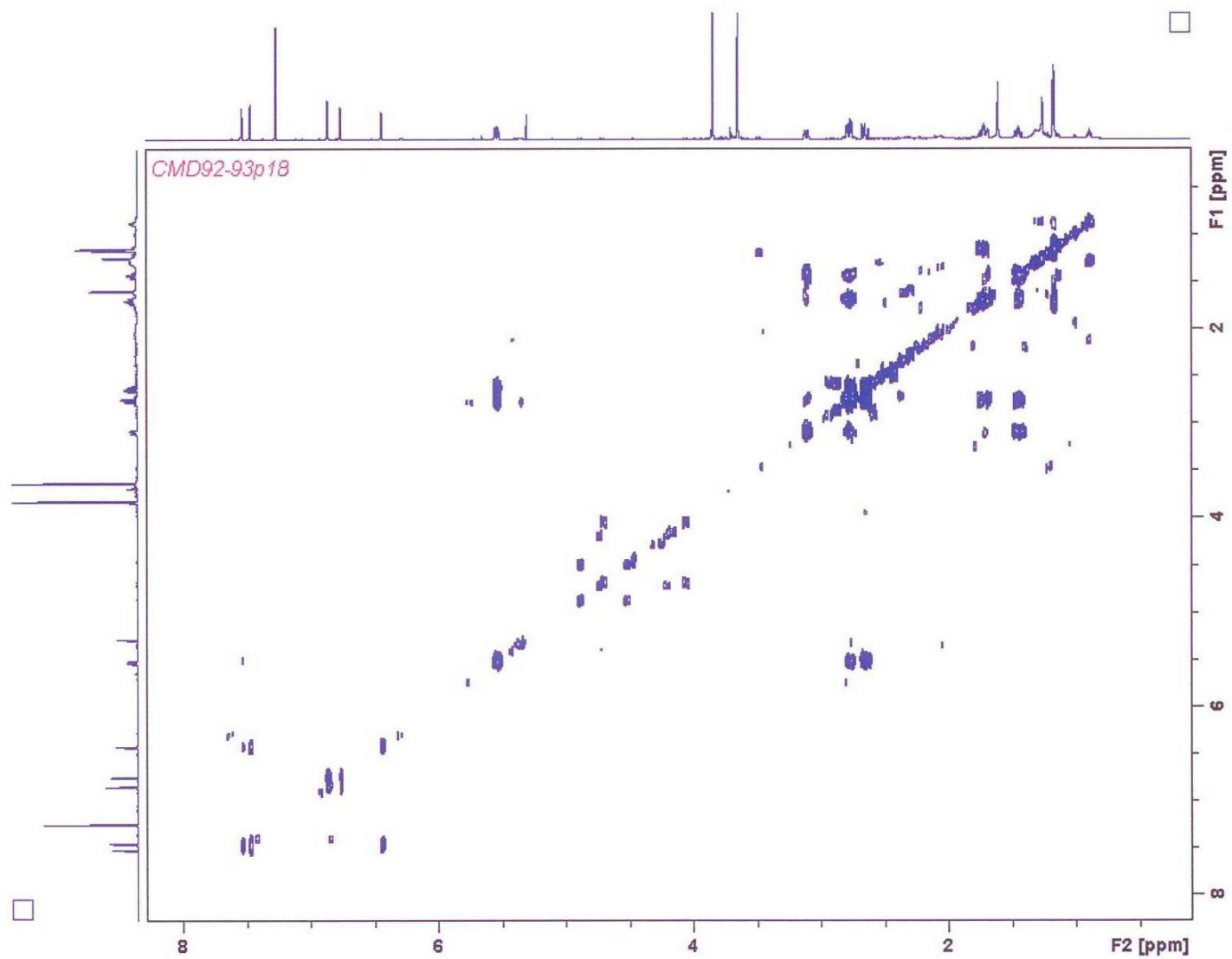


Fig. 4.32: COSY spectrum of CMD-D in CDCl_3

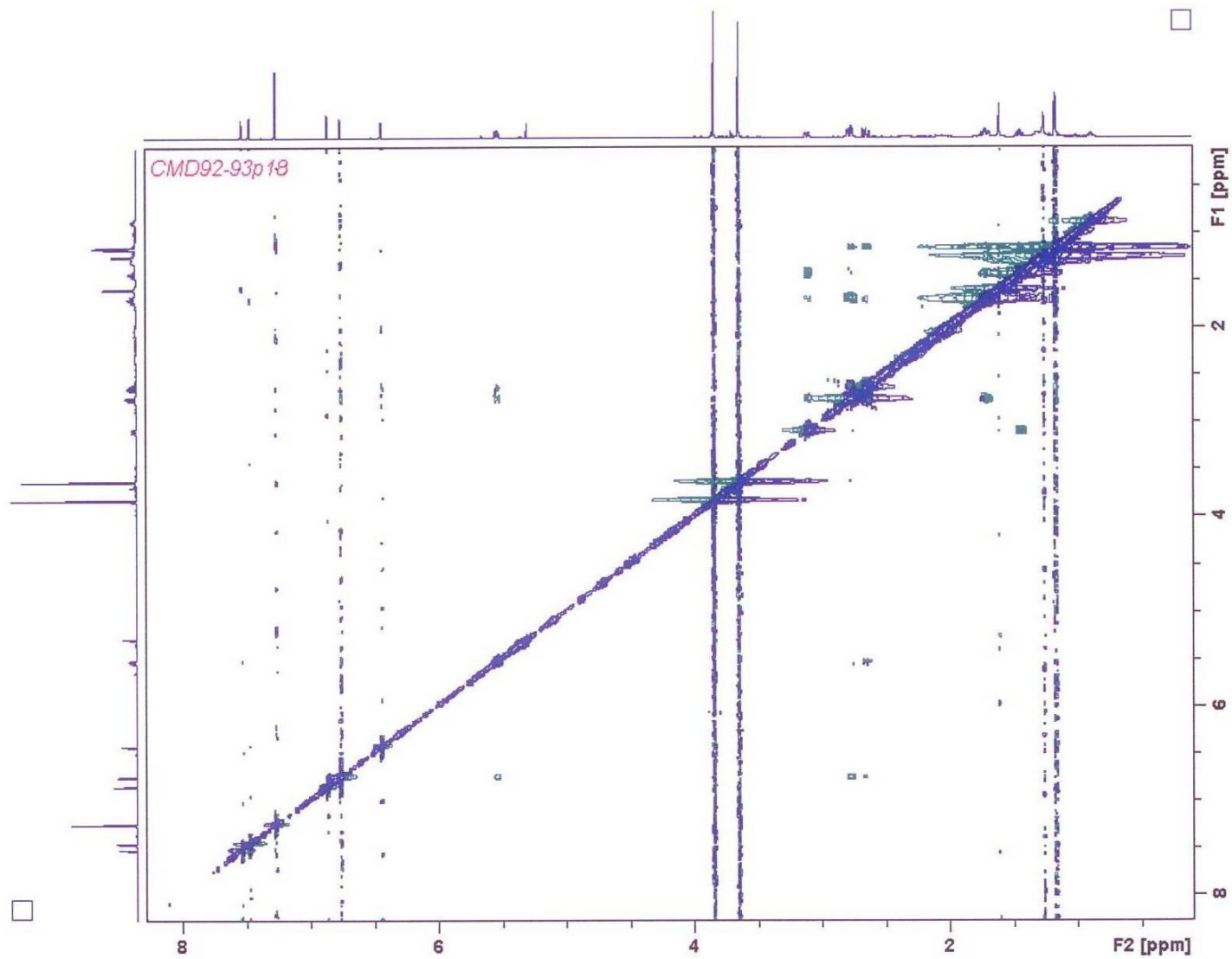
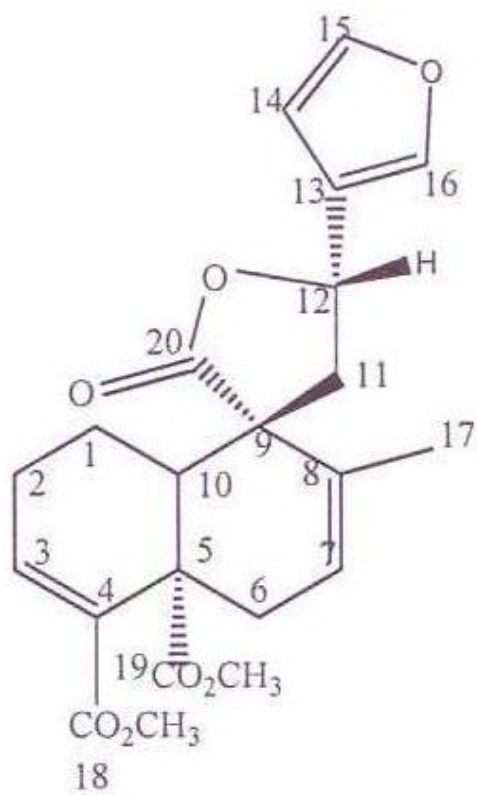


Fig. 4.33: NOESY spectrum of CMD-D in CDCl₃

4.2.5 Structural elucidation of compound CMD-E

Compound **CMD-E** was isolated as a white solid. Resonances showing olefinic protons resonances at δ_{H} 6.39 *d*, 7.44 *t* and 7.45 *s* (Tchissambou *et al.*, 1990) which is characteristic of a β -substituted furanyl ring were observed in the ^1H NMR spectrum (Fig 4.34). Resonances showing singlets of olefinic protons at δ_{H} 6.98 that was placed at position 7 and δ_{H} 5.83 assigned to position 3 were observed. In addition, resonances of three-proton singlets at δ_{H} 3.70 *s* and 3.71 *s* and were taken to be of two ester methyl groups were observed. An oxymethine proton resonance was observed at δ_{H} 5.50. The ^{13}C NMR spectrum (Fig 4.35) showed resonances of four sp^2 carbons of a β -substituted furanyl ring, three of them methine carbons at δ_{C} 108.2, 144.4, 139.6 and a fully substituted carbon at δ_{C} 125.8. Three carbonyl carbons resonances at δ_{C} 166.5, 172.0 and 175.9 were also observed. Carbon-carbon double bond resonances at δ_{C} 140.4 and 135.2 were observed in the ^{13}C NMR spectrum (Fig 4.35) and was placed at position 7. Another carbon-carbon double bond resonances at 127.2 and 130.6 that was placed at position 3 was observed.

Correlations were observed between the olefinic proton at $\delta_{\text{H}-7}$ 6.98 with $\delta_{\text{C}-5}$ 45.8 (quaternary) in the HMBC spectrum (Fig 4.40), further confirming the proposed chemical structure. In the NOESY spectrum (Fig 4.38), ^1H - ^1H peaks were observed at $\delta_{\text{H}-12}$ 5.50 with $\delta_{\text{H}-1\alpha}$ 2.34; $\delta_{\text{H}-1\beta}$ 2.34 with $\delta_{\text{H}-11\beta}$ 2.69; $\delta_{\text{H}-12}$ 5.50 with $\delta_{\text{H}-16}$ 7.45 indicating that compound **CMD-E** had similar relative configuration at C-12 with crotoacrylifuran. The ^1H NMR and ^{13}C NMR of **CMD-E** were compared with reported literature (Beth *et al.*, 2016) and was found to be similar to a new derivative of crotoacrylifuran **CMD-E** and was given the name 7,8-dehydrocrotoacrylifuran [**33**]. It has been previously isolated from the roots of *Croton megalocarpoides* (Beth *et al.*, 2016).



33

Table 5 : Correlation Table of ¹H (500 MHz) and ¹³C (125 MHz) NMR Data^a for compound CMD-E: 7,8-dehydrocrotocorylifuran in CDCl₃

No	¹³ C NMR ^a (125 MHz) CDCl ₃	¹³ C NMR ^b (125 MHz) CDCl ₃	¹ H NMR ^a (500 MHz) CDCl ₃	¹ H NMR ^b (500 MHz) CDCl ₃
1	19.4	19.4	2.34-2.44 <i>m</i> 1.56-1.77 <i>m</i>	2.34-2.44 <i>m</i> 1.56-1.77 <i>m</i>
2	26.6	26.6	2.56 <i>t</i> 1.56-1.77 <i>m</i>	2.56 <i>t</i> 1.56-1.77 <i>m</i>
3	127.2	127.2	5.83 <i>d</i>	5.83 <i>d</i>
4	130.6	130.6		
5	45.8	45.8		
6	33.4	33.4	1.56-1.77 <i>m</i> 2.34-2.44 <i>m</i>	1.56-1.77 <i>m</i> 2.34-2.44 <i>m</i>
7	140.4	140.4	6.98 <i>dd</i>	6.98 <i>dd</i>
8	135.2	135.2		
9	52.9	52.9		
10	50.5	50.5	2.00 <i>dd</i>	2.00 <i>dd</i>
11	42.4	42.4	2.34-2.44 <i>m</i> 2.69 <i>dd</i>	2.34-2.44 <i>m</i> 2.69 <i>dd</i>
12	72.0	72.0	5.50 <i>t</i>	5.50 <i>t</i>
13	125.8	125.8		
14	108.2	108.2	6.39 <i>d</i>	6.39 <i>d</i>
15	144.4	144.4	7.44 <i>t</i>	7.44 <i>t</i>
16	139.6	139.6	7.45 <i>s</i>	7.45 <i>s</i>
17	19.5	19.5	1.25 <i>s</i>	1.25 <i>s</i>
18	166.5	166.5		
19	172.0	172.0		
20	175.9	175.9		
18-acetoxy	51.8	51.8	3.70 <i>s</i>	3.70 <i>s</i>
19-acetoxy	52.4	52.4	3.71 <i>s</i>	3.71 <i>s</i>

^a Assignment aided by HMQC and HMBC experiments

^b Literature data of 7,8-dehydrocrotocorylifuran (Beth *et al.*, 2016)

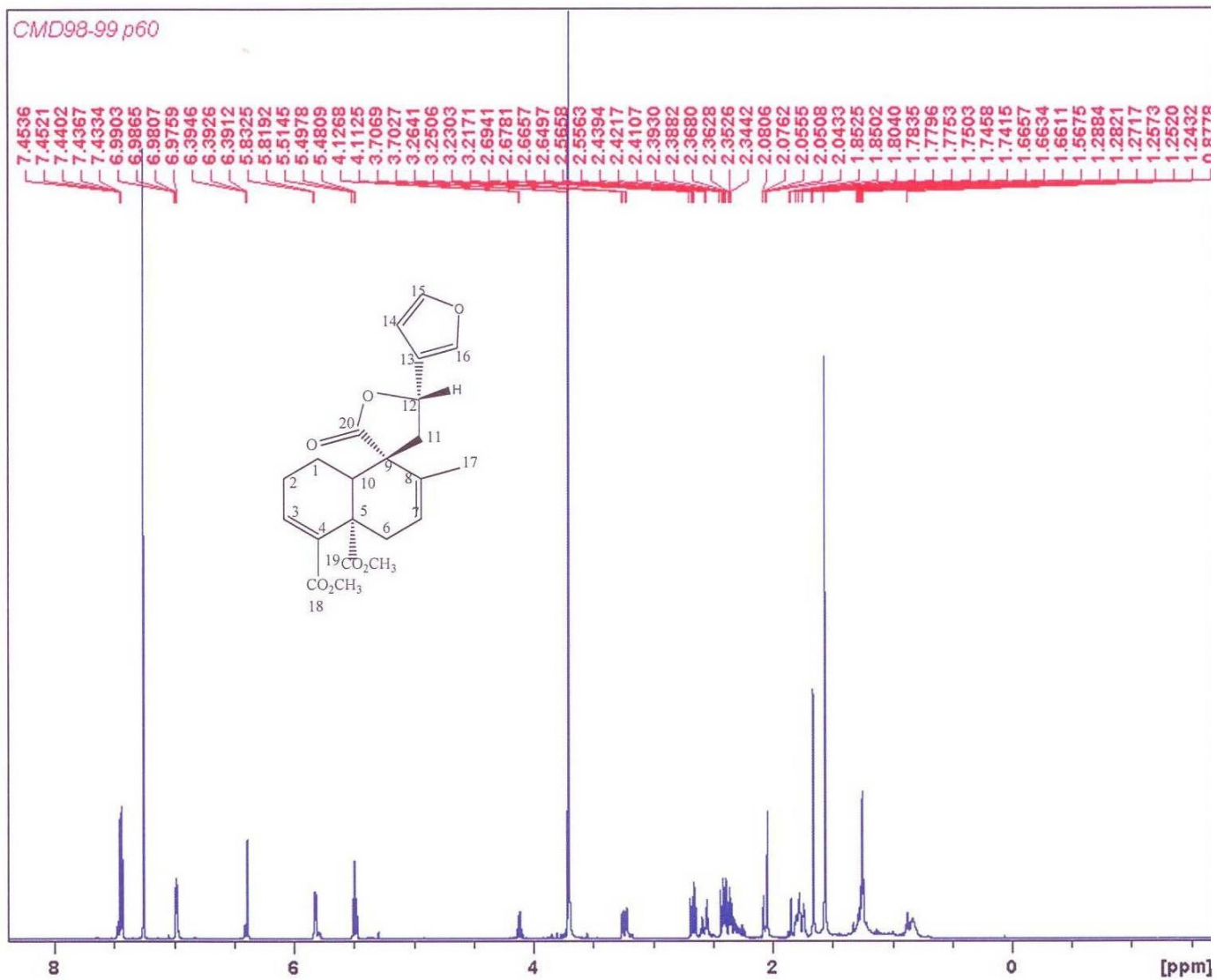


Fig. 4.34: ^1H NMR (500MHz) spectrum of CMD-E in CDCl_3

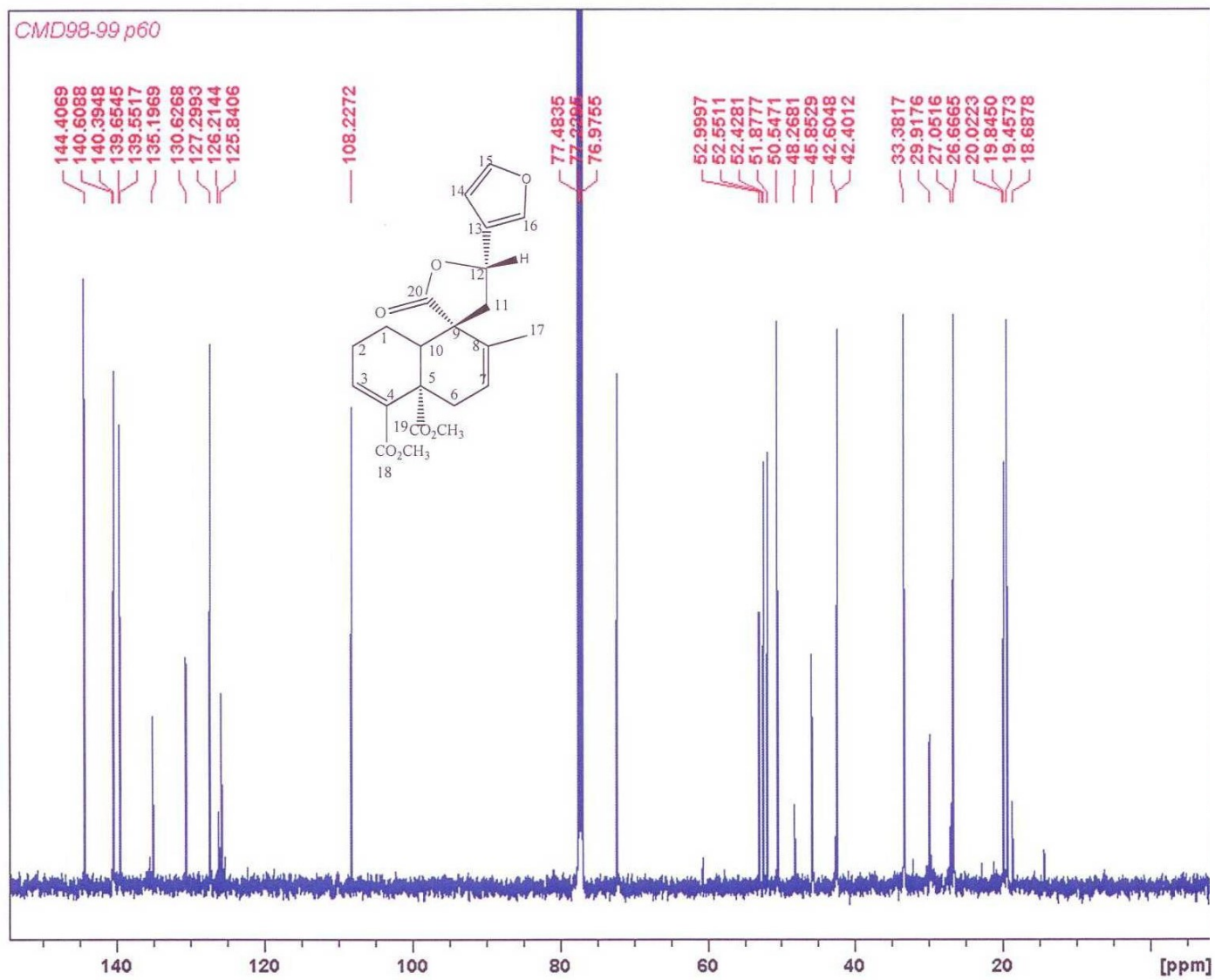


Fig. 4.35: ¹³CNMR (125 MHz) spectrum of CMD-E in CDCl₃

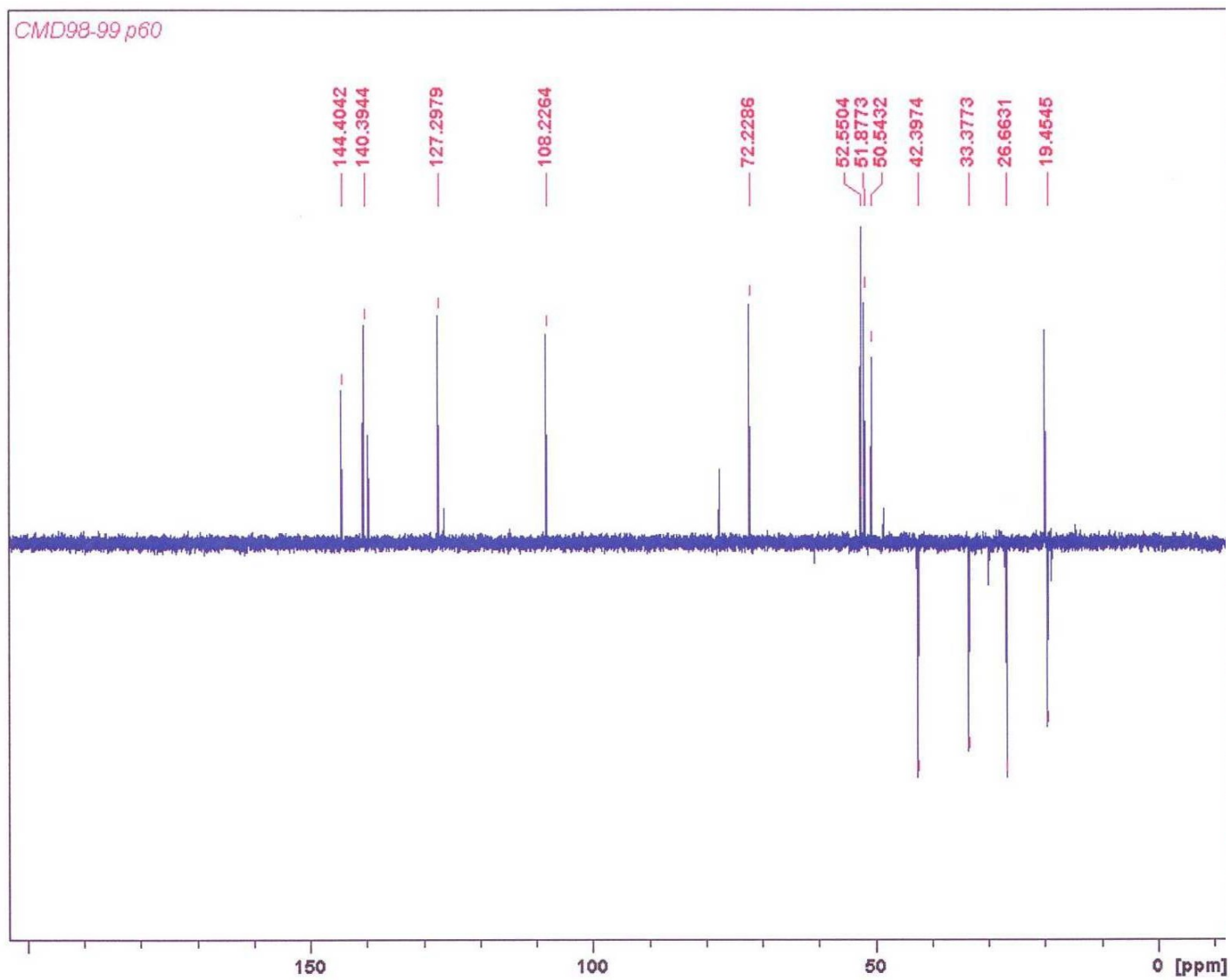


Fig. 4.36: DEPT spectrum of CMD-E in CDCl_3

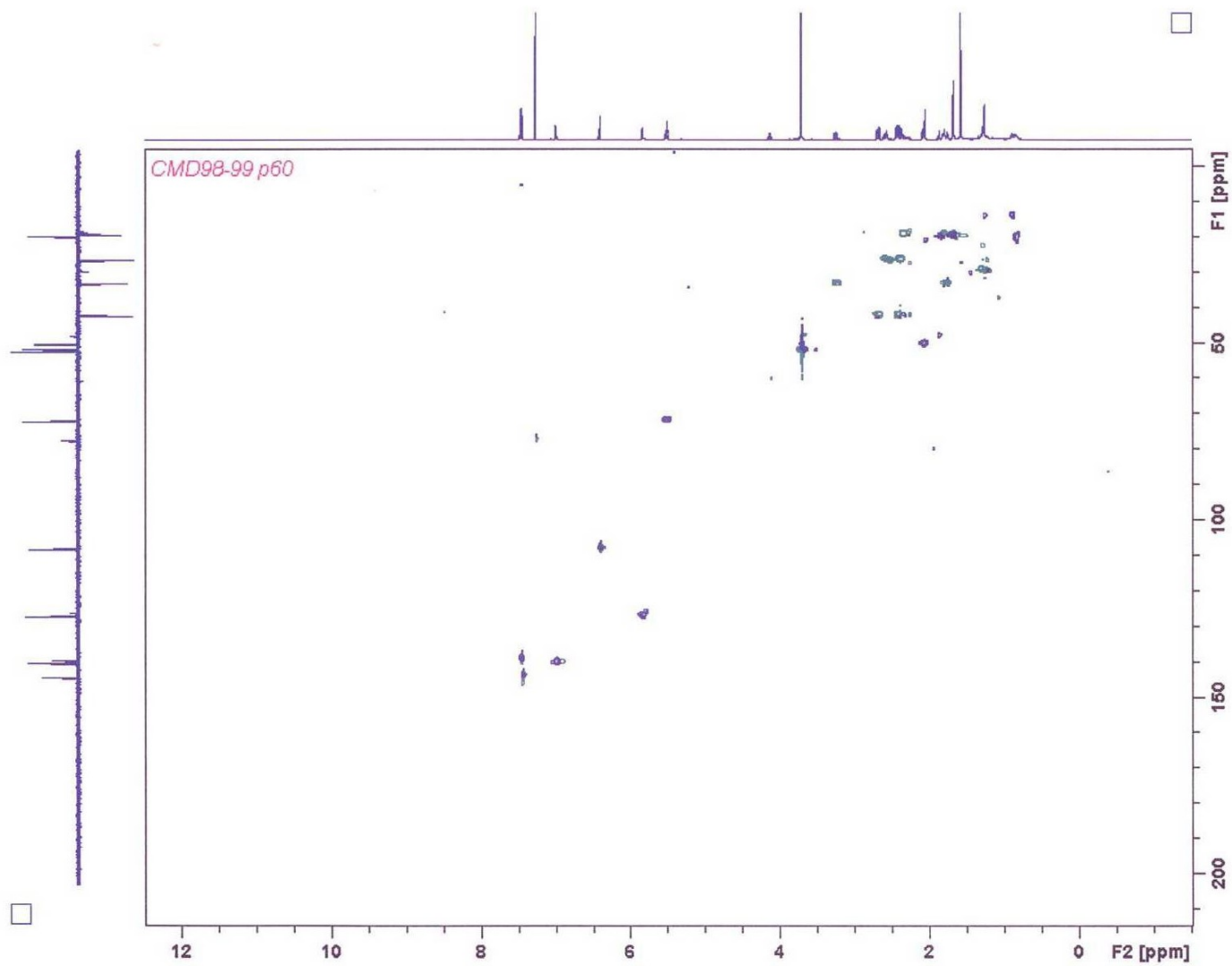


Fig. 4.37: HSQC DEPT spectrum of CMD-E in CDCl_3

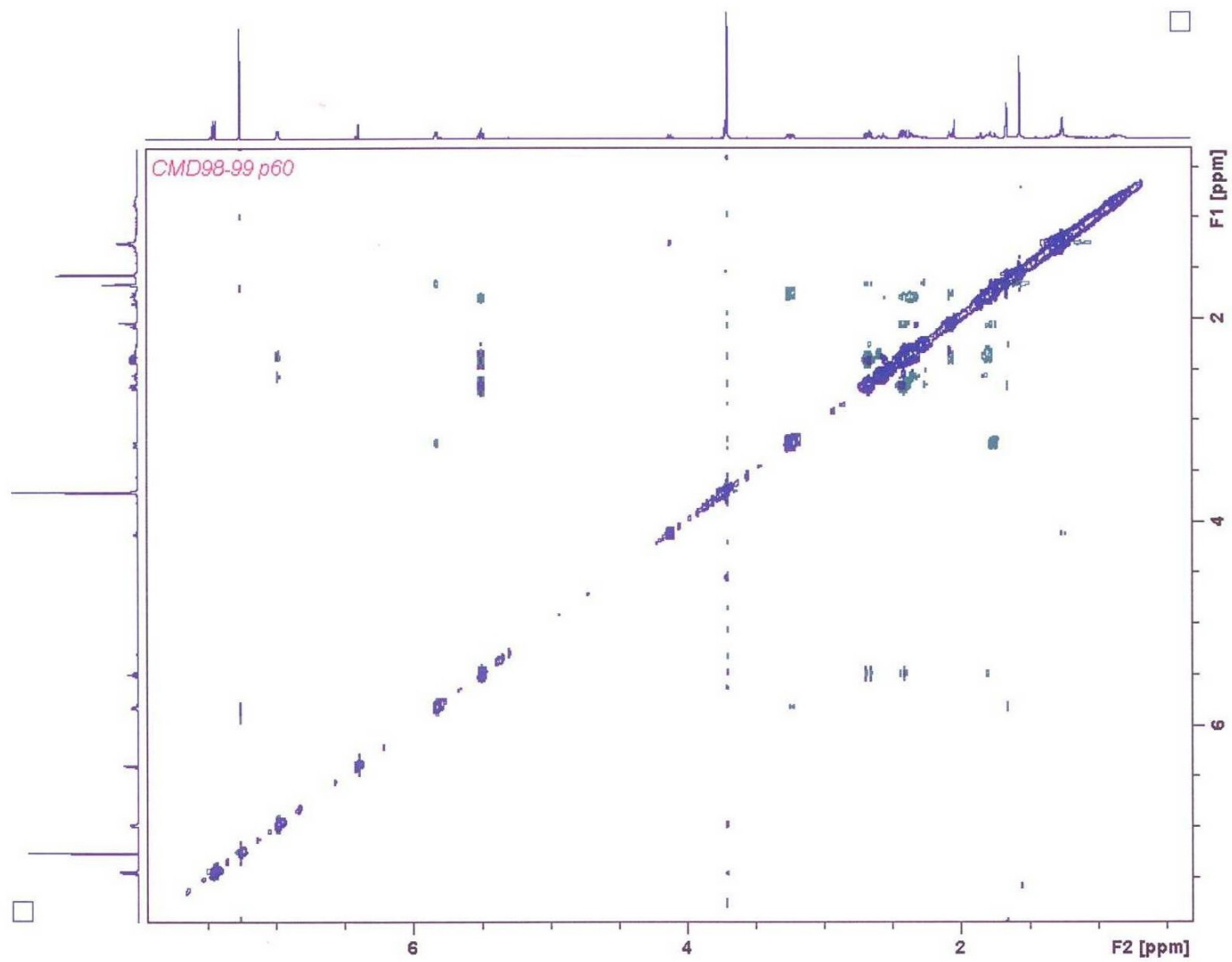


Fig. 4.38: NOESY spectrum of CMD-E in CDCl_3

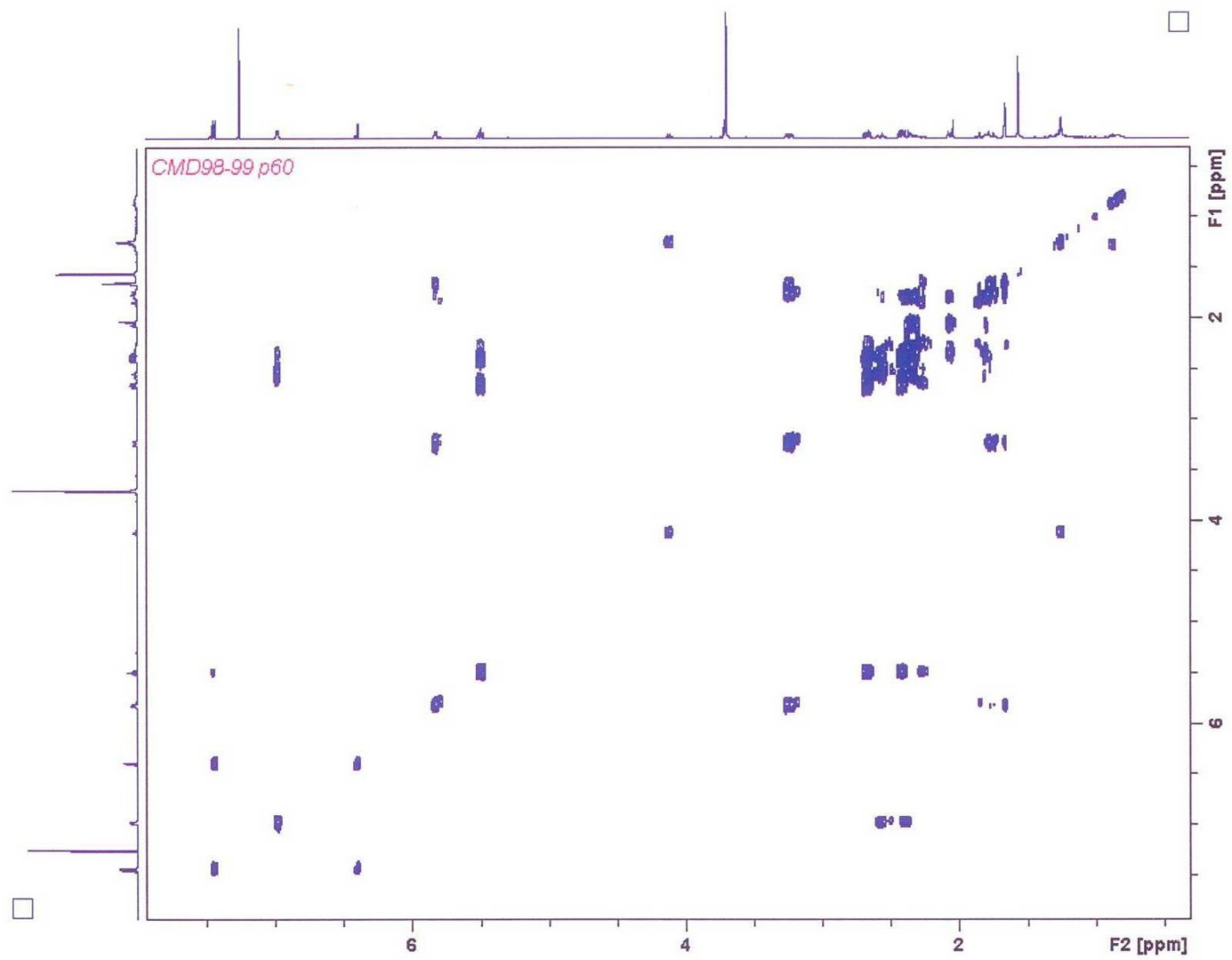


Fig. 4.39: COSY spectrum of CMD-E in CDCl₃

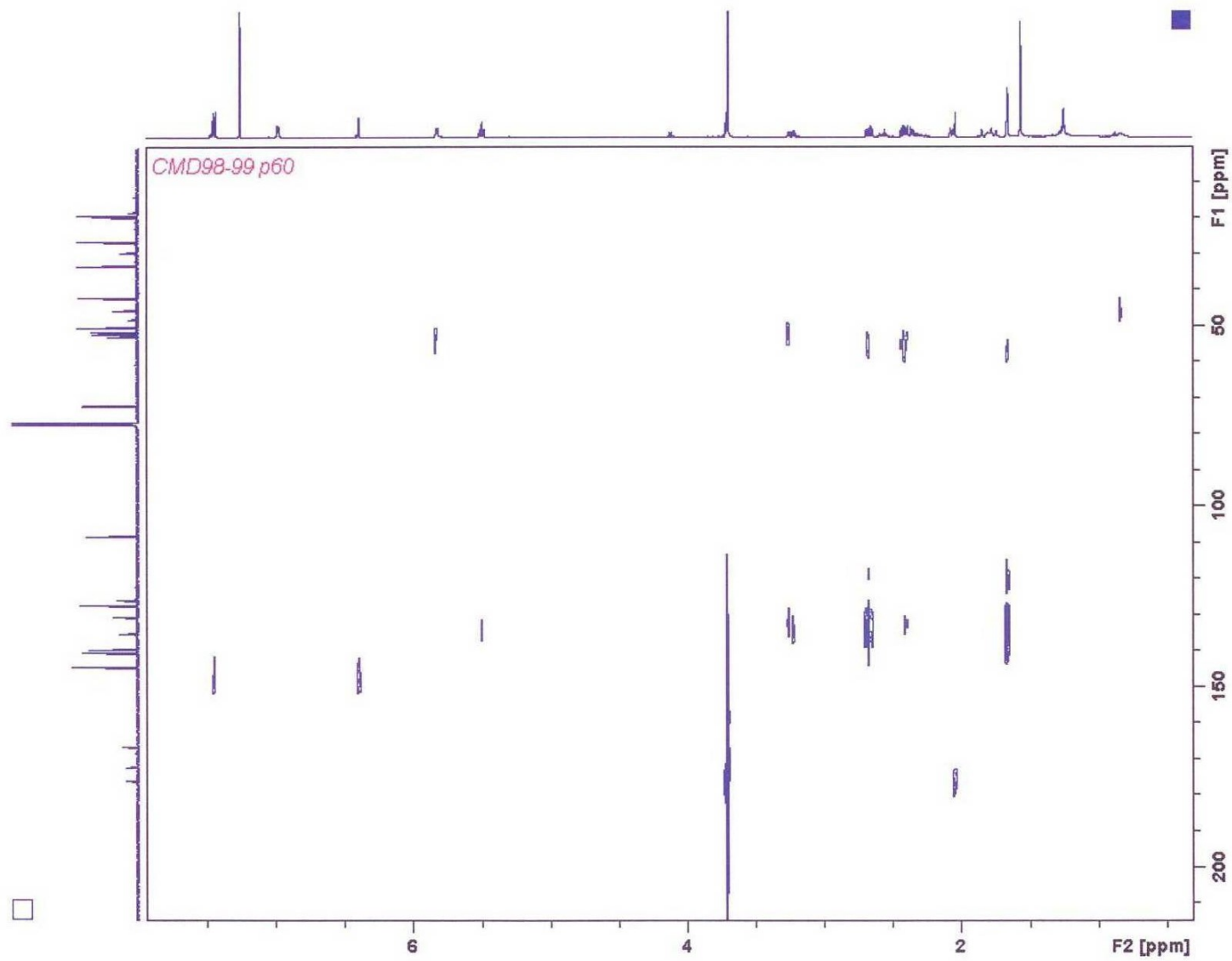


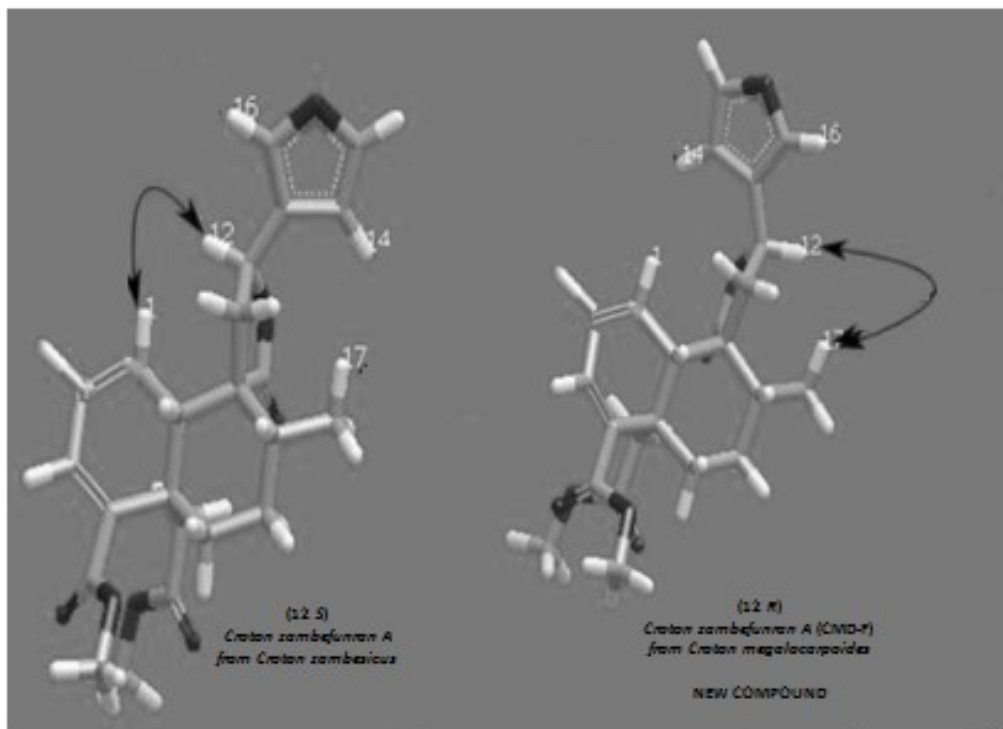
Fig. 4.40: HMBC spectrum of CMD-E in CDCl_3

4.2.6 Structural elucidation of compound CMD-F

Compound **CMD-F** was isolated as a white solid. Its mass spectrum (Fig 4.41) had a molecular ion peak at m/z 423.7 for $[M + Na^+]$ consistent with the proposed molecular formula $C_{22}H_{24}O_7$. The FTIR spectrum (Fig.4.42) showed an absorption band at 1730, 1699 cm^{-1} of lactone and ester respectively. The 1H and ^{13}C NMR (Fig 4.43 and Fig 4.44 respectively) signals revealed presence of six vinyl proton at δ_H 6.01, 6.15, 6.98, 6.40, 7.47, 7.49. The resonances at δ_H 6.40 *brt*, 7.47 *t* and 7.49 *brs* are characteristics of a β -substituted furan ring. The remaining three vinyl protons at δ_H 6.01, 6.15, 6.98 were assigned to H- 1, H- 2 and H-3 respectively. Three methyl groups resonances were identified as a secondary group δ_H 1.13 and two methyl esters (δ_H 3.60 and 3.81). Three carbonyl groups were observed at δ_C 166.9, 172.0 and 176.0. The shielded carbonyl at δ_C 166.9 is suggestive of a conjugated carbonyl while the deshielded carbonyl group at δ_C 176.0 is suggestive of a carbonyl of a lactone. The ^{13}C NMR spectrum (Fig 4.44) showed resonances of four sp^2 carbons of a β -substituted furanyl ring, three of them methine carbons at δ_C 108.4, 144.4, 140.0 and a fully substituted carbon at δ_C 126.0. Carbon resonances at δ_C 133.0, 125.5, 135.6 and 136.4 were assigned to the olefinic carbons at position 1, 2, 3 and 4 respectively. The spectral data of **CMD-F** contained had an additional conjugated double bond when compared to that of crotoerylifuran **CMD-B**, which was isolated from *Croton zambesicus* (Ngadjui *et al.*, 1999).

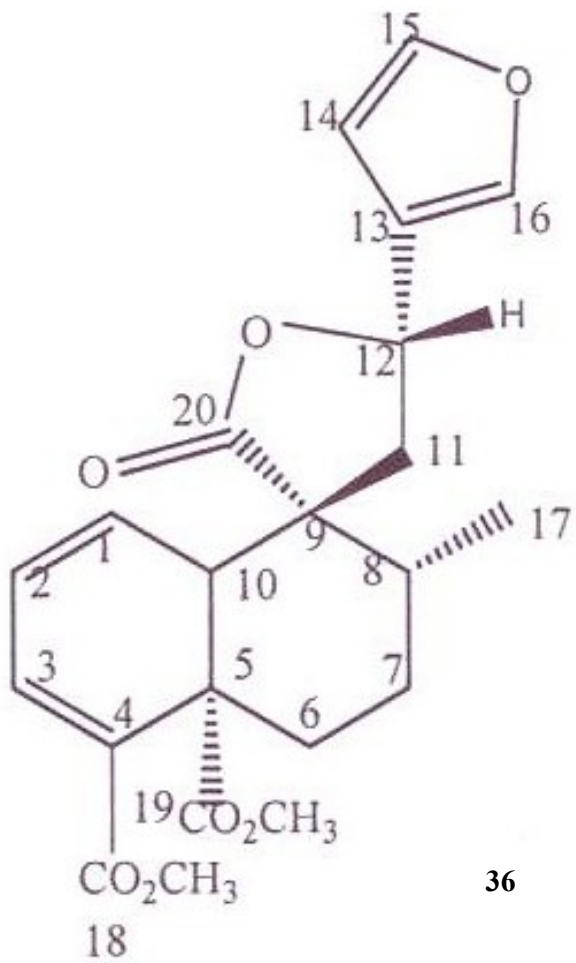
The 1H NMR and ^{13}C NMR of **CMD-F** were compared with reported literature (Ngadjui *et al.*, 1999) and was found to be similar to crotozambefuran A (15,16-epoxy-1,3,13(16),14-clerodatetraen 20,12-olide-18,19-dioic acid dimethylester), which was isolated from stem bark of another croton plant *Croton zambesicus* (Ngadjui *et al.*, 1999). From the Crotozambefuran A [34] reported in literature (Ngadjui *et al.*, 1999), a correlation was observed between H-12 and H-1 in its NOESY spectrum confirming the (C-12*S*) configuration.

However, in the NOESY spectrum (Fig 4.49) of **CMD-F**, there is correlation between H-12 and 3H-17 confirming the 12 *R* configuration which indicates that the compound **CMD-F** is new and an epimer (C-12*R*) [35] of the known Crotozambefuran A (C-12*S*) [34]. Crotozambefuran A (C-12*S*) [34] and **CMD-F** (C-12*R*) [35] are three dimensional models illustrating the correlations between H-12/H-1 and H-12/H-17 respectively. It is trivially named as 12- *epi*-Croton zambefuran and identified as 12-*epi*-15,16-epoxy-1,3,13(16),14-clerodatetraen-20,12-olide-18,19-dioic acid dimethyl ester [35][36]. This is the first report of this compound in nature to the best of our knowledge.



34

35



36

Table 6: Correlation Table ^1H (500 MHz) and ^{13}C (125 MHz) NMR Data^a for compound CMD-F :12 -*epi*-Croton zambefuran in CDCl_3

No	^{13}C NMR ^a (125 MHz) CDCl_3	^{13}C NMR ^b (125 MHz) CDCl_3	^1H NMR ^a (500 MHz) CDCl_3	^1H NMR ^b (500 MHz) CDCl_3
1	133.0 <i>d</i>	133.0 <i>d</i>	6.01 <i>dd</i>	6.01 <i>dd</i>
2	125.5 <i>d</i>	125.5 <i>d</i>	6.15 <i>ddd</i>	6.20 <i>ddd</i>
3	135.6 <i>d</i>	135.6 <i>d</i>	6.98 <i>d</i>	7.00 <i>d</i>
4	136.4 <i>s</i>	136.4 <i>s</i>	-	-
5	47.1 <i>s</i>	47.1 <i>s</i>	-	-
6a	32.0 <i>t</i>	32.0 <i>t</i>	3.13 <i>dt</i>	3.13 <i>dt</i>
6b	31.8 <i>t</i>	31.8 <i>t</i>	1.30 <i>brdt</i>	1.30 <i>brdt</i>
7a	28.2 <i>t</i>	28.2 <i>t</i>	2.06 <i>ddd</i>	2.06 <i>ddd</i>
7b	28.2 <i>t</i>	28.2 <i>t</i>	1.56 <i>brdd</i>	1.56 <i>brdd</i>
8	42.0 <i>d</i>	42.0 <i>d</i>	1.84 <i>m</i>	1.84 <i>m</i>
9	50.1 <i>s</i>	50.1 <i>s</i>	-	-
10	49.6 <i>d</i>	49.6 <i>d</i>	3.02 <i>t</i>	3.02 <i>t</i>
11a	41.8 <i>t</i>	41.8 <i>t</i>	2.65 <i>dd</i>	2.65 <i>dd</i>
11b	41.4 <i>t</i>	41.4 <i>t</i>	2.50 <i>dd</i>	2.50 <i>dd</i>
12	73.0 <i>d</i>	73.0 <i>d</i>	5.50 <i>t</i>	5.50 <i>t</i>
13	126.0 <i>s</i>	126.0 <i>s</i>	-	-
14	108.4 <i>d</i>	108.4 <i>d</i>	6.40 <i>br t</i>	6.46 <i>brt</i>
15	144.4 <i>d</i>	144.4 <i>d</i>	7.47 <i>t</i>	7.46 <i>t</i>
16	140.0 <i>d</i>	140.0 <i>d</i>	7.49 <i>brs</i>	7.51 <i>brs</i>
17	17.3 <i>q</i>	17.3 <i>q</i>	1.13 <i>d</i>	1.13 <i>d</i>
18	166.9 <i>s</i>	166.9 <i>s</i>	-	-
19	172.0 <i>s</i>	172.0 <i>s</i>	-	-
20	176.0 <i>s</i>	176.0 <i>s</i>	-	-
OMe-18	51.6 <i>q</i>	51.6 <i>q</i>	3.81 <i>s</i>	3.79 <i>s</i>
OMe-19	51.8 <i>q</i>		3.60 <i>s</i>	3.59 <i>s</i>
OMe-20	-			

^a Assignment aided by HMQC and HMBC experiments

^b Literature data on Croton zambefuran A (Ngadjui *et al.*, 2001)

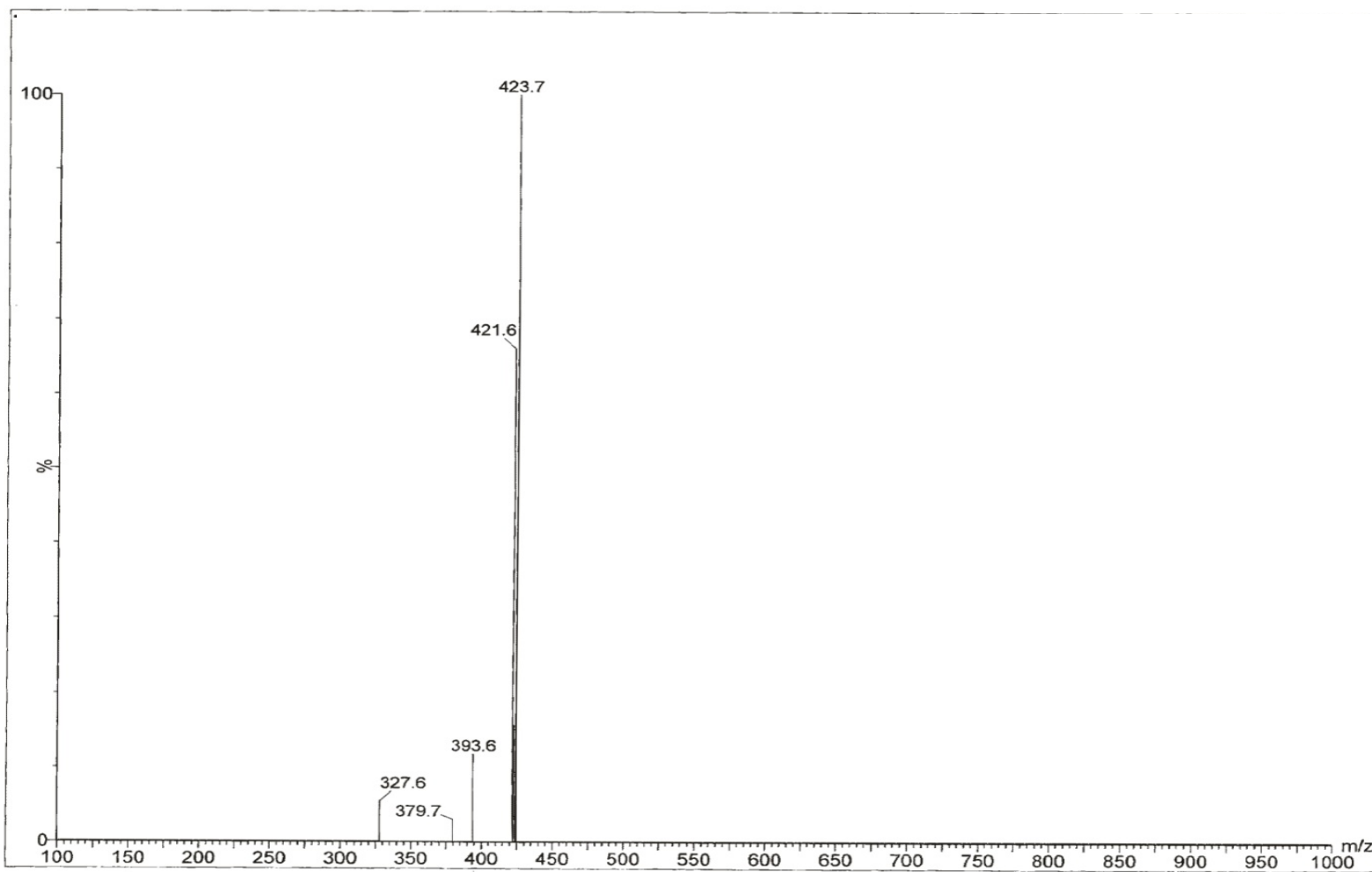


Fig. 4.41: MS spectrum of CMD-F

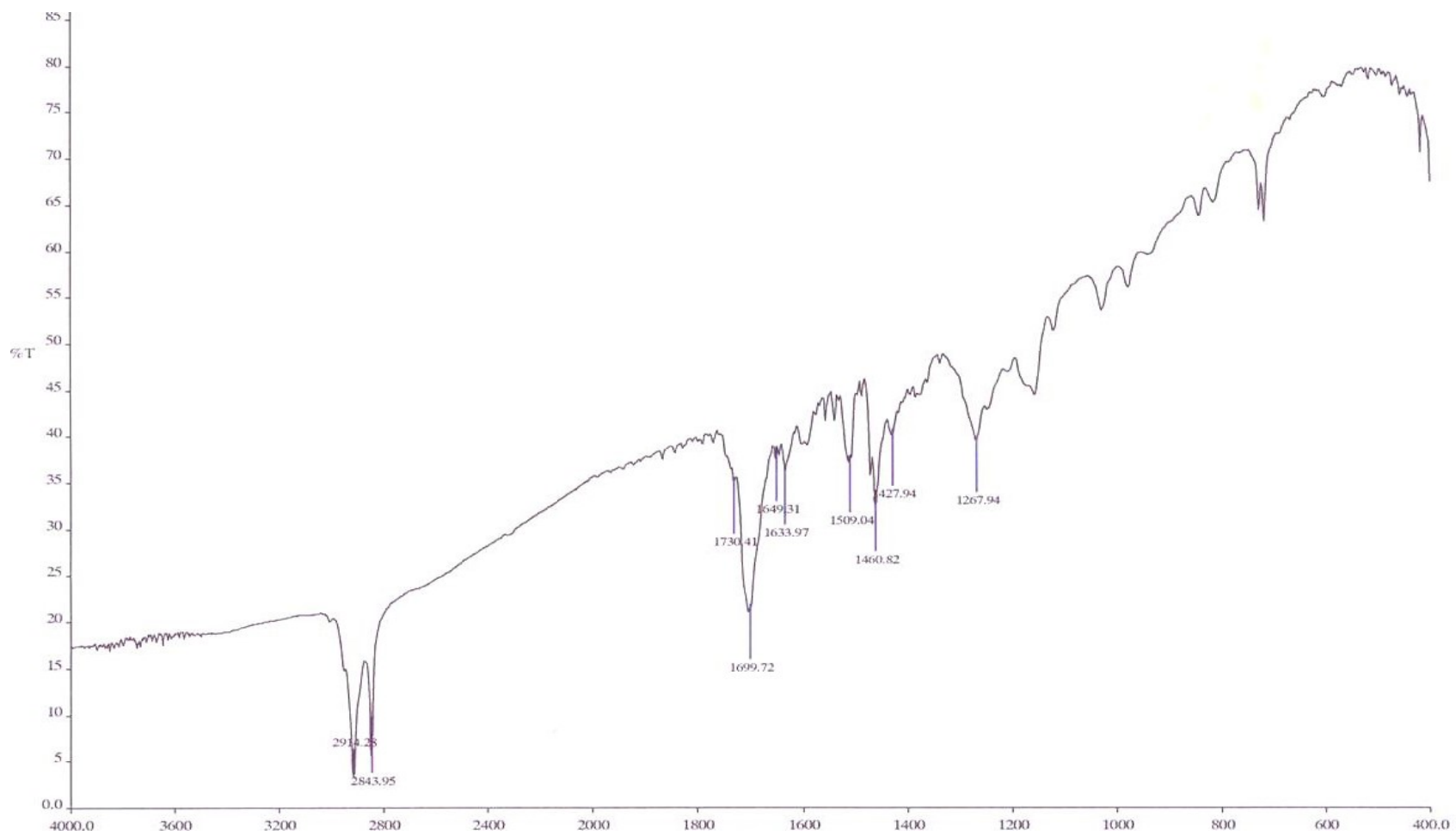


Fig. 4.42: IR spectrum of CMD-F

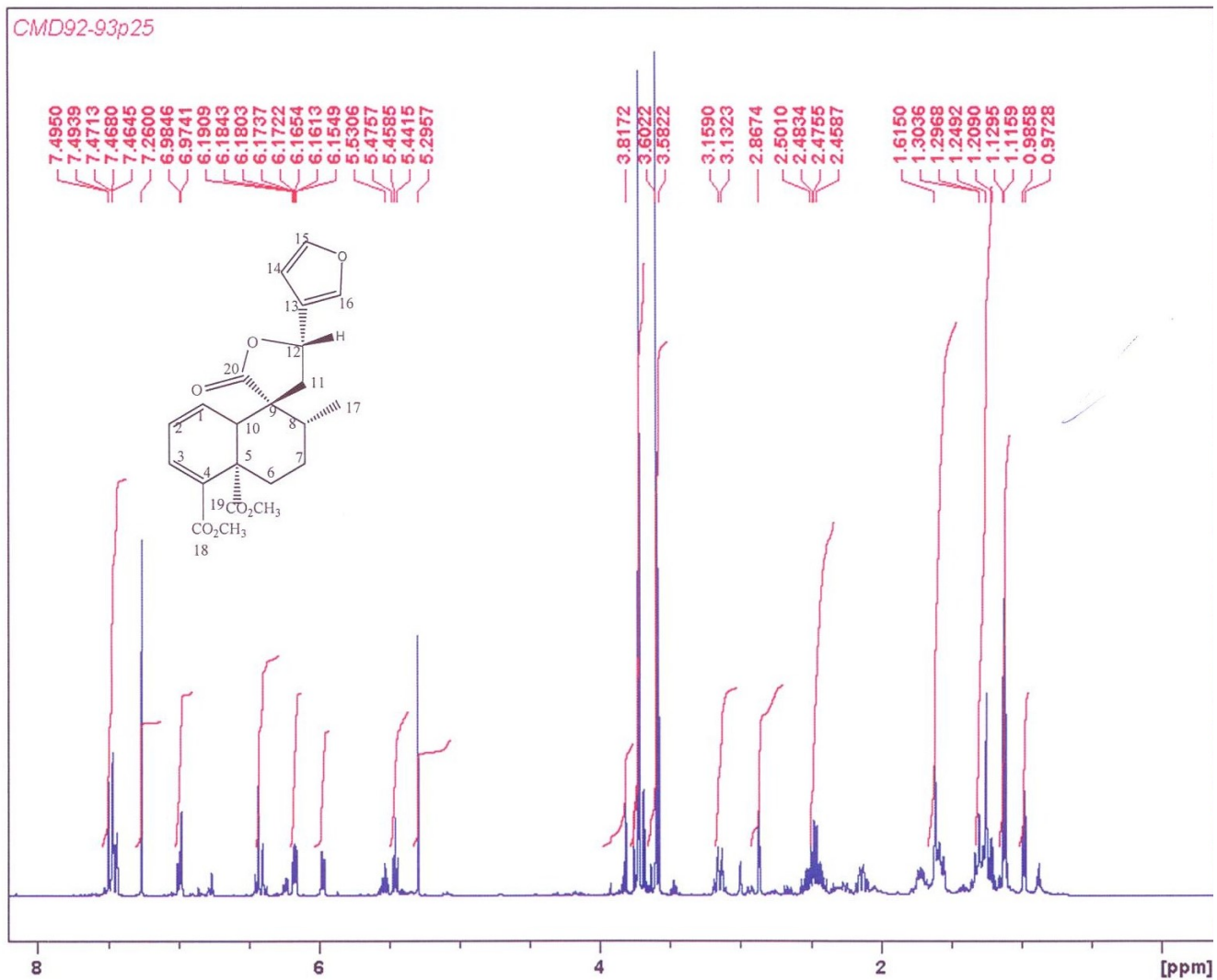


Fig. 4.43: ^1H NMR (500MHz) spectrum of CMD-F in CDCl_3

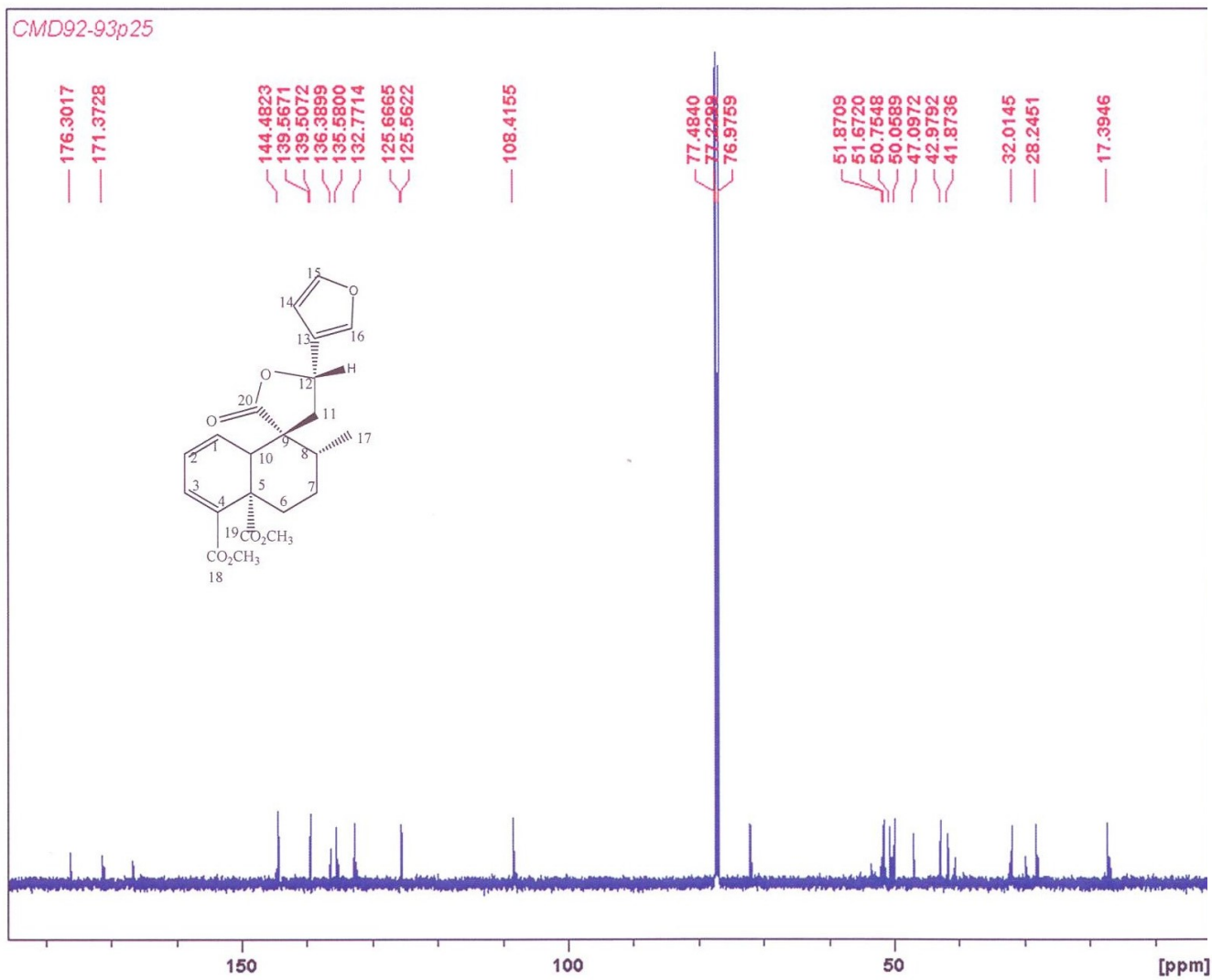


Fig. 4.44: ¹³CNMR spectrum of CMD-F in CDCl₃

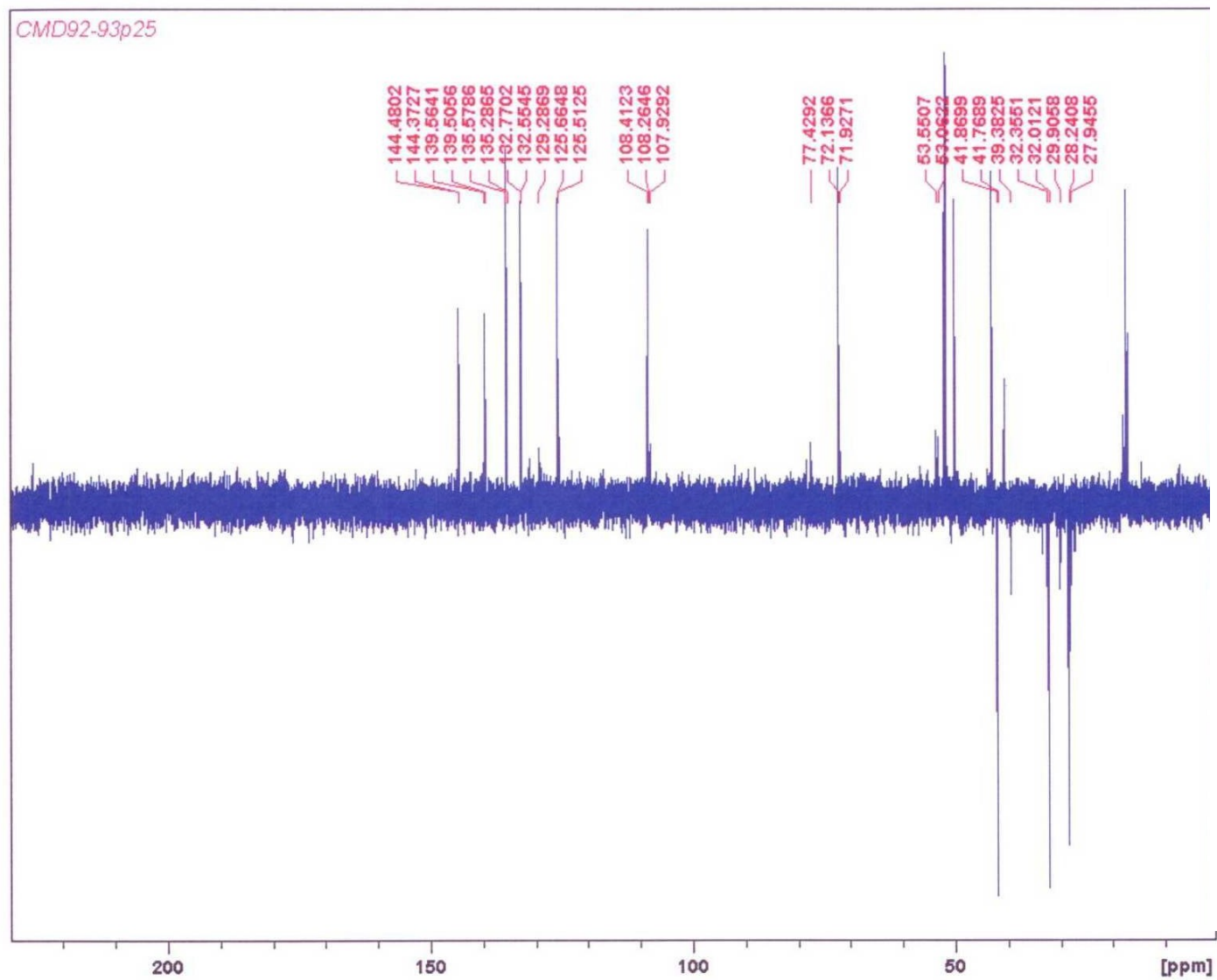


Fig. 4.45: DEPT spectrum of CMD-F in CDCl_3

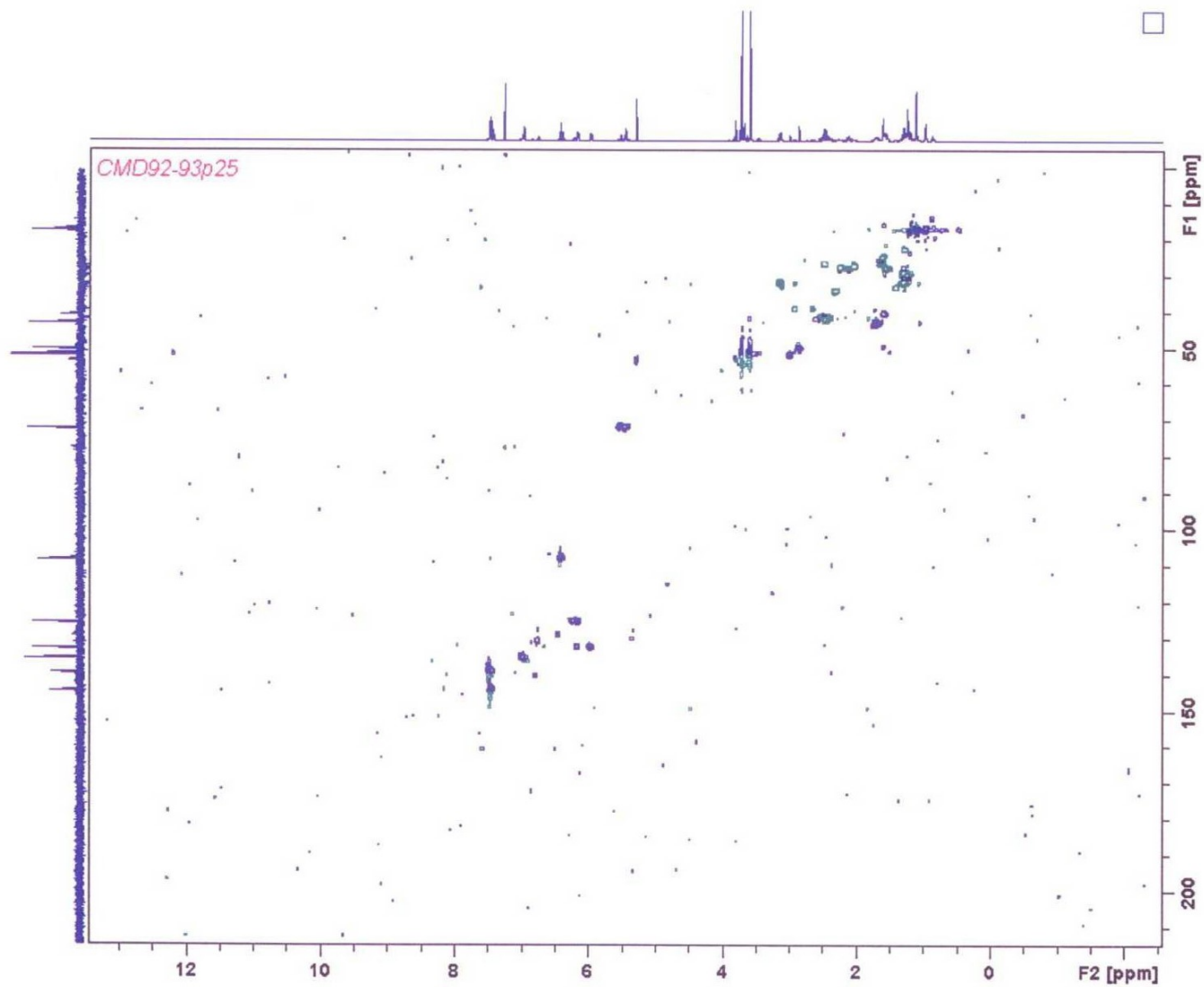


Fig. 4.46: HSQC DEPT spectrum of CMD-F in CDCl_3

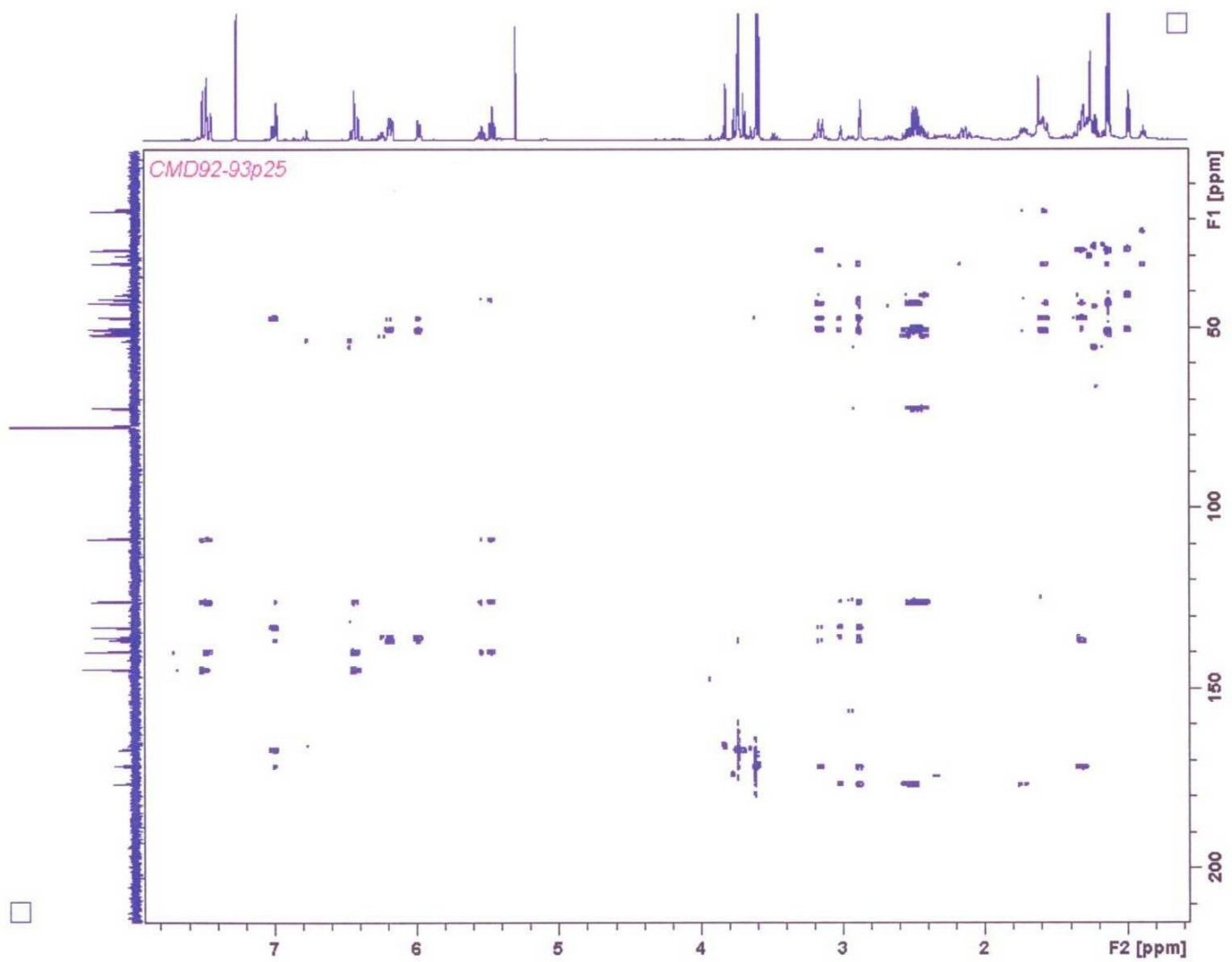


Fig. 4.47: HMBC spectrum of CMD-F in CDCl_3

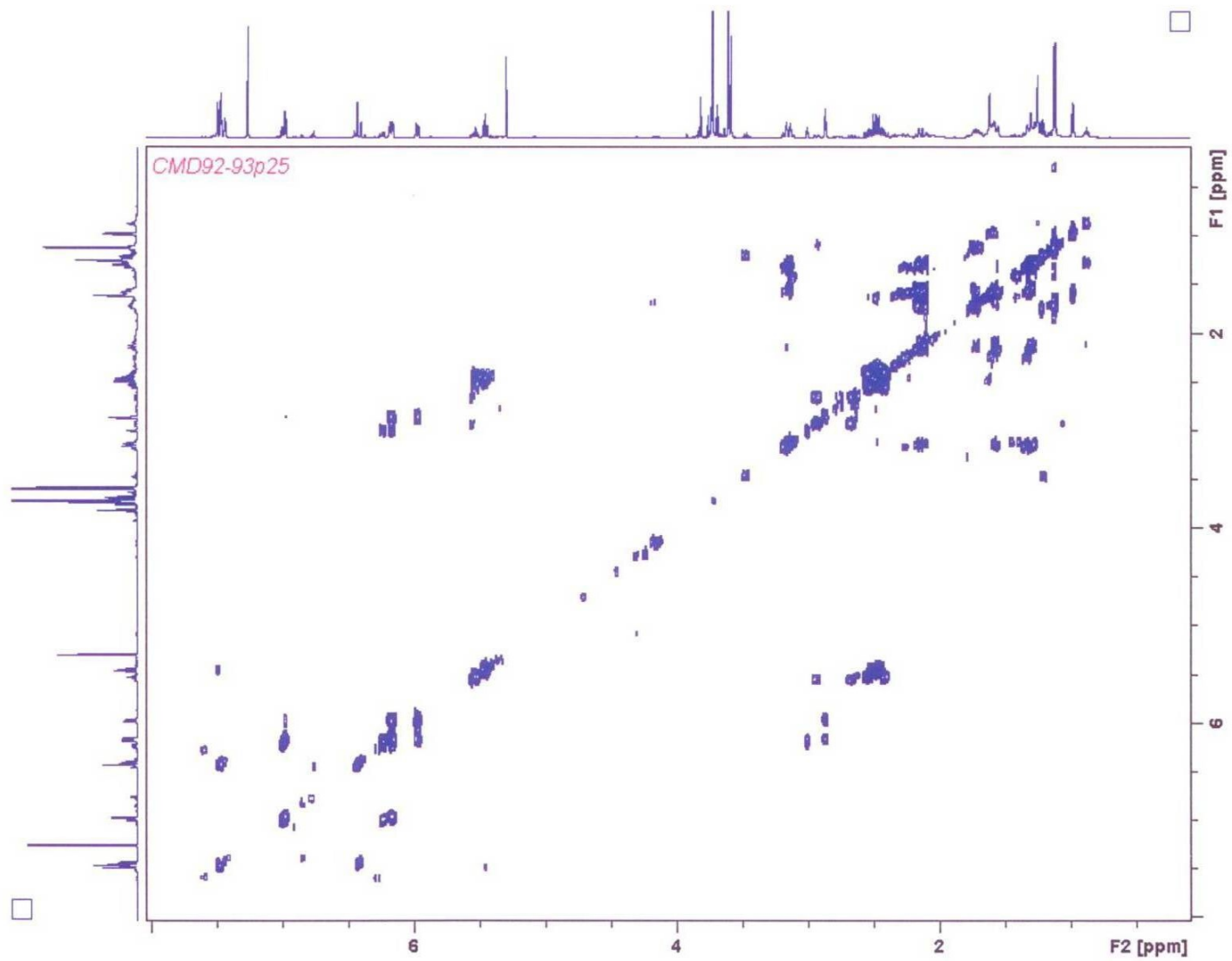


Fig. 4.48: COSY spectrum of CMD-F in CDCl₃

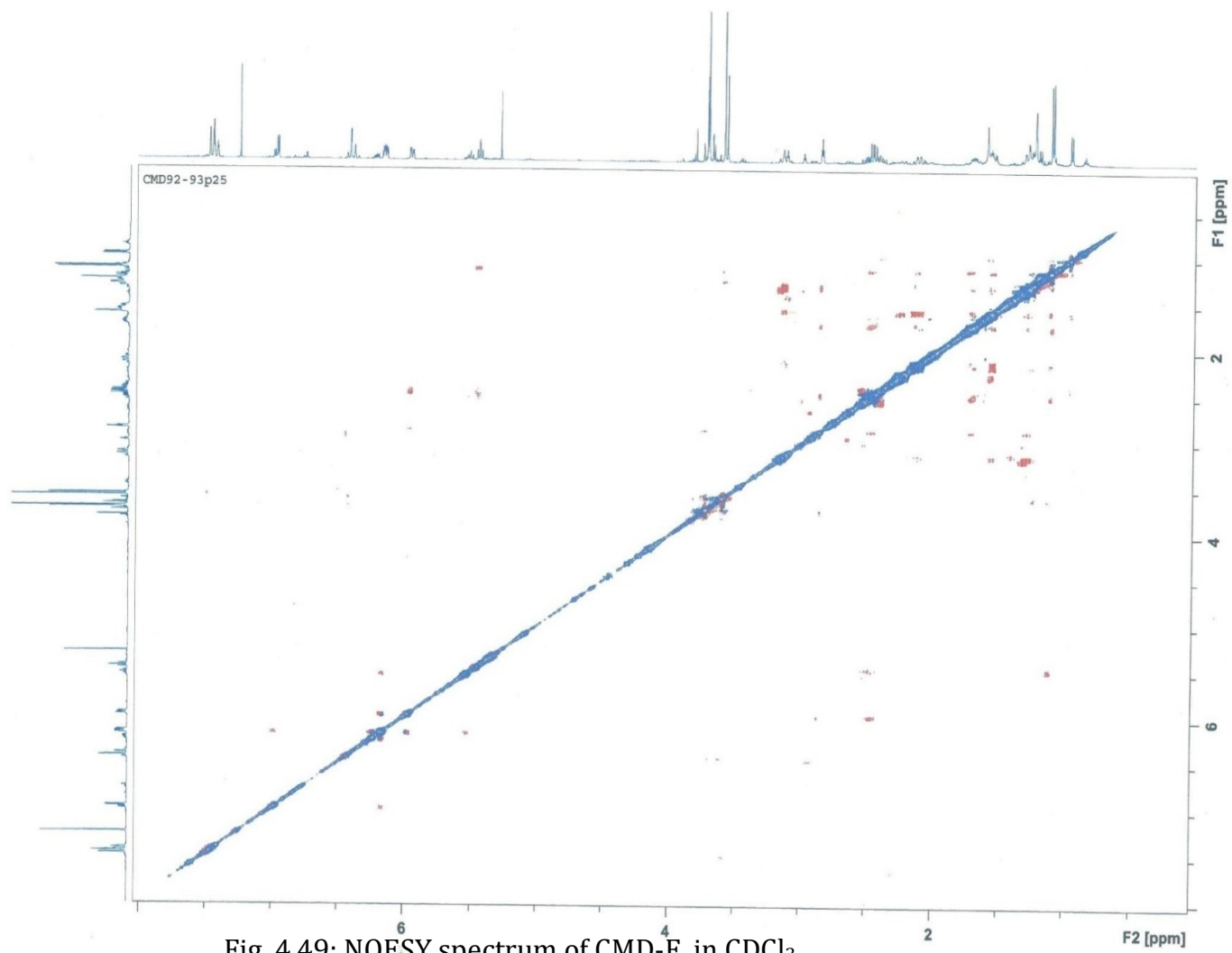


Fig. 4.49: NOESY spectrum of CMD-F in CDCl₃

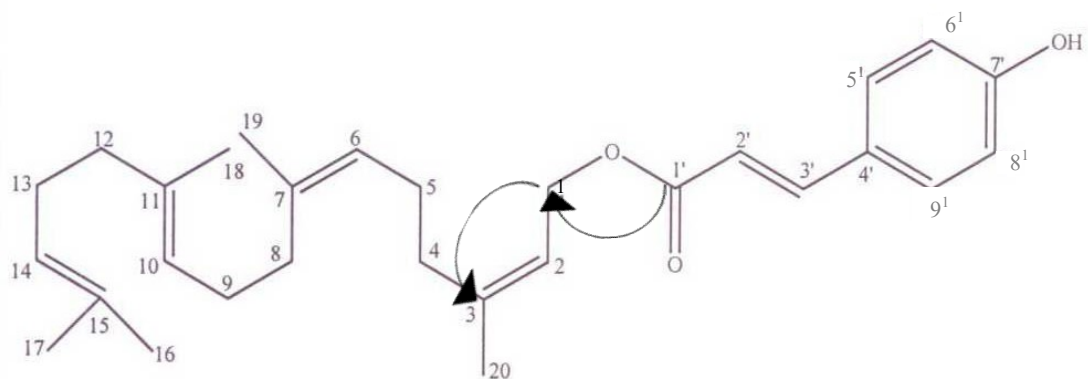
4.2.7 Structural elucidation of compound CMD-G

Compound **CMD-G** was isolated as a white solid. Its mass spectrum (Fig 4.50) had a molecular ion peak at m/z 459.8 for $[M + Na^+]$ consistent with the proposed molecular formula $C_{29}H_{40}O_3$. The FTIR spectrum (Fig 4.51) showed an O-H stretching absorption band at 3400 cm^{-1} and 1740 cm^{-1} for a carbonyl group. The ^{13}C NMR spectrum (Fig 4.53) of compound **CMD-G** showed twenty nine carbon resonances. The carbonyl carbon resonance at δ_C 167.7 was attributed to a conjugated carbonyl. An oxymethylene carbon resonance at δ_C 61.6 was also observed. A correlation was observed in the HMBC spectrum (Fig 4.56) of carbonyl carbon resonance δ_C 167.7 with an oxymethylene doublet proton resonance at δ_H 4.71 (d , $J=7.1\text{ Hz}$) indicating that the conjugated carbonyl is an ester and the oxymethylene proton is attached to an unsaturated carbon atom (sp^2). Proton resonances at δ_H 7.61(1H, $J=16.0\text{ Hz}$), 7.43 (2H, $J=8.0\text{ Hz}$), 6.80 (2H, $J=8.0\text{ Hz}$) and 6.32(1H, $J=16.0\text{ Hz}$) which are indicative of an aromatic ring were observed. Compound **CMD-G** therefore possesses an aromatic ring. The proton resonance at δ_H 5.43 did not correspond to a carbon resonance in the HSQC DEPT spectrum (Fig 4.55). It is thus assigned as the hydrogen of a hydroxyl group which is attributed to the para position of the aromatic ring at C-7'. The pair of doublets in the ^1H NMR spectrum (Fig 4.52) at δ_H 7.61 and δ_H 6.32 had similar coupling constant at $J=16.0\text{ Hz}$ suggesting the presence of a trans double bond. Another pair of two proton doublets at δ_H 7.43 and 6.80 with similar coupling constant of $J=8.0\text{ Hz}$ for ortho coupled aromatic resonances typical of a pair of parasubstituted aromatic system was also observed. These pair of parasubstituted proton resonances were assigned to H5'/H6' and H8'/H9'. The carbonyl carbon resonance at δ_C 167.7 showed correlations in the HMBC spectrum (Fig 4.56) to the trans-couple pair of doublets at δ_H 7.61 and δ_H 6.32. The downfield proton resonance at δ_H 7.61 was assigned as H-2' as it further showed a correlation in the HMBC

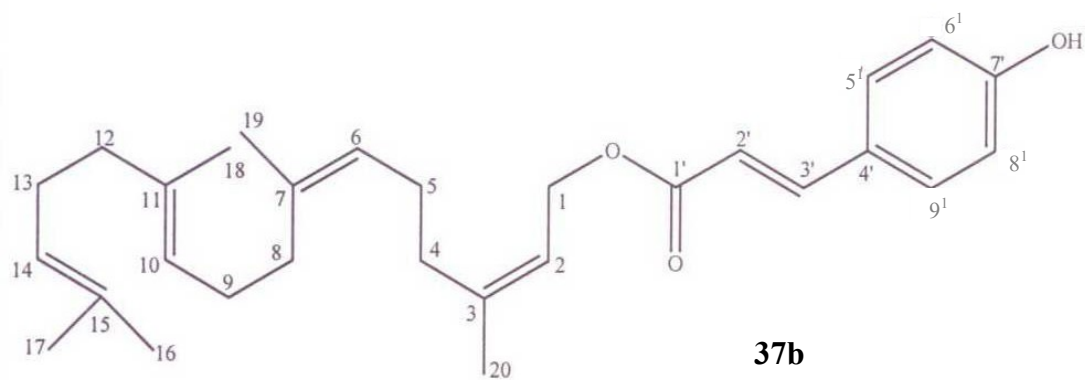
spectrum (Fig 4.56) to the fully substituted carbon resonance at δ_C 158.0 for C-4'. Furthermore, the H-3' proton resonance at δ_H 6.32 showed a correlation in the HMBC spectrum (Fig 4.56) with a carbon resonance at δ_{C-4} 158.0. These nine carbon resonances on comparison with literature suggested that the group is *p*-hydroxy coumarate (Renata *et al.*, 2012). This left a balance of twenty carbon resonances.

The oxymethylene doublet resonance at δ_H 4.71 was observed to couple with a double bond proton at δ_H 5.43 in the COSY spectrum (Fig 4.57). The 1H NMR spectrum (Fig 4.52), proton resonances at δ_H 5.43, 4.71 and three overlapped double bond proton resonances at δ_H 5.10 were observed. In addition, five methyl proton singlets at 1.68 , 1.60 , 1.60 , 1.60 and 1.70 were observed. From the HSQC spectrum(Fig 4.55), the carbon resonances at δ_C 123.8, 142.5, 124.4, 135.7, 124.4, 135.2, 124.6 and 131.4 were assigned to C-2, C-3, C-6, C-7, C-10, C-11, C-14 and C-15. On comparison with literature, these twenty carbon resonances were comparable to those of the known geranyl geraniol (Fedeli *et al.*, 1966).

Correlations were observed between carbonyl carbon resonance δ_{C-1} 167.7 of the *p*-hydroxy coumarate with an oxymethylene doublet proton resonance at δ_{H-1} 4.71 (*d*, $J=7.1$ Hz) in the geranyl geraniol moiety and between δ_{H-1} 4.71 with δ_{C-3} 142.5 in the HMBC spectrum (Fig 4.56) as illustrated in [37a]. The above NMR data suggested that this compound was a new lactonized geranyl geraniol with *p*. coumaric acid. It was determined as 1-(*p*-hydroxy coumaric acid) – geranyl geran-1-ol [37b]. This is the first report of this compound in nature to the best of our knowledge.



37a



37b

Table 7a: Correlation Table of ^1H (500 MHz) and ^{13}C (125 MHz) NMR Data^a for compound CMD-G: *p*-hydroxy coumaric acid and Literature^b in CDCl_3

No	^{13}C NMR ^a (125 MHz) CDCl_3	^{13}C NMR ^b (125 MHz) CDCl_3	^1H NMR ^a (500 MHz) CDCl_3	^1H NMR ^b (500 MHz) CDCl_3
1'	167.7	167.7	-	-
2'	144.6	144.9	7.61(1H,d)	7.62(1H,d)
3'	115.9	115.9	6.32(1H,d)	6.32(1H,d)
4'	158.0	158.0	-	-
5'/9'	115.8	115.8	6.80(2H,d)	6.79(2H,d)
6'/8'	130.1	130.1	7.43(2H,d)	7.46(2H,d)
7'	127.5	127.5	-	-
HO-7	130.2	115.4	5.62	5.62

^a Assignment aided by HMQC and HMBC experiments

^b Literature data of *p*-hydroxy coumaric acid (Renata *et al.*, 2012)

Table 7b: Correlation Table of ^1H (500 MHz) and ^{13}C (125 MHz) NMR Data^a for compound CMD-G: Geranyl geran-1-ol and Literature^b in CDCl_3

No	^{13}C NMR ^a (125 MHz) CDCl_3	^{13}C NMR ^b (125 MHz) CDCl_3	^1H NMR ^a (500 MHz) CDCl_3	^1H NMR ^b (500 MHz) CDCl_3
1	61.6	60.9	4.71 d	4.63 d
2	123.8	123.5	5.43 dd	5.43 dd
3	142.5	141.9	-	-
4	39.9	39.6	2.00 dd	2.00 dd
5	27.4	26.8	2.00 dd	2.00 dd
6	124.4	123.9	5.10 ddd	5.10 ddd
7	135.7	135.5	-	-
8	39.9	39.8	2.00 dd	2.00 dd
9	26.7	26.7	2.10 dd	2.10 dd
10	124.4	124.3	5.10 ddd	5.10 ddd
11	135.2	135.0	-	-
12	39.8	39.8	2.05 dd	2.05 dd
13	26.4	26.4	2.10 dd	2.10 dd
14	124.6	124.5	5.10 ddd	5.10 ddd
15	131.4	131.3	-	-
16	25.9	25.7	1.68 s	1.68 s
17	17.9	17.9	1.60 s	1.60 s
18	16.2	16.2	1.60 s	1.60 s
19	16.2	16.2	1.60 s	1.60 s
20	16.7	16.5	1.70 s	1.70 s

^a Assignment aided by HMQC and HMBC experiment

^b Literature data of geranylgeraniol (Fedeli *et al.*, 1966)

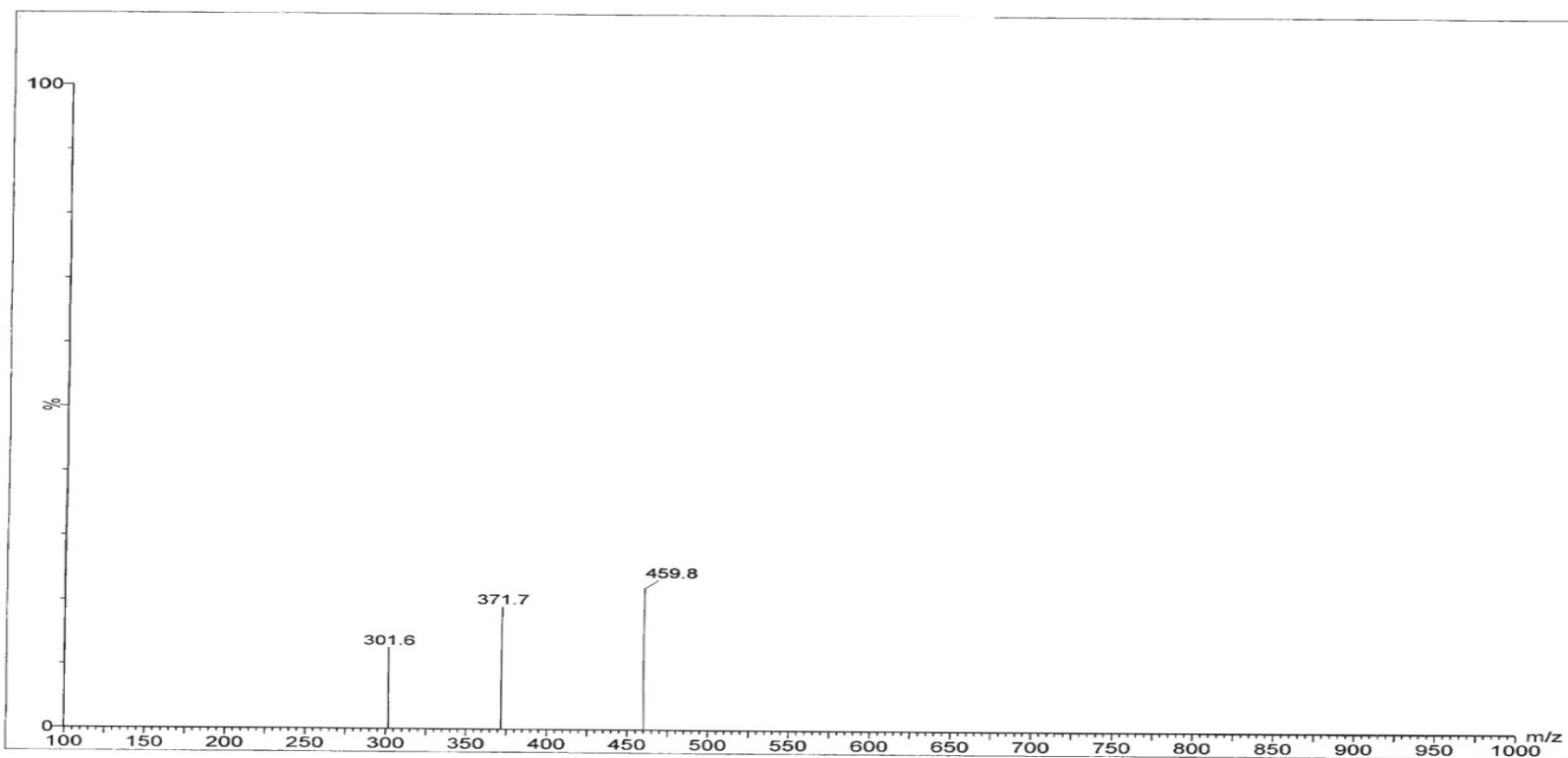
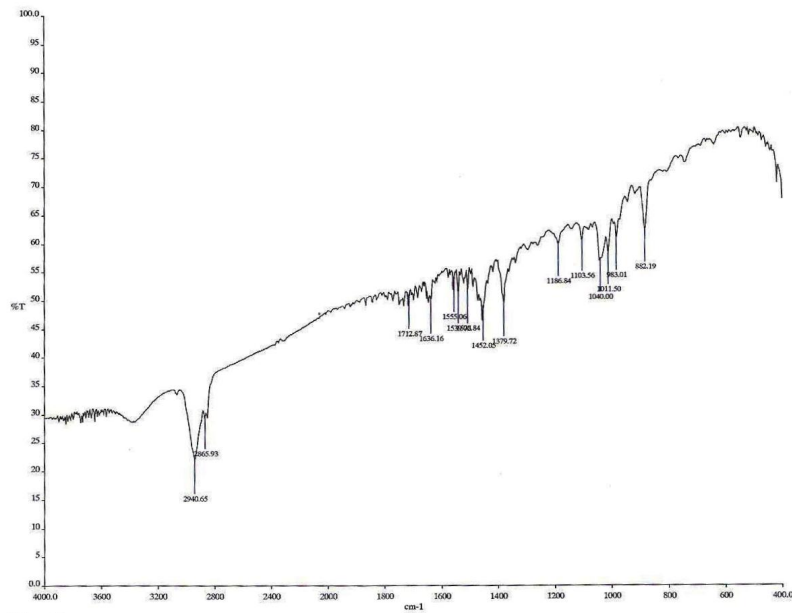


Fig 4.50:MS spectrum of CMD-G in CDCl₃



Top 3

Fig. 4.51 : IR spectrum of CMD-G

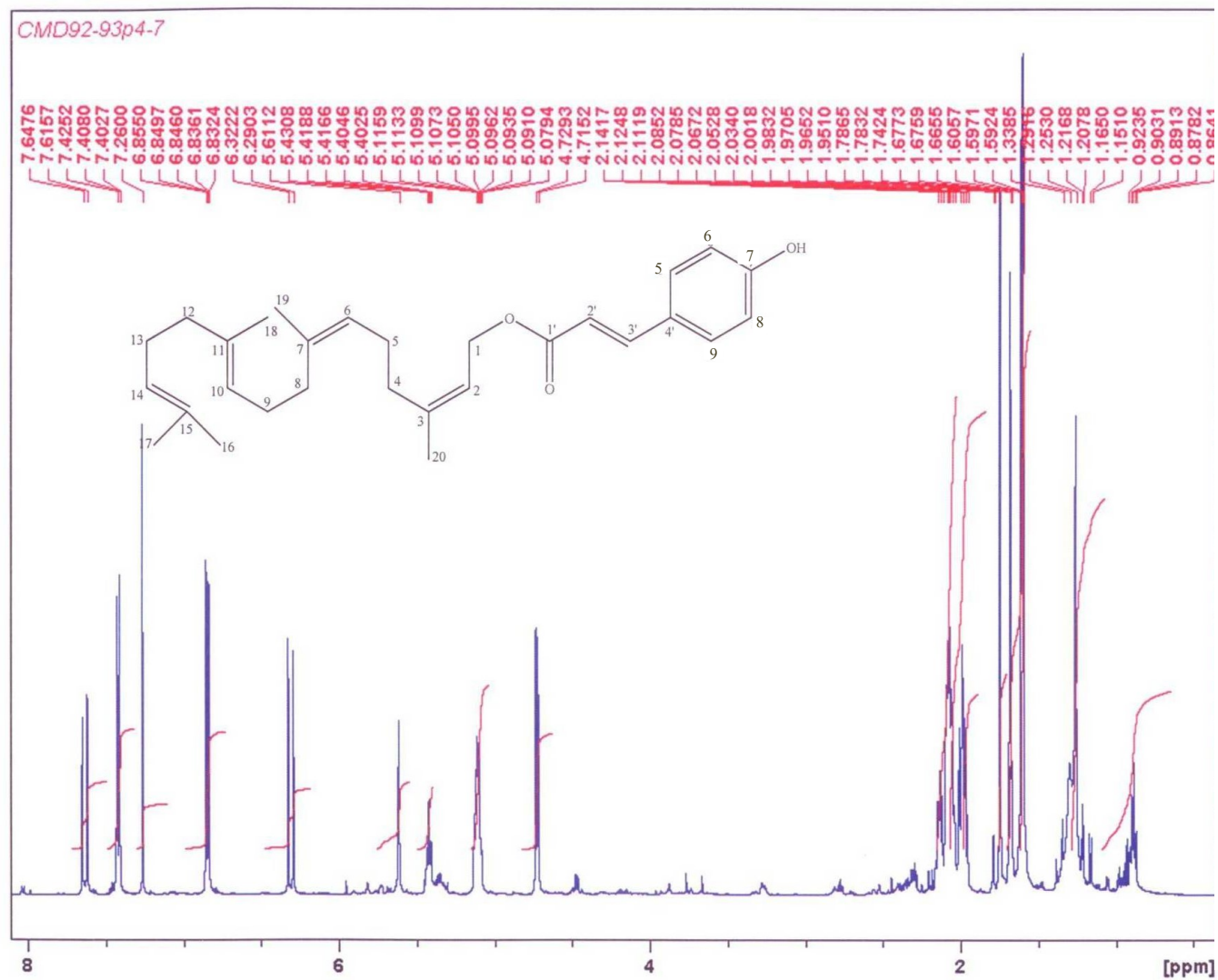


Fig. 4.52: ^1H NMR (500MHz) spectrum of CMD-G in CDCl_3

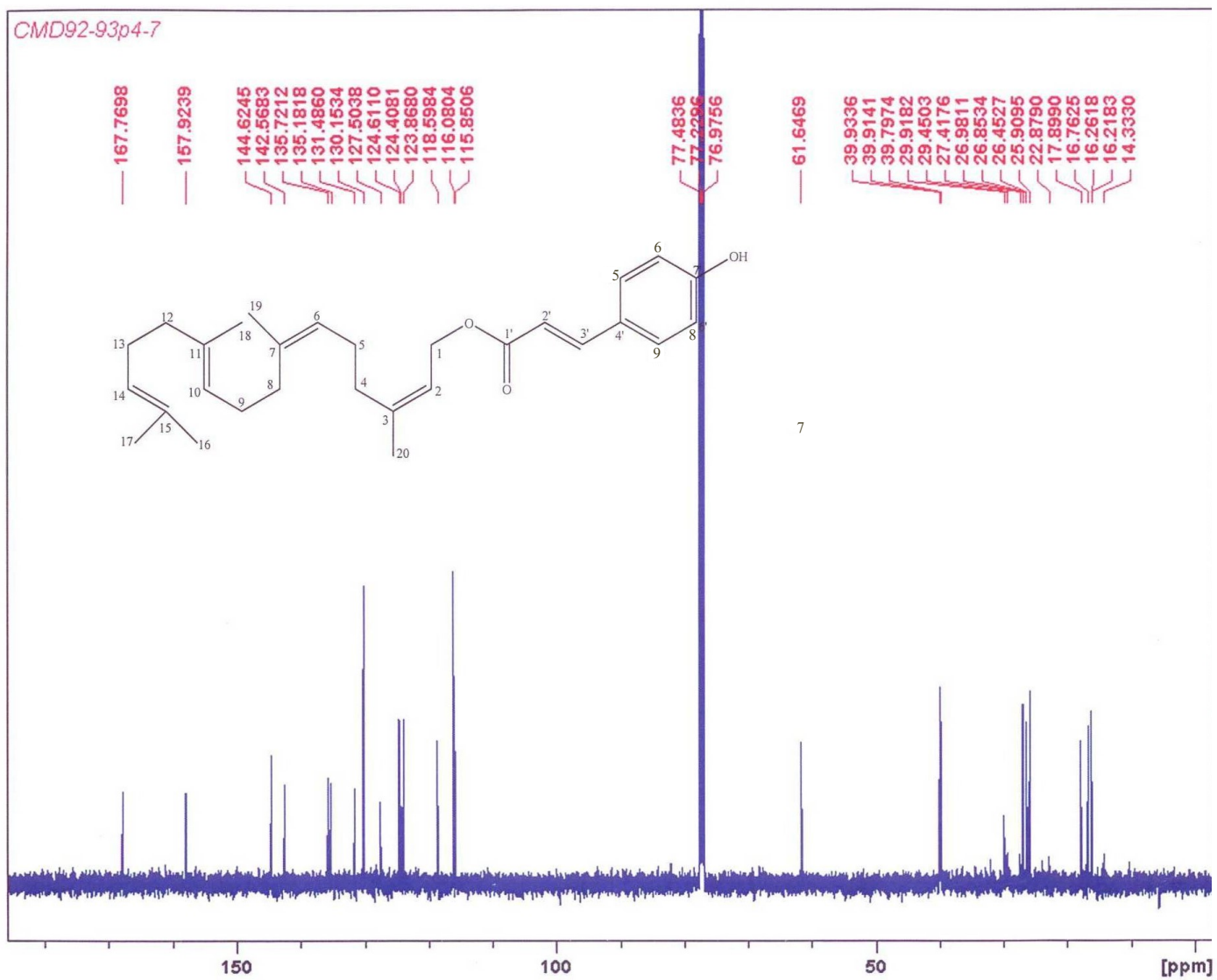


Fig. 4.53: ¹³CNMR (125 MHz) spectrum of CMD-G in CDCl₃

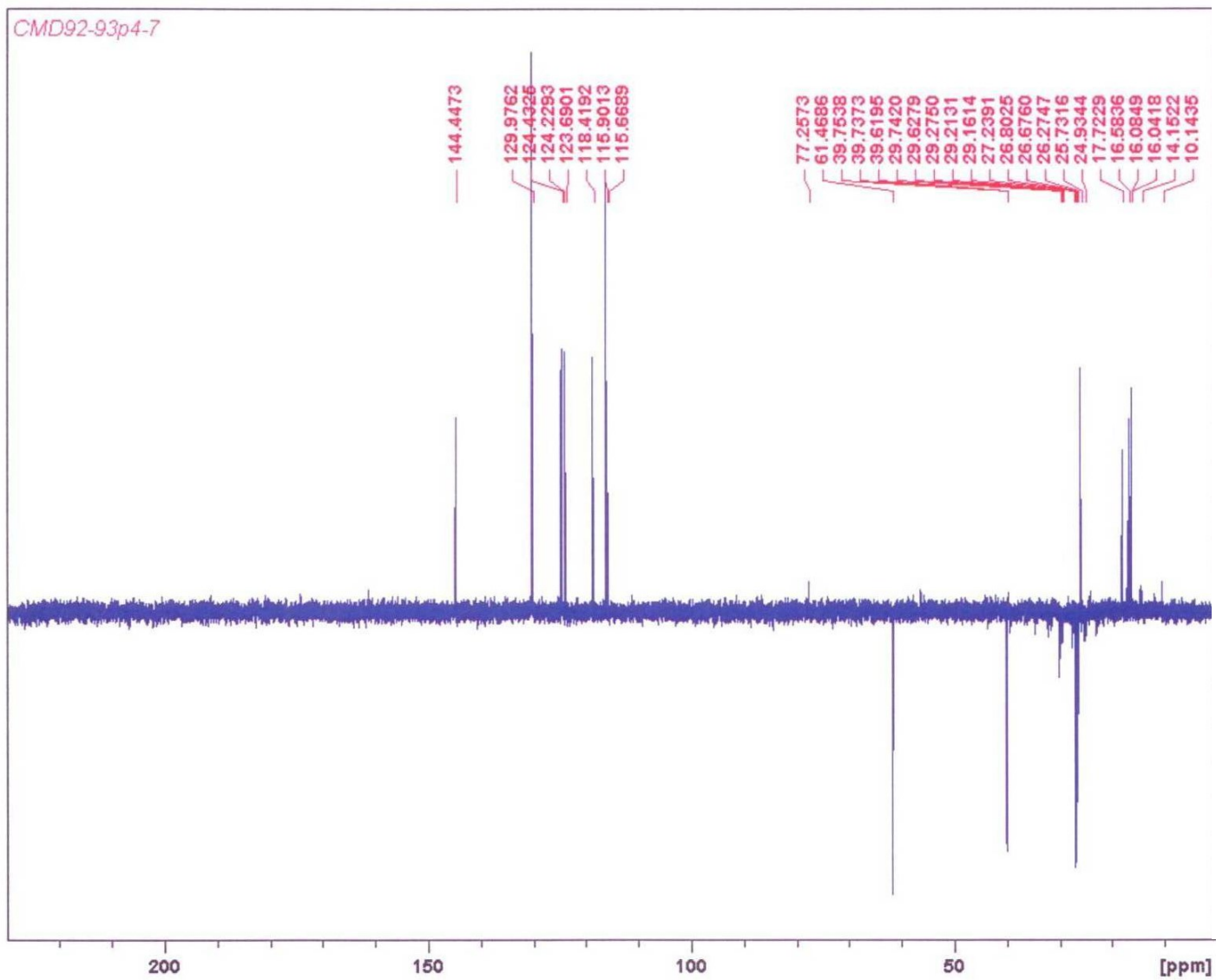


Fig. 4.54: DEPT spectrum of CMD-G in $CDCl_3$

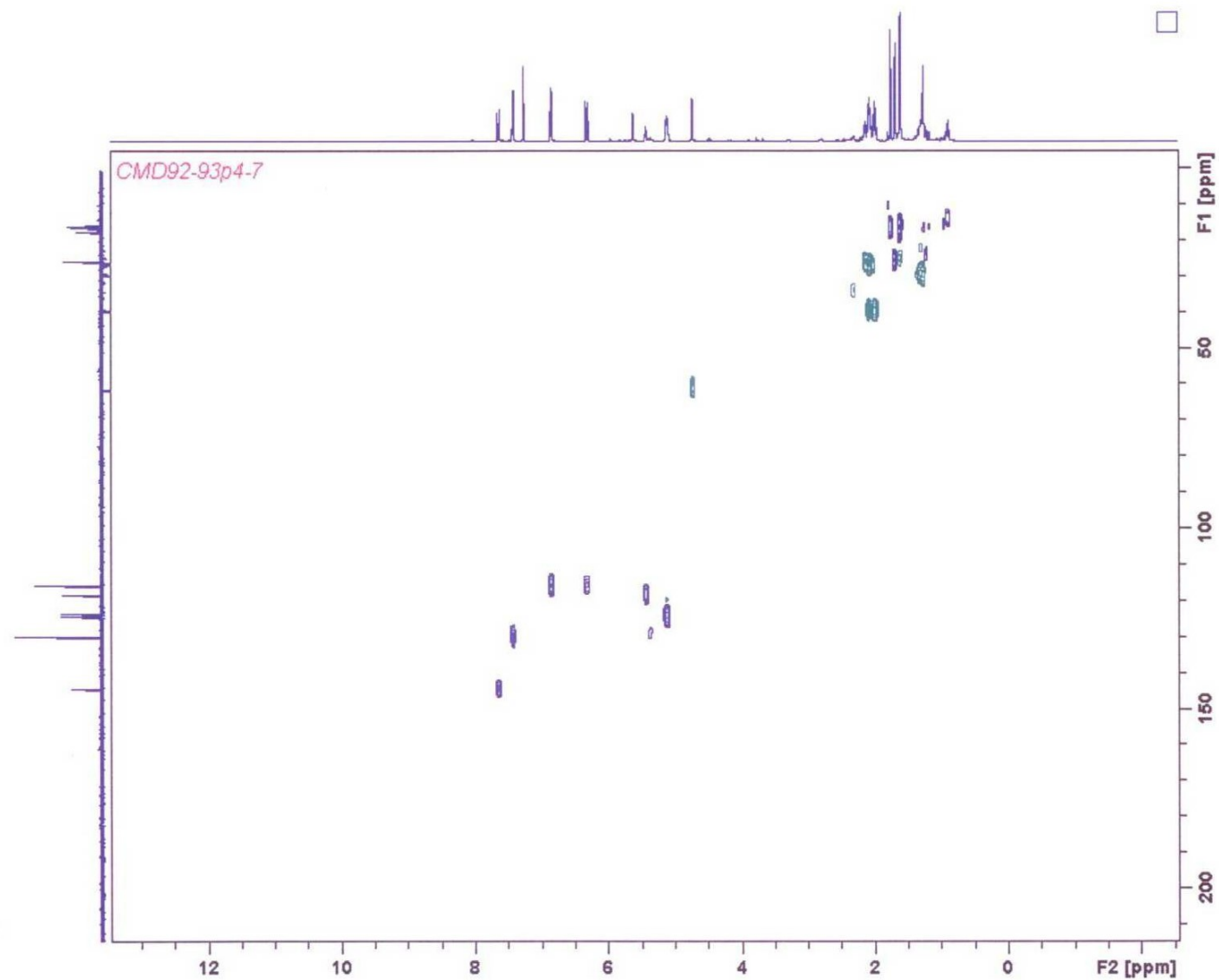


Fig. 4.55: HSQC DEPT spectrum of CMD-G in CDCl_3

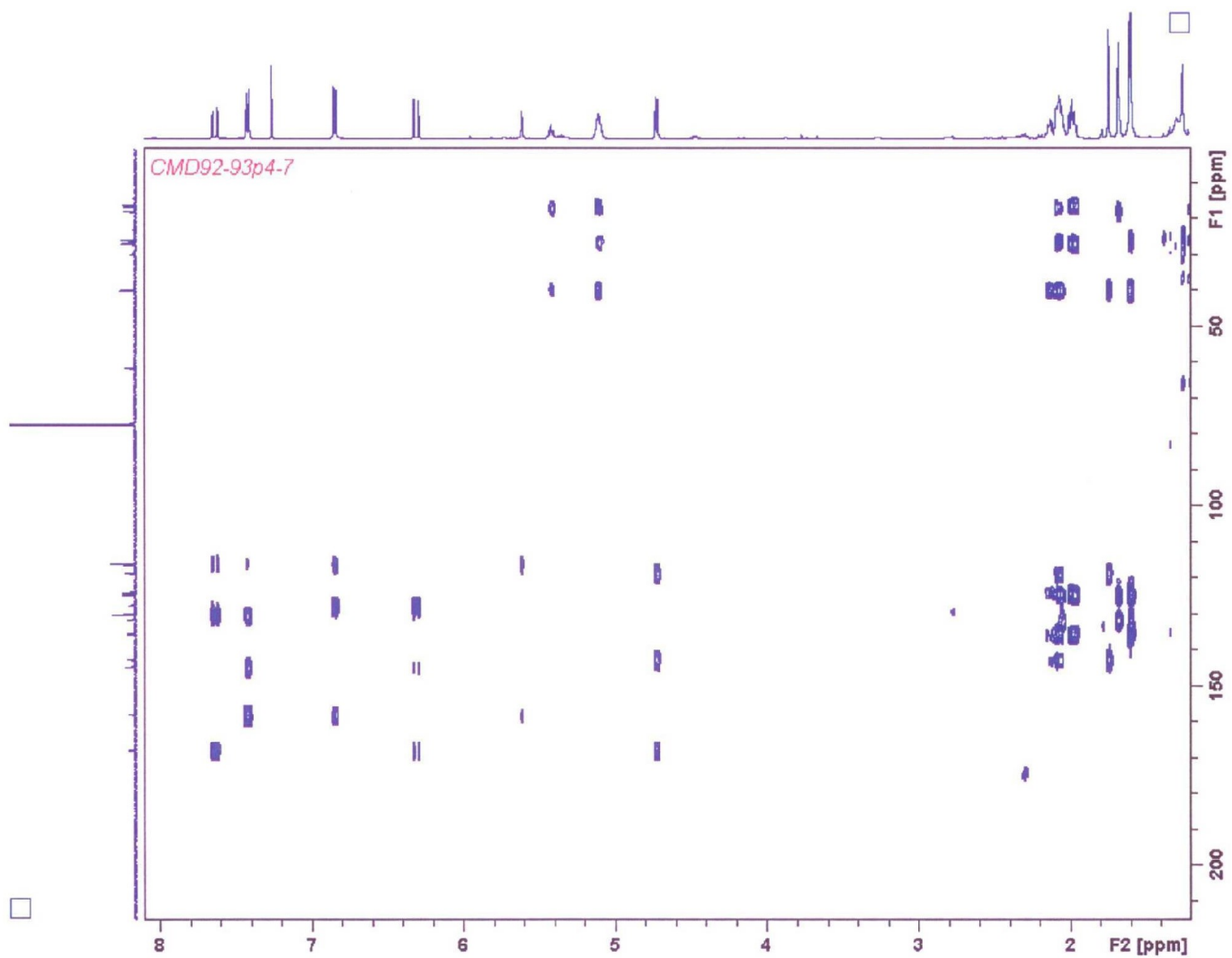


Fig. 4.56: HMBC spectrum of CMD-G in CDCl₃

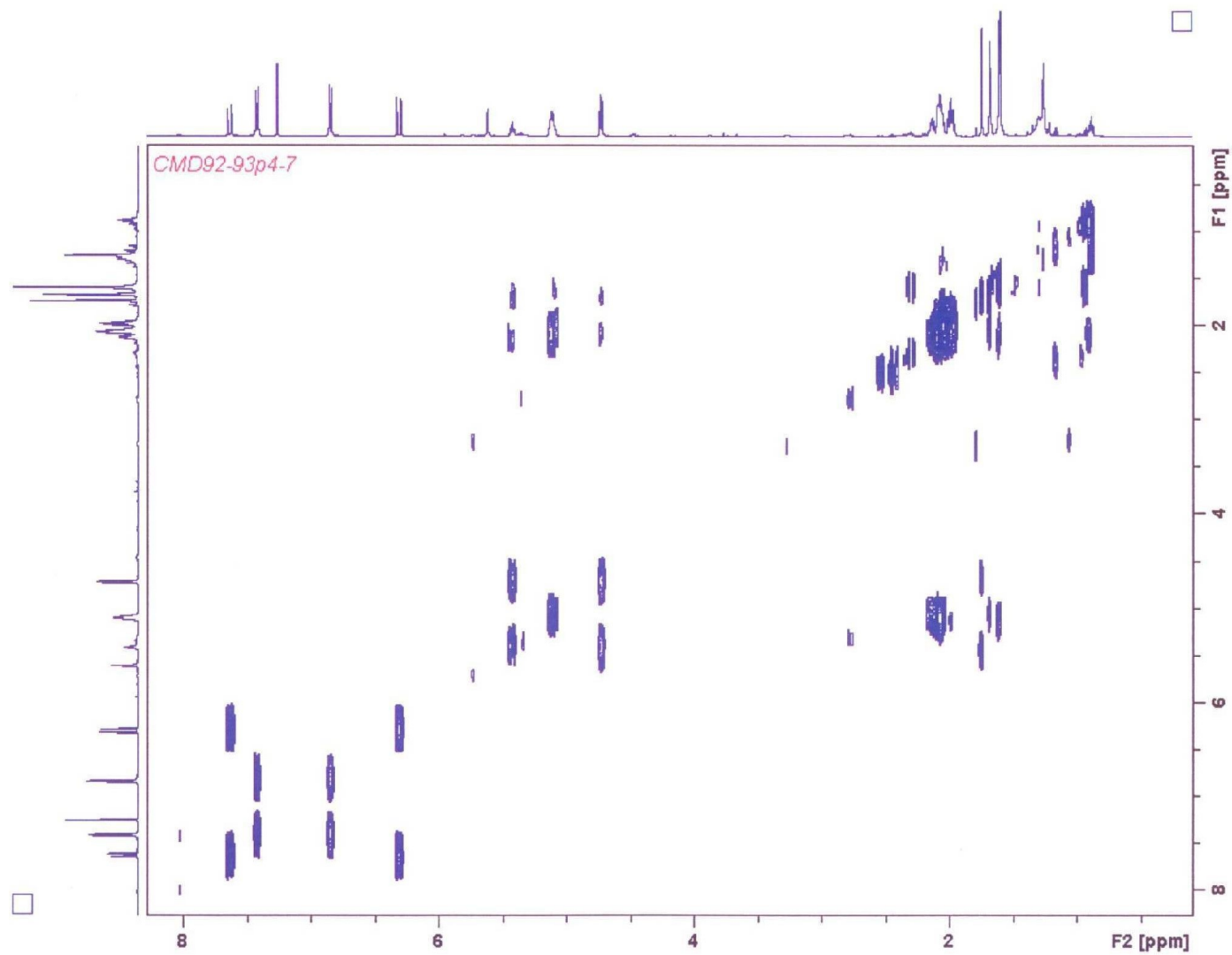


Fig. 4.57: COSY spectrum of CMD-G in $CDCl_3$

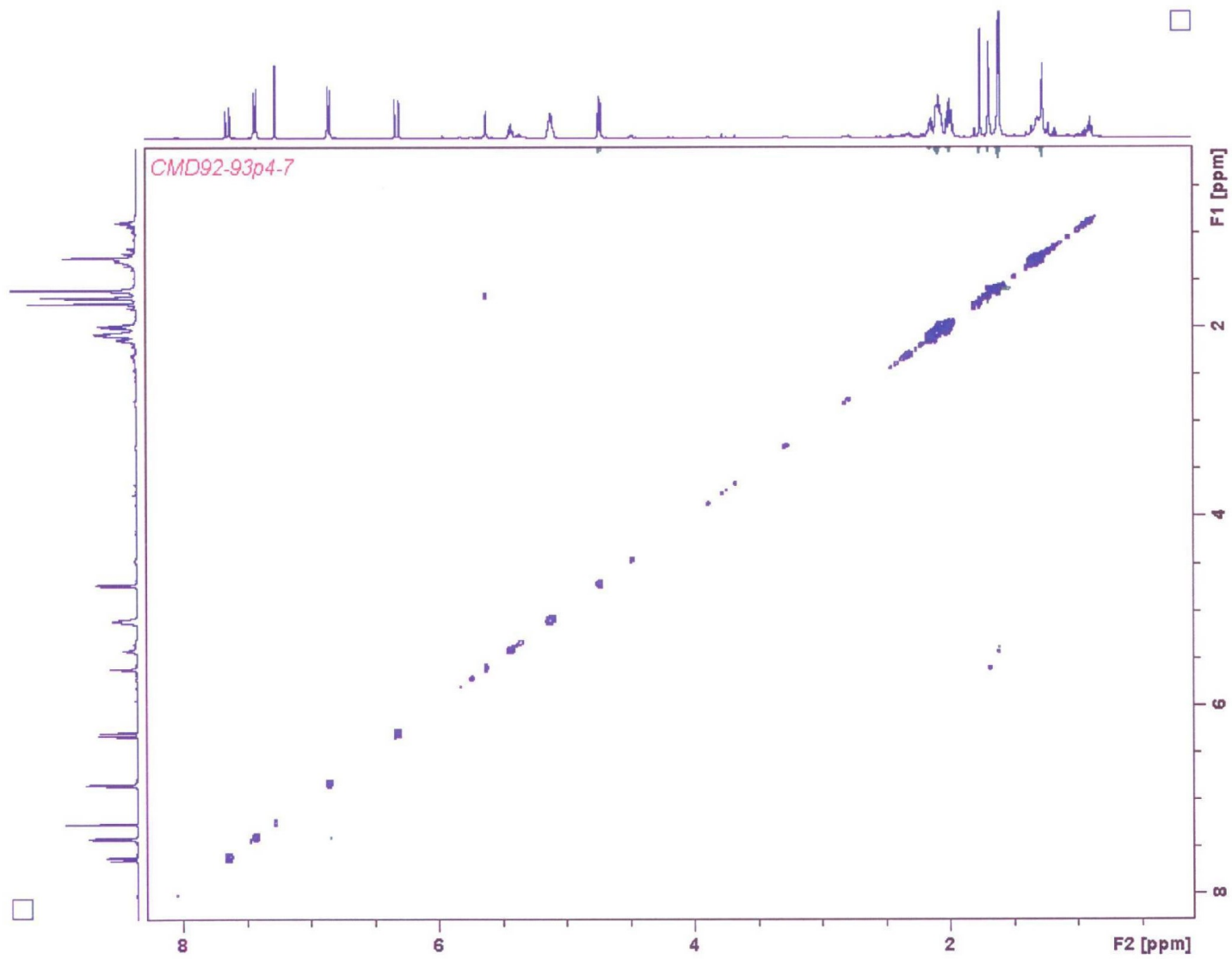
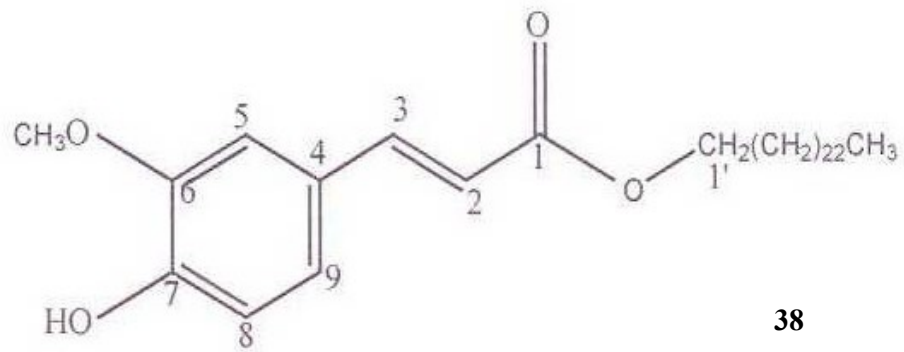


Fig. 4.58: NOESY spectrum of CMD-G in CDCl₃

4.2.8 Structural elucidation of compound **CMD-H**

Compound **CMD-H** was isolated as a white solid from the DCM extract of *C. megalocarpoides*. The FTIR spectrum (Fig.4.59) showed absorption bands at 3472 and 1769 cm^{-1} . The ^{13}C -NMR spectrum (Fig 4.61) for compound **CMD-H** showed one carbonyl carbon resonance at δ_{C} 167.6 and eight double bond carbon resonances at 116.0, 144.9, 127.1, 109.5, 148.1, 147.0, 114.9 and 123.2.

The ^1H NMR spectrum (Fig 4.60) showed the presence of a typical methoxy group proton resonance at δ_{H} 3.90(s), trans double bond proton resonances at δ_{H} 6.27 and 7.60. The integral of the proton resonances that occurred at δ_{H} 0.85, 1.25 and 1.67 (2H, t, $J = 6.6$ Hz) for the aliphatic chain showed approximately 49 protons. Proton resonances at δ_{H} 7.02, 6.89 and 7.03 were assigned as H-5, H-8 and H-9 respectively. The corresponding carbon resonances occurred at δ_{C} 109.5 (C-5), 114.9 (C-8) and 123.2 (C-9) in the ^{13}C NMR spectrum (Fig 4.61). In the NOESY spectrum (Fig 4.67), a correlation between the methoxy group (δ_{H} 3.90, s) and the H-5 resonance allowed for the placement of the methoxy group on C-6. A search in the literature showed that compound **CMD-H** exhibited ^1H NMR and ^{13}C NMR data that were similar to those of the known lignoceryl-trans-ferulate (Kuo, 1999). Compound **CMD-H** [38] was determined to be the known lignoceryl-trans-ferulate.



38

Table 8: Correlation Table of ^1H (500 MHz) and ^{13}C (125 MHz) NMR Data^a for compound CMD-H: lignoceryl-trans-ferulate in CDCl_3

No	^{13}C NMR ^a (125 MHz) CDCl_3	^{13}C NMR ^b (125 MHz) CDCl_3	^1H NMR ^a (500 MHz) CDCl_3	^1H NMR ^b (500 MHz) CDCl_3
1	167.6C	167.6C	-	
2	116.0CH	116.0CH	6.27 d	6.29 d
3	144.9CH	144.9CH	7.60 d	7.60 d
4	127.1C	127.1C	-	-
5	109.5CH	109.5CH	7.02 d	7.03 d
6	148.1C	148.1C	-	-
7	147.0C	147.0C	-	-
8	114.9CH	114.9CH	7.03 dd	7.06 dd
9	123.2CH	123.2CH	6.89 d	6.91 d
1''	64.8CH ₂	64.8CH ₂	4.17 t	4.18 t
2''	29.2CH ₂	29.2CH ₂	1.67 t	1.70 t
3''-22''	32.1,29.2,29.6,2 9.5,26.2,22.9CH 2	32.1,29.2,29.6,29. 5,26.2,22.9CH ₂	1.25 br s [*]	1.25 br s [*]
23''	14.33 CH ₃	14.33 CH ₃	0.85 t	0.87 t
OCH ₃	56.1 CH ₃	56.1 CH ₃	3.90 s	3.93 s
OH	-	-	5.96 br s	5.83 br s

*Refer to superimposed proton resonances

^a Assignment aided by HMQC and HMBC experiments

^b Literature data of lignoceryl ferulate (kuo,1999)

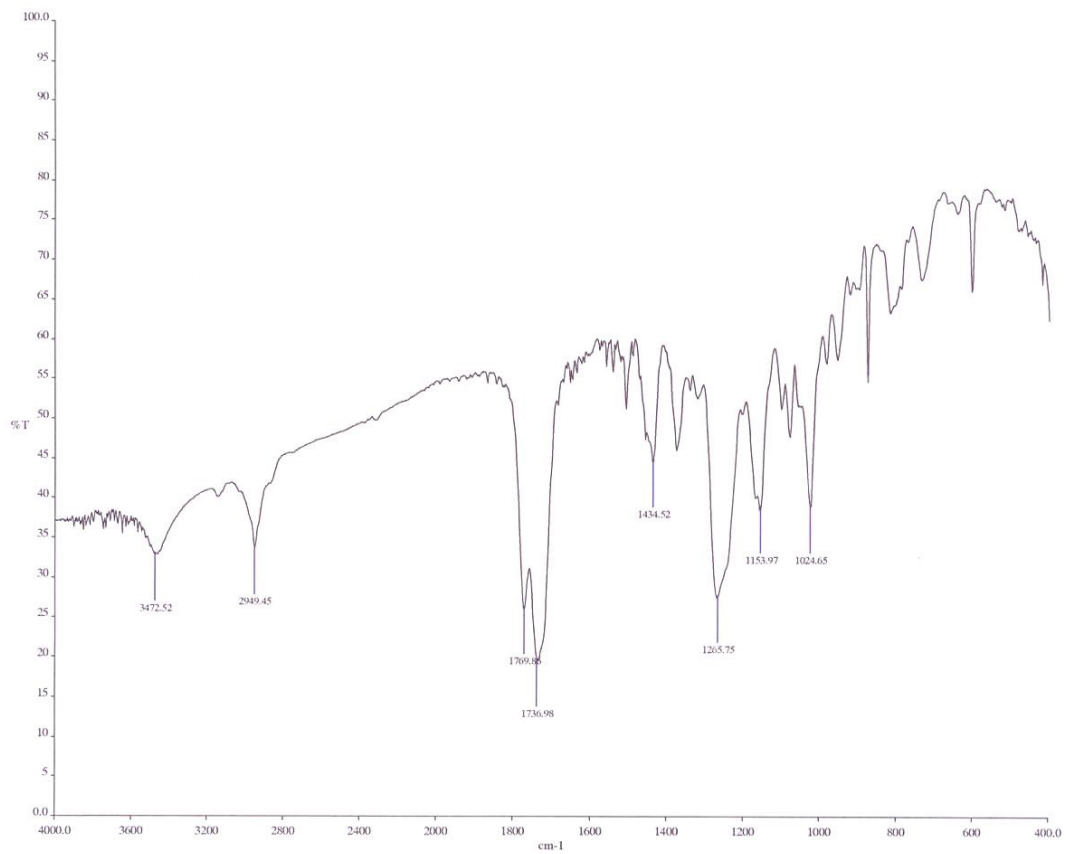


Fig. 4.59: IR spectrum of CMD-H in CDCl₃

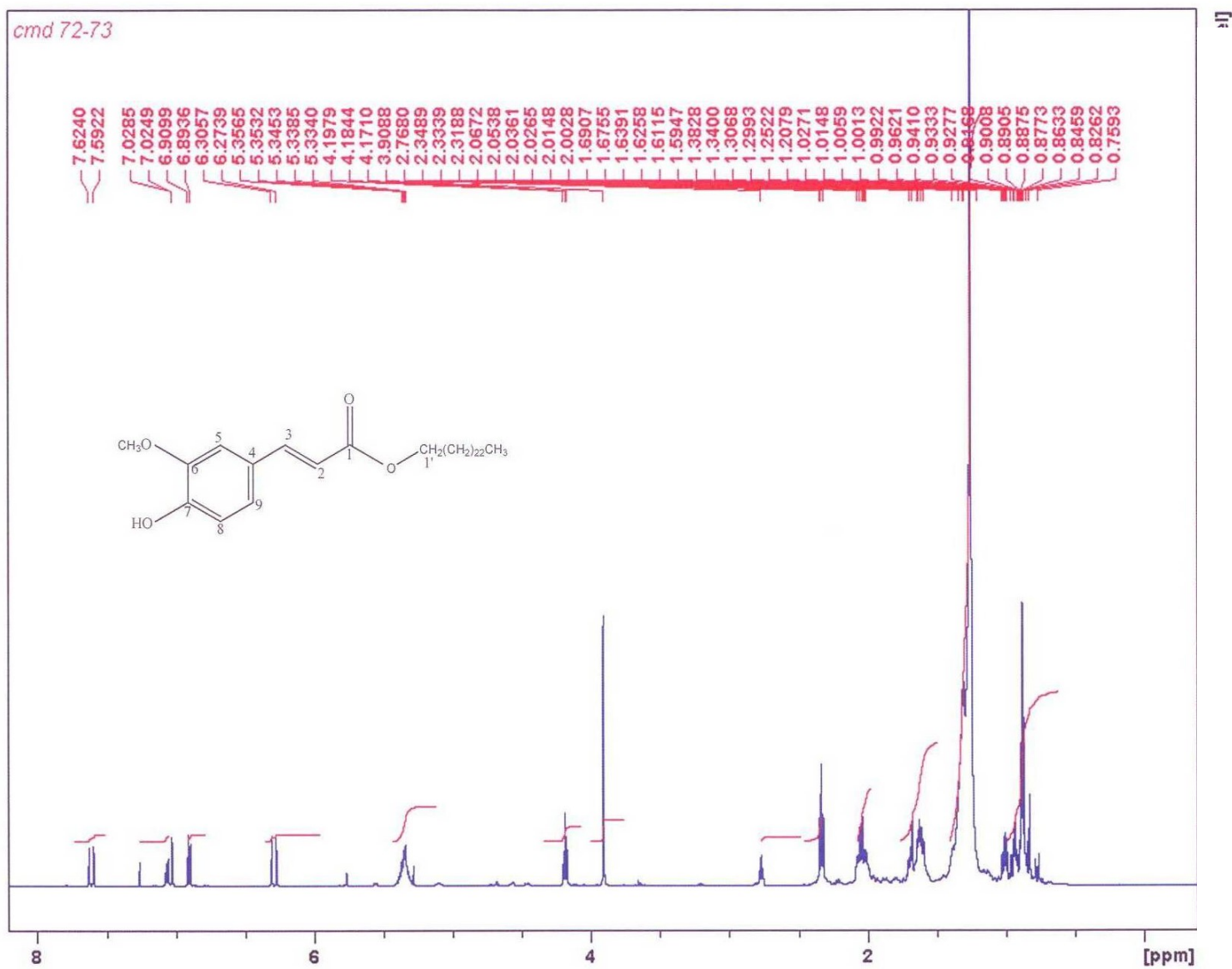


Fig. 4.60: ¹H-NMR (500MHz) spectrum of CMD-H in CDCl₃

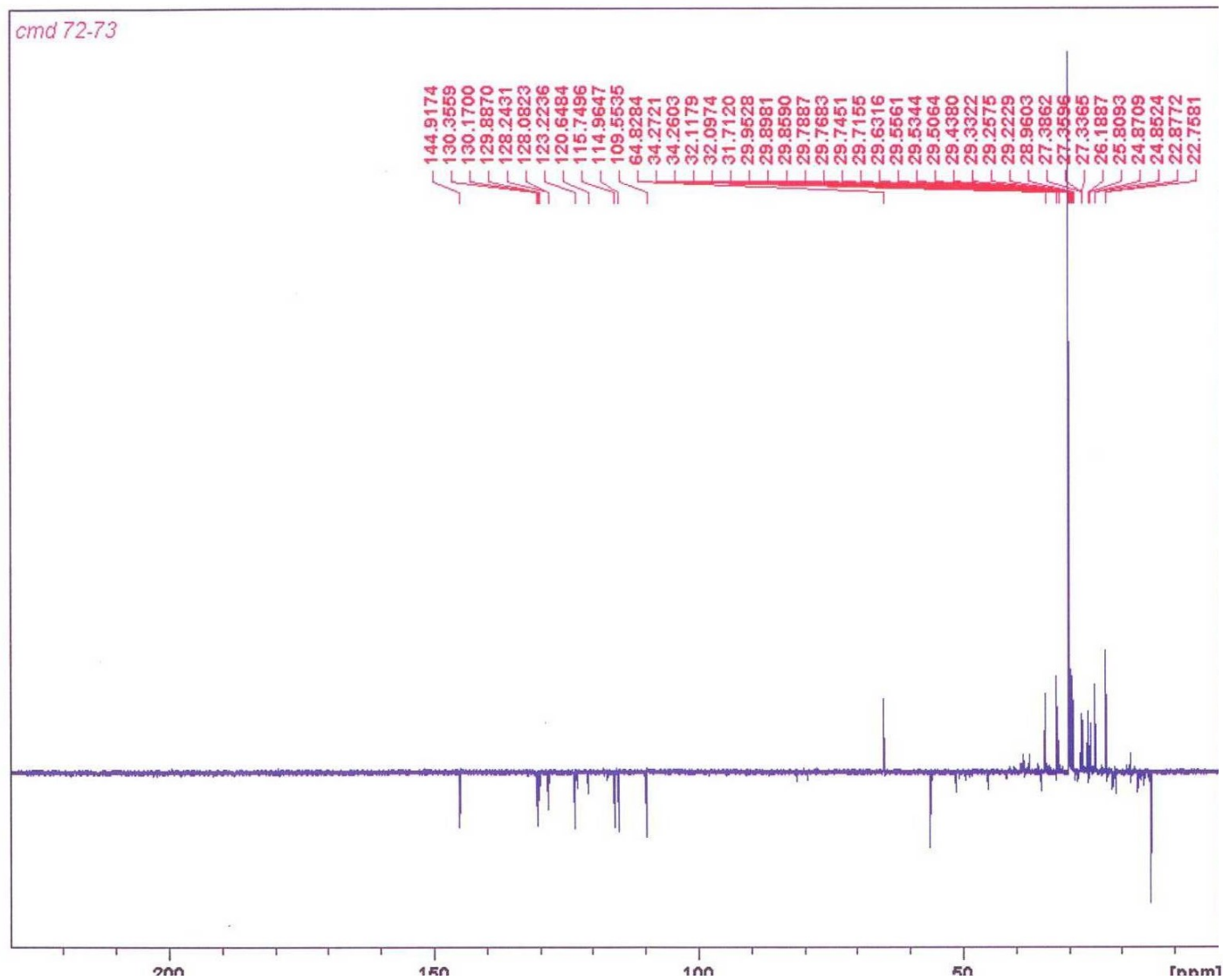


Fig. 4.62: DEPT spectrum of CMD-H in CDCl_3

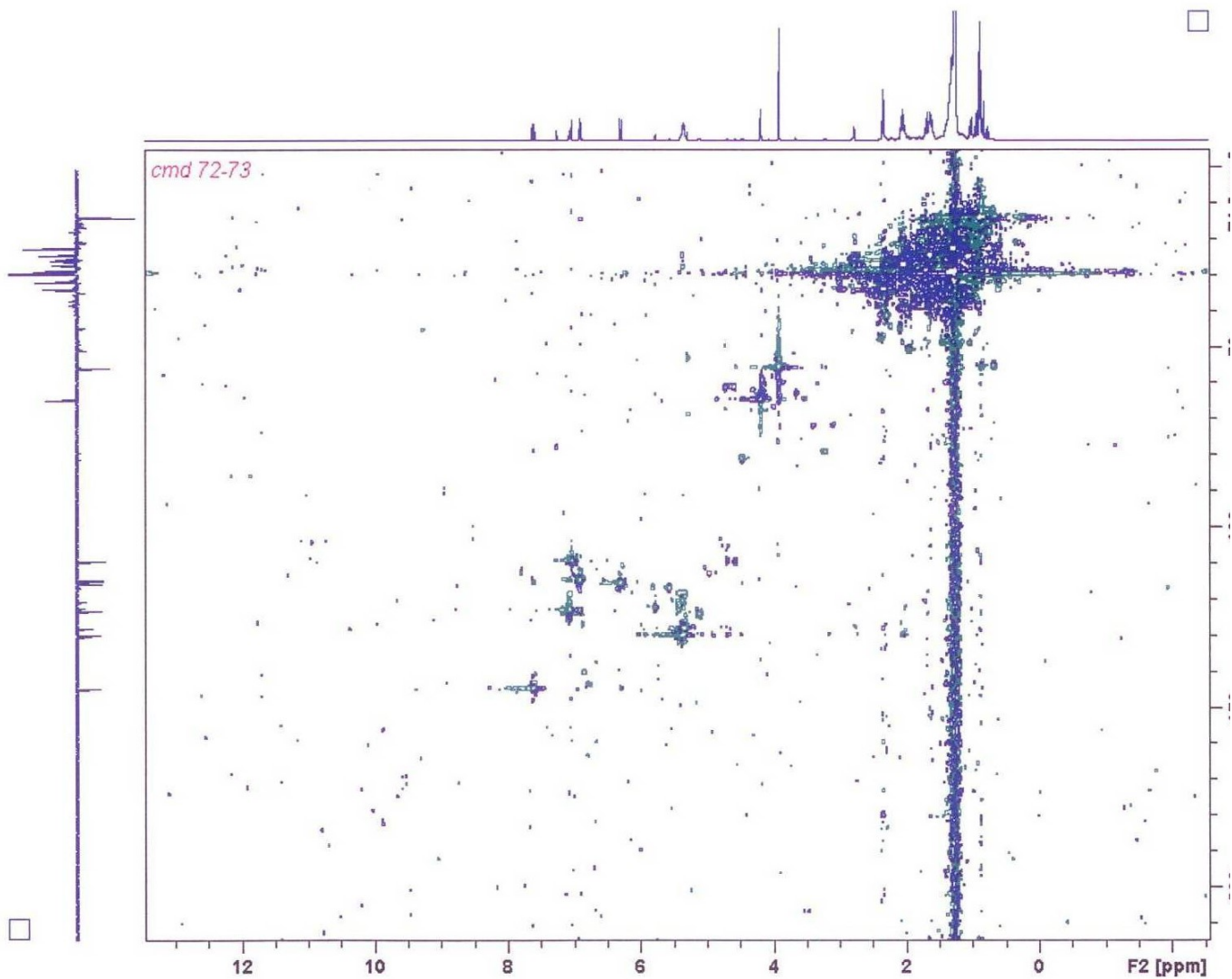


Fig. 4.63 : HSQC DEPT spectrum of CMD-H in CDCl₃

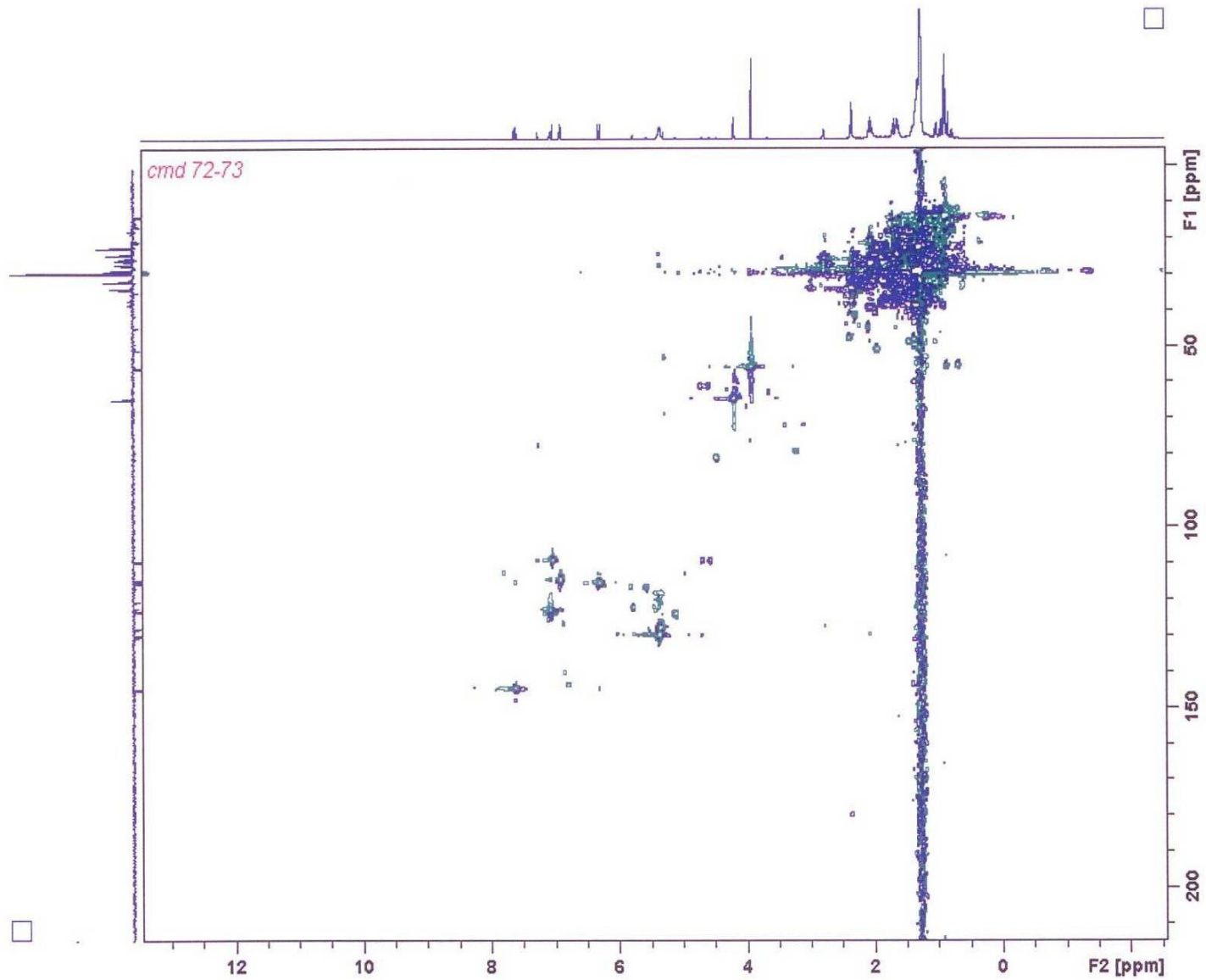


Fig. 4.64: HSQC DEPT spectrum of CMD-H in CDCl_3 (expanded)

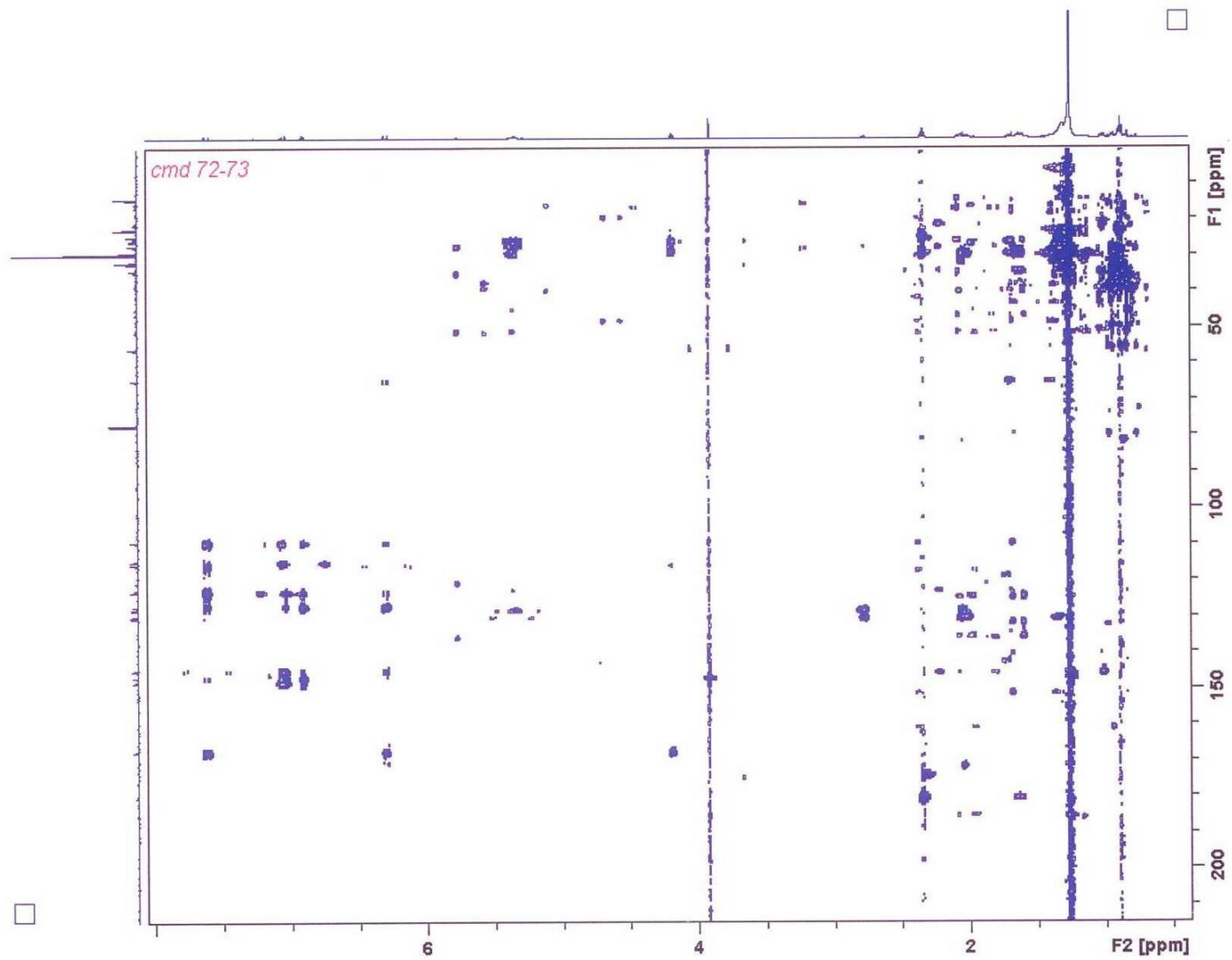


Fig. 4.65: HMBC spectrum of CMD-H in CDCl_3 (expanded)

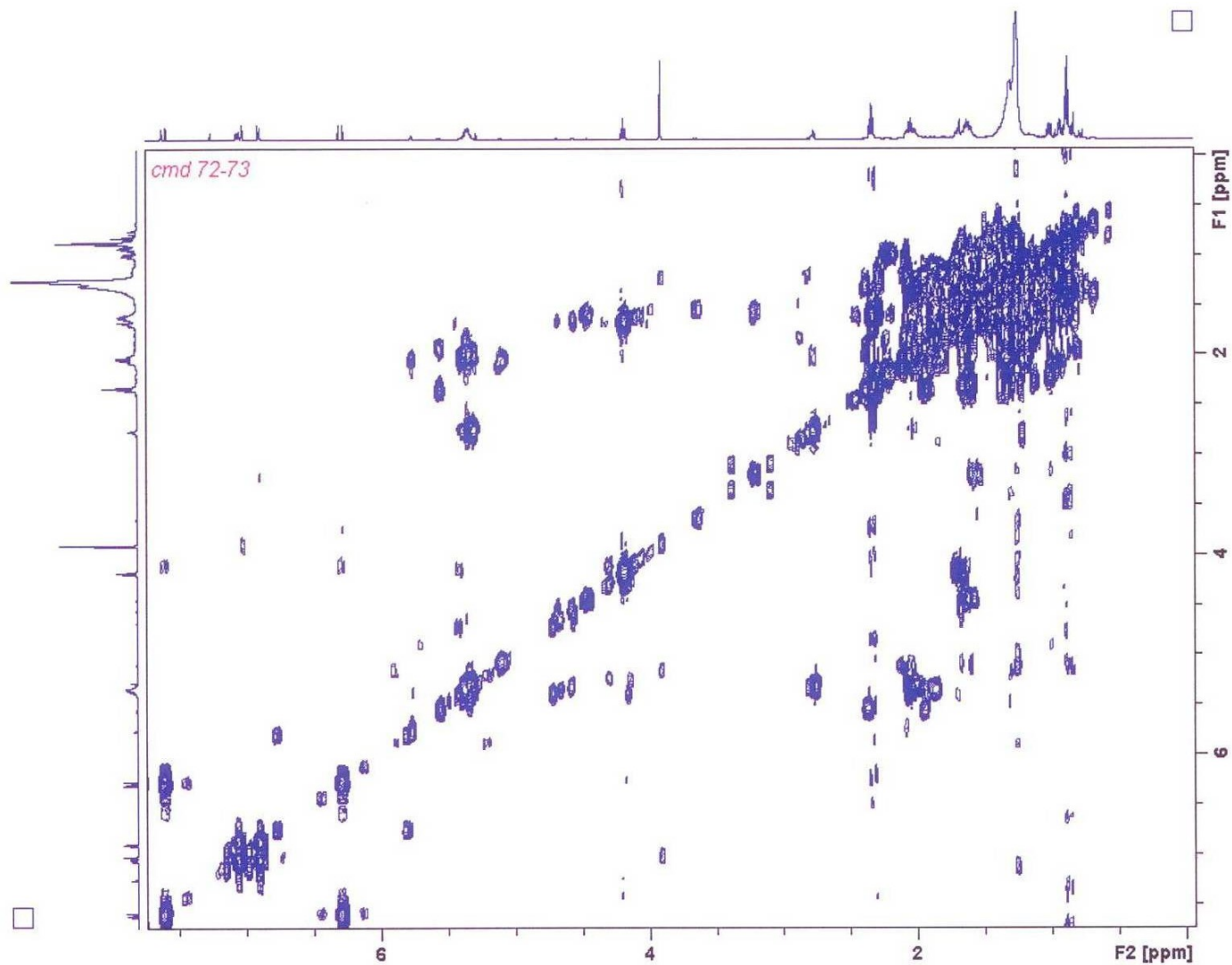


Fig. 4.66: COSY spectrum of CMD-H in CDCl_3

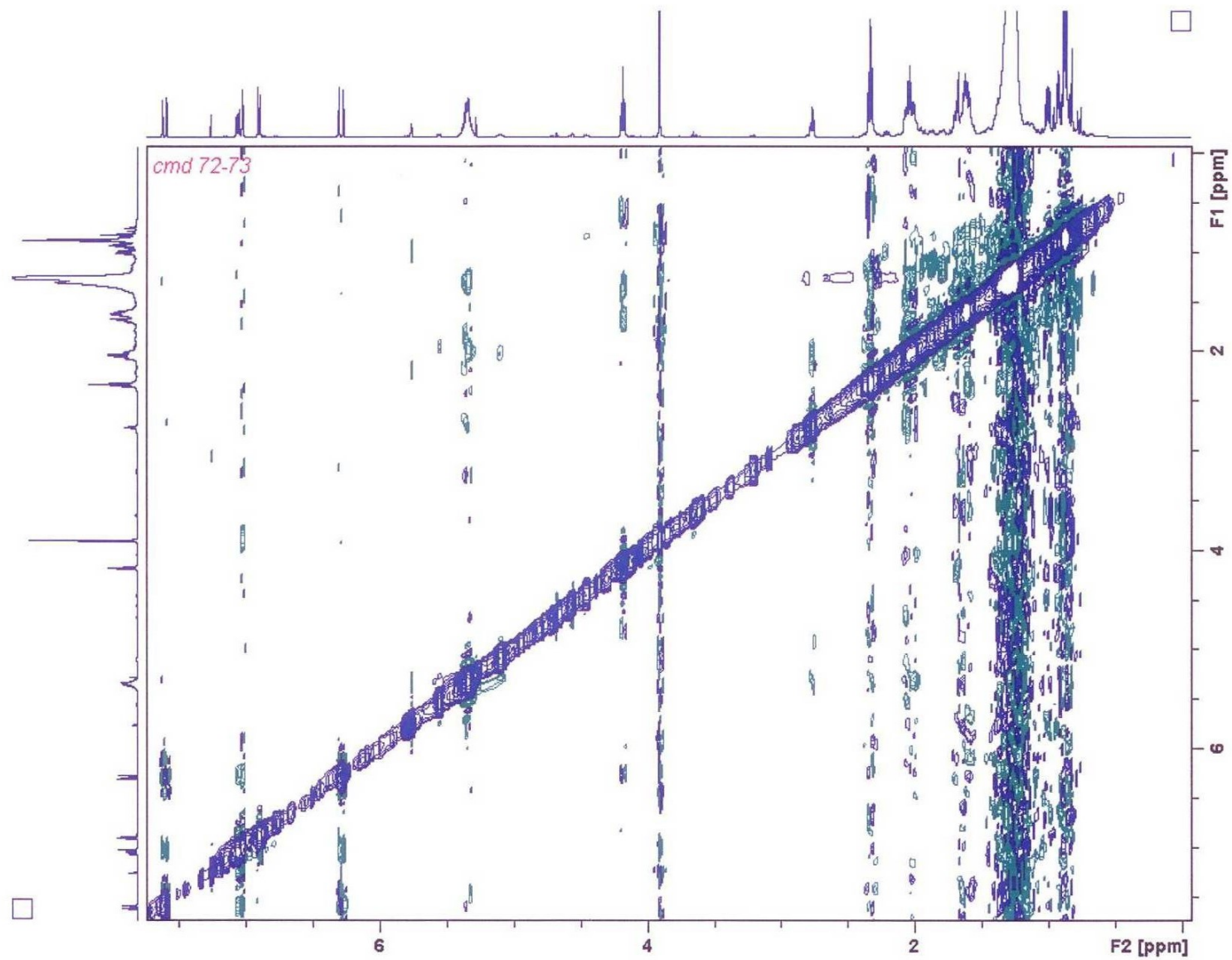


Fig. 4.67: NOESY spectrum of CMD-H in CDCl₃

4.3 ISOLATION AND CHARACTERIZATION OF PA-A TO PA-D FROM *Physalis angulata*

The methanol extract of *Physalis angulata* was subjected to flash column chromatography using various mixtures of hexane and ethyl acetate as solvents and it yielded 130 fractions. Similar fractions were pulled together based on their R_f values on thin layer chromatography (TLC) to give 8 fractions PAM-01 to PAM -08. Fraction PAM-04 (50 % hexane and 50% ethyl acetate) which contains solids was then packed in a column (5 mm x 35 cm) and elution was carried out, starting with the solvent mixture of 50 % hexane and 50% ethyl acetate. Twenty five fractions were collected and pulled together based on TLC to give four fractions- PAM4-1, PAM4-2, PAM4-3 and PAM4-4. PA-A (1.8 mg) was purified from PAM4-1; PA-B (3.4 mg) was purified from PAM4-2. Then PAM4-3 was loaded on sephadex LH-20 column and six fractions were obtained (PAM4-3-1 to PAM4-3-6. PAM-C (1.2 mg) was purified from PAM4-3-1. PA-D (1.2 mg) was purified from PAM4-4.

4.3.1 STRUCTURAL ELUCIDATION OF COMPOUND PA-A

Compound **PA-A** was isolated from the whole plant extract of *Physalis angulata*. The FTIR spectrum (Fig. 4.68) showed an absorption band at 3298 cm^{-1} that was attributed to a hydroxyl group. The ^1H NMR spectrum (Fig. 4.69) for compound PA-A showed an oxymethylene proton resonance at $\delta_{\text{H}} 4.14$ (2H, d, $J = 6.90$ Hz), an alkene proton resonance at $\delta_{\text{H}} 5.41$ (t, $J = 6.90$ Hz), a vinyl methyl proton at $\delta_{\text{H}} 1.66$ s, four methyl protons resonance at $\delta_{\text{H}} (0.81-0.84)$, which integrated to 12H at $\delta_{\text{H}} 0.81$ (d, $J = 7.05$ Hz), $\delta_{\text{H}} 0.81$ (d, $J = 7.05$ Hz), $\delta_{\text{H}} 0.83$ (d, $J = 7.05$ Hz,) and $\delta_{\text{H}} 0.84$ (d, $J = 7.05$ Hz). The ^{13}C NMR (Fig. 4.70) and DEPT spectrum (Fig. 4.72) revealed the presence of twenty carbons comprising five methyl, ten methylene, four methine and one quaternary carbon. The ^{13}C signals at $\delta_{\text{C}} 59.7$ suggested that PA-A has one OH functional group. The carbon resonance at $\delta_{\text{C}} 140.6$ and 123.3 were

attributed to double bond. The proton signals and their respective carbon atoms were assigned based on the HSQC spectrum (Fig 4.73). Thus the ^1H signal at δ_{H} 4.14 was attributed to H-1 and carbon δ_{C} 59.7 at C-1 respectively. The ^{13}C signals at δ_{C} 123.3, 140.6, 40.1 were attributed to C2, C3, and C4 respectively. The 2D HMBC spectrum (Fig. 4.74) revealed that the proton at H2 correlated with C3, H4 with C3, H20 correlated to C3.

The ^{13}C NMR chemical shifts for compound **PA-A** were compared to the ^{13}C NMR data for phytol from literature (Takaya, 2003) as showed in table 9. The data confirmed that compound PA-A is phytol [**39**] isolated previously from *Raphanus sativus* L. (Takaya, 2003) and many other sources but reported here for the first time from *Physalis angulata*.

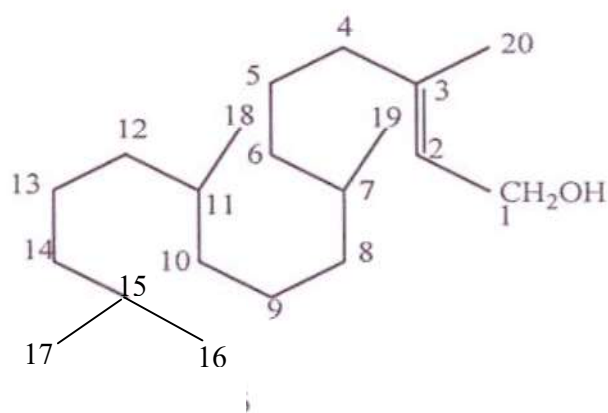


Table 9: Correlations table ^1H (500 MHz) and ^{13}C (125 MHz) NMR Data^a for compound PA-A: Phytol and literature^b in CDCl_3

No	^{13}C NMR ^a (125 MHz) CDCl_3	^{13}C NMR ^b (125 MHz) CDCl_3	^1H NMR ^a (500 MHz) CDCl_3	^1H NMR ^b (500 MHz) CDCl_3
1	59.7 CH_2	59.4	4.14 t $J = 5.0\text{Hz}$	4.13 t $J = 6.7\text{Hz}$
2	123.3 CH	123.0	5.41 q $J = 6.9\text{Hz}, 0.8$	5.39 t $J = 6.7\text{Hz}$
3	140.6 C	140.3	-	-
4	40.1 CH_2	39.9	1.99m	2.00 t $J = 6.1\text{Hz}$
5	25.4 CH_2	25.1	} 1.02 – 1.49 m	} 1.05 – 1.46 m
6	36.9 CH_2	36.6		
7	33.0 CH	32.8		
8	37.6 CH_2	37.4		
9	24.7 CH_2	24.4		
10	37.7 CH_2	37.4		
11	32.9 CH	32.7		
12	37.5 CH_2	37.4		
13	25.0 CH_2	24.7		
14	39.6 CH_2	39.4		
15	28.2 CH	28.0	1.49m	1.50m
16	22.9 CH_3	22.7	0.83 d $J = 7.05\text{Hz}$	0.84 d $J = 6.5\text{Hz}$
17	23.0 CH_3	22.8	0.84 d $J = 7.05\text{Hz}$	0.84 d $J = 6.5\text{Hz}$
18	20.0 CH_3	19.7	0.81 d $J = 7.05\text{Hz}$	0.82 d $J = 6.5\text{Hz}$
19	19.9 CH_3	19.7	0.81 d $J = 7.05\text{Hz}$	0.82 d $J = 6.5\text{Hz}$
20	16.4 CH_3	16.2	1.66s	1.65s

^a Assignment aided by HMQC and HMBC experiments

^b Literature data of Phytol (Takaya, 2003)

TOPE 9

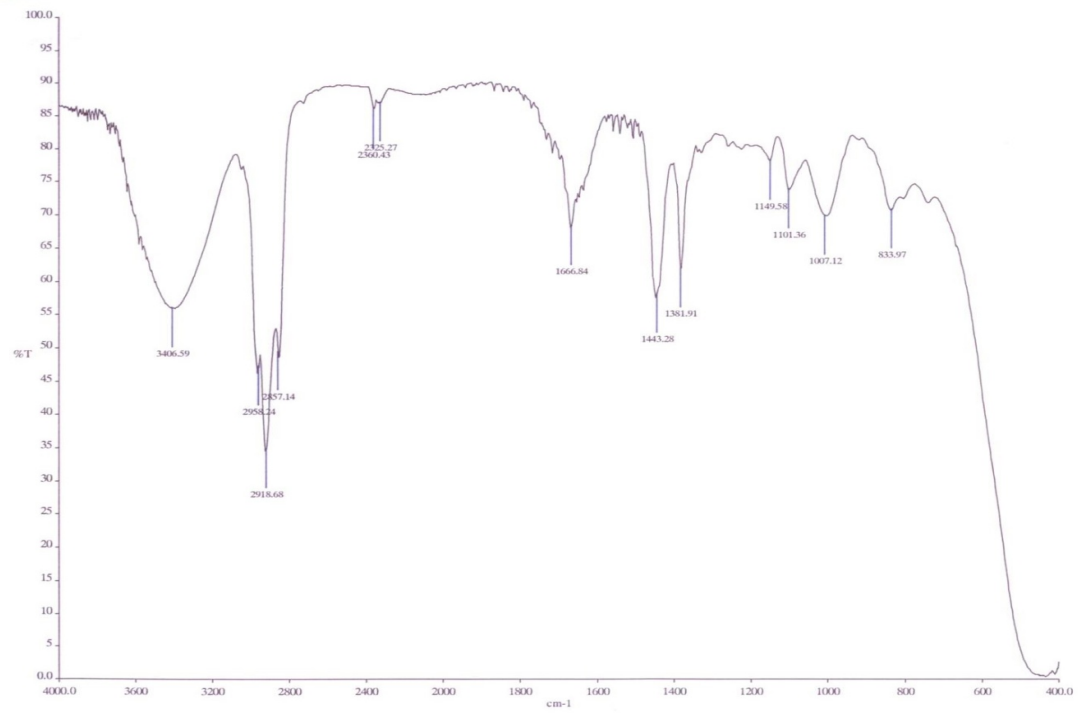


Fig. 4.68: IR spectrum of PA-A in $CDCl_3$

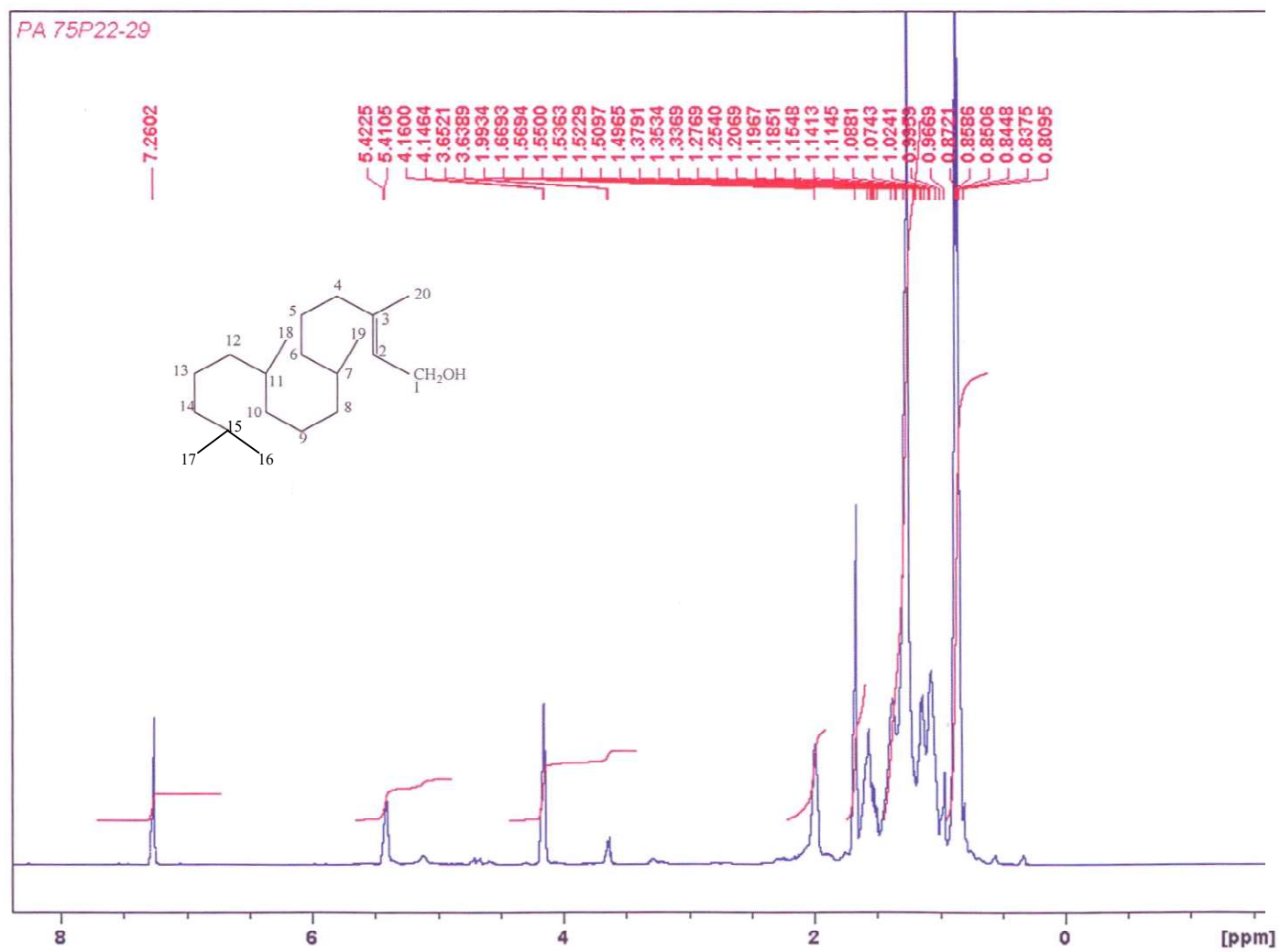


Fig. 4.69: ¹H-NMR (500MHz) spectrum of PA-A in CDCl₃

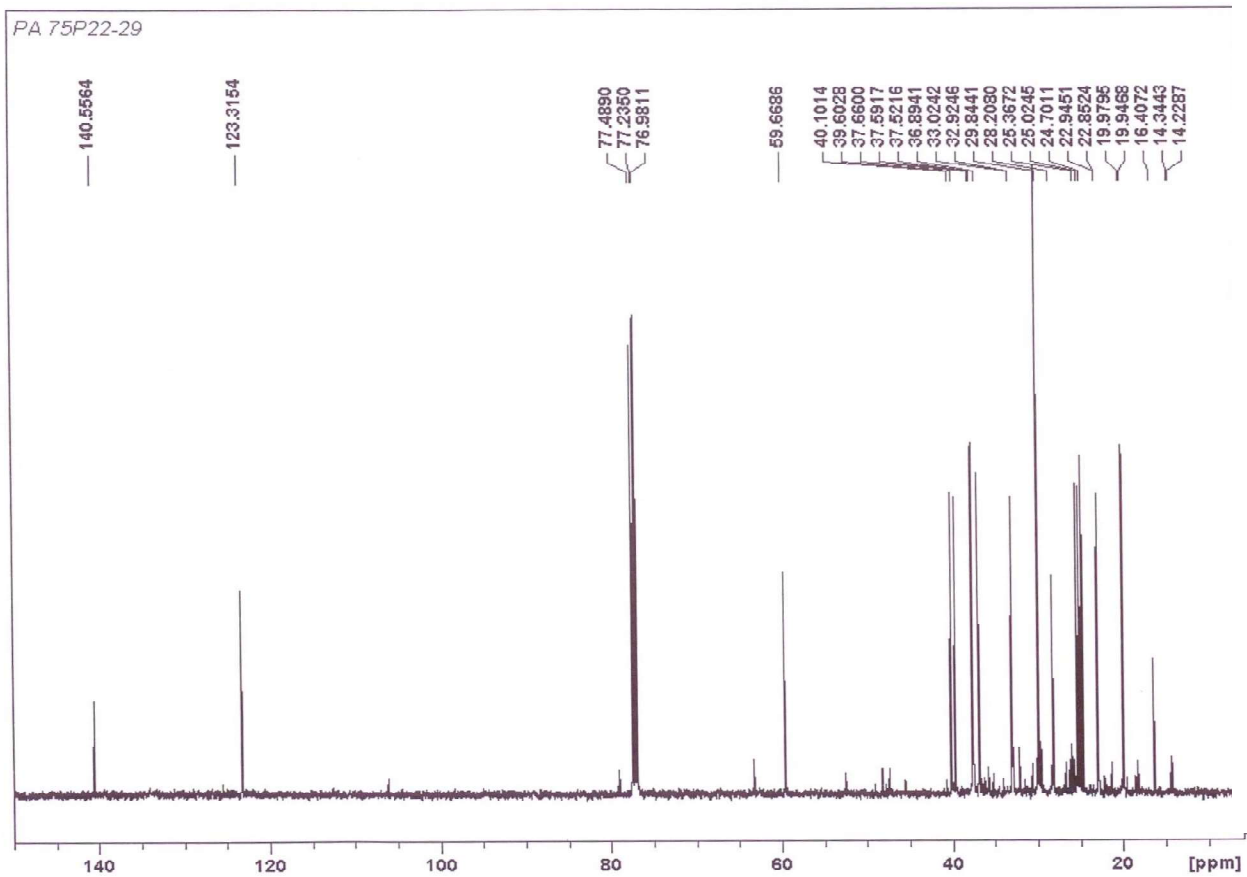


Fig. 4.71: ^{13}C -NMR (125 MHz) spectrum of PA-A in CDCl_3 (expanded)

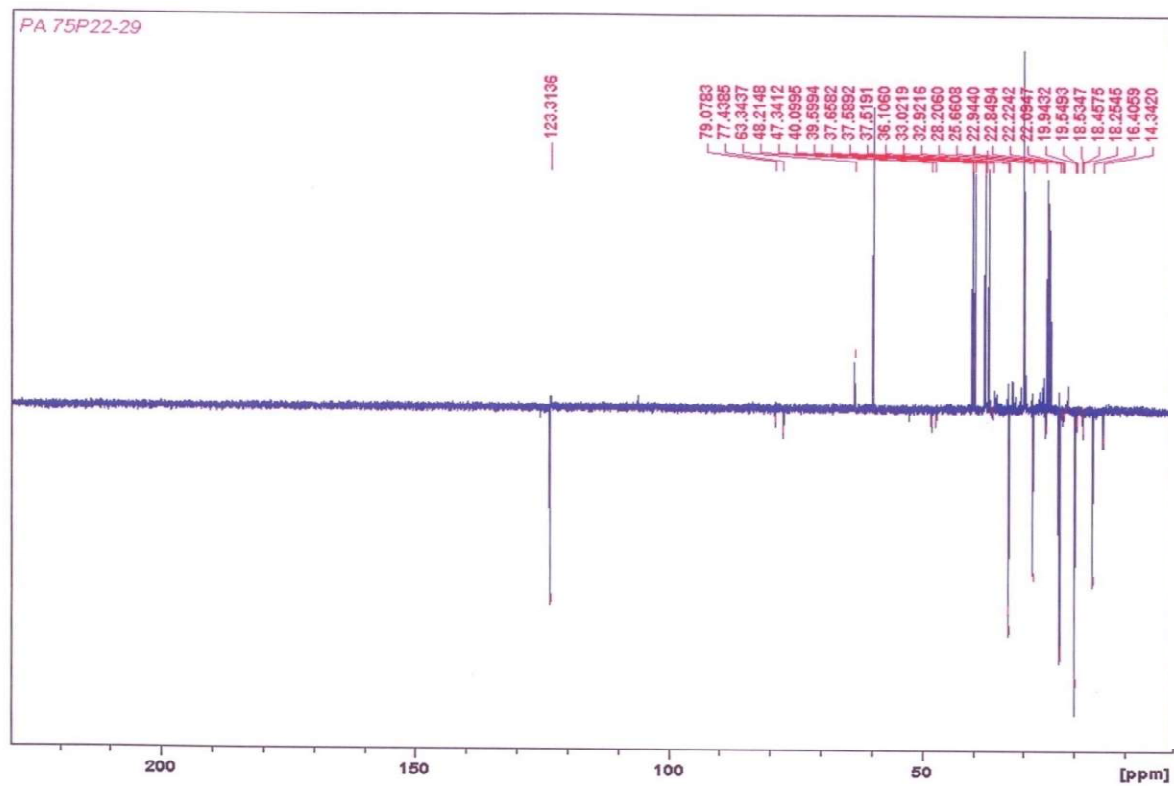


Fig. 4.72: DEPT spectrum of PA-A in CDCl_3

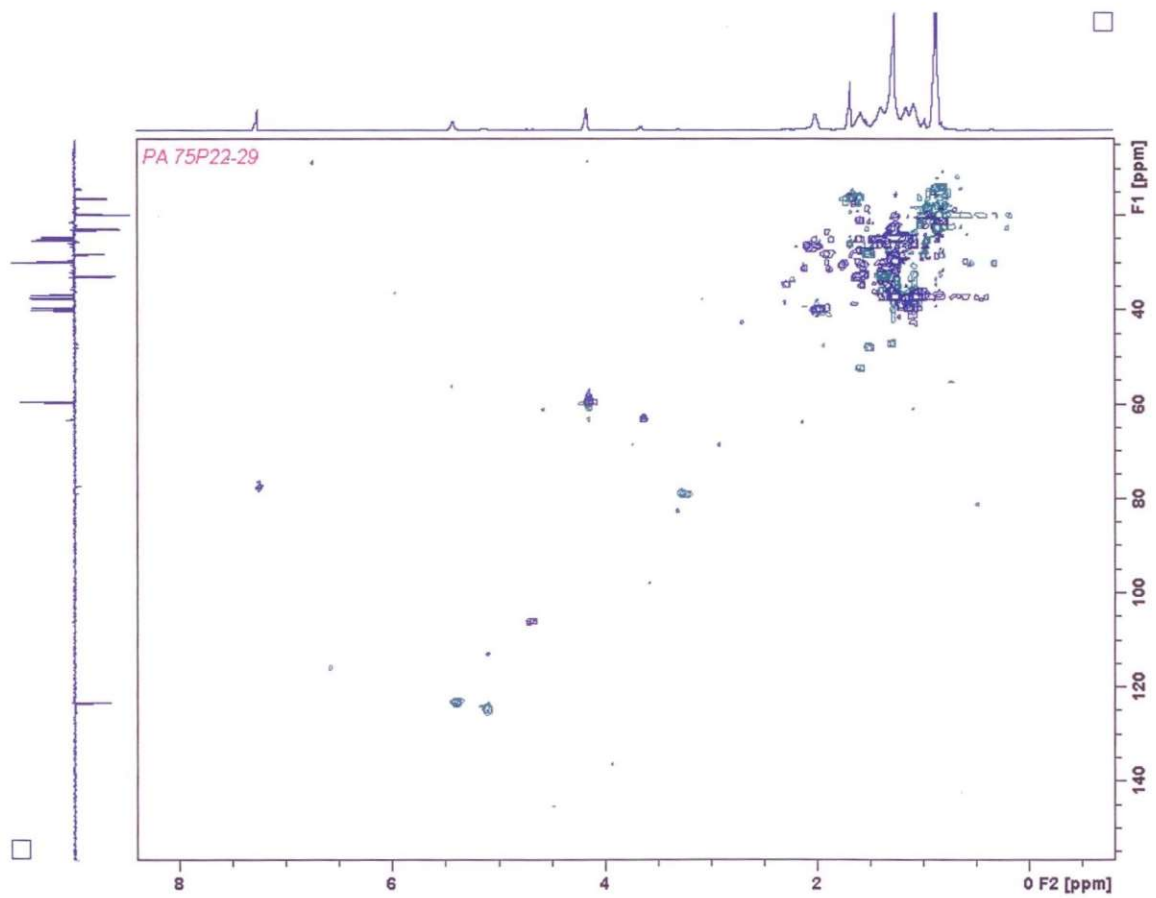


Fig. 4.73: HSQC DEPT spectrum of PA-A in CDCl_3

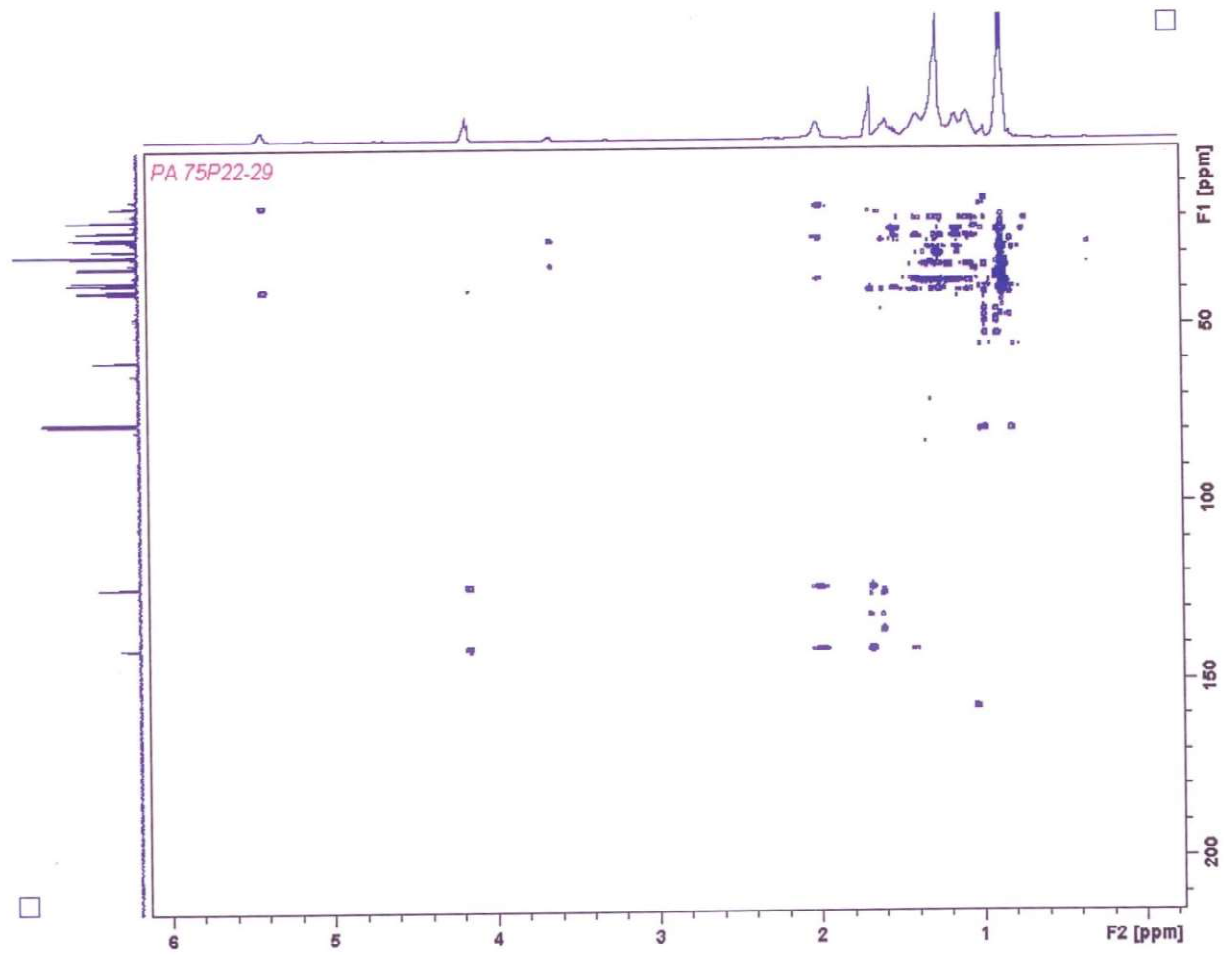


Fig. 4.74: HMBC spectrum of PA-A in CDCl_3

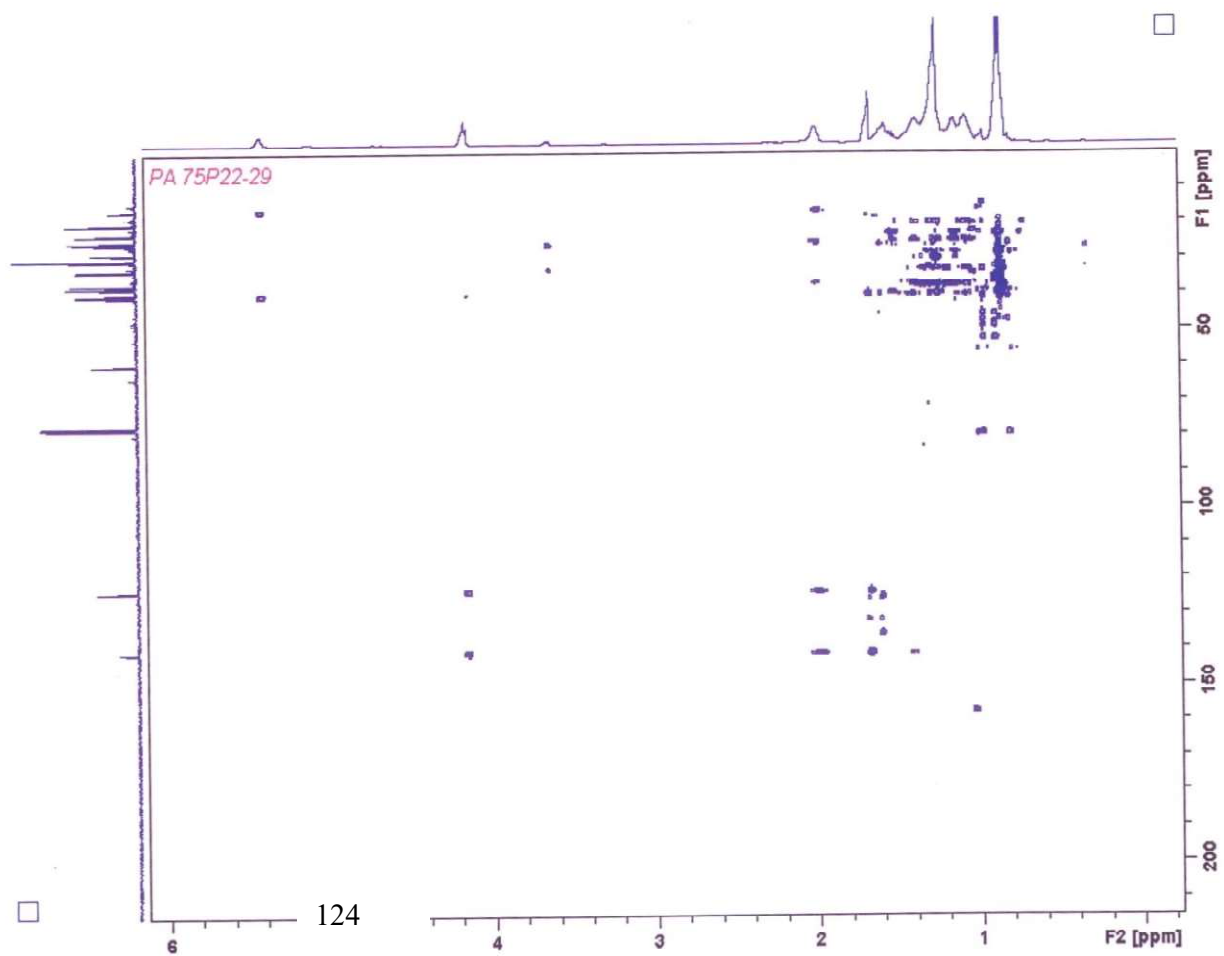
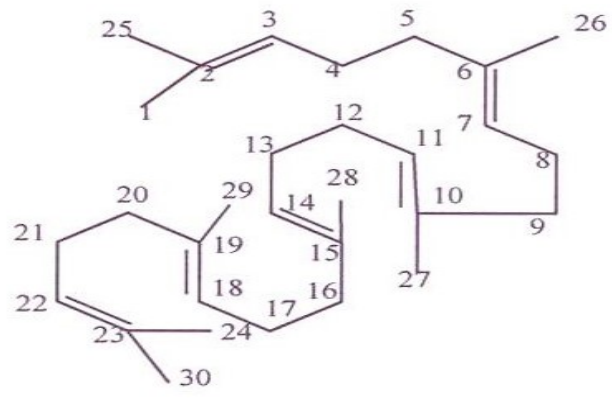


Fig. 4.75: HMBC spectrum of PA-A in CDCl_3 (expanded)

4.3.2 STRUCTURAL ELUCIDATION OF COMPOUND PA-B

Compound **PA-B** was isolated as yellow oil from the whole plant of *Physalis angulata*. The ^1H NMR spectrum (Fig. 4.76) of **PA-B** showed six olefinic proton resonances at δ_{H} 5.11 which were assigned to H-3/22, H-7/18 and H-11/14 using HMBC spectrum (Fig 4.80). The ^{13}C NMR spectrum (Fig.4.77) displayed fifteen carbon resonances representing thirty carbons while the DEPT spectrum (Fig. 4.78) showed the presence of eight methyls, ten methylenes, six methines and six trisubstituted carbons. The presence of three methine carbon resonating at δ_{C} 124.4, δ_{C} 124.5 and δ_{C} 124.6 (^{13}C NMR spectrum- Fig. 4.77) and ten methylene proton (m, δ_{H} 2.05, H-4, H-5, H-8, H-9, H-123,H-13, H-16, H17, H-20 and H-21), a singlet at δ_{H} 1.68 (6H, s, H-1 and H-24) together with two broad singlets at δ_{H} 1.60s (6H, bs) and δ_{H} 1.67s (3H, bs) (^1H NMR spectrum, Fig. 4.76) correspond respectively, to an in-chain, allylic methyl group and three out chain allylic groups of a polyprenoid system. The out of chain methyl groups resonating at δ_{C} 17.9, δ_{C} 16.5 and δ_{C} 16.3 indicated the geometry of the six trisubstituted double bonds while signals appearing at δ_{C} 25.9, confirmed its in-chain position in ^{13}C NMR spectrum (Fig. 4.77).

The ^1H and ^{13}C NMR spectral features of this compound were compared with the reported literature (He *et al.*, 2002) as shown in table 10 and was found to be similar to squalene, an acyclic triterpenoid, which is a very common compound in many natural sources, fish liver oils and many vegetables oil (Barreto *et al.*, 2013). Squalene [40] has been isolated previously from *Croton muscicapa* and *Amaranths grain* (He *et al.*, 2002) but reported here for the first time from *Physalis angulata*.



40

Table 10: Correlations table ^1H (500 MHz) and ^{13}C (125 MHz) NMR Data^a for compound PA-B: Squalene and literature^b in CDCl_3

No	^{13}C NMR ^a (125 MHz) CDCl_3	^{13}C NMR ^b (125 MHz) CDCl_3	^1H NMR ^a (500 MHz) CDCl_3	^1H NMR ^b (500 MHz) CDCl_3
1/24	25.9 CH_3	25.7 CH_3	1.68s	1.67s
2/23	131.2 C	131.2 C	-	-
3/22	124.4 CH	124.2CH	5.11m	5.11m
4/21	26.6 CH_2	26.7 CH_2	2.10 m	2.10 m
5/20	39.7 CH_2	39.7 CH_2	1.98 m	1.98 m
6/19	135.0 C	134.9C	-	-
7/18	124.5 CH	124.3CH	5.11 m	5.12 m
8/17	26.6 CH_2	26.6 CH_2	2.07 m	2.07 m
9/16	40.0 CH_2	40.0 CH_2	1.98 m	1.97 m
10/15	135.1 C	135.1C	-	-
11/14	124.6 CH	124.2 CH	5.11 m	5.11 m
12/13	28.2 CH_2	28.2 CH_2	2.01 dd	2.01 dd
25/30	17.9 CH_3	17.6 CH_3	1.60s	1.60s
26/29	16.5 CH_3	16.0 CH_3	1.67s	1.66s
27/28	16.3 CH_3	16.0 CH_3	1.60s	1.60s

^a Assignment aided by HMQC and HMBC experiments

^b Literature data of squalene (Barreto *et al.*, 2013)

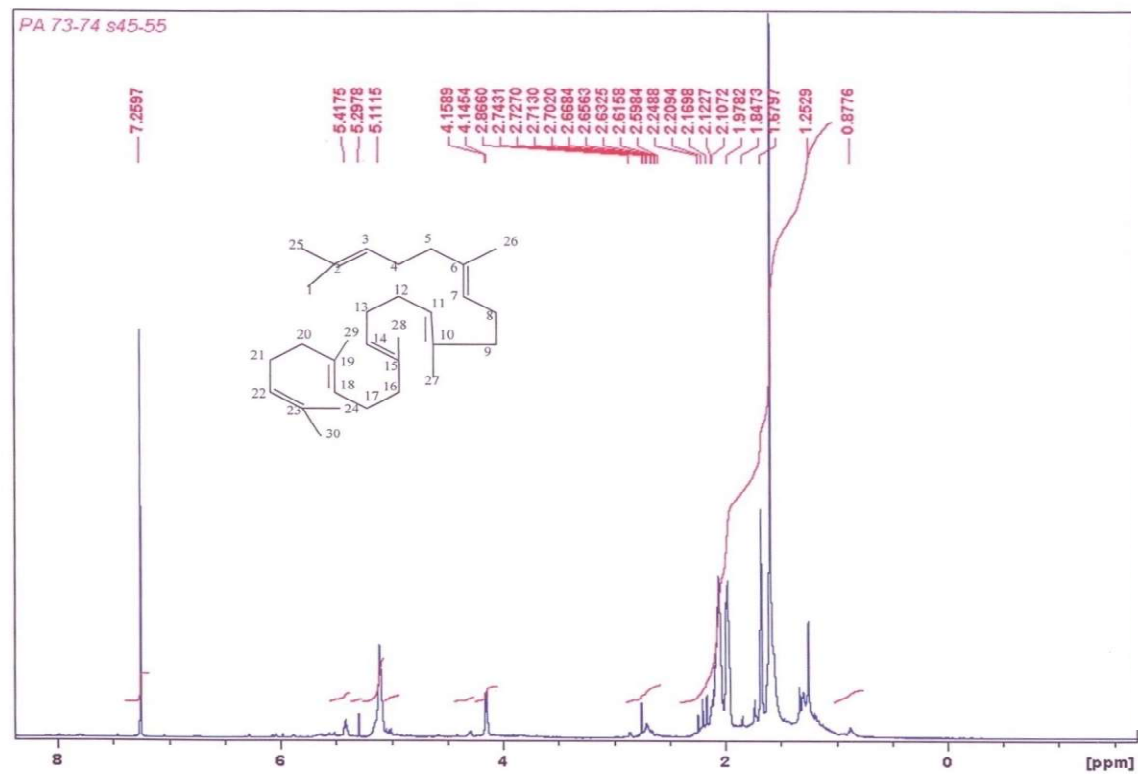


Fig. 4.76: $^1\text{H-NMR}$ (500MHz) spectrum of PA-B in CDCl_3

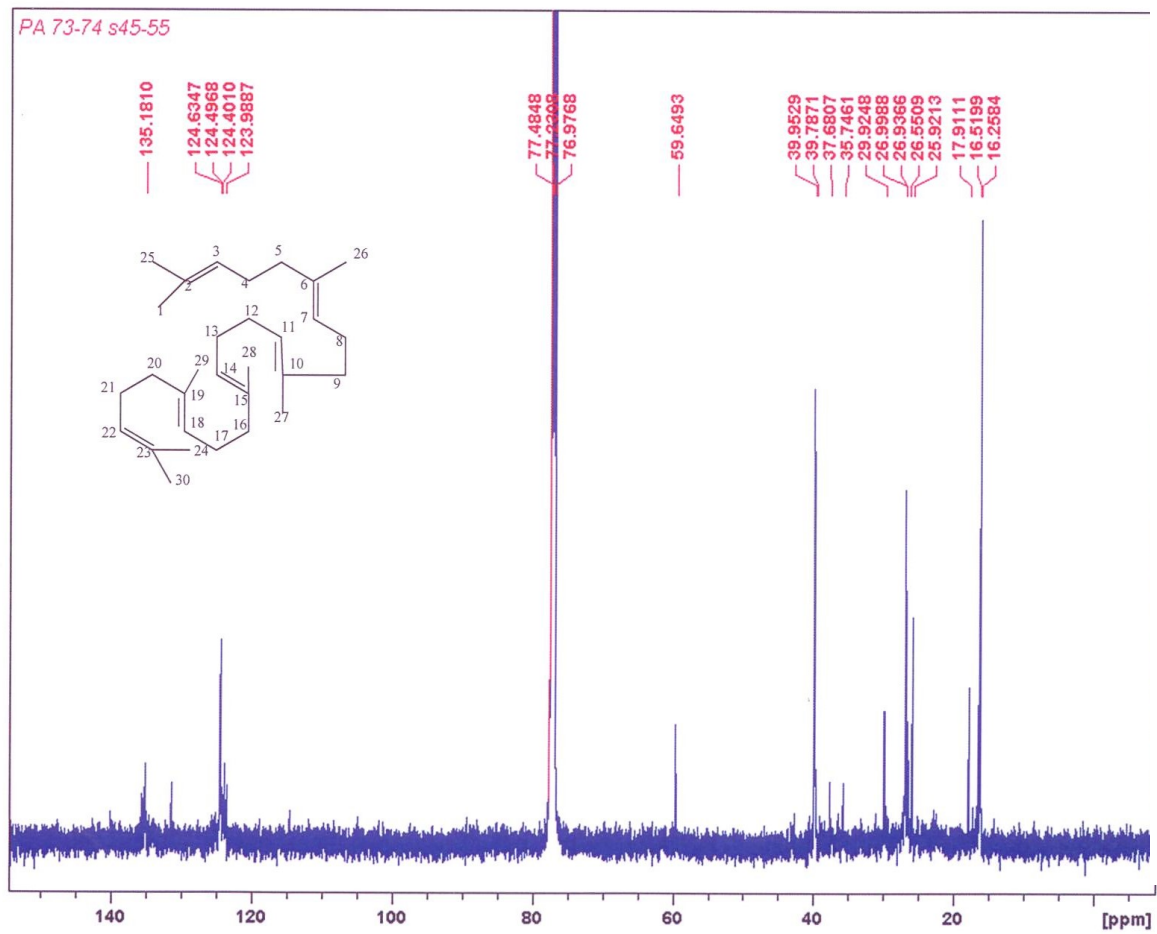


Fig. 4.77 ^{13}C -NMR (125 MHz) spectrum of PA-B in CDCl_3

Fig. 39: ^{13}C -NMR (500MHz) spectrum of PA2 in CDCl_3

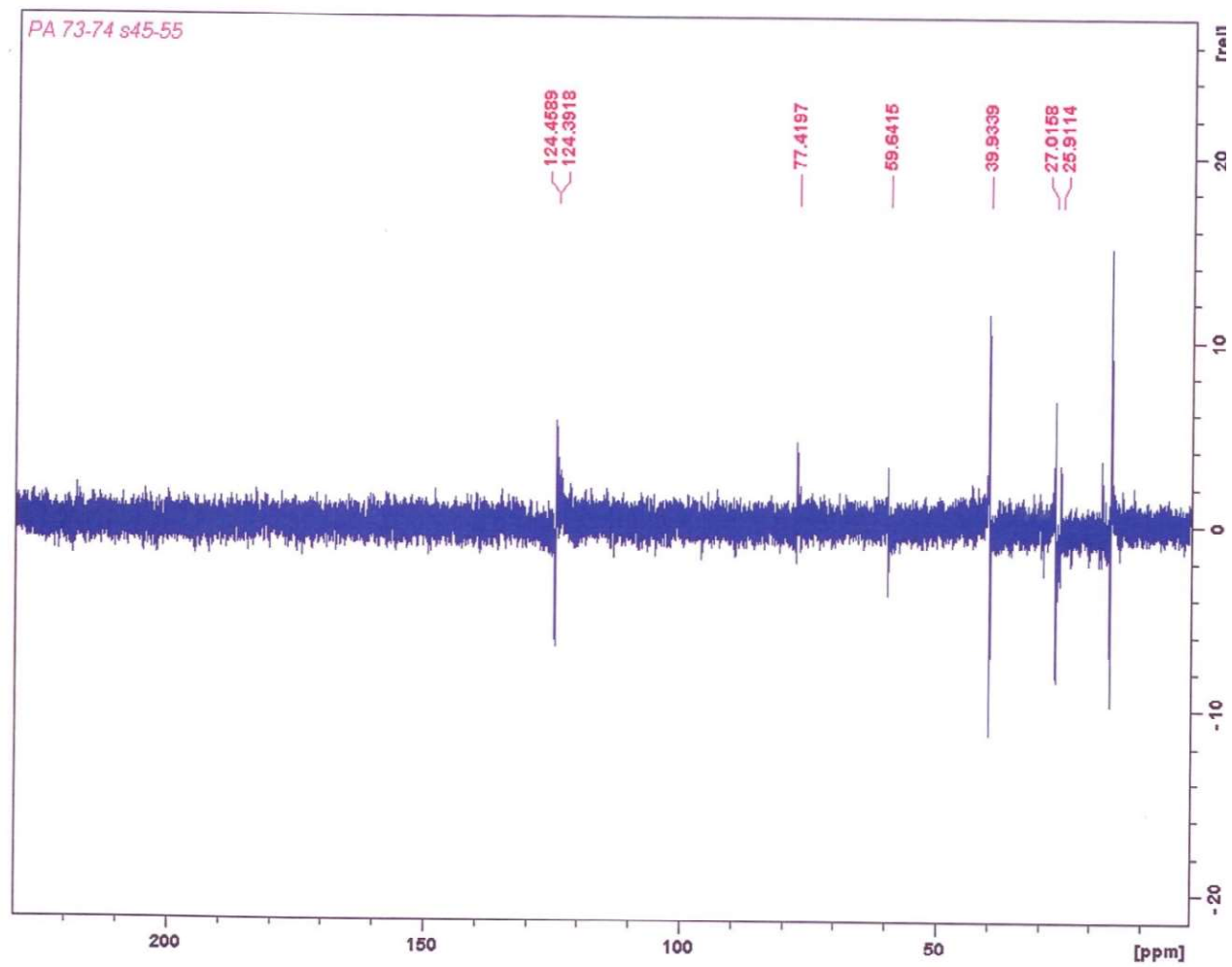


Fig. 4.78: DEPT spectrum of PA-B in CDCl_3

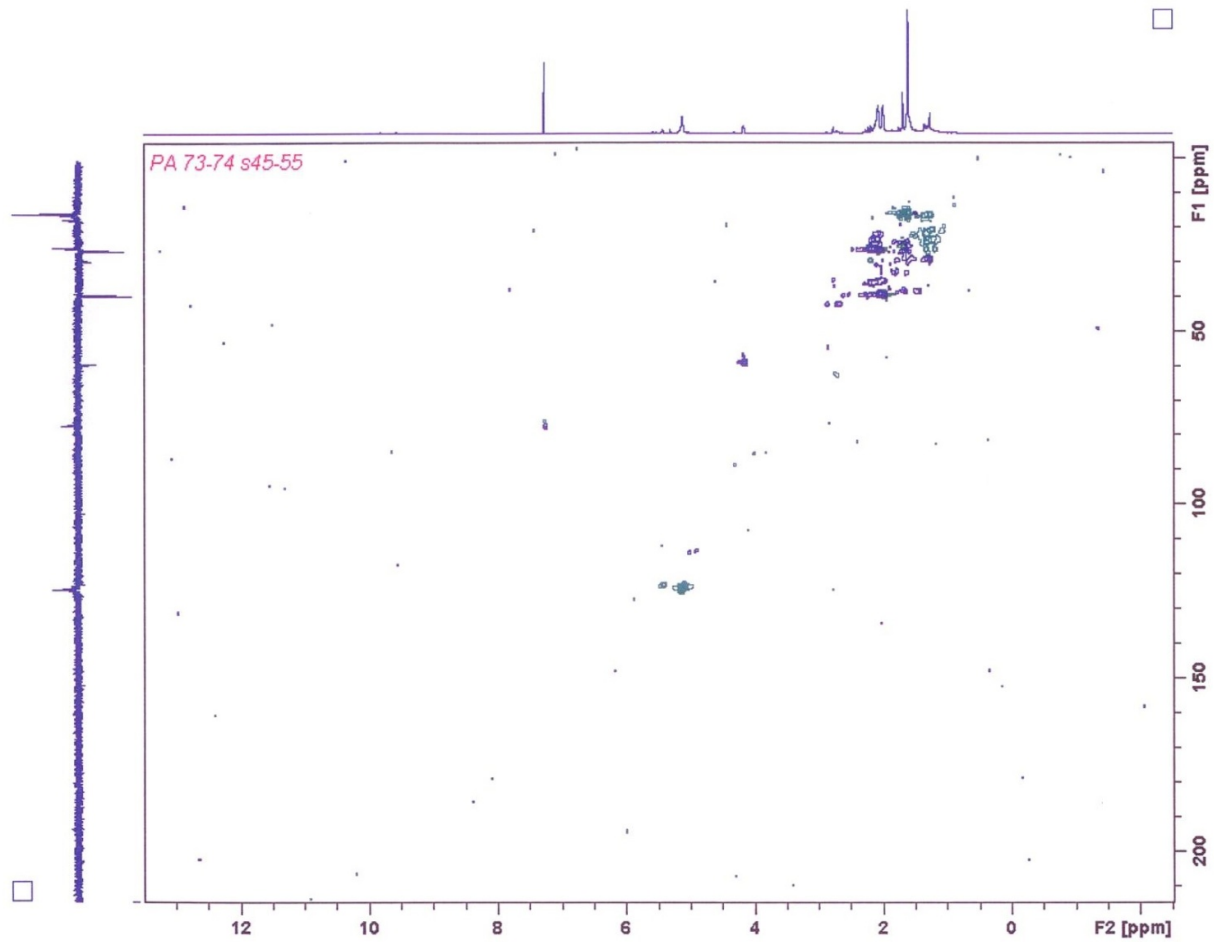


Fig. 4.79: HSQC DEPT spectrum of PA-B in CDCl_3

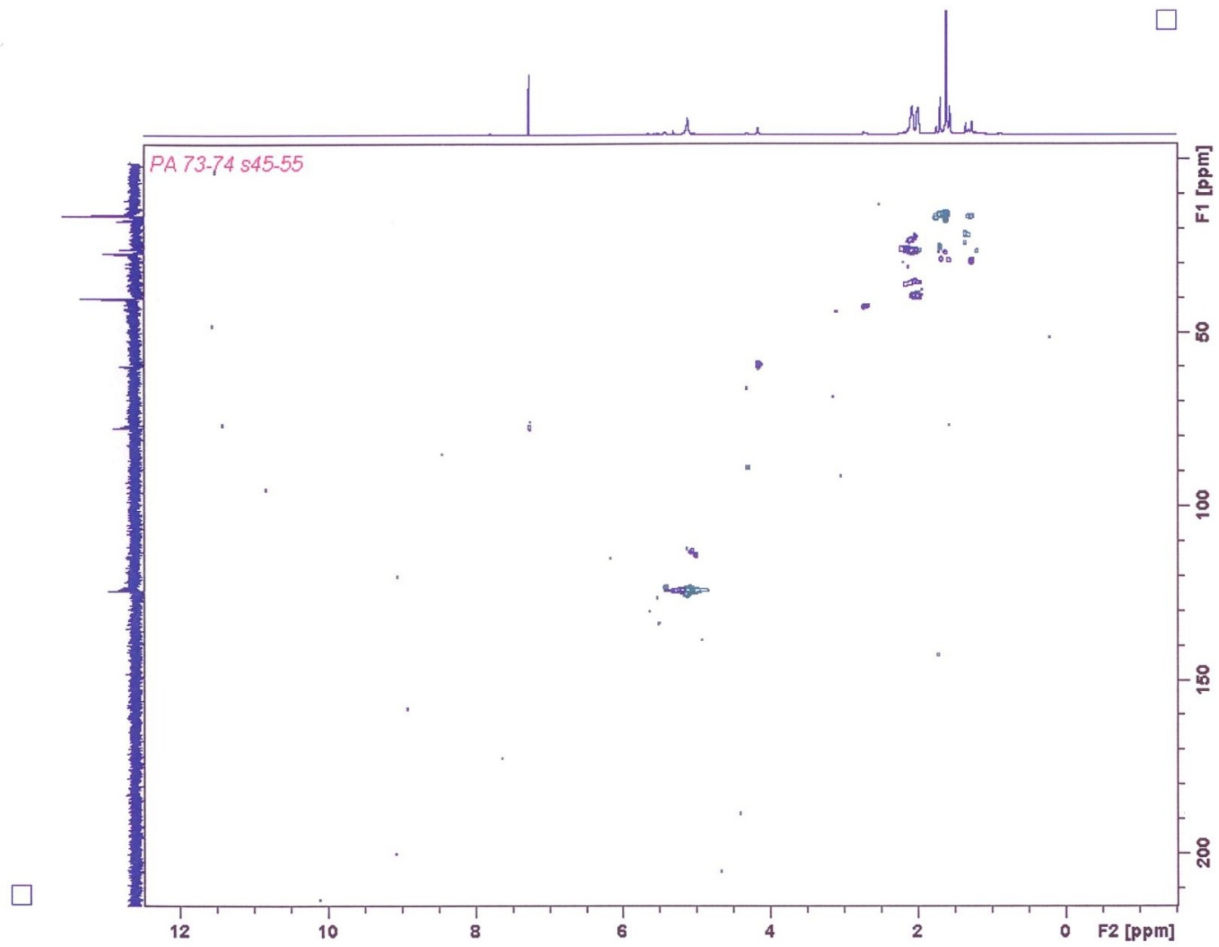
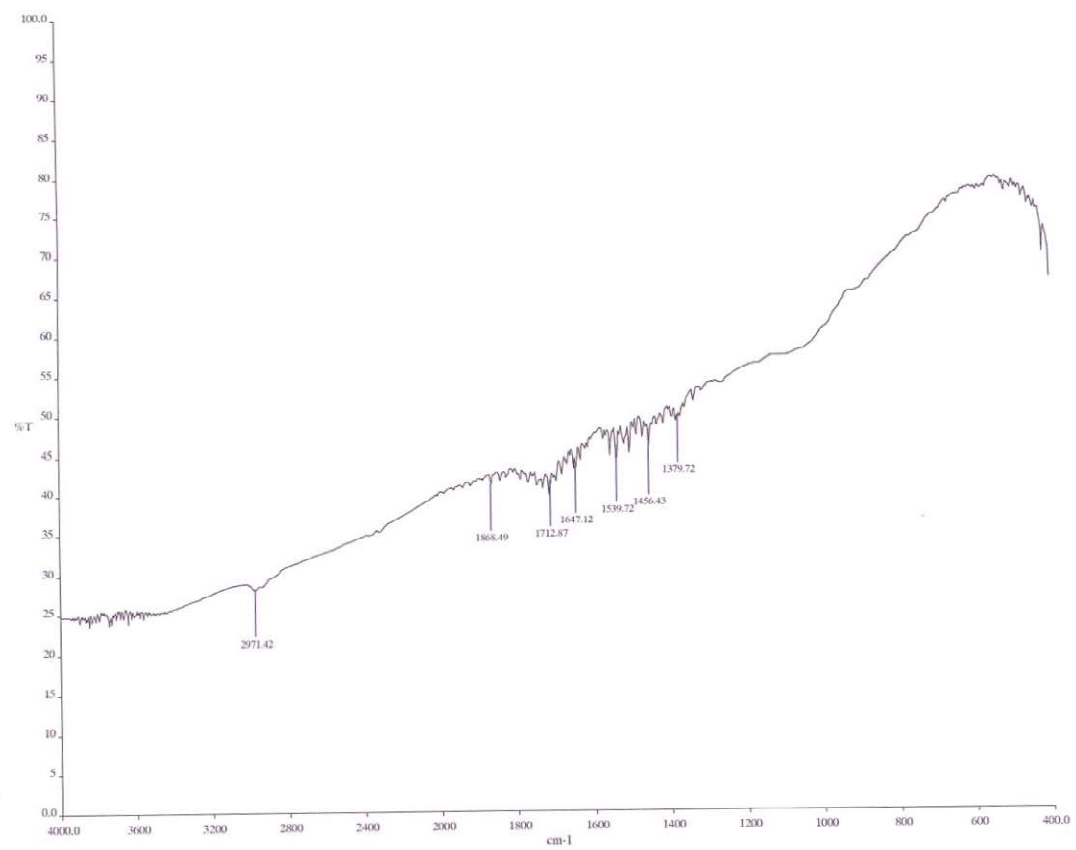


Fig. 4.80 HMBC spectrum of PA-B in CDCl_3



Top 10

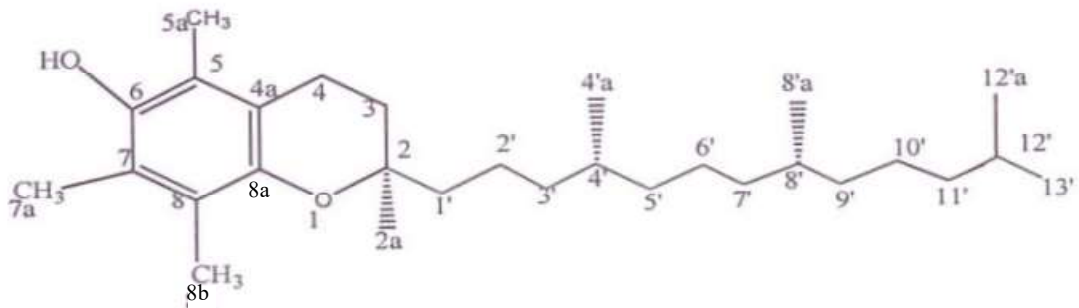
Fig. 4.81: IR spectrum of PA-B in CDCl₃

4.3.3 STRUCTURAL ELUCIDATION OF COMPOUND PA-C:

The FTIR spectrum (Fig. 4.82) of compound **PA-C** showed stretch absorption bands at 2925 and 2854 cm^{-1} suggesting the presence of methyl groups.

The ^1H NMR spectrum (Fig. 4.83) exhibited signals for one singlet methyl group δ_{H} 1.22, four doublet methyl groups δ_{H} 0.85, [3H, d, $J=6.4$ Hz], δ_{H} 0.85, [3H, d, $J=6.8$ Hz], 0.87 (3H, d, $J=7.6$ Hz), 0.87 (3H, d, $J=6.8$ Hz), three vinyl methyl at δ_{H} 2.10 (6H,s), 2.15(3H,s), eleven methylene protons at δ_{H} 1.51 (2H,d), 1.38 (2H,m), 1.22 (2H,m), 0.87 (3H,d), 1.22 (2H,m), 1.26 (2H,m), 1.36 (1H,m), 0.87 (3H,d), 1.10 (2H,m) δ_{H} 1.77 (1H, d), 2.59 (2H, dt) and a low field exchangeable hydroxyl proton δ_{H} 4.16 (s).

The DEPT spectrum (Fig. 4.85) showed eight CH_3 , eleven CH_2 , three CH and seven quaternary carbon. A downfield signal at δ_{C} 74.5 together with its HMBC correlation with the methyl signal at δ_{H} 1.22 and two methylene signals at δ_{C} 23.0 and δ_{C} 31.7 were part of a chromane system. The ^1H and ^{13}C NMR spectral features of **PA-C** [41] were compared with the reported literature (Benjamat *et al.*, 2017) and was found to be similar to α -tocopherol, which is a common compound in wheat germ oil, seed oils, sunflower and olive oils and a known potent antioxidant. **PA-C** was determined to be the known α -tocopherol. It has been isolated previously from fruits and leaves of *Cratogeomys cochinchinense* (Benjamat *et al.*, 2017) but reported here for the first time from *Physalis angulata*.



41

Table 11: Correlations table ^1H (500 MHz) and ^{13}C (125 MHz) NMR Data^a for compound PA-C: α -tocopherol and literature^b in CDCl_3

No	^1H NMR ^a (500 MHz)	^1H NMR ^b (500 MHz)	^{13}C NMR ^a (125 MHz)	^{13}C NMR ^b (125 MHz) in CDCl_3
2	-	-	74.5(C)	74.3(C)
2a	1.22(3H,s)	1.23(3H,s)	23.0(CH_3)	23.7(CH_3)
3 α	1.77(1H, dt)	1.79H, dt)	31.7(CH_2)	31.6(CH_2)
3 β	1.80 (1H,m)	1.80 (1H,m)		
4	2.59 (2H, brt)	2.63 (2H, br t)	20.9(CH_2)	20.8(CH_2)
4a	-	-	117.5(C)	117.0(C)
5	-	-	118.6(C)	118.4(C)
6	-	-	144.8(C)	144.4(C)
7	-	-	121.0(C)	121.0(C)
8	-	-	122.7(C)	122.3(C)
8a	-	-	145.8(C)	145.4(C)
5a	2.10(3H,s)	2.10(3H,s)	11.4(CH_3)	11.2(CH_3)
7a	2.15(3H,s)	2.15(3H,s)	12.4(CH_3)	12.1(CH_3)
8b	2.10(3H,s)	2.10(3H,s)	11.9(CH_3)	11.8(CH_3)
6-OH	4.16(1H,s)	4.16(1H,s)	-	-
1 ¹	1.51(2H, dd)	1.50(2H, dd)	39.6(CH_2)	39.8(CH_2)
2 ¹	1.38 (2H,m)	1.36(2H,m)	21.2(CH_2)	21.0(CH_2)
3 ¹	1.22(2H,m)	1.22(2H,m)	37.5(CH_2)	37.5(CH_2)
4 ¹	1.36(1H,m)	1.36(1H,m)	32.9(CH)	32.7(CH)
4 ^{1a}	0.87(3H, d)	0.85(3H, d)	19.8(CH_3)	19.7(CH_3)
5 ¹	1.22(2H,m)	1.22(2H,m)	37.5(CH_2)	37.5(CH_2)
6 ¹	1.26(2H,m)	1.24(2H,m)	24.6(CH_2)	24.5(CH_2)
7 ¹	1.08(2H,m)	1.08(2H,m)	37.5(CH_2)	37.5(CH_2)
8 ¹	1.36(1H,m)	1.37(1H,m)	32.9(CH)	32.7(CH)
8 ^{1a}	0.87(3H, d)	0.85(3H, d)	19.9(CH_3)	19.7(CH_3)
9 ¹	1.10(2H,m)	1.10(2H,m)	37.5(CH_2)	37.5(CH_2)
10 ¹	1.80(2H,m)	1.80(2H,m)	24.7(CH_2)	24.8(CH_2)
11 ¹	1.10(2H,m)	1.10(2H,m)	39.6(CH_2)	39.4(CH_2)
12 ¹	1.50(1H,m)	1.50(1H,m)	28.2(CH)	28.0(CH)
12 ^{1a}	0.85(3H, d)	0.85(3H, d)	22.8(CH_3)	22.6(CH_3)
13 ¹	0.85(3H, d)	0.85(3H, d)	22.8(CH_3)	22.6(CH_3)

^a Assignment aided by HMQC and HMBC experiments

^b Literature data of α - tocopherol (Benjamat *et al.*, 2017)

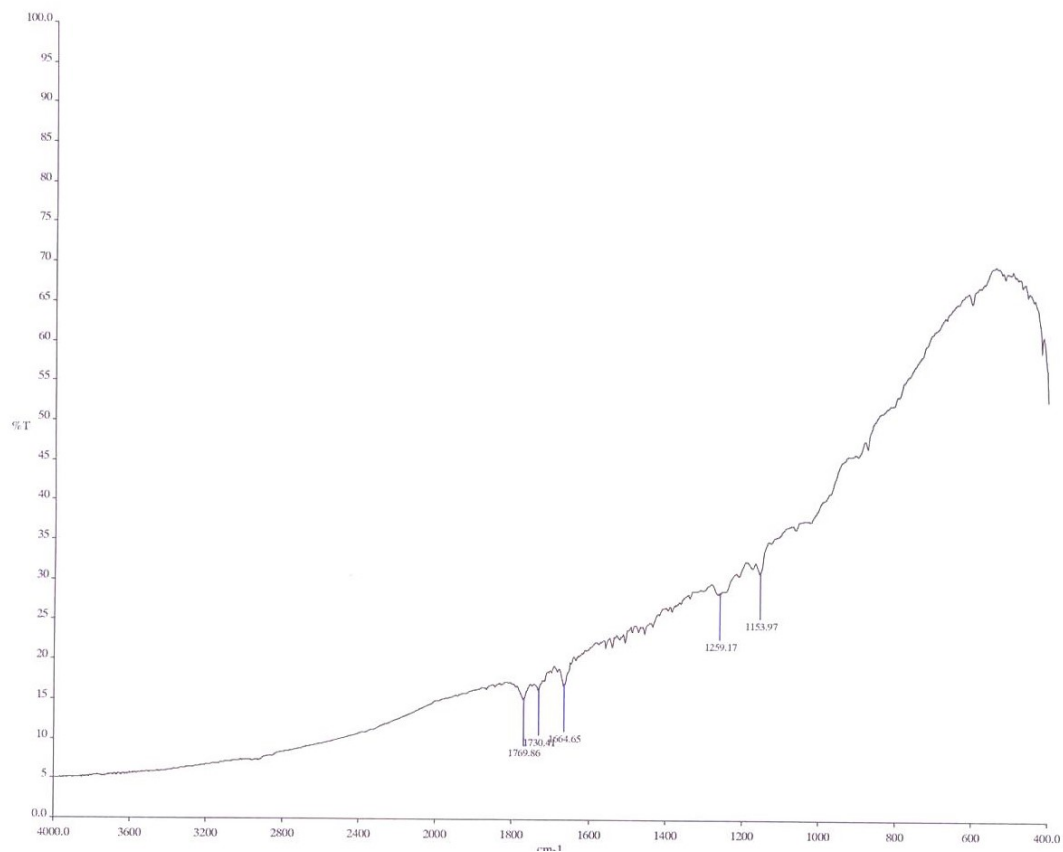


Fig. 4.82: IR spectrum of PA-C in CDCl₃ (expanded)

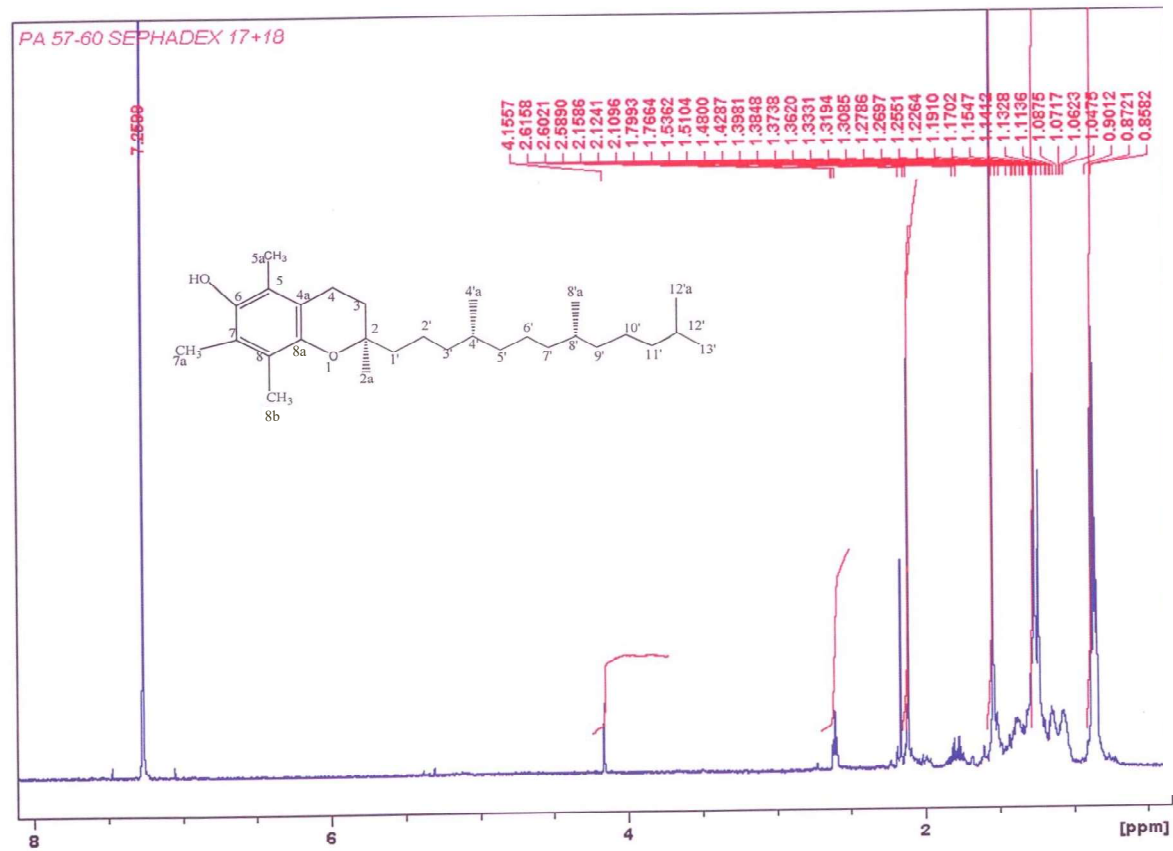


Fig. 4.83: ^1H NMR (500MHz) spectrum of PA-C in CDCl_3

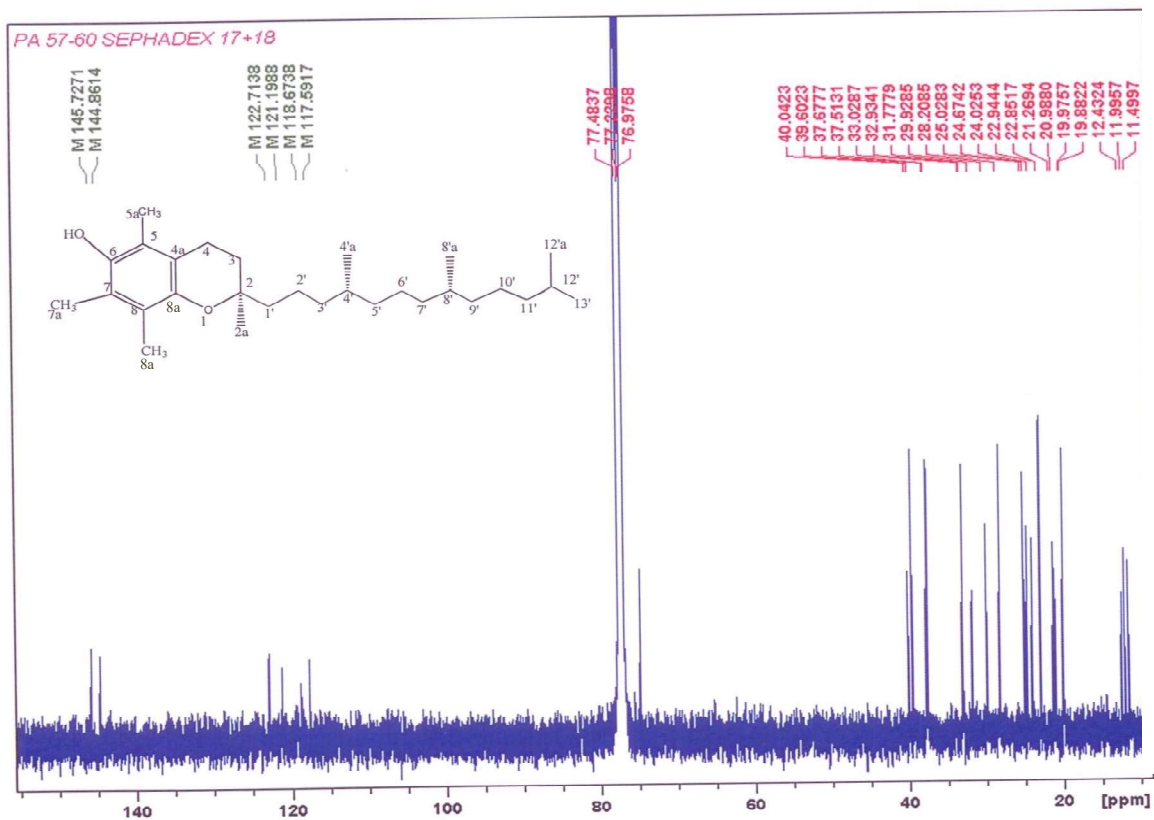


Fig. 4.84: ^{13}C NMR (125 MHz) spectrum of PA-C in CDCl_3

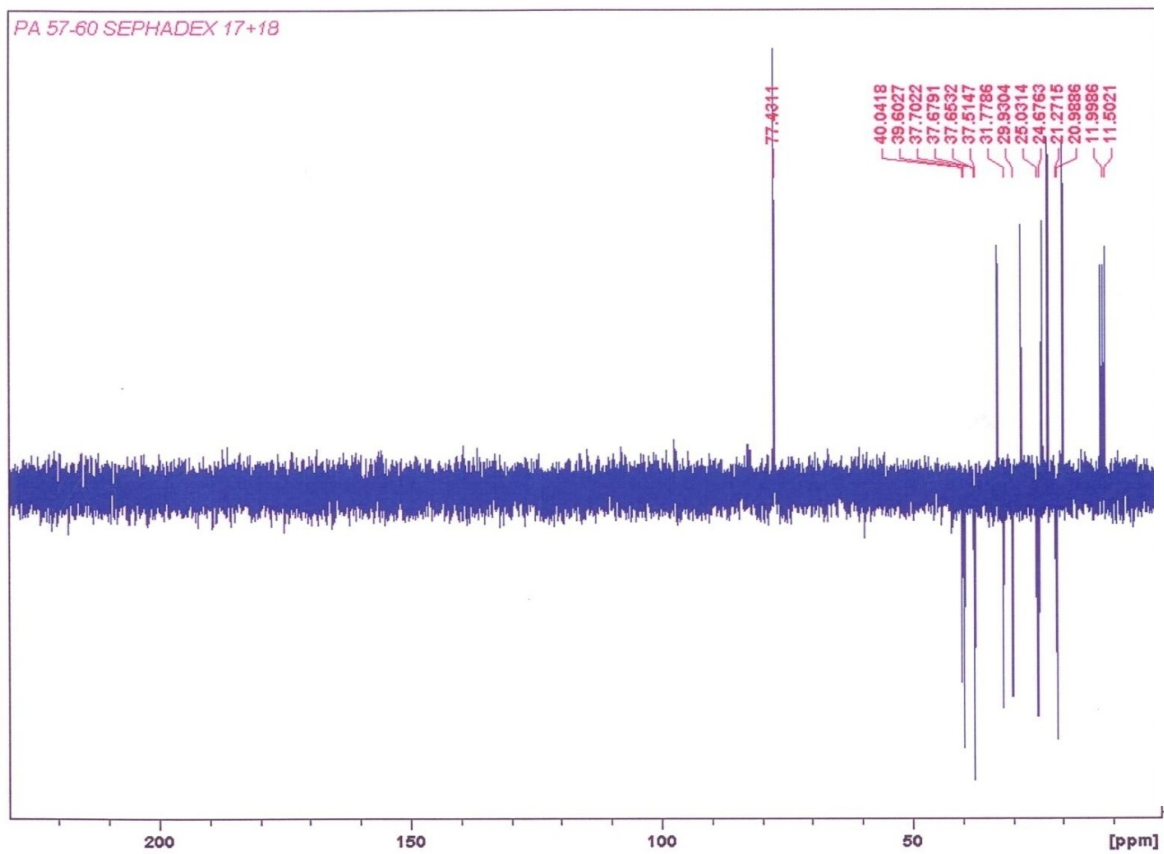


Fig. 4.85: DEPT spectrum of PA-C in CDCl_3

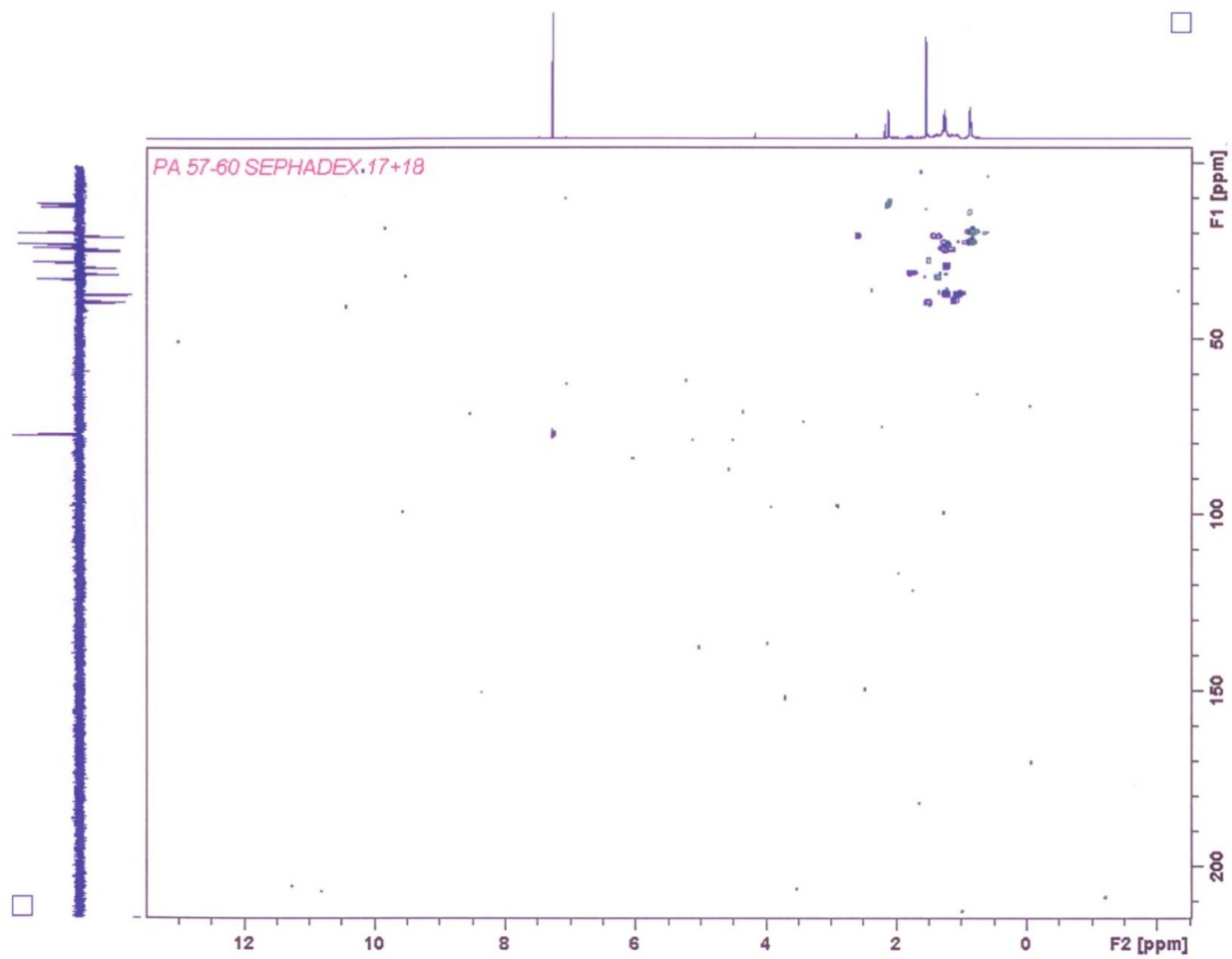


Fig. 4.86: HSQC DEPT spectrum of PA-C in CDCl_3

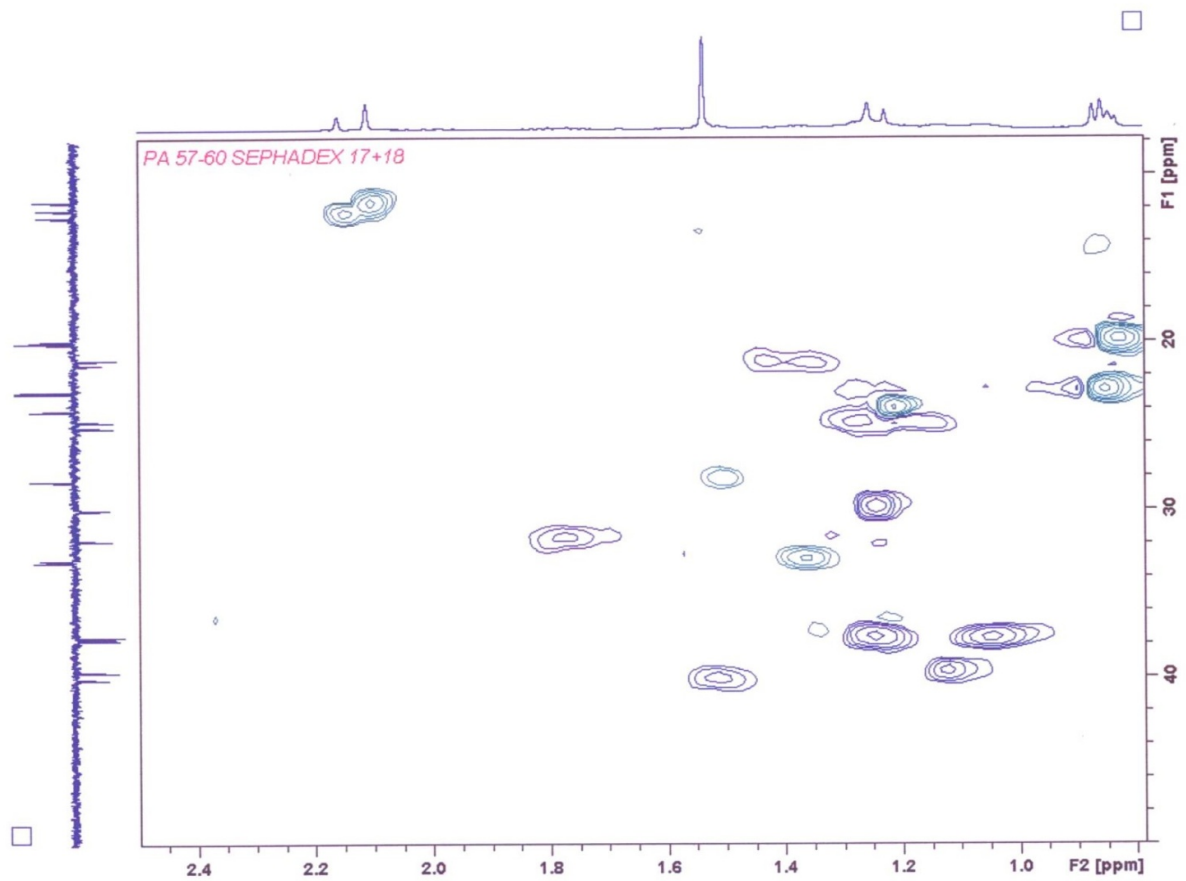


Fig. 4.87: HSQC DEPT spectrum of PA-C in CDCl_3 (expanded)

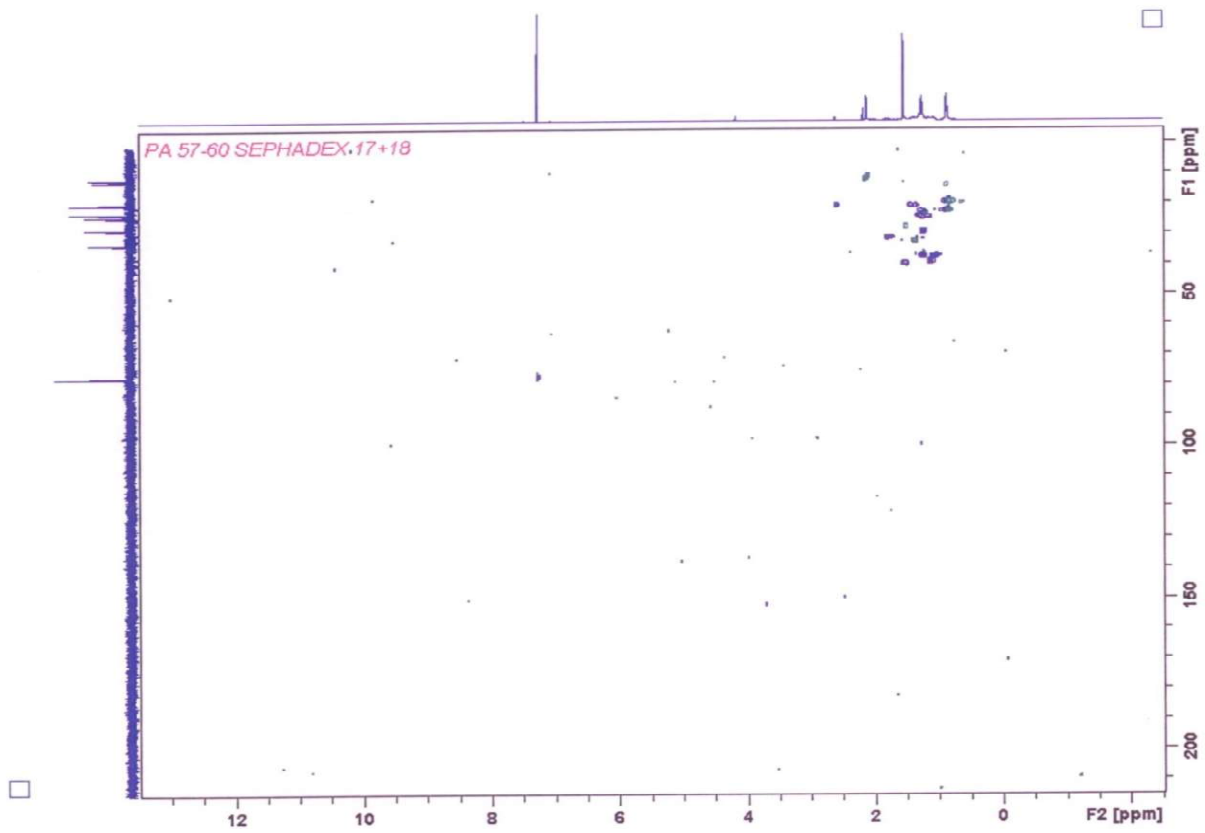


Fig. 4.88: HMBC spectrum of PA-C in CDCl_3

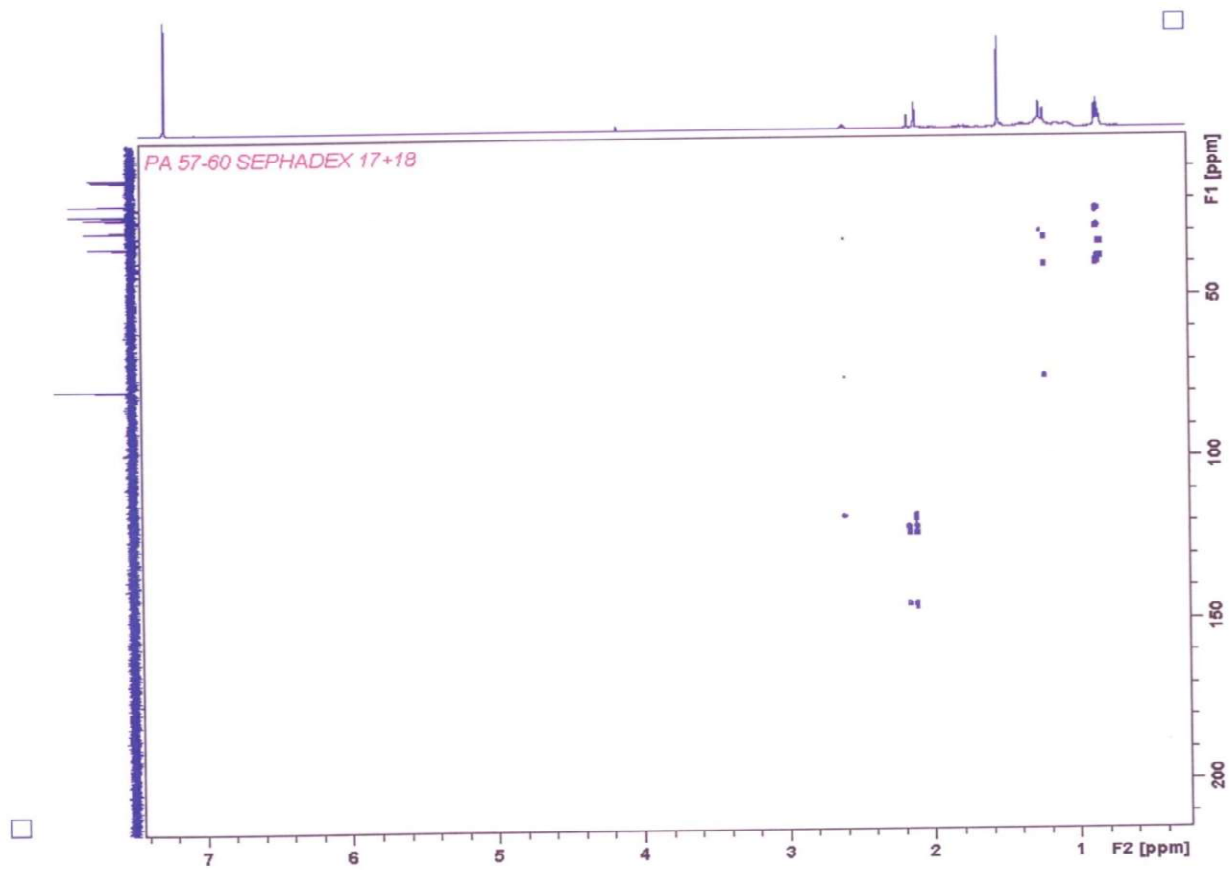


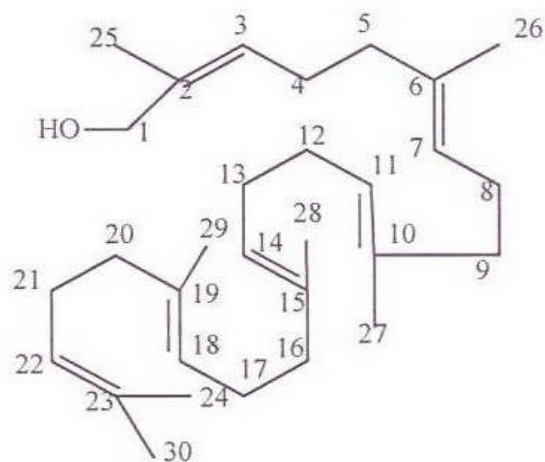
Fig. 4.89: HMBC spectrum of PA-C in CDCl_3 (expanded)

4.3.4 Structural elucidation of compound PA-D

Compound **PA-D** was isolated as a white solid. Its mass spectrum (Fig. 4.90) had a molecular ion peak at m/z 329.6 for $[M+Na^+]$ consistent with the proposed molecular formula $C_{20}H_{51}O$. The FTIR spectrum (Fig. 4.91) of compound **PA-D** showed absorption bands at 3415 cm^{-1} that was attributed to a hydroxyl group, 2954 and 2852 cm^{-1} attributed to CH stretches. Six olefinic proton resonances were observed at δ_H 5.11 in the 1H NMR spectrum (Fig. 4.92) which were assigned to H-3/22, H-7/18 and H-11/14 using HMBC spectrum (Fig. 4.96). The ^{13}C NMR spectrum (Fig. 4.93) displayed fifteen carbon resonances representing thirty carbons. Eight methyls, ten methylenes, one oxymethylene, six methines and six trisubstituted carbons were also observed in the DEPT spectrum (Fig. 4.94). Three methine carbon resonating at δ_C 124.3, δ_C 124.5 and δ_C 124.6 which corresponded to six methine carbons were observed in the ^{13}C NMR spectrum (Fig. 4.93). The out of chain methyl groups resonating at δ_C 17.9, δ_C 16.5 and δ_C 16.2 indicated the geometry of the six trisubstituted double bonds while signals appearing at δ_C 25.9, confirmed its in-chain position in the ^{13}C NMR spectrum (Fig. 4.93). Two overlapped methylene proton resonance at δ_H 2.07 m and 1.98 m and four overlapped methyl proton resonances at δ_H 1.67 s and 1.60 s were also observed. The oxymethylene proton resonances was observed at δ_H 4.16 ($J = 6.0\text{ Hz}$) while the oxymethylene carbon resonance was observed at δ_C 59.7. From the ^{13}C NMR spectrum (Fig. 4.93) double bond quaternary carbon resonance were observed at δ_C 131.4, 135.1 and 135.2.

Comparism between the ^{13}C NMR resonance for squalene and those of **PA-D** showed that carbon resonance at δ_C 140.1 and 59.7 were missing in that of squalene. In addition the HMBC spectrum (Fig. 4.96) showed a correlation between the oxymethylene proton resonance δ_H 4.16 with carbon resonance at δ_C 140.1 indicating

that the OH is attached to C-1 and not C-24. This was further supported by the correlation also observed in the HMBC spectrum (Fig 4.96) between the vinylic proton resonance at δ_H 5.11 with the downfield double bond carbon resonance at δ_C 140.1. Furthermore, a correlation was observed between this downfield double bond carbon resonance at δ_C 140.1 and a methyl group at δ_C 17.9. The hydroxyl group was assigned to C-1 position. This compound was characterized as squalen-1-ol [42]. This is the first report of this compound in nature to the best of our knowledge.



42

Table 12: ^1H (500 MHz) and ^{13}C (125 MHz) NMR Data^a for compound PA-D: squalen-1-ol (1-hydroxy squalene)^a and Squalene in literature^b in CDCl_3

No	^{13}C NMR ^a (125 MHz) CDCl_3	^{13}C NMR ^b (125 MHz) CDCl_3	^1H NMR ^a (500 MHz) CDCl_3	^1H NMR ^b (500 MHz) CDCl_3
1	59.7 CH_2	25.7 CH_3	4.16s	1.67s
2	140.1 C	131.2 C	-	-
23	131.4 C	131.2 C		
3/22	124.3 CH	124.2CH	5.11m	5.11m
4/21	26.8 CH_2	26.7 CH_2	2.10 m	2.10 m
5/20	39.9 CH_2	39.7 CH_2	1.98 m	1.98 m
6/19	135.1 C	134.9 C	-	-
7/18	124.5 CH	124.4CH	5.11 m	5.12 m
8/17	26.5 CH_2	26.6 CH_2	2.07 m	2.07 m
9/16	39.9 CH_2	40.0 CH_2	1.98 m	1.97 m
10/15	135.2 C	135.1C	-	-
11/14	124.6 CH	124.3 CH	5.11 m	5.11 m
12/13	27.8 CH_2	28.2 CH_2	2.01 dd	2.01 dd
24	25.9 CH_3	25.9 CH_3	1.68 s	1.67 s
25/30	17.9 CH_3	17.6 CH_3	1.60s	1.60s
26/29	16.2 CH_3	16.0 CH_3	1.67s	1.66s
27/28	16.5 CH_3	16.0 CH_3	1.60s	1.60s

^a Assignment aided by HMQC and HMBC experiments

^b Literature data of squalene (Barreto *et al.*, 2013)

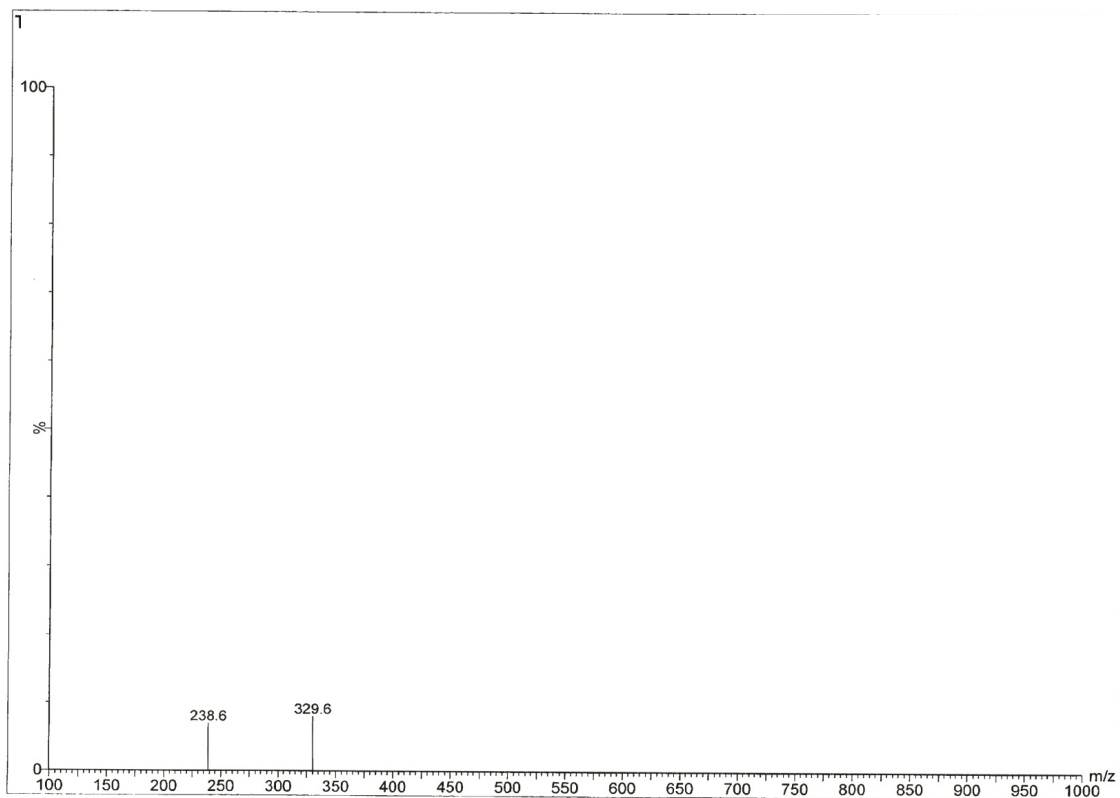


Fig. 4.90: MS spectrum of PA-D

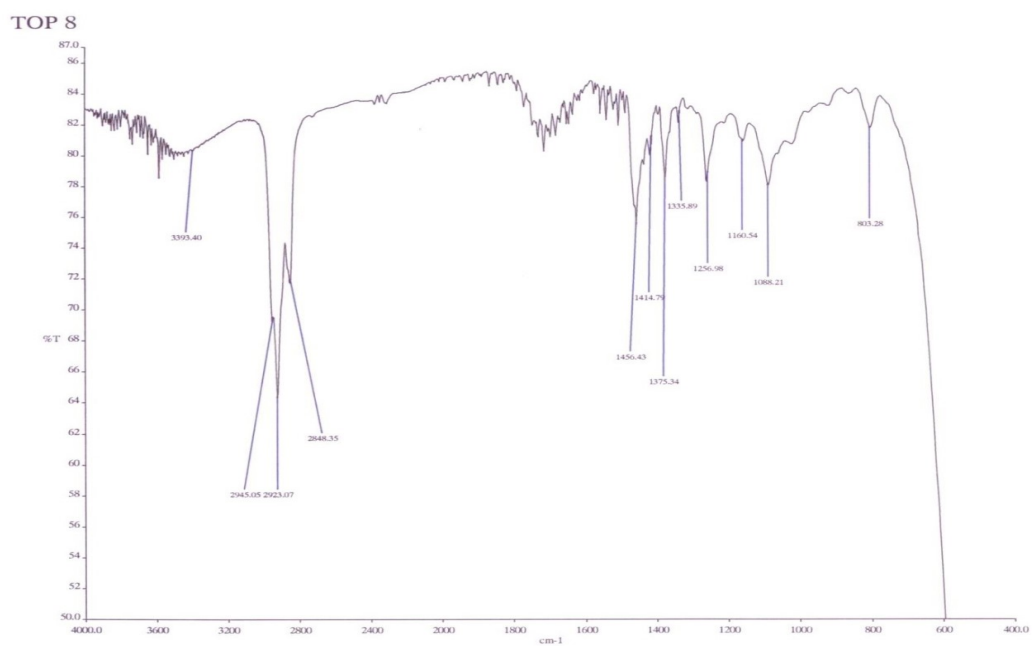


Fig. 4.91: IR spectrum of PA-D

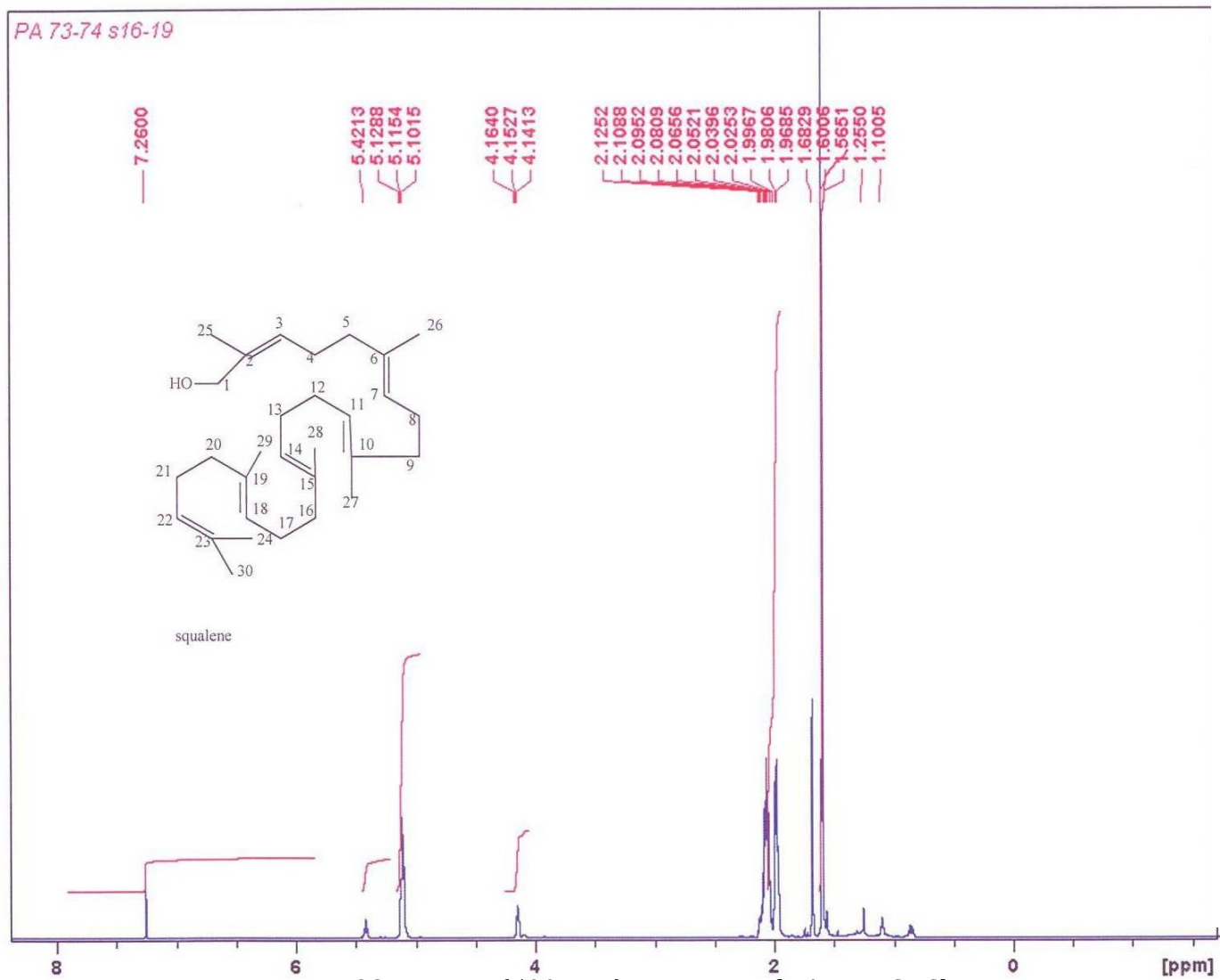


Fig. 4.92: ^1H NMR (500MHz) spectrum of PA-D in CDCl_3

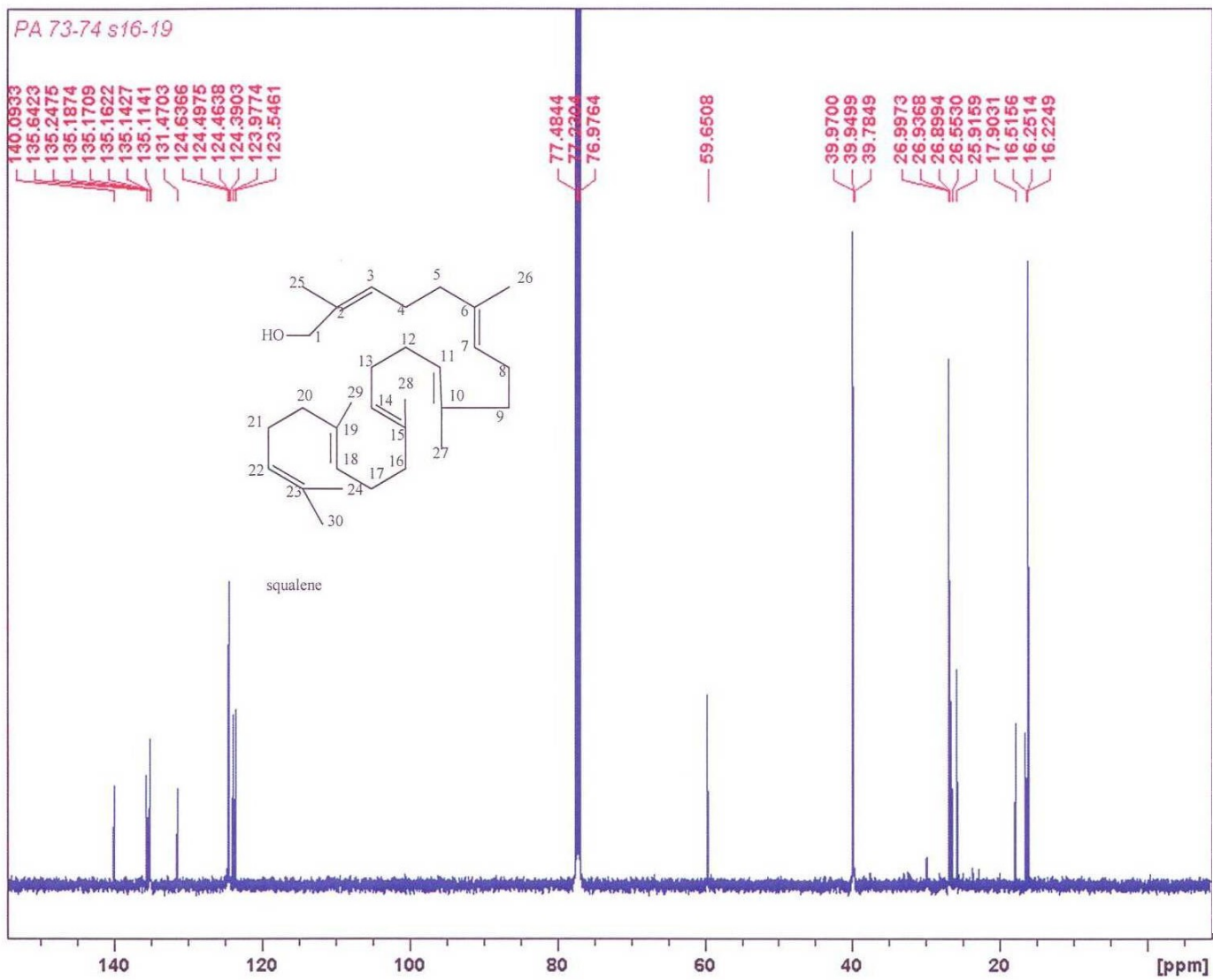


Fig. 4.93: ^{13}C NMR spectrum of PA-D in CDCl_3

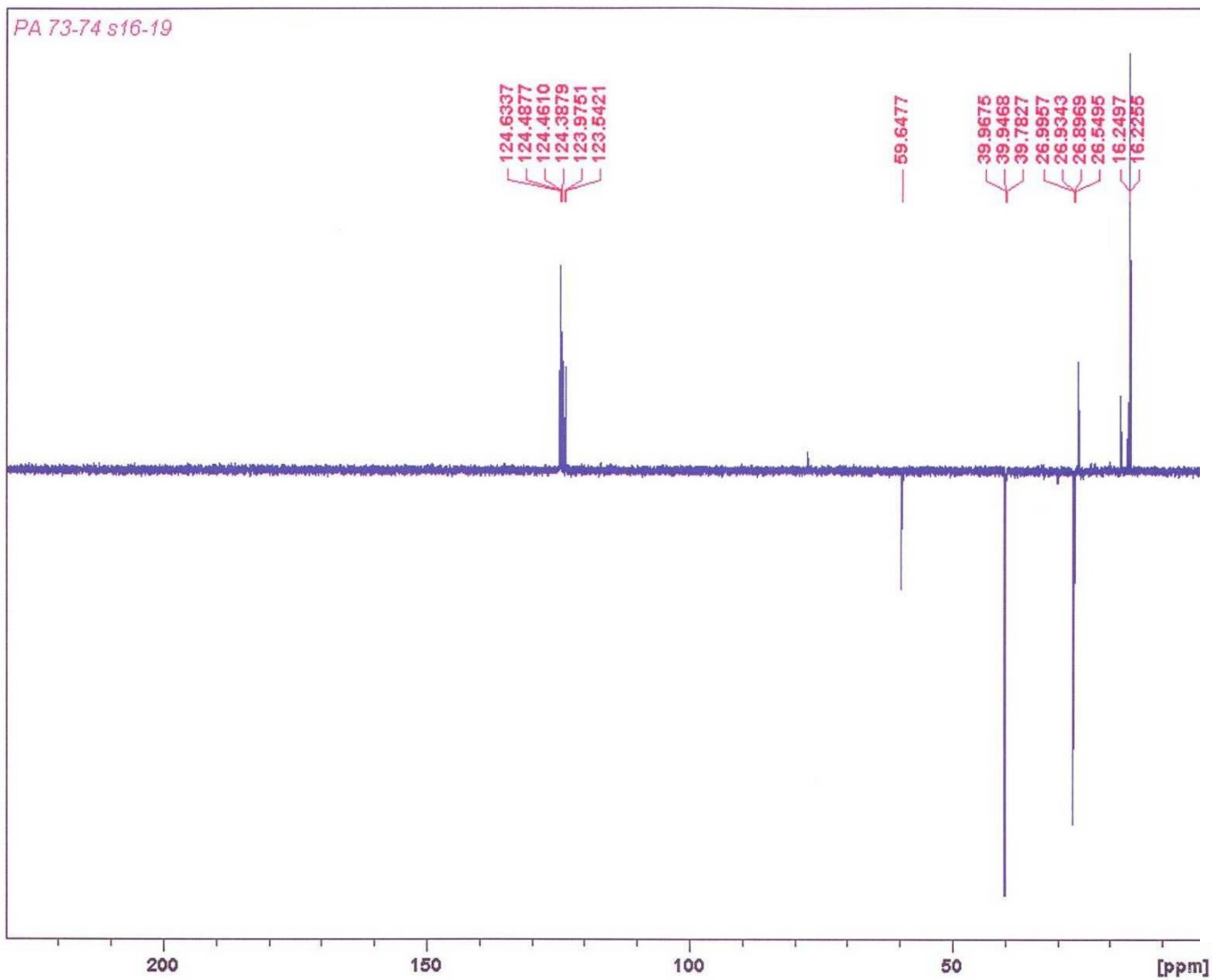


Fig. 4.94: DEPT spectrum of PA-D in CDCl_3

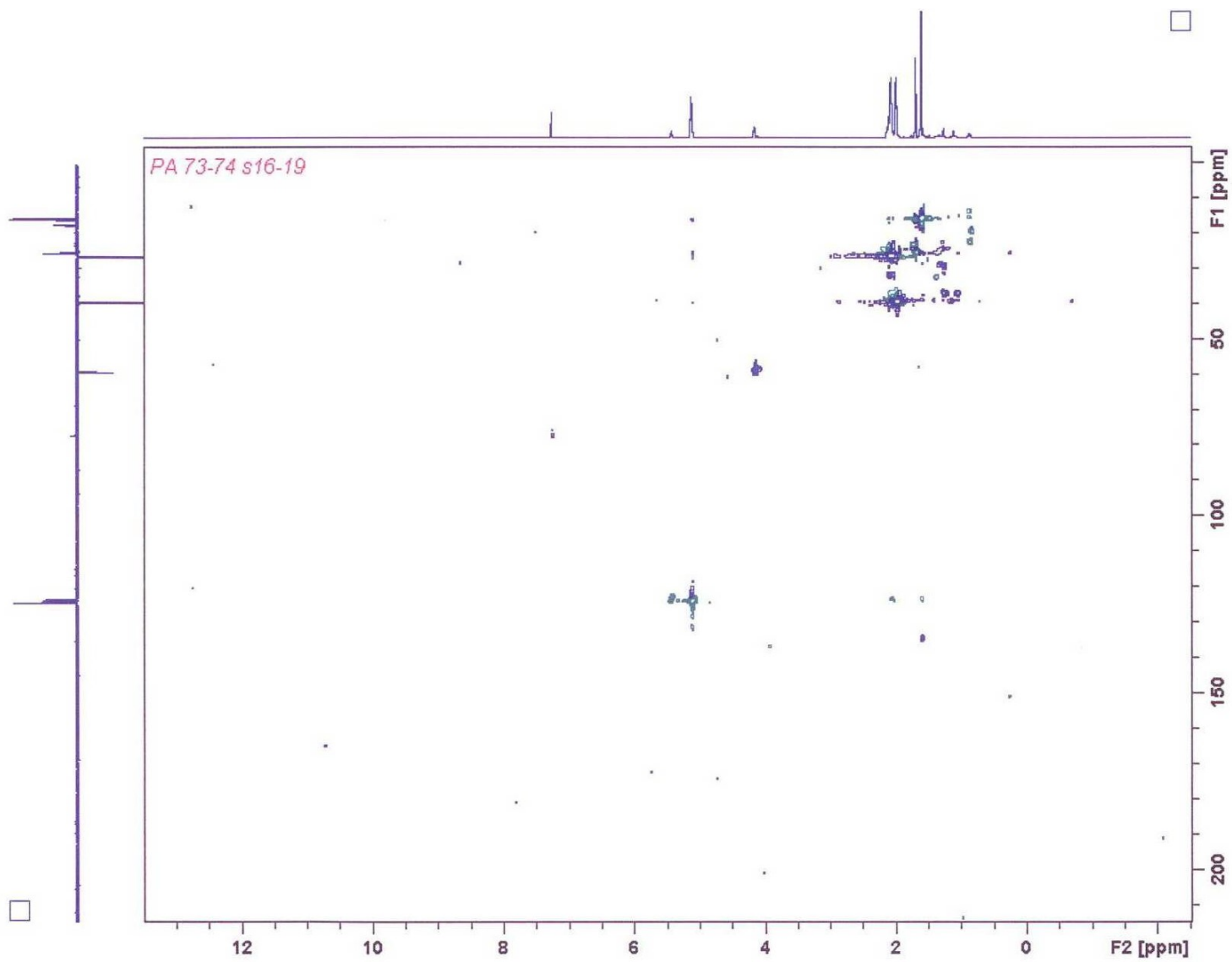


Fig. 4.95: HSQC DEPT spectrum of PA-D in CDCl_3

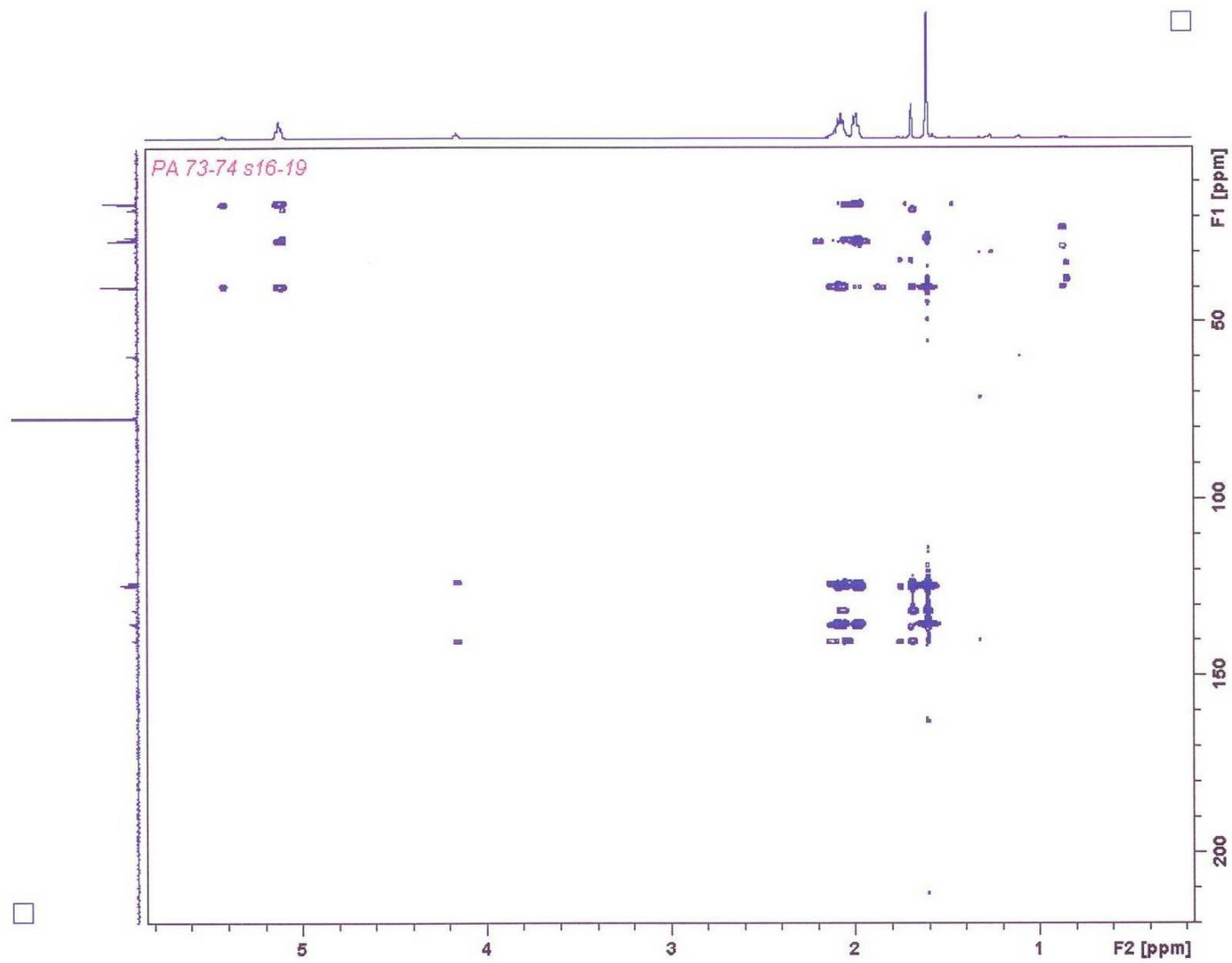


Fig. 4.96: HMBC spectrum of PA-D in CDCl_3

4.4 RESULT OF ANTIOXIDANT ANALYSIS (SCAVENGING EFFECT OF DPPH) ON DICHLOROMETHANE EXTRACT OF *Croton megalocarpoides* AND METHANOL EXTRACT OF *Physalis angulata*

ABSORBANCE VALUES AT 517 nm.

Lower absorbance of the reaction mixture indicated higher free radical activity. The dichloromethane extract of *Croton megalocarpoides* showed concentration –dependent free radical scavenging ability as shown in table 13. *Croton megalocarpoides* extract demonstrated modest antioxidant activity with the highest % radical scavenging activity 58.0 % at concentration of 1.0 mg/mL with IC₅₀ of 0.79 mg/mL. *Physalis angulata* extract antioxidant activities increase with increase in concentration. *Physalis angulata* extract showed the highest % radical scavenging activity 73.0 % at concentration of 1.0 mg/mL with IC₅₀ of 0.06 mg/mL. This indicates that *Croton megalocarpoides* and *Physalis angulata* are potential sources of natural antioxidants.

Table 13: Result of Antioxidant Analysis (Scavenging Effect of DPPH on Dichloromethane Extract of *Croton megalocarpoides*)
Absorbance values at 517nm

Concentration (mg/mL)	ABSORBANCE (nm)			
	Sample	Ascorbic acid	Scavenging Activity %	
			Sample	Ascorbic acid
1.0	0.333	0.151	58.0	91.5
0.5	0.327	0.172	58.8	90.3
0.252	0.438	0.175	44.8	89.7
0.125	0.427	0.179	46.2	89.0
0.0625	0.429	0.182	45.9	89.9

Table 14: Result of Antioxidant Analysis (Scavenging Effect of DPPH) on methanol extract of *Physalis angulata*,

Absorbance values at 517nm

Concentration (mg/mL)	ABSORBANCE (nm)			
	Sample	Ascorbic acid	Scavenging Activity %	
			Sample	Ascorbic acid
1.0	0.455	0.151	73.0	91.5
0.5	0.459	0.172	70.4	90.3
0.252	0.461	0.175	67.2	89.7
0.125	0.466	0.179	60.3	89.3
0.0625	0.470	0.182	56.4	89.0

4.5 RESULT OF ANTIOXIDANT ANALYSIS (SCAVENGING EFFECT OF DPPH) OF ISOLATED COMPOUNDS FROM *Croton megalocarpoides* AND *Physalis angulata*

Isolated compound CMD-A showed significant antioxidant activity at concentration of 1.0 mg/mL - 0.0625 mg/mL with % scavenging activity from 55.9 - 58.4. Isolated compounds CMD-B –CMD-E do not show significant antioxidant activity at concentration of 1.0 - 0.0625 mg/mL. The % scavenging activity of these isolated compounds (CMD-B –CMD-E) ranges from 26.9 - 33.8. The new isolated compounds CMD-F and CMD-G showed significant antioxidant activity at concentration of 1.0 mg/mL- 0.5 mg/mL with % scavenging activity ranging from 39.6 - 50.1 and IC₅₀ values of 0.72 and 0.74 mg/mL respectively. Compounds isolated from *Physalis angulata* (PA-A - PA-D) showed good antioxidant activity at concentration of 1.0 mg/mL - 0.625 mg/mL with % scavenging activity ranging from 48.8 % - 68.0%. The new isolated compound from *Physalis angulata* PA-D showed good antioxidant activity from concentration of 1.0 mg/mL to 0.625 mg/mL with % scavenging activity ranging from 55.2 -56.7 with IC₅₀ of 0.76 mg/mL.

Table 15: Result of Antioxidant Analysis (Scavenging Effect of DPPH) on isolated chemical compounds from *Croton megalocarpoides* and *Physalis angulata*

Absorbance values at 517nm

Concentration (mg/mL)	ABSORBANCE (nm)			
	Sample	Ascorbic acid	Scavenging Activity %	
			Sample	Ascorbic acid
	CMD-A		CMD-A	
1.0	0.735	0.151	58.4	91.5
0.5	0.748	0.182	57.7	90.0
0.25	0.756	0.172	57.2	90.3
0.125	0.770	0.179	56.4	89.8
0.0625	0.780	0.179	55.9	89.8
	CMD-B		CMD-B	
1.0	1.185	0.151	32.9	91.5
0.5	1.190	0.182	32.6	90.0
0.25	1.210	0.172	31.5	90.3
0.125	1.250	0.179	29.3	89.8
0.0625	1.290	0.179	26.9	89.8
	CMD-C		CMD-C	
1.0	1.170	0.151	33.8	91.5
0.5	1.178	0.182	33.3	90.0
0.25	1.181	0.172	32.8	90.3
0.125	1.186	0.179	32.8	89.8
0.0625	1.190	0.179	32.6	89.8

Concentration (mg/mL)	ABSORBANCE (nm)			
	Sample	Ascorbic acid	Scavenging Activity %	
			Sample	Ascorbic acid
	CMD-D		CMD-D	
1.0	1.181	0.151	33.2	91.5
0.5	1.187	0.182	32.8	90.0
0.25	1.196	0.172	32.3	90.3
0.125	1.213	0.179	31.4	89.8
0.0625	1.234	0.179	30.2	89.8
	CMD-E		CMD-E	
1.0	1.179	0.151	33.3	91.5
0.5	1.182	0.182	33.1	90.0
0.25	1.187	0.172	32.8	90.3
0.125	1.193	0.179	32.5	89.8
0.0625	1.206	0.179	31.7	89.8
	CMD-F		CMD-F	
1.0	1.009	0.151	42.89	91.5
0.5	1.066	0.182	39.67	90.0
0.25	1.102	0.172	37.60	90.3
0.125	1.133	0.179	35.89	89.8
0.0625	1.158	0.179	34.46	89.8
	CMD-G		CMD-G	
1.0	0.898	0.151	50.12	91.5
0.5	0.914	0.182	48.27	90.0
0.25	1.109	0.172	37.23	90.3
0.125	1.381	0.179	21.84	89.8
0.0625	1.381	0.179	21.84	89.8

Concentration (mg/mL)	ABSORBANCE (nm)			
	Sample	Ascorbic acid	Scavenging Activity %	
			Sample	Ascorbic acid
	CMD-H		CMD-H	
1.0	1.110	0.151	37.2	91.5
0.5	1.118	0.182	36.7	90.0
0.25	1.126	0.172	36.3	90.3
0.125	1.164	0.179	34.2	89.8
0.0625	1.198	0.179	26.5	89.8
	PA-A		PA-A	
1.0	0.795	0.151	55.0	91.5
0.5	0.801	0.182	54.7	90.0
0.25	0.817	0.172	53.8	90.3
0.125	0.836	0.179	52.7	89.8
0.0625	0.904	0.179	48.8	89.8
	PA-B		PA-B	
1.0	0.769	0.151	56.5	91.5
0.5	0.770	0.182	56.4	90.0
0.25	0.780	0.172	55.9	90.3
0.125	0.793	0.179	55.1	89.8
0.0625	0.793	0.179	55.1	89.8
	PA-C		PA-C	
1.0	0.564	0.151	68.0	91.5
0.5	0.571	0.182	67.7	90.0
0.25	0.621	0.172	64.8	90.3
0.125	0.678	0.179	61.6	89.8
0.0625	0.735	0.179	58.4	89.8

Concentration (mg/mL)	ABSORBANCE (nmp)			
	Sample	Ascorbic acid	Scavenging Activity %	
			Sample	Ascorbic acid
	PA-D		PA-D	
1.0	0.764	0.151	56.7	91.5
0.5	0.887	0.182	49.8	90.0
0.25	1.174	0.172	33.5	90.3
0.125	1.185	0.179	32.9	89.8
0.0625	1.246	0.179	29.4	89.8

CHAPTER FIVE

5.0 CONCLUSION

Twelve compounds were isolated from the two medicinal plants- *Croton megalocarpoides* and *Physalis angulata* . Two new compounds and six other compounds were isolated for the first time from the stem bark of *Croton megalocarpoides* . The two new compounds were named as 12-*epi*-Croton zambefuran A **CMD-F** and 1-(*p*-hydroxy coumaric acid)-geranyl geran-1-ol **CMD-G**. The other six compounds were identified as lupeol (**CMD-A**), 15,16-epoxy-3,13(16),14-clerodatriene-20,12-olide-18,19-dioic acid dimethylester **CMD-B**, 18,19,-dimethoxycarbonyl-3 α acetoxy,4 β -hydroxy-15,16-epoxy-clerodane-7,13(16),14-triene-12,20-olide **CMD-C**, 1,2-dehydrocrotonocorylifuran-2-one **CMD-D**, 7,8-dehydrocrotonocorylifuran **CMD-E** and lignoceryl-trans-ferulate **CMD-H**. A new squalene derivative and three other compounds were also isolated for the first time from *Physalis angulata*. The squalene derivative was named as 1-hydroxy-squalene (**PA-D**) .The other compounds were identified as phytol (**PA-A**), squalene (**PA-B**) and α -tocopherol (**PA-C**). The extracts and isolated chemical compounds from *Croton megalocarpoides* and *P.angulata* investigated for antioxidant activities showed that the antioxidant activities of extracts of both plants increased with increase in their concentration. The two extracts exhibited the highest % radical scavenging activities at 58.0 and 73.0 respectively (IC₅₀ of 0.79 and 0.06 mg/mL).

The new isolated compounds (12-*epi*-Croton zambefuran A **CMD-F** and 1-(*p*-hydroxy coumaric acid)- geranyl geran-1-ol **CMD-G**) showed significant antioxidant activity at concentration of 1-0.5 mg/mL with IC₅₀ values from 0.72 to 0.74 mg/mL. The 1-hydroxy-squalene (**PA-D**) also showed significant antioxidant activity at concentration of 1-0.0625 mg/mL with IC₅₀ value of 0.76. It can be correlated that the antioxidant activity of *Croton megalocarpoides* and *Physalis angulata* could be attributed to the presence of these isolated

compounds that showed antioxidant activity which could be responsible for the ethno-medicinal uses of these two plants.

REFERENCES

- Barahona MV, Sanchez- Fortun S. 1999. Toxicity of Carbamates to the brine shrimp *Artemia salina* and the effect of atropine, BW 284c51, Iso-OMPA and 2-PAM on carbonyl toxicity. *Env. Pollut*, 104: 469-476
- Barreto, M B., Gomes, C.L., de Freitas, J.V.B., Pinto, F.d.C.L., Silveira, E. R., Gramosa, N.V., Torres, A.S.C., 2013. Flavonoids and Terpenoids from *Croton Muscicapa* (*Euphorbiaceae*). *Quimica Nova* 36, 675-679.
- Beth N, Langat M.k, Harry E, Larry A.W, Ilias M, Mulholland D.A, kerubo L.O, Midiwo J.O. 2016. New *ent* clerodane and abietane diterpenoids from the roots of Kenyan *Croton megalocarpoides*. *Planta medica* 82(11/12). 1079-1086.
- Beentje H.J. 1994. Kenyan Trees, Shrubs, Lianas, Majestic Printing Works Ltd. Nairobi, Kenya: 190-192.
- Benjamat C, Thanesuan N, Songchan P, Anumat B. 2017. Chemical constituents of fruits and leaves of *Crotoxylum cochinchinense* and their cytotoxic activities. *Naresuan University Journal: Science and Technology*, 25 (3), 22-30.
- Bohm, B. A. 1994. Flavonoid and Condensed tannins from Leaves of *Vaccinium vaticulatum* and *V. calycinium*. *Pacific Sci.* 48: 458-463.
- Burkill, H.M. 1985. The useful plants of West Tropical Africa. 2nd Edition. Volume 1, Families A-D, Royal Botanic Gardens, Kew, Richmond, United Kingdom. 960
- Cao G, Alesso H.M, Gutler R.G 1993. Oxygen radical absorbance capacity assay for antioxidants free radical. *Biology and medicine* 14. 303-311.
- Chapman, V. 1997. Natural Product. Dictionary of Natural product. Chapman and Hall. 866-1042.
- Cooper R, George N. 2015. Natural Products Chemistry .Sources, Separations and Structures. CRC press. 203-210.
- Dudley H.W. 1980. Spectroscopy method in organic chemistry. McGraw Hill. 252-257

- Edeoga, H. O.; Okwu D.E. Mbaebia G.A 2005. Phytochemical Constituents of Some Nigerian medicinal plants. *African journal of Bio-technology*. 47; 685-688
- Evans W.C , Trease G.E.1989.Pharmacognosy.Balliere Tindall,13th Edition. 97-105
- Fedeli E, Capella P, Cirmelle M, Jacini G.1966. Isolation of geranyl geraniol from the unsaponifiable fraction of Linseed oil. *Journal of Lipid Research* 17, 438-441.
- Feka P.D, Mohammed S.Y. Shaibu M.A, Solomon R.S. 2013. Phytochemical screening and antimicrobial efficacy of *Physalis angulata* extracts. *Journal of Pharmacology* 18-24.
- Finar, L. 1973. Organic Chemistry “Natural Product”. Academic Press, 5th Edition. 458-470.
- Gelosa D, Sliepcevich A.2009. Fundamentals of chemistry, Chromatography techniques, Politecnio di Milano,Encclopeadia of life support systems, 1,16-27.
- Gongalez A.G, Ferro E.A, Ravelo A.G 1987. Triterpenes from *Mayterus horrid* *Phytochemistry* 26, 2785-2788.
- Grubben G.J, Denton O.A. 2004 .*Plant products of Tropical Africa 2.Vegetables* Wageningen.PROTA foundation. 167-171.
- Harbone J.B, Williams C.A 2000. Advances in flavonoid research since 1992.*Phytochemistry* 55 :481-504.
- Harbone, J.B. 1993. A Guide to Modern Techniques of Plants Analysis. Phytochemical .3:46-60.
- Harbone J.B.1984.Phytochemical methods. Chapman and Hall. 245-248.
- Harwig J. Scott P.1971 .Brine Shrimp *Arternia Salina L* Larvae as a screening system for fungal toxins. *Appl Microbial* 1011-1016.
- He, H.P., Cai, Y. Z., Sun, M., Corke, H., 2002. Extraction and Purification of Squalene from *Amaranthus grain*. *Journal of Agricultural and Food Chemistry* 50, 368-372.
- IUCN.1993.International Union of Conservation of Nature Report
- <http://www.plantzafrica.com/planted/crotonmegalocarpoide.htm> retrieved on the 14th November,2017

<http://www.ethnopharmacologia.org/phototheque/Physalisangulata1.jpg> retrieved on the 14th November, 2017.

Jaki .B, Ogala. J, Burji H. Sticher.O.1999. Biological Screening of cyanobacteria for antimicrobial and molluscidal activity brine shrimp lethality and cytotoxicity. *Pharm Biol.*37:138-143.

Ksumoto, I.T. 1993. "Screening for some Indonesian Medicinal for Inhibiting Effects on Limited.35, 153-159.

Kumar M, Rawat P, Gautan A.k Singh R.2010. Antio-osteoporotic constituents from Indian medicinal plants.*Phytomedicine 17*: 993-999.

Kuo Y.H, Chen W.C 1999. Chemical constituents of the pericarp of *Platyclus orientalis*, *Journal of Chinese chemical society.* 46, 819-825.

Lawal O. Uzokwe E. Igboanugo I, Adio F. Awuson A. 2010. Ethno medical information on collection and identification of some medical Plants in research Institute of South-West Nigeria. *Afri. J. Pharm* 4 (9);32

Manuchair.E(2002).*Pharm. dynamic basis of herbal medicine.CRC press.*14(2).356-360.

Martinez .M, Ramo. J, Torreblanca. A, Diaz – Mayans J.1998 effect of Cadmium exposure on zinc levels in the brine shrimp *Artemia partenogenetica*. *Aqua culture.*172: 315-325.

McLaughlin J.L, Chang C.J., Smith, D.L.1991: Bench top "Bioassay for the discovery bioactive natural products: an update in studies in natural products chemistry (edited by; All Rahman) Elseview, 383-409.

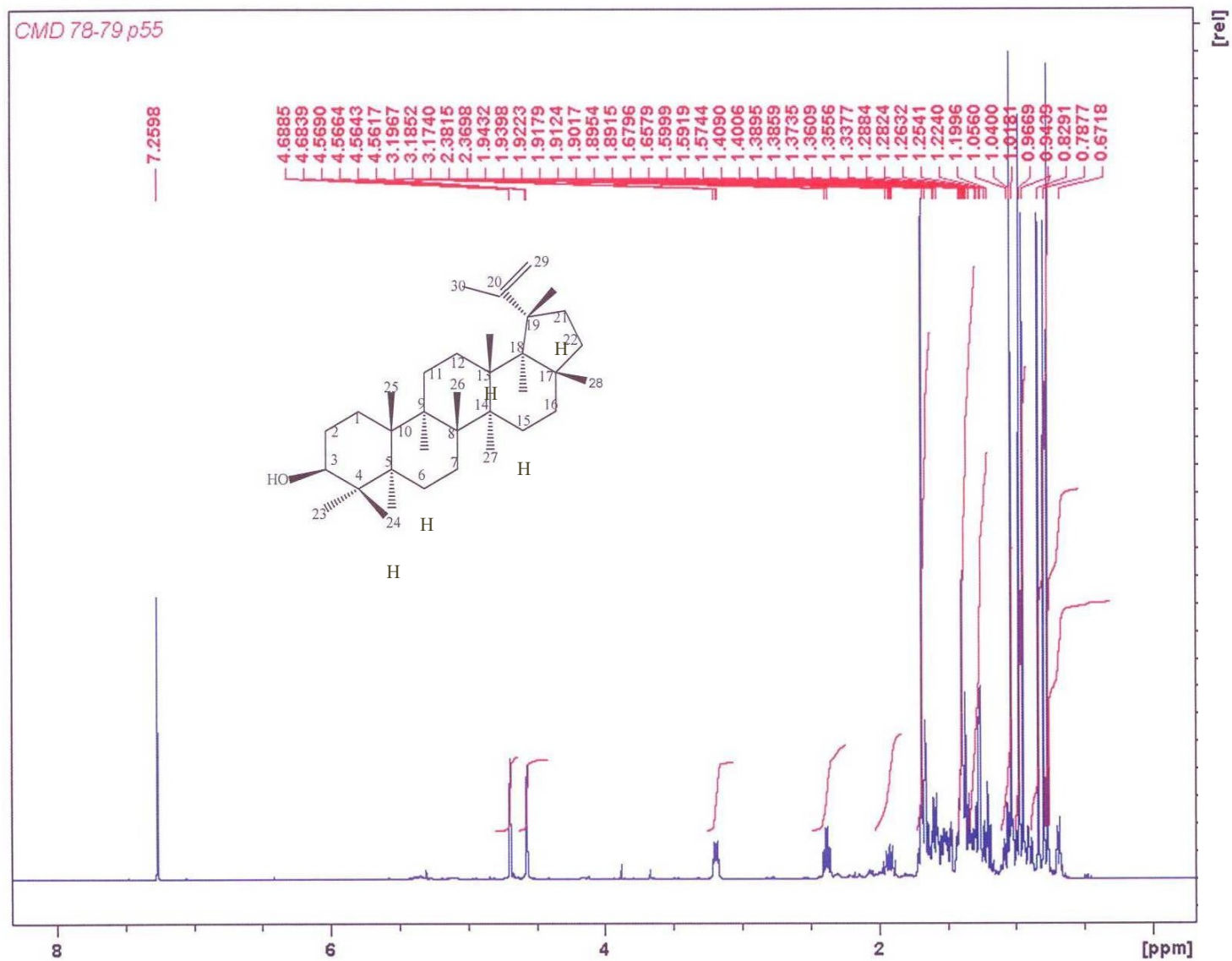
Morrison,R.T, Bough R.N.2004.Spectroscopy and structure. *Organic Chemistry.* Prentice Hall,6; 586-600.

Motaleb A.M. 2011. Selected Medicinal plants of Chittagong Hill tracts. Published by IUCN (International Union for conservation of Nature. 116.

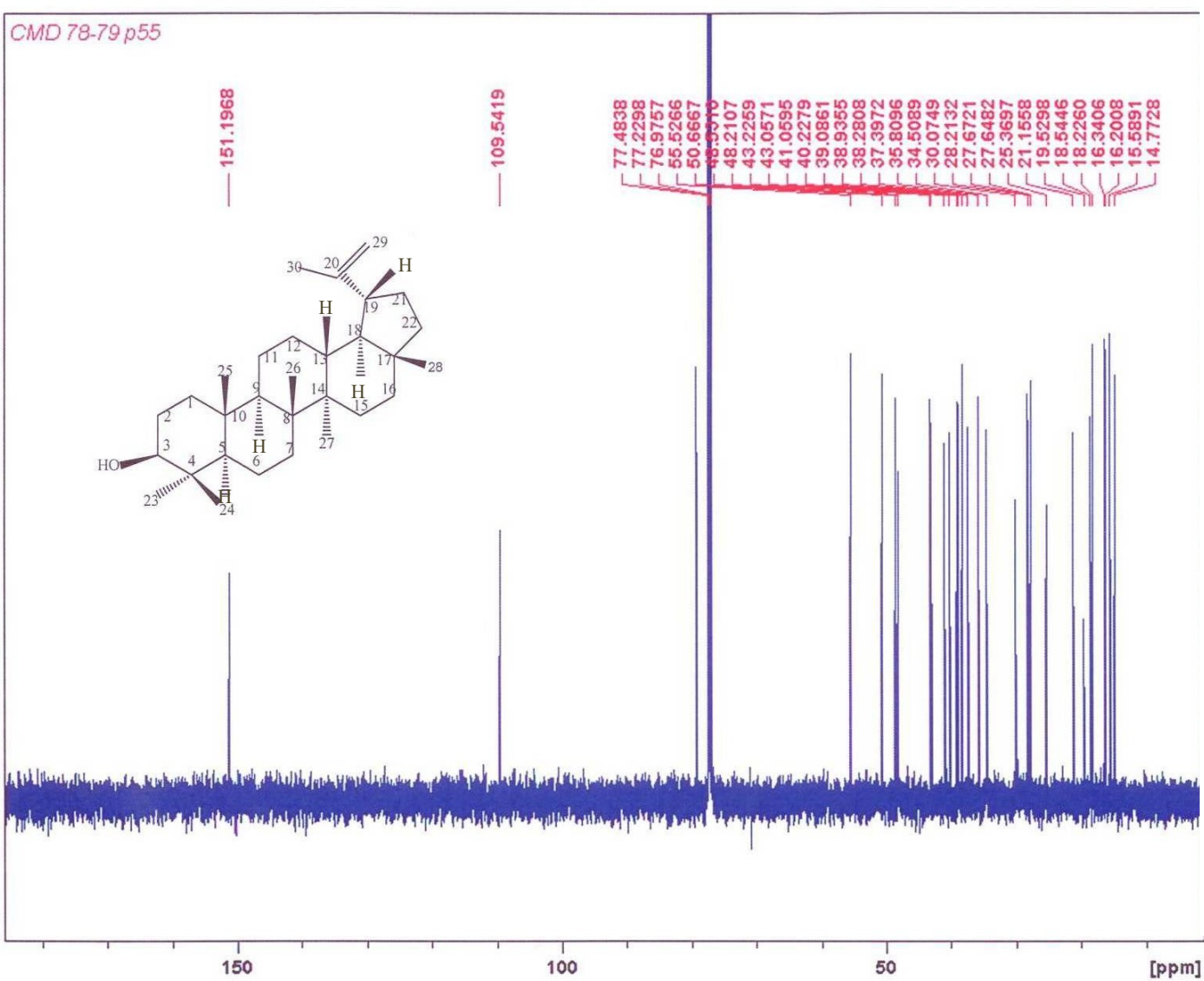
Naqvi S.A, Khan M.S, Whora S.B.1976. Antibacterial, antifungal and anthelmintic Studies on *Ochrocarpus longifolius*. *Planta medica* 29, 98-103.

- Ngadjui B.T, Abegaz B.M, Keumedjo F, Folefoe G., Kapche G.W. 2002. Diterpenoids from the stem bark of *Croton zambesicus*. *Phytochemistry*. 60:345-349.
- Onocha P.A. Oloyede G.K. Abegunde L.M. 2016. Antioxidant, Toxicity and Phytochemical Screening of Extracts Obtained from *Mariscus alterifoliosus* Vahl. *Journal of Natural Sciences Research*. ISSN 2225-0921 (Online) 6(5) 1-5.
- Onocha P.A. Oloyede G.K. Afolabi Q.O. 2011. Chemical Composition, Cytotoxicity and Antioxidant Activity of Essential Oils of *Acalypha hispida* Flowers. *International Journal of Pharmacology*, 7: 144-148.
- Padhee D. K. 2001. Medicinal plants of Orissa. Conservation and utilization of medicinal and aromatic plants. Allied Publisher Limited. 22.
- Peka. M, Danzl. C., Disfler.W. .2000. Novel Antibacterial quaternary alkaloid from *Vepris Lowsii*, *Planta Medica* 44, 139-742.
- Philip.M .1996 .Separation Techniques. Advanced chemistry Cambridge University Press. 205-208.
- Prior R.L, Hoang H ,Basu B.D.1981.Indian medicinal plants, Lalit Mohan Basu, Allahabad, India.2. 204-208.
- Rajab M.S, Cantrell C.L, Franzblau S.G, Fischer N.H.1998.Antimycobacterial activity of Phytol and its derivatives,a preliminary structure-activity study.*Planta med* 64:2-4
- Reddy H.L, Couvreur P.2009. Squalene: A natural triterpene for use in disease management and therapy. *Advance Drug Delivery Reviews* 61. 1412-1426.
- Renata S, Malgorzata K, Monika K, Lewandowski W. 2012. Spectroscopic (FTIR, FT-Raman, ¹H and ¹³ C NMR and theoretical studies of p -coumaric acid and alkali metal p –coumarates. *Spectroscopy* 27. /SPE-2012-0568.IOS Press. 35-48.
- Renaud S.C, Guegen R, Schenlies J. 1998 .Alcohol and mortality in middle age man from eastern France. *Epidemiology*, Scopys. 184-188.
- Savithamma N .Linga M,Rao J.Suhrulatha D.2011.Screening of medicinal plants for secondary metabolites. *Middle East Journal of Scientific Research*.813 579-584.

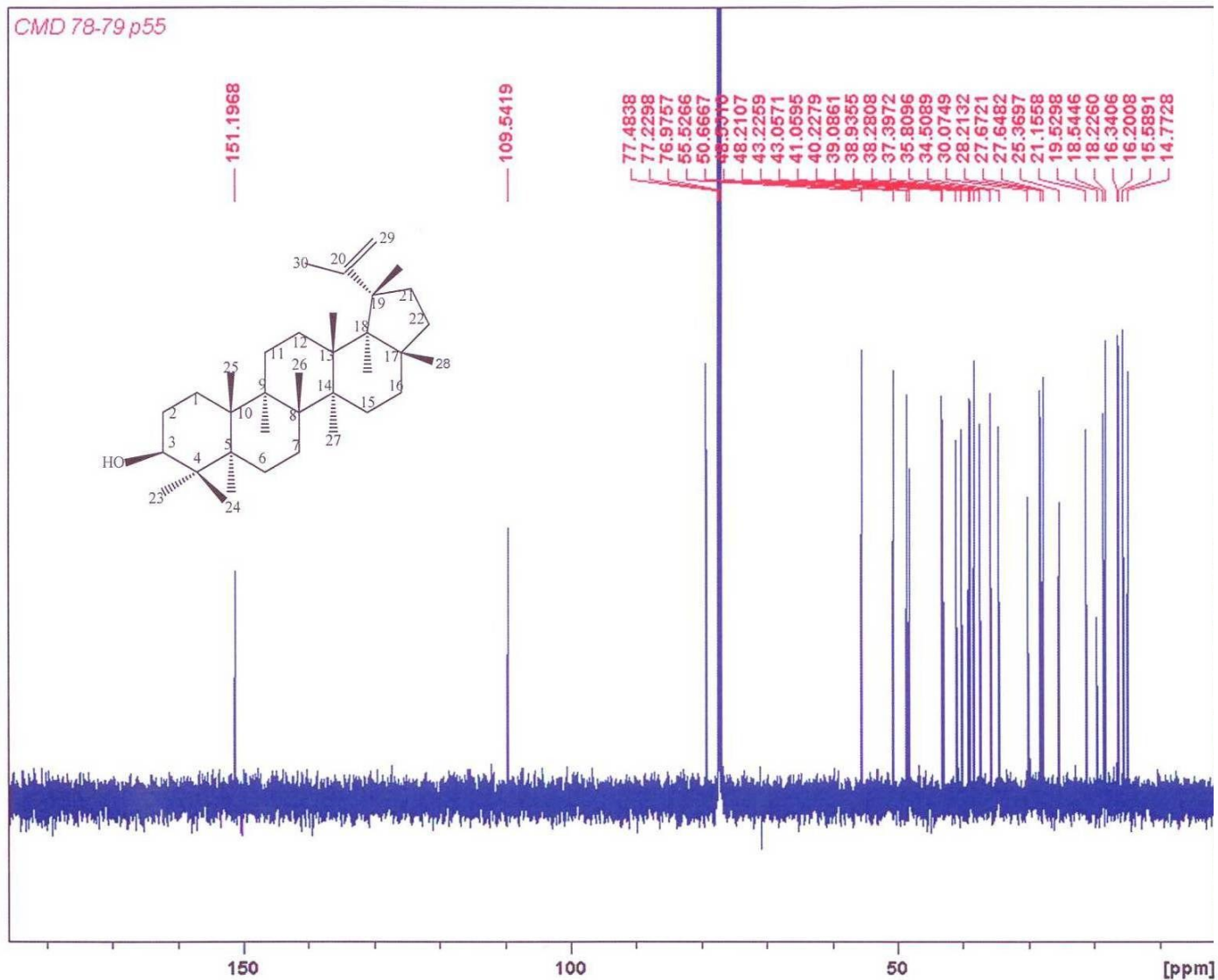
- Shivi D. and Kamlash T. 1980. Plants used by the Bhat Community for regulating fertility. *Eco. Bot.* 34 (3): 273-275.
- Sleet R.B, Brandel.K.1983. Improved methods for harvesting and counting synchronous populations of *Artemia nauphi* for use in developmental toxicology. *Ecotoxicol Env. Safety.*, 7: 435-446.
- Sofowora A.1993..Medicinal plants and Traditional Medicine in Africa.Spectrum Books. Ibadan, Nigeria.. 34-188.
- Solis,P.N, Wright, C.W. Anderson, M.M, Gupta, M.P, Phillipson JD:1993 A microwell cytotoxicity assay using *Artemia salina*. *Plant Med* 59: 250-252.
- Tabuti J.R, Lye K.A, Dhyllon S.S.2003. Traditional herbal drugs of Budamogii, Uganda. Plants use and administration. *Journal of Ethnopharmacology* 88(1) 19-44.
- Talha A. Murat C. Adnan K. 2013. The effect of flavonoid in the treatment of hepatopulmonary syndrome. *Journal of the Korean Surgical Society.* 85(5) 219-224.
- Takaya, Y., Kondo, Y., Furukuwa, T, Niwa, M, 2003. Anti-oxidant constituents of radish sprout (Kaiware-daikon), *Raphanus sativus* L. *Journal of Agricultural and Food Chemistry.* 51, 8061-8066.
- Tchissambou L, Chiarioni A, Richie C.and Khoung –huuf.1990.Crotocorylifuran and Crotohaumanoxide, new diterpenes from *Croton haumanianus* J.Leonard.*Tetrahedron letters* 46(15):5199-5202.
- Temple N.J. 2000. Antioxidants and diseases. More questions than answers. *Nutrition Research.* 20. 449-459.
- Tolstiva T.G, Sorokina I.V, Tolstikov A.G, Flekhter O.B (2006). Biological activity and Pharmacological prospects of lupine terpenoids: Natural lupane derivatives. *Russian Journal of Bioorganic Chemistry* 32.37-49.
- Townsend, C.C. 1988. *Amaranthaceae*. Flora of Tropical West Africa. A.A. Balkema Rotterdam, Netherlands. 136.



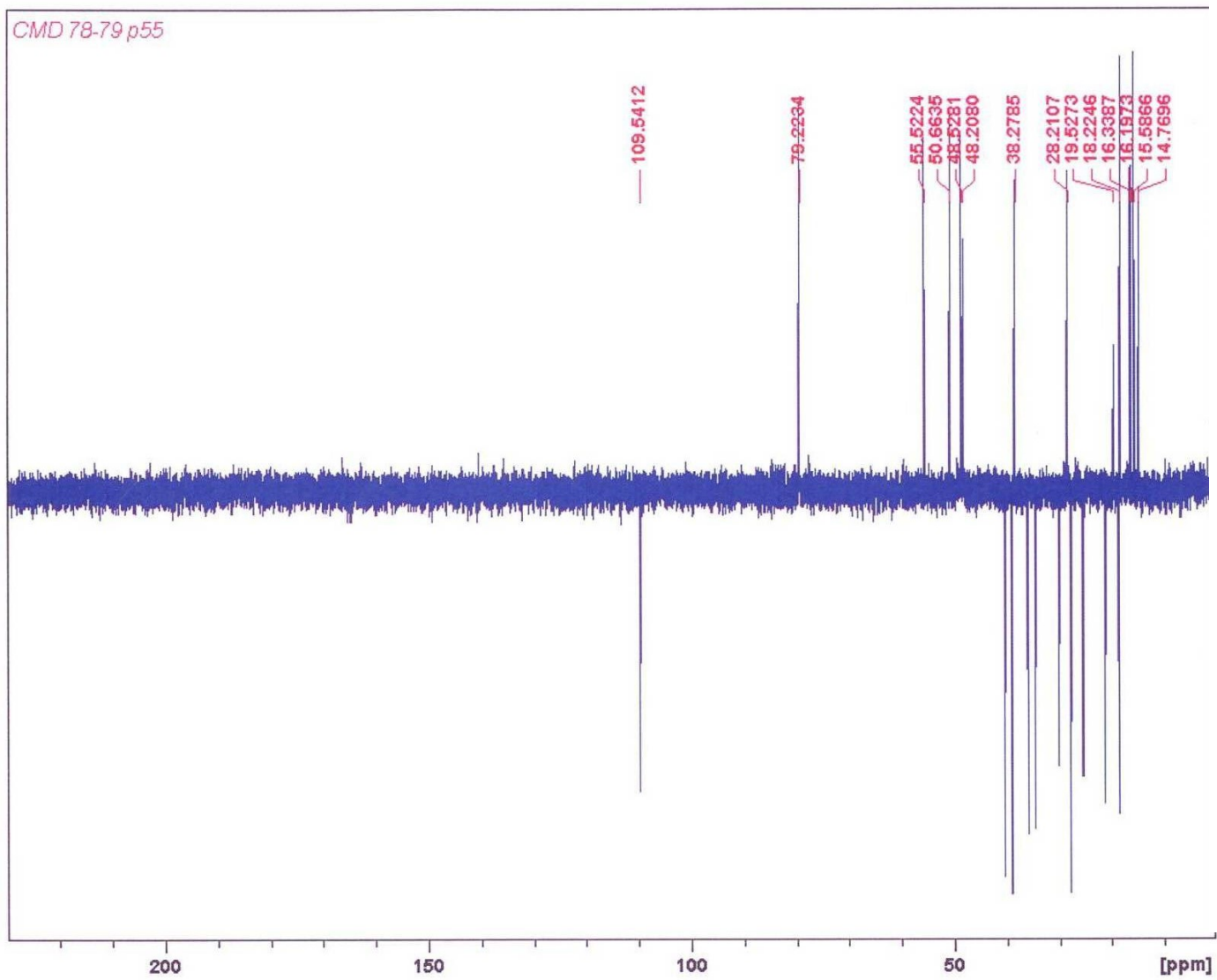
Appendix 1: $^1\text{H-NMR}$ (500MHz) spectrum of CMD-A in CDCl_3



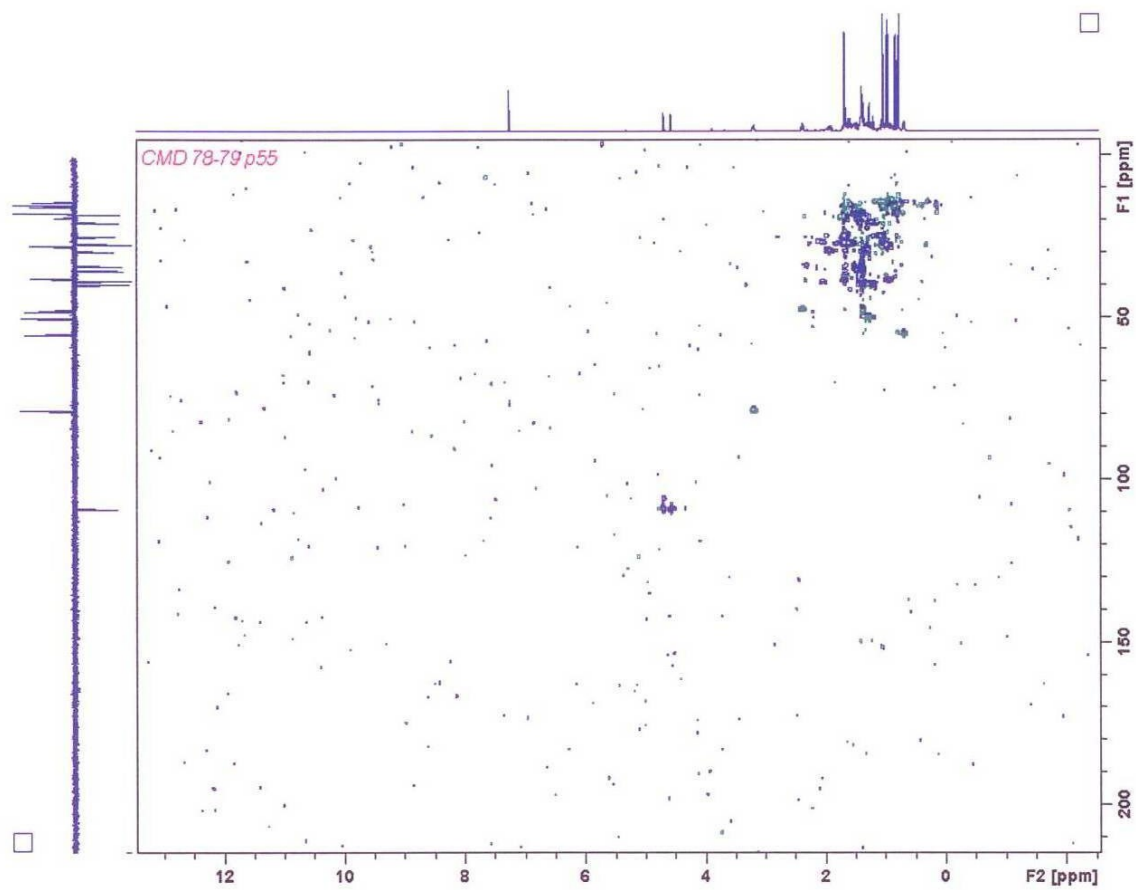
Appendix 2: ¹³C-NMR (125 MHz) spectrum of CMD-A in CDCl₃



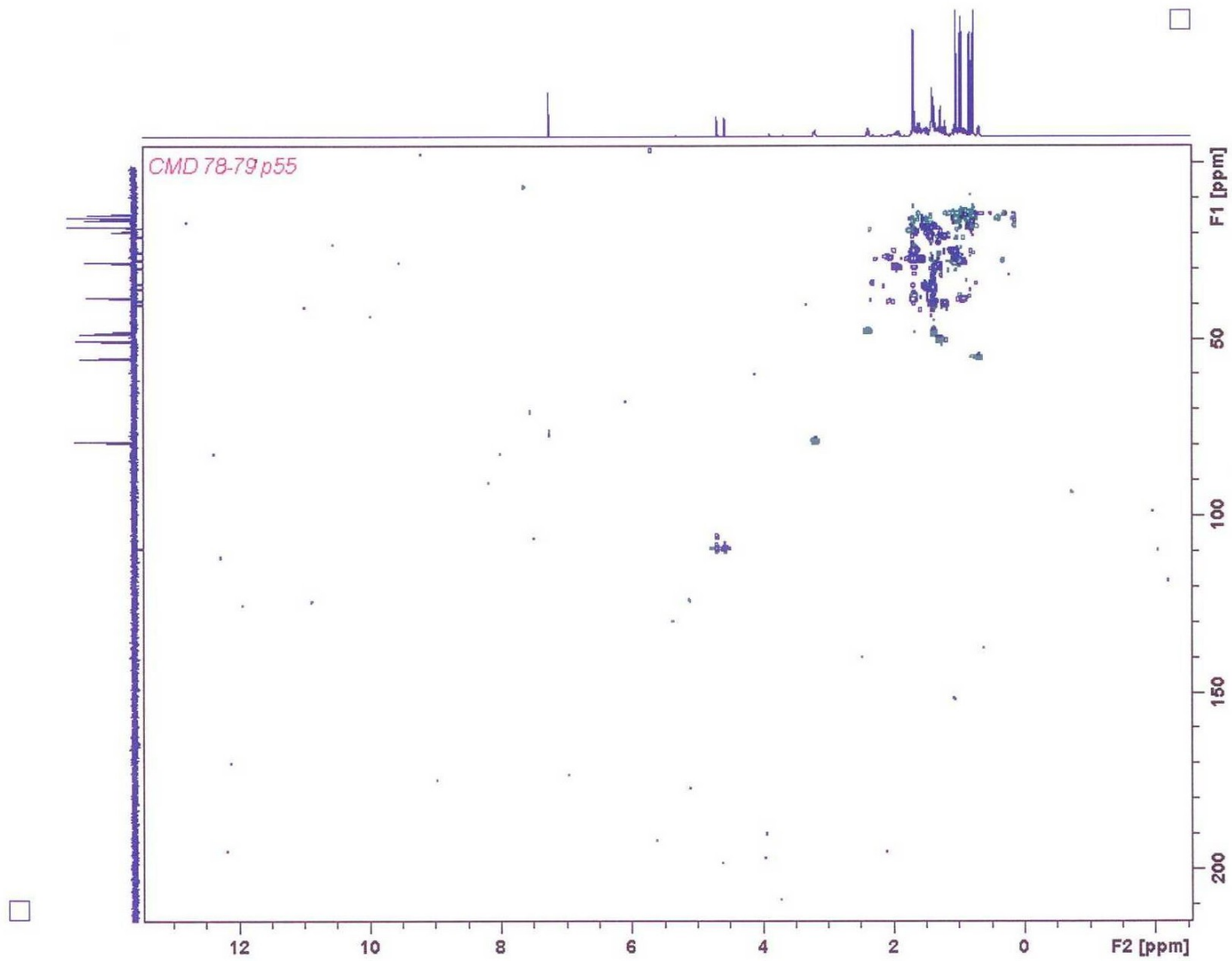
Appendix 3 : ^{13}C -NMR (125 MHz) spectrum of CMD-A in CDCl_3



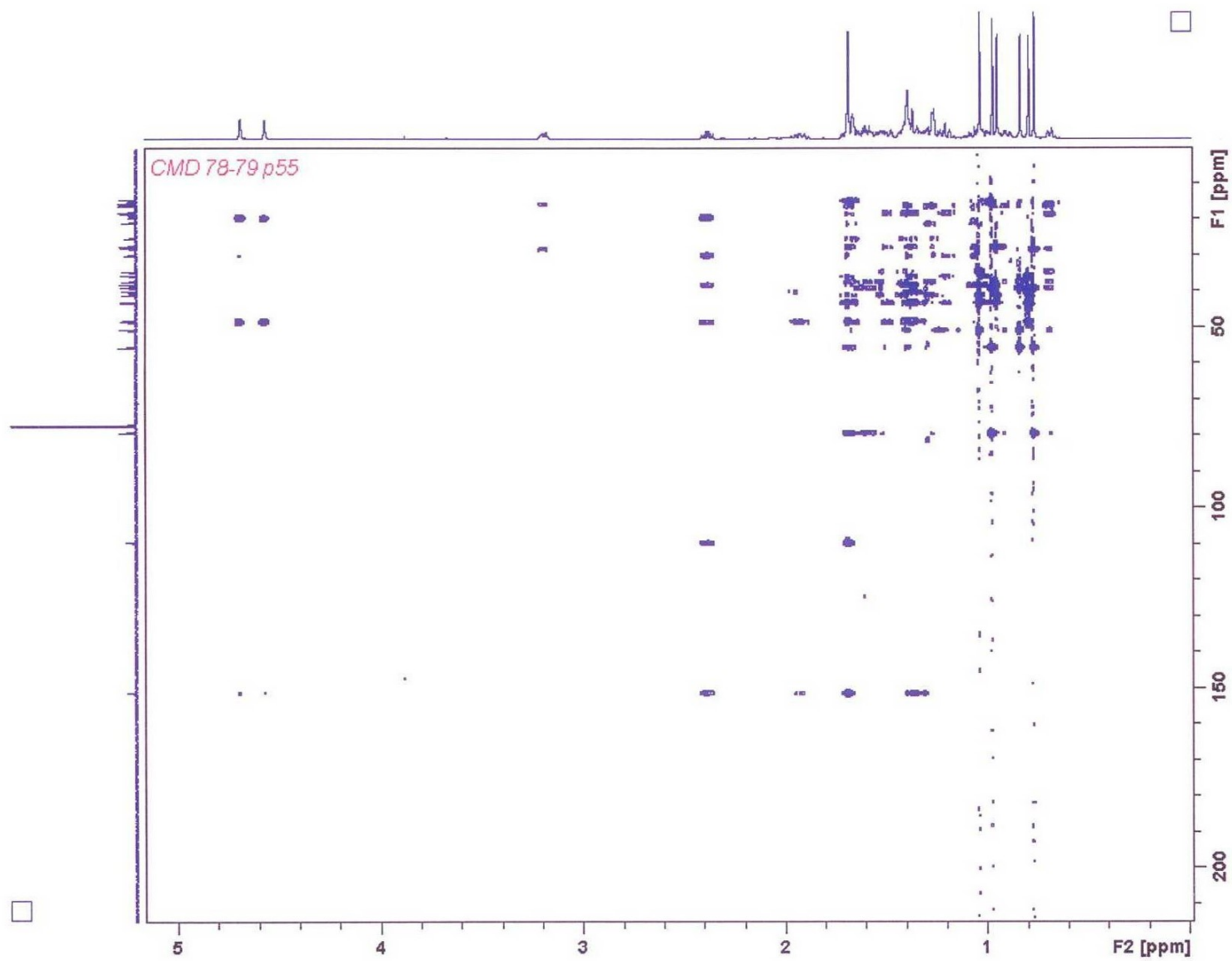
Appendix 4 : DEPT spectrum of CMD-A in CDCl_3



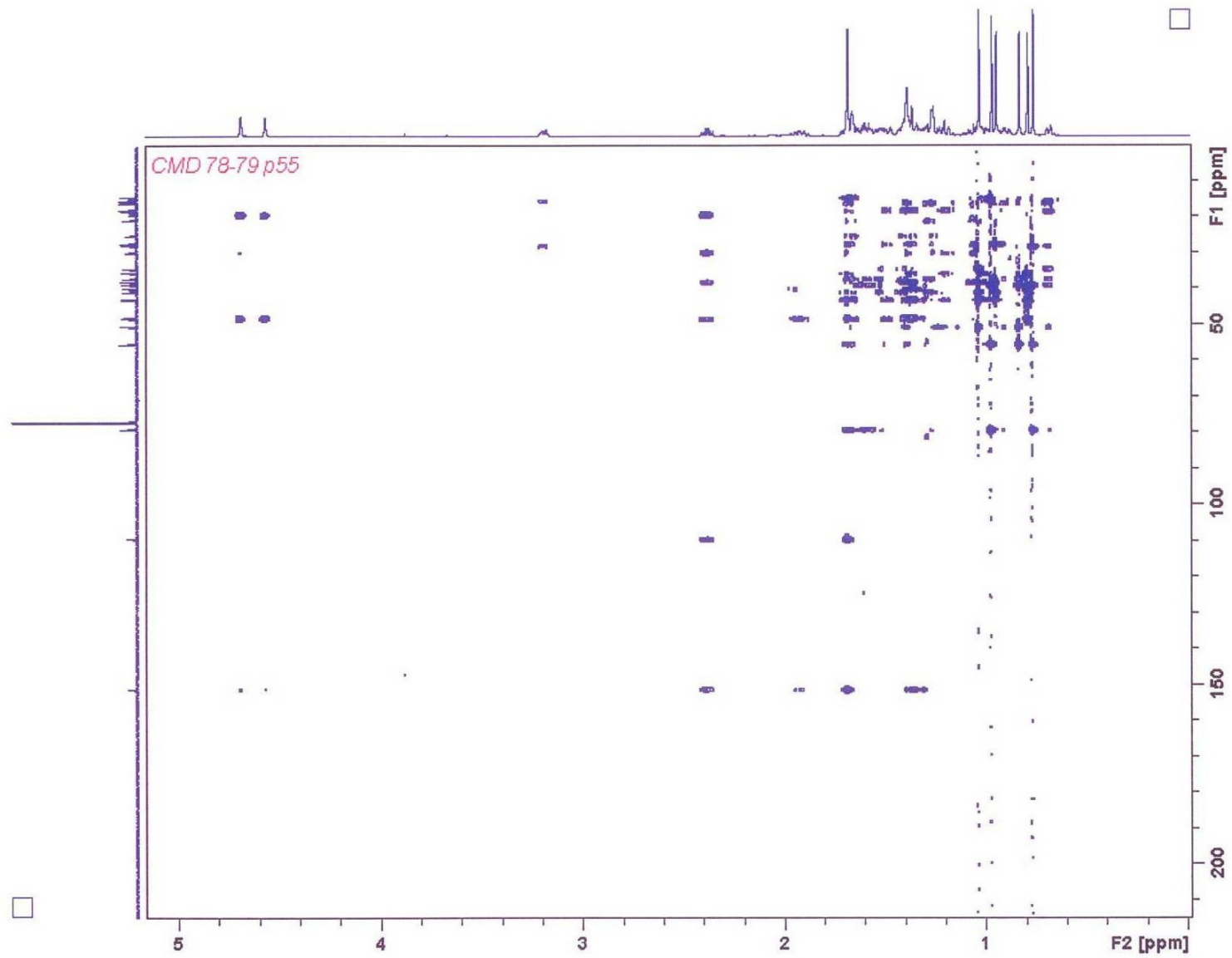
Appendix.5: HSQC DEPT spectrum of CMD-A in CDCl_3



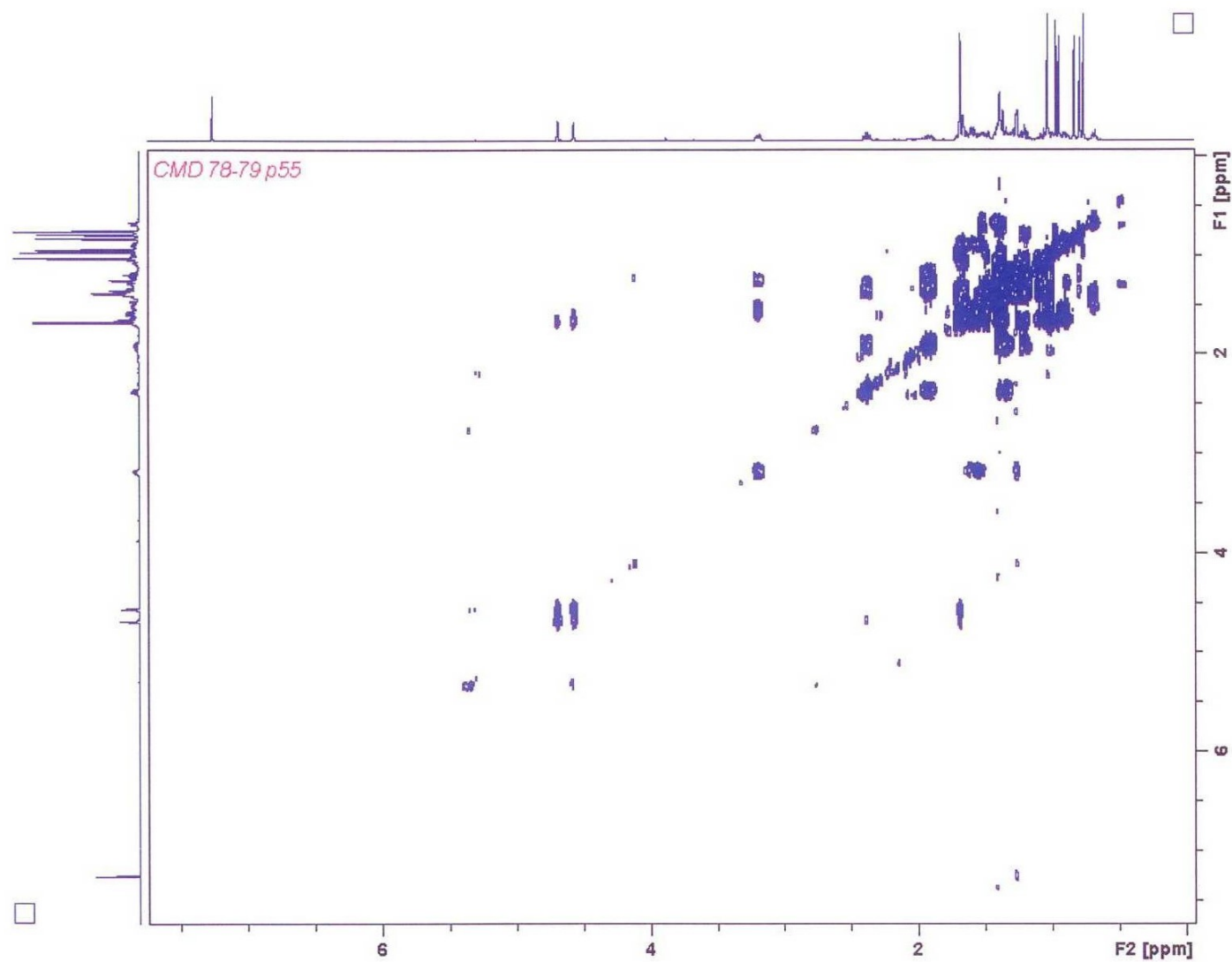
Appendix.6: HSQC DEPT spectrum of CMD-A in CDCl_3



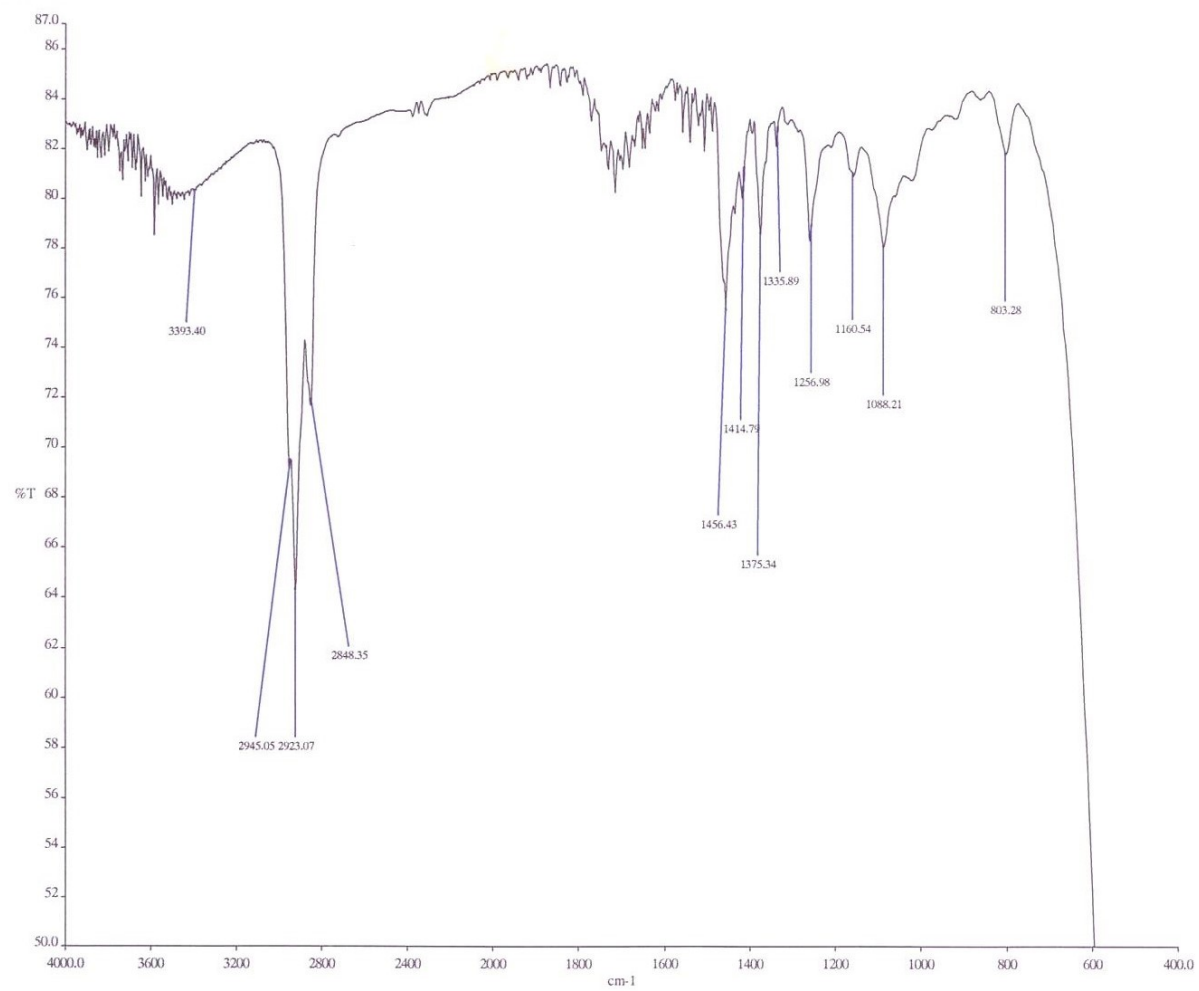
Appendix 7 : HMBC spectrum of CMD-A in CDCl_3



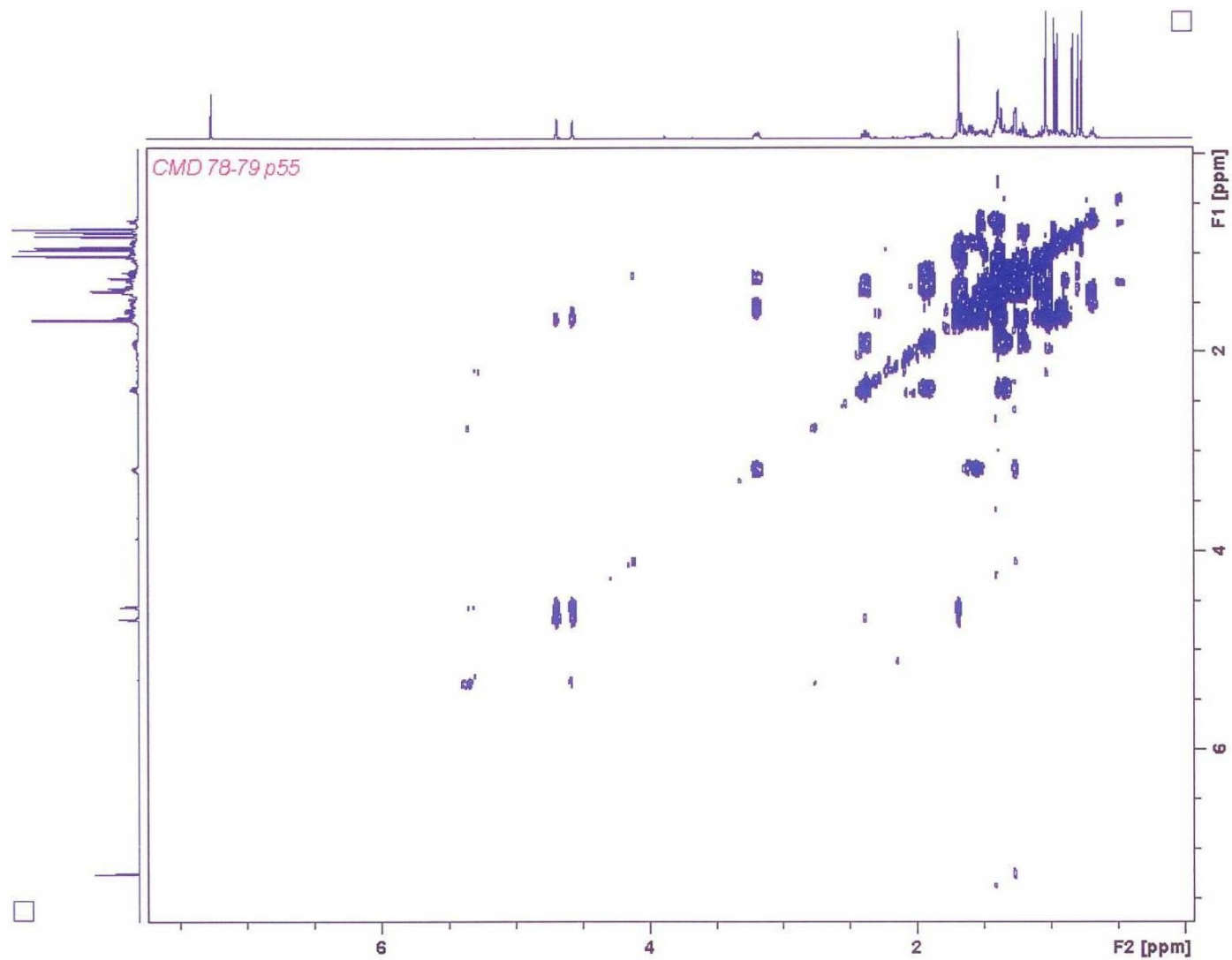
Appendix.8: COSY spectrum of CMD-A in CDCl_3



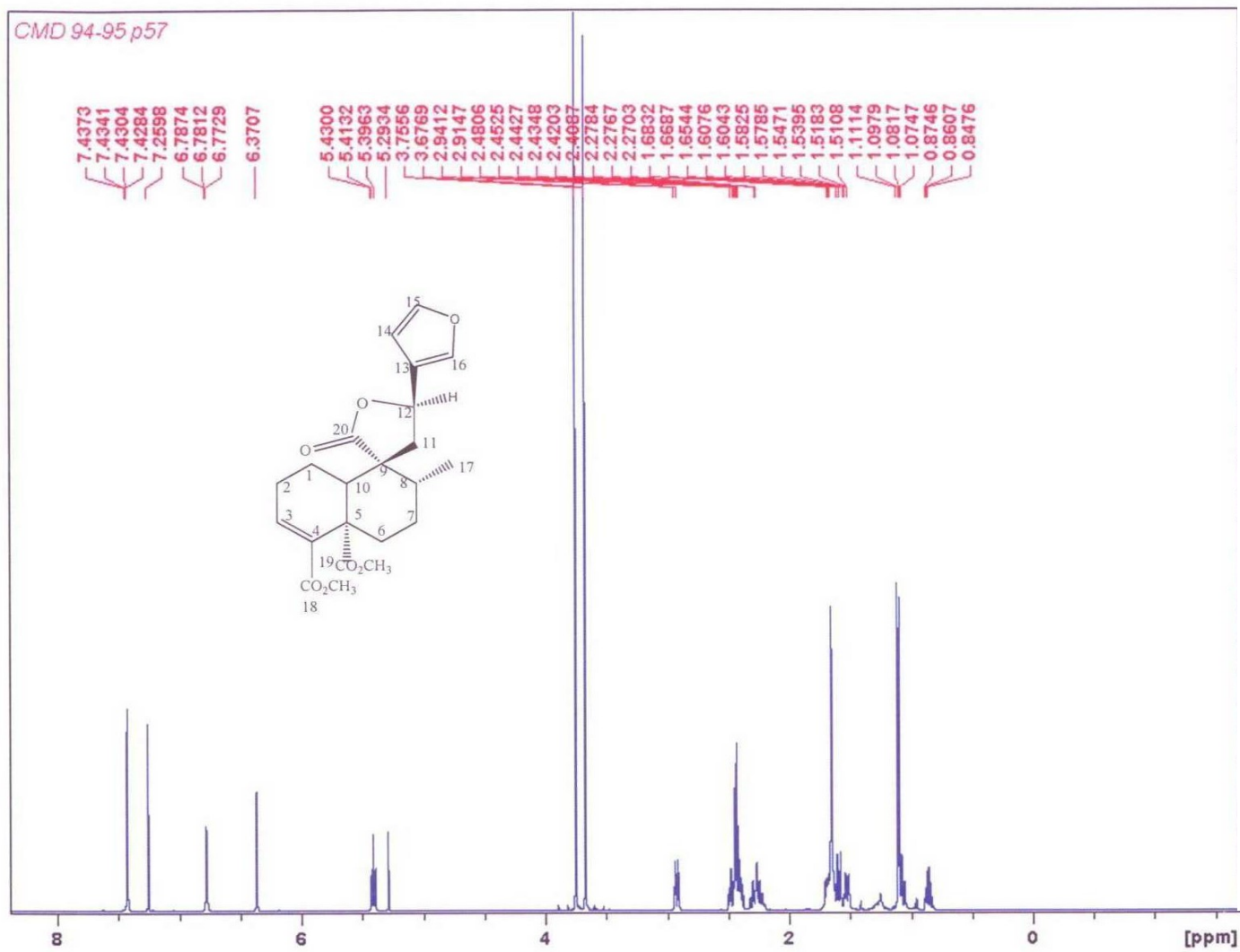
Appendix 9: NOESY spectrum of CMD-A in CDCl₃



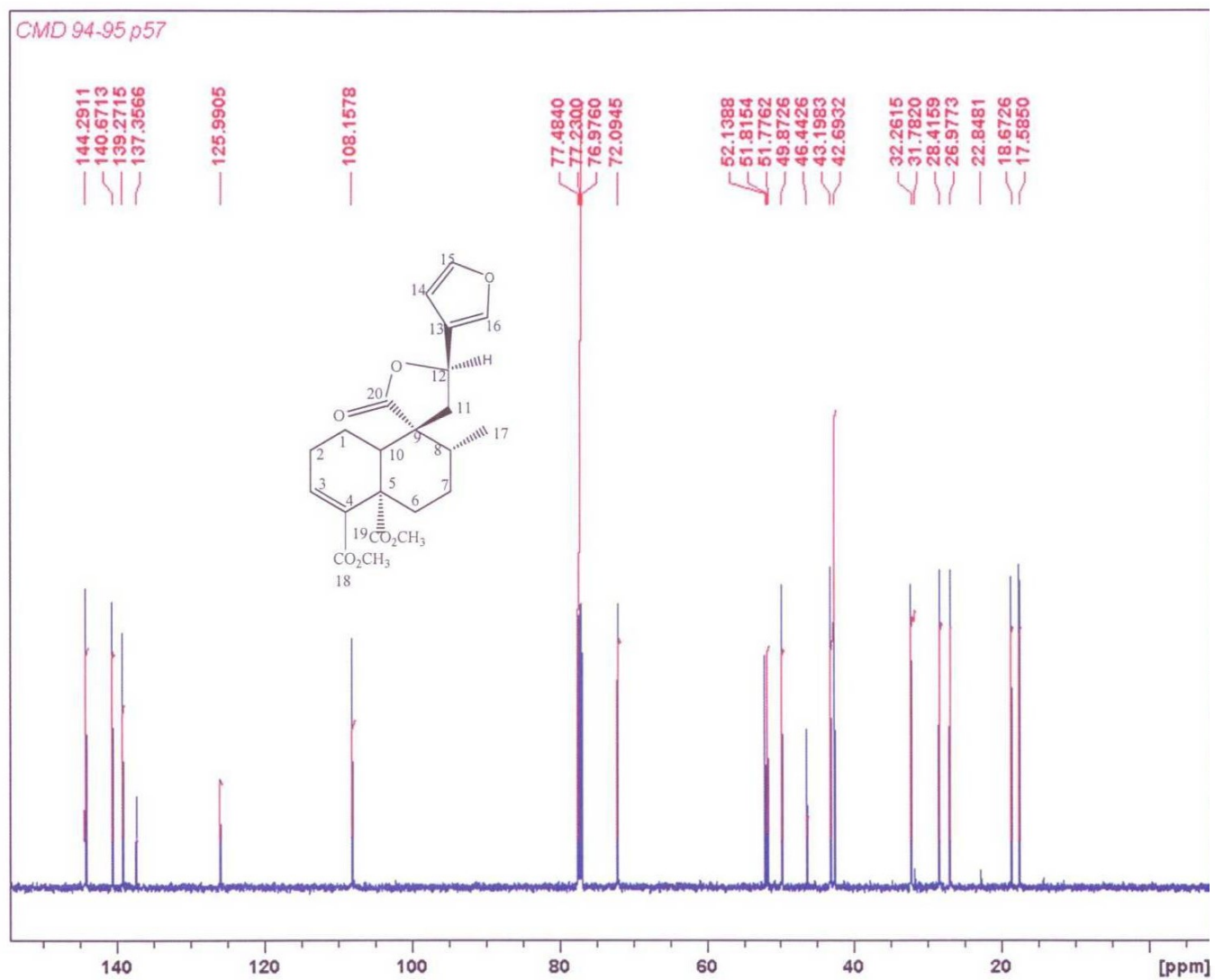
Appendix 10: IR spectrum of CMD-A in CDCl₃



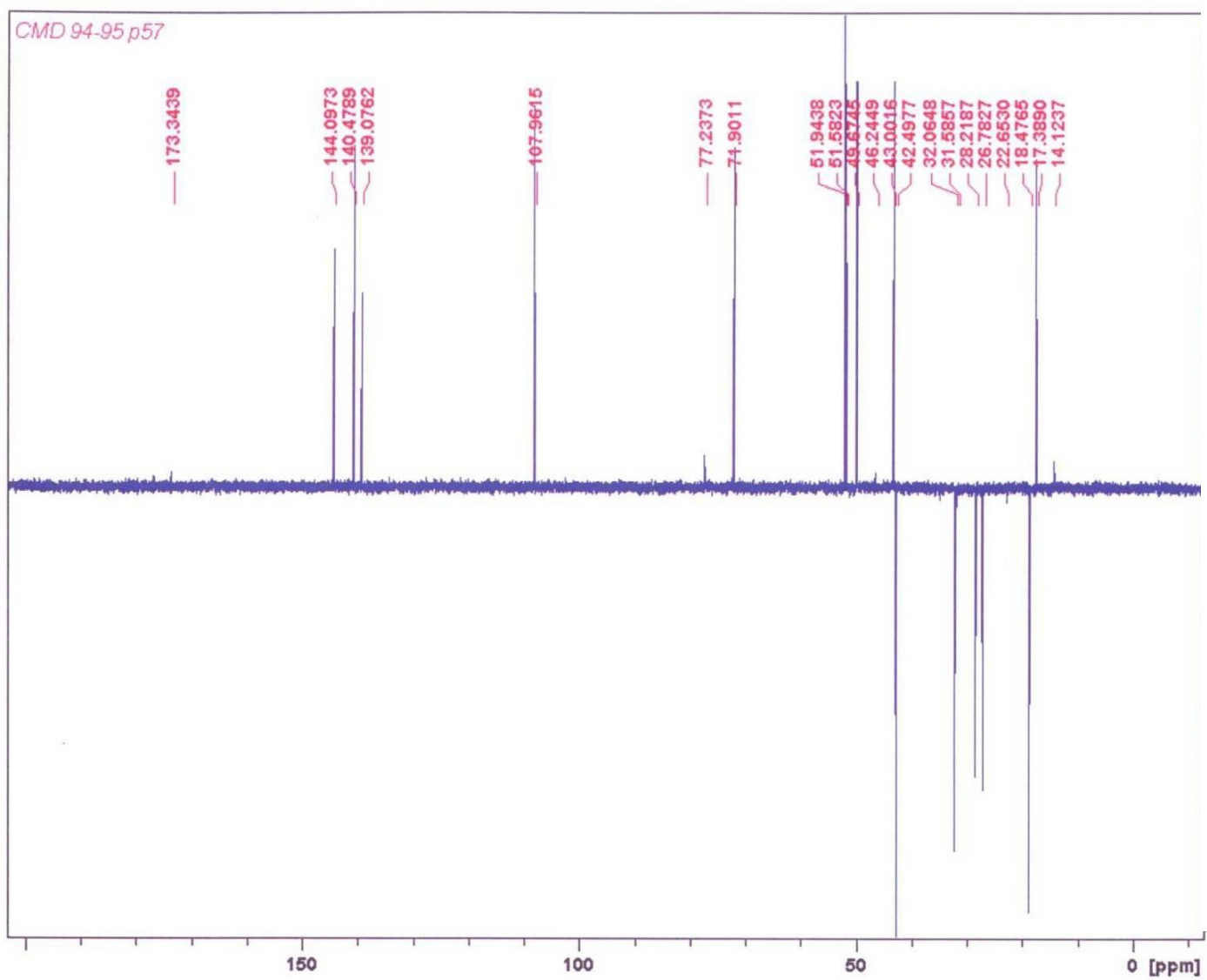
Appendix 11: NOESY spectrum of CMD-A (expanded)



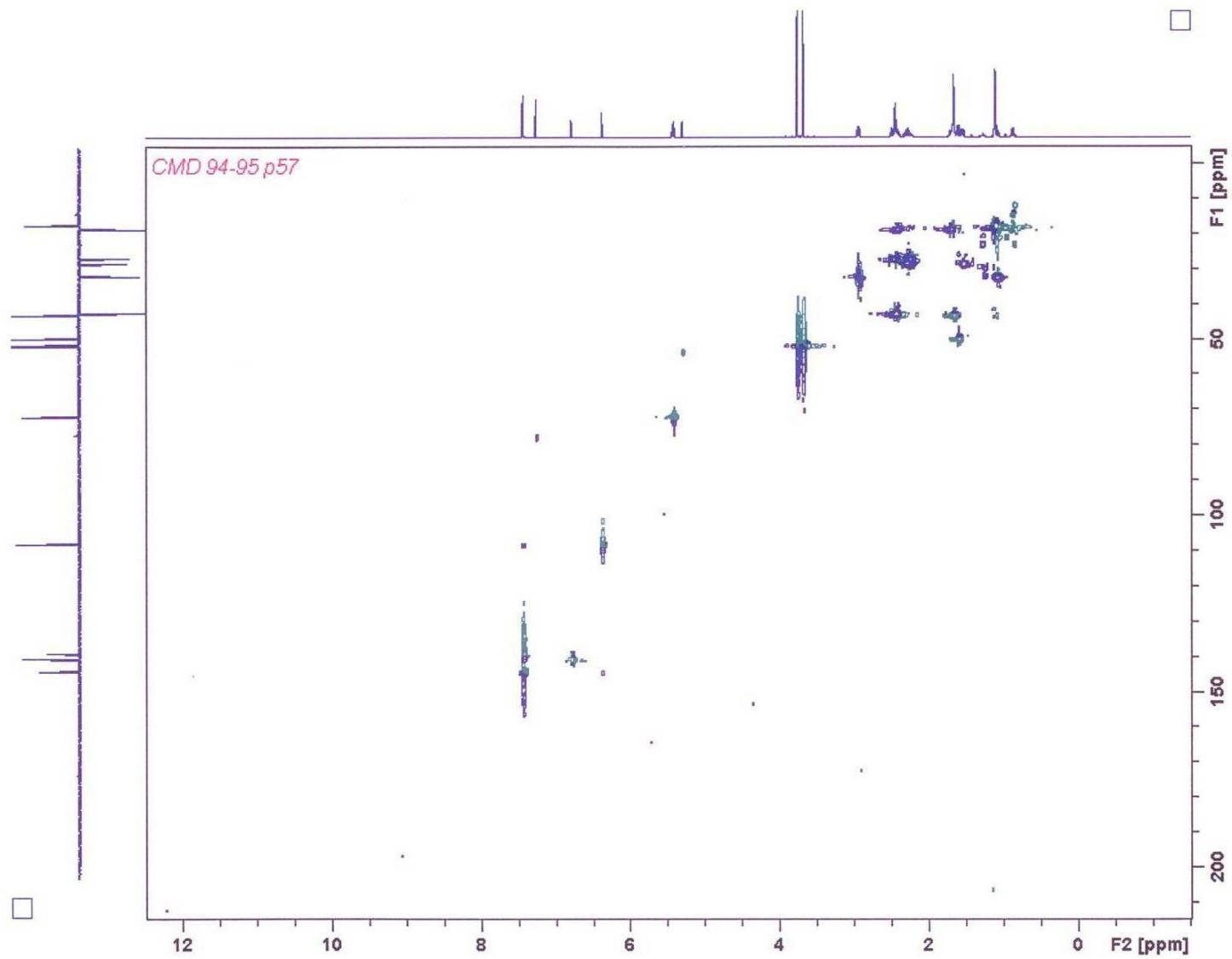
Appendix 12: ^1H NMR (500MHz) spectrum of CMD-B in CDCl_3



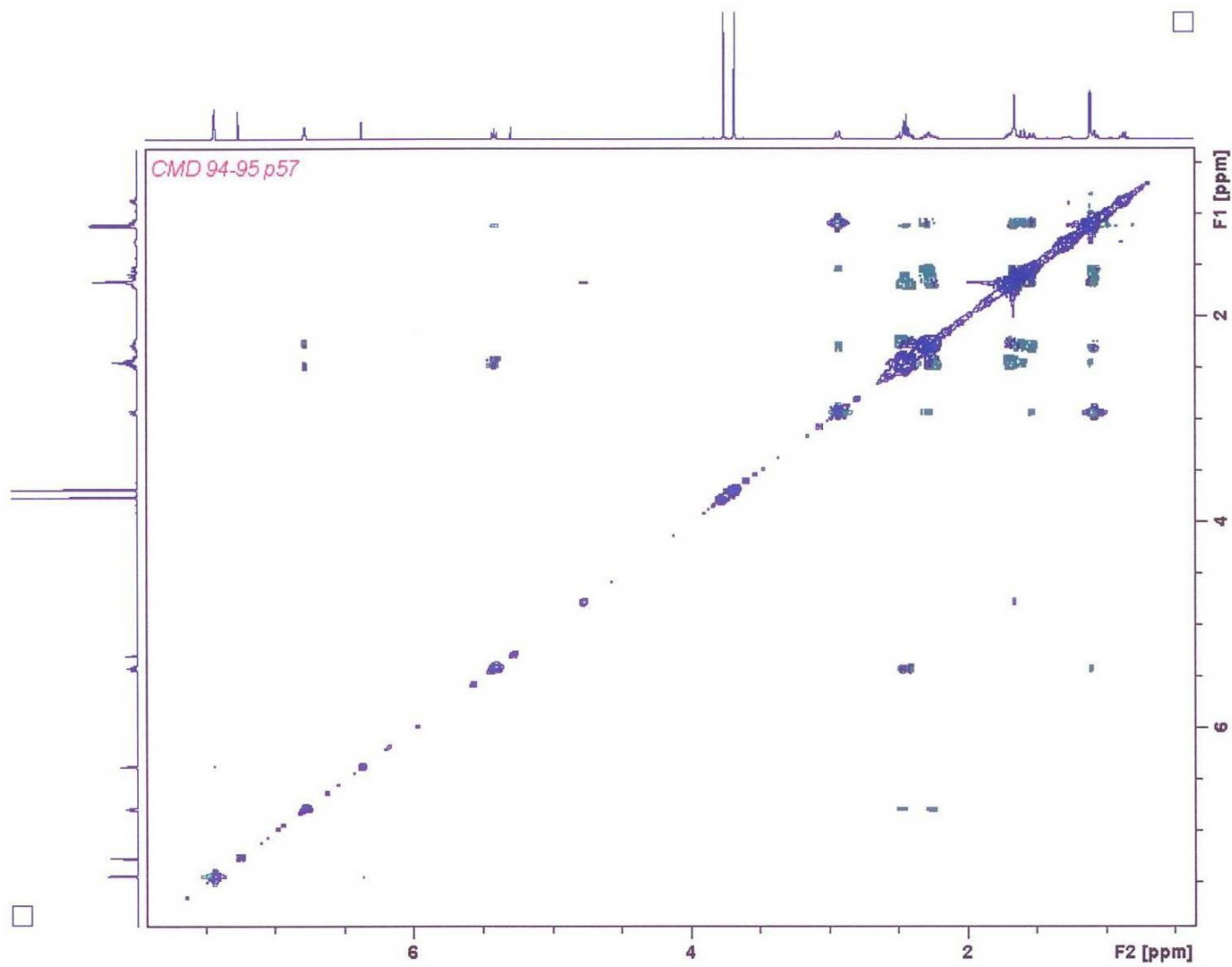
Appendix 13: ¹³CNMR (125 MHz) spectrum of CMD-B in CDCl₃



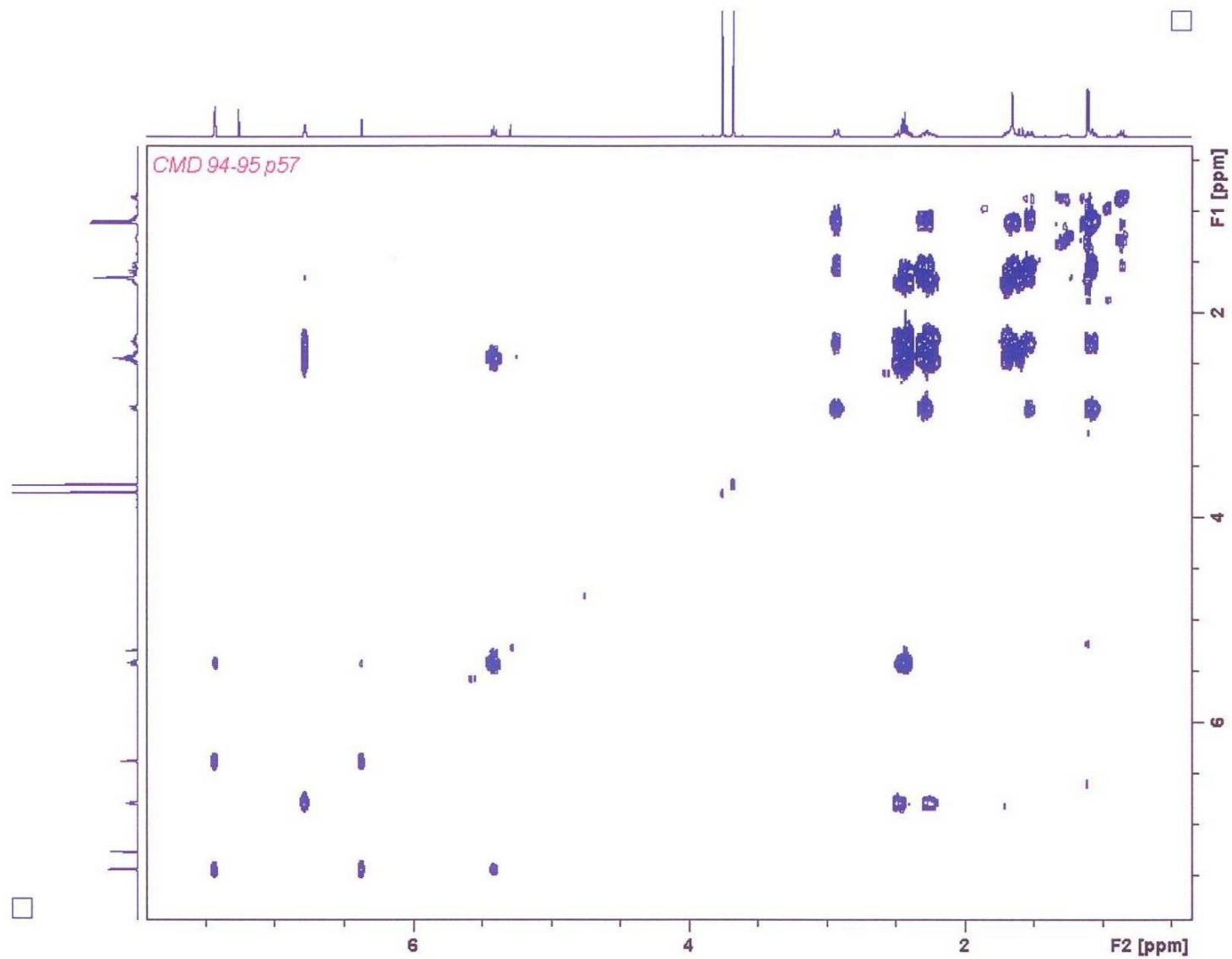
Appendix 14: DEPT spectrum of CMD-B in CDCl_3



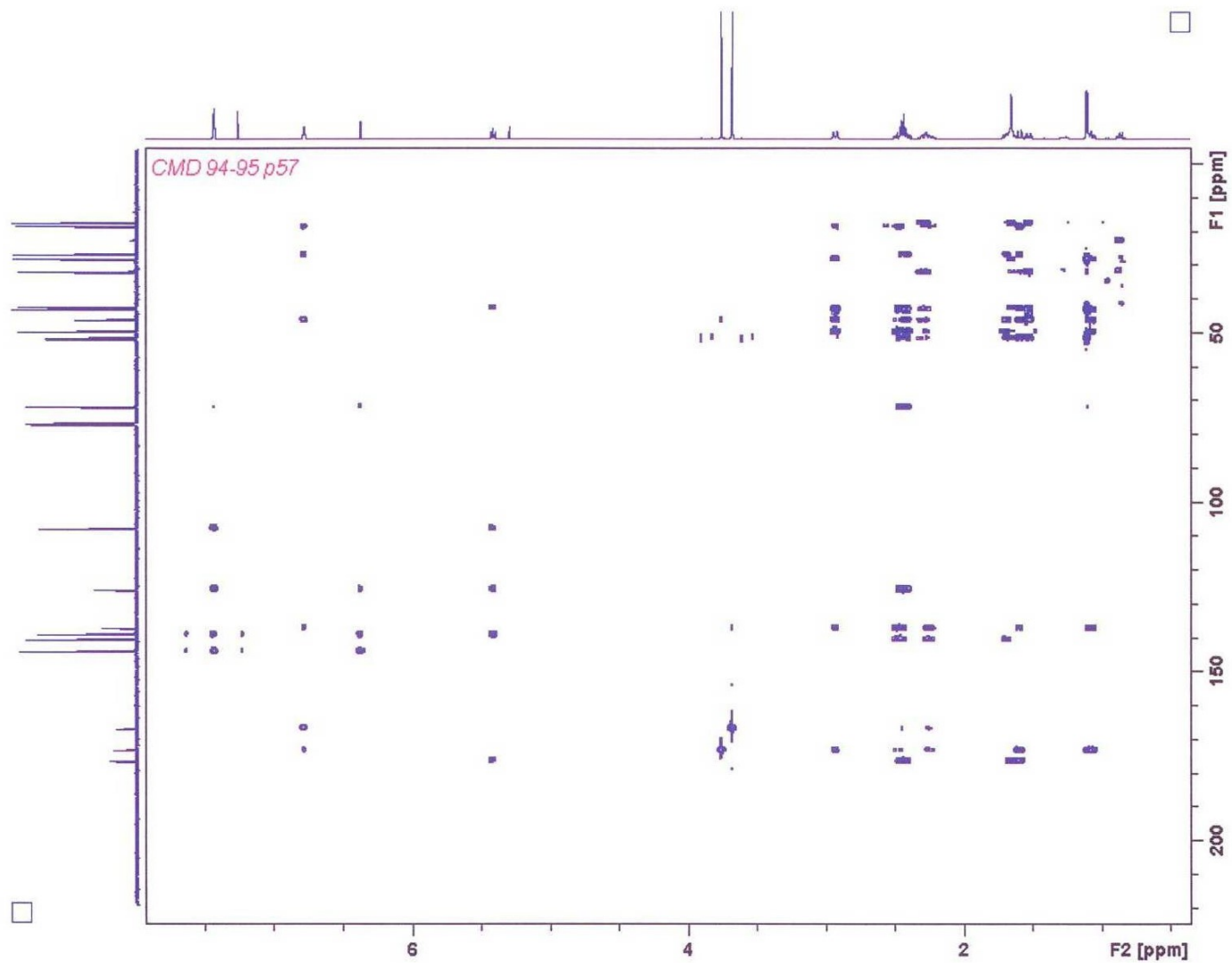
Appendix.15: HSQC DEPT spectrum of CMD-B in CDCl_3



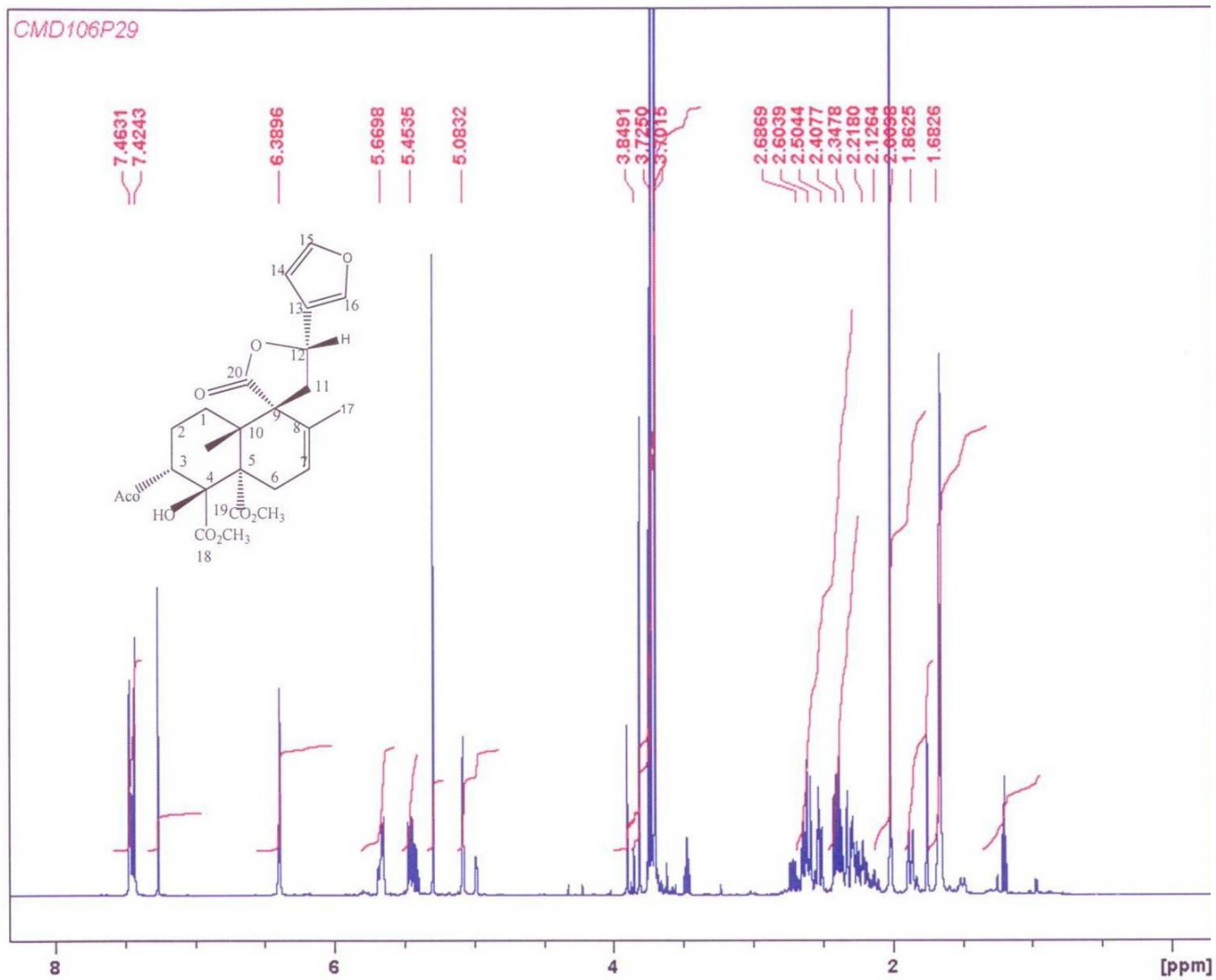
Appendix 16: HMBC spectrum of CMD-B in CDCl_3



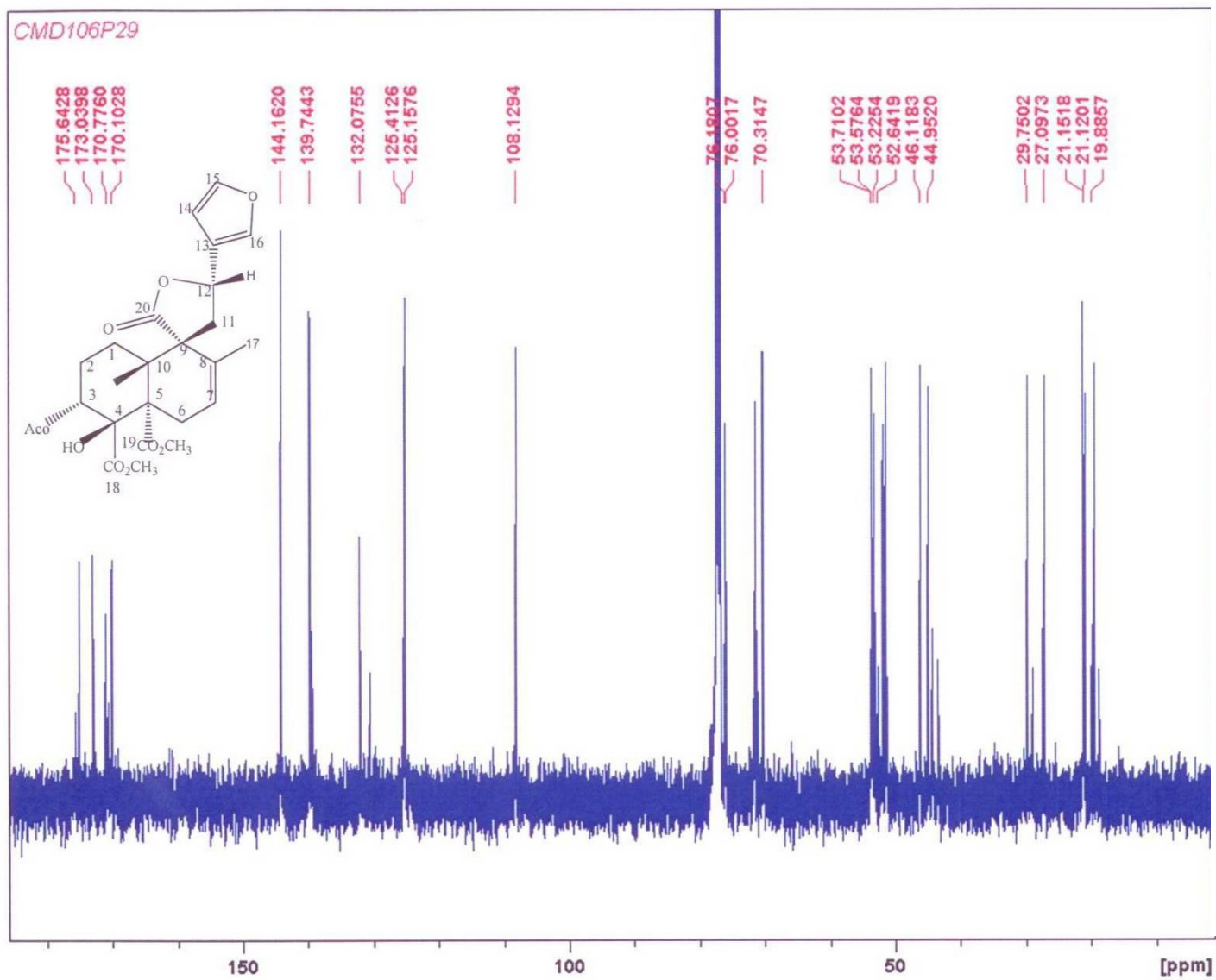
Appendix.17: COSY spectrum of CMD-B in CDCl_3



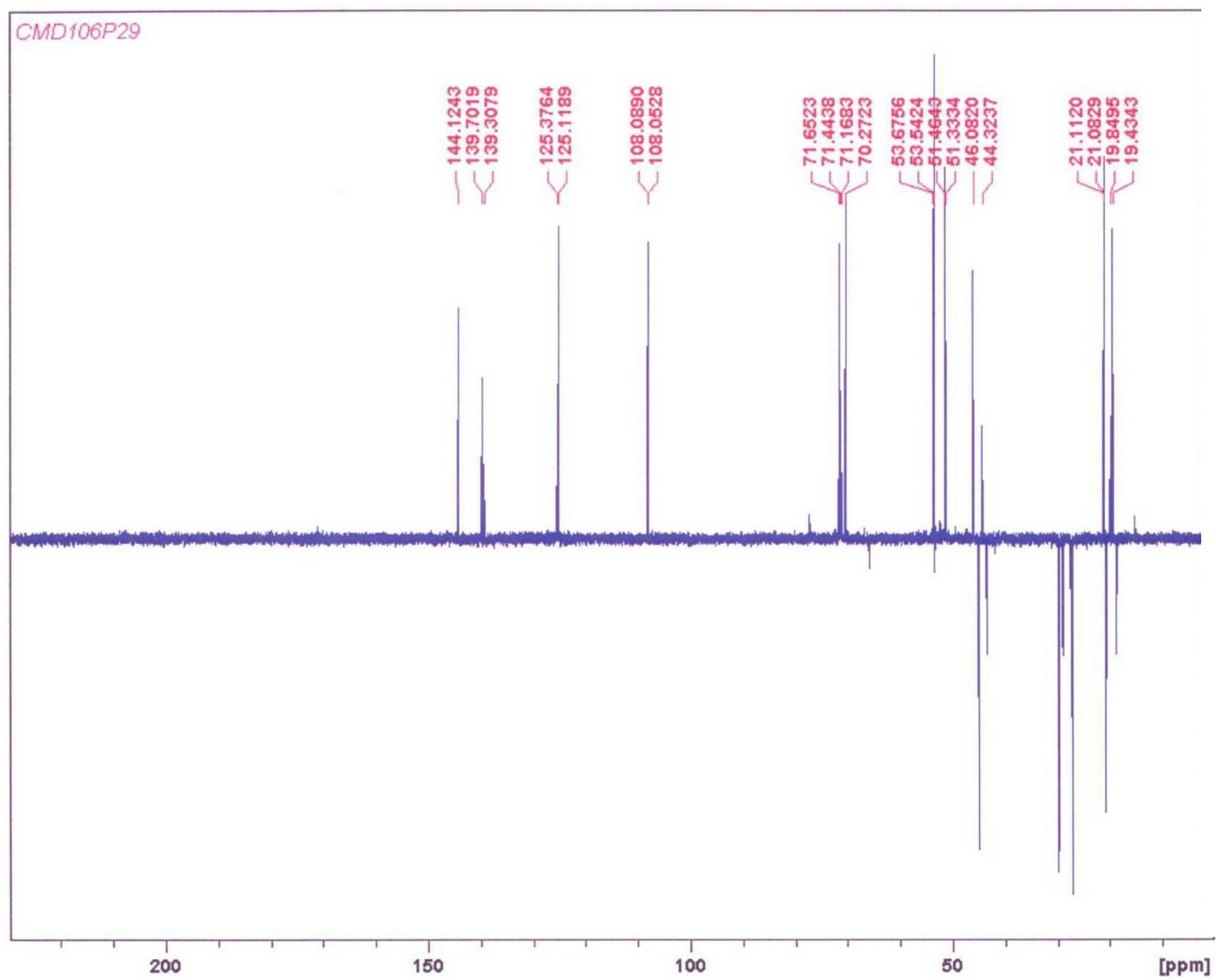
Appendix 18: NOESY spectrum of CMD-B in CDCl₃



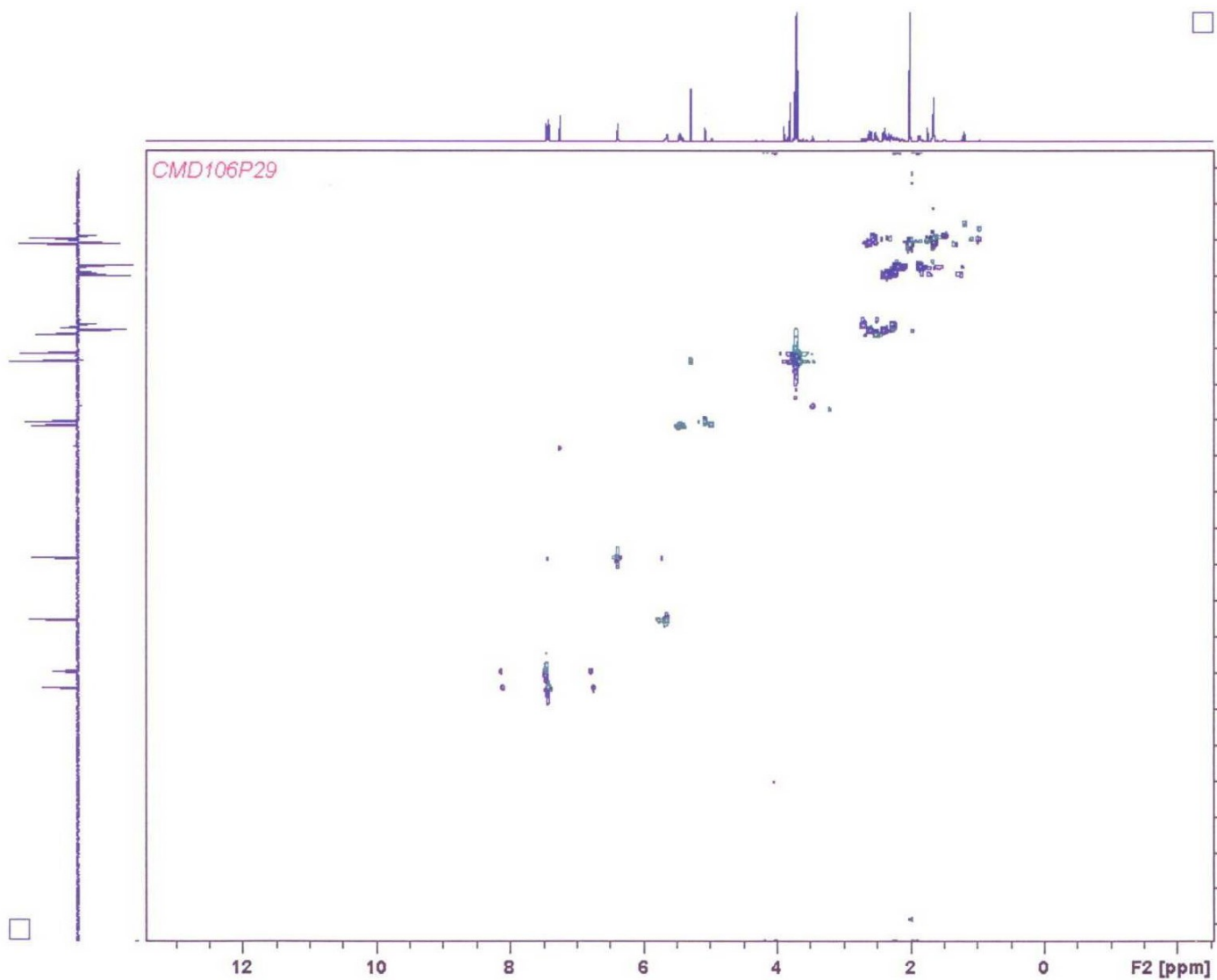
Appendix.19: ¹HNMR (500MHz) spectrum of CMD-C in CDCl₃



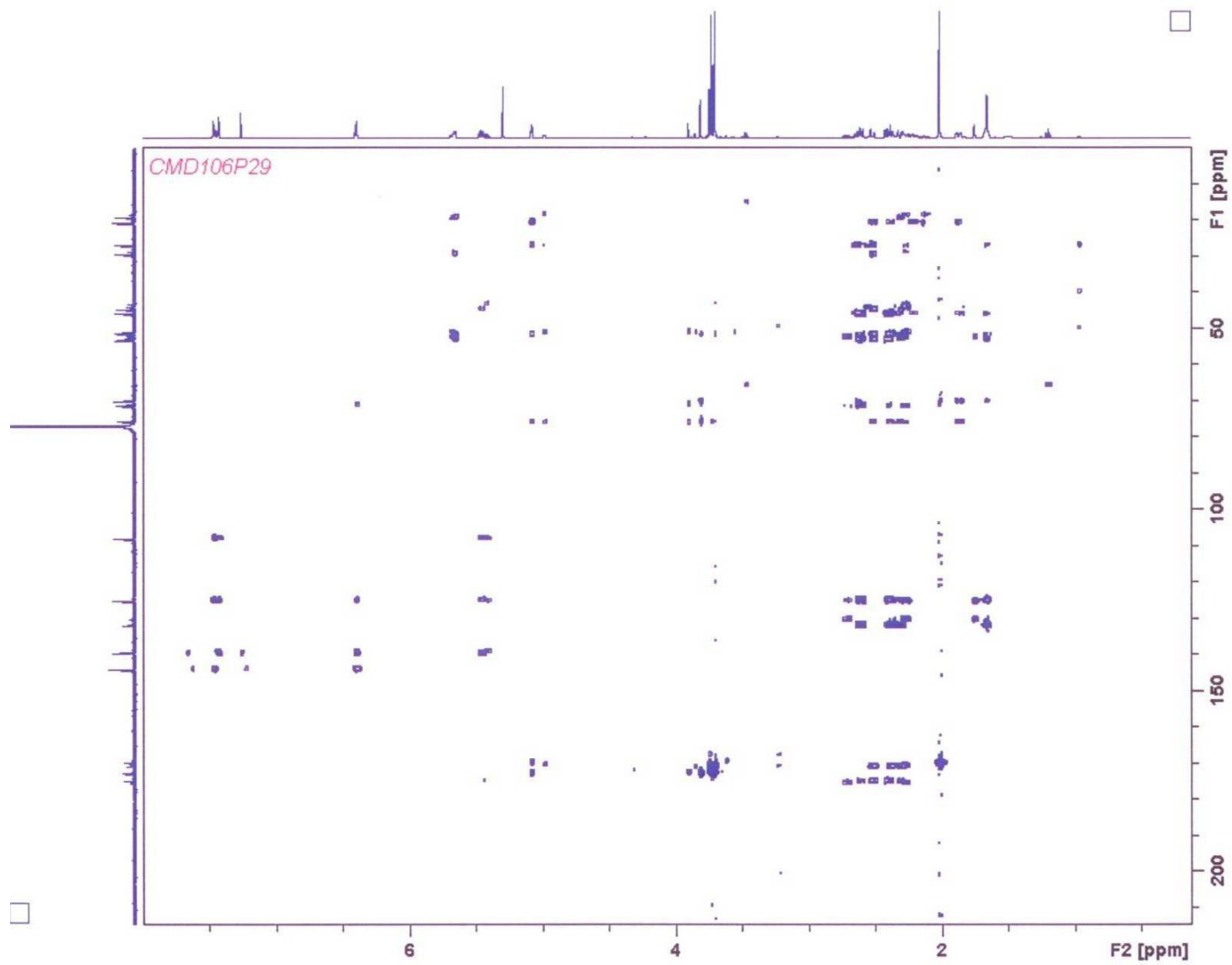
Appendix 20: ^{13}C NMR (125 MHz) spectrum of CMD-C in CDCl_3



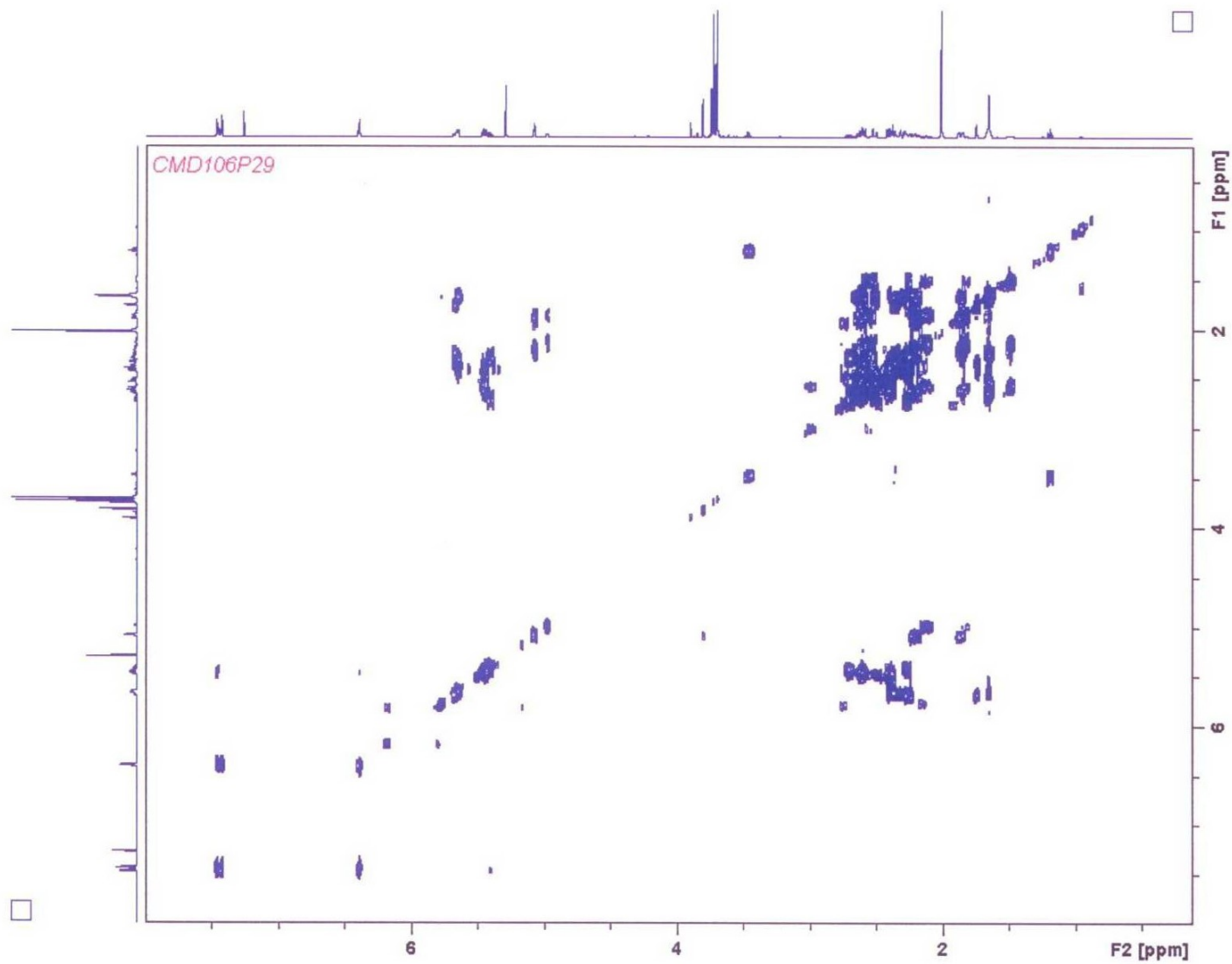
Appendix 21: DEPT spectrum of CMD-C in CDCl_3



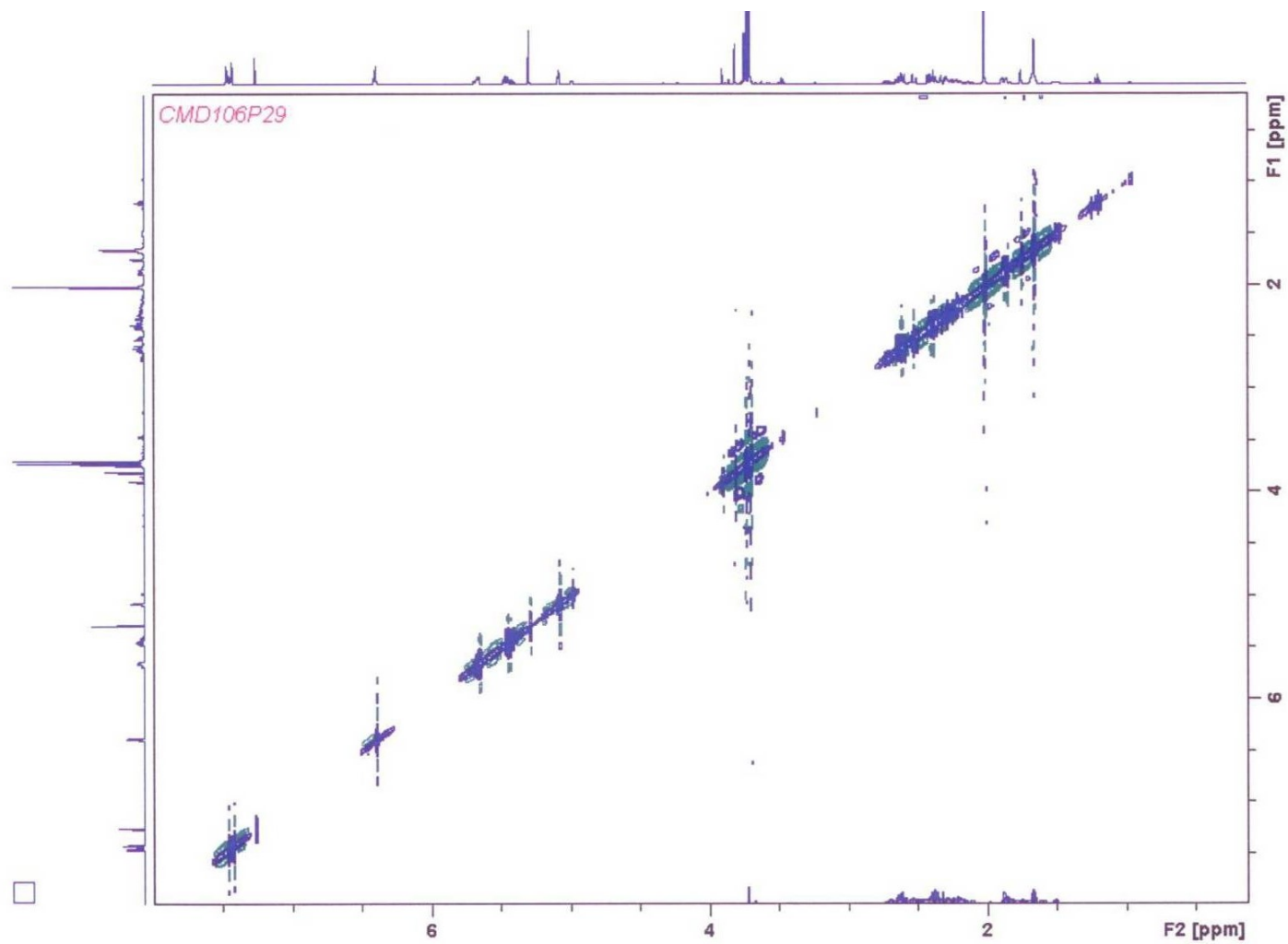
Appendix 22: HSQC DEPT spectrum of CMD-C in CDCl_3



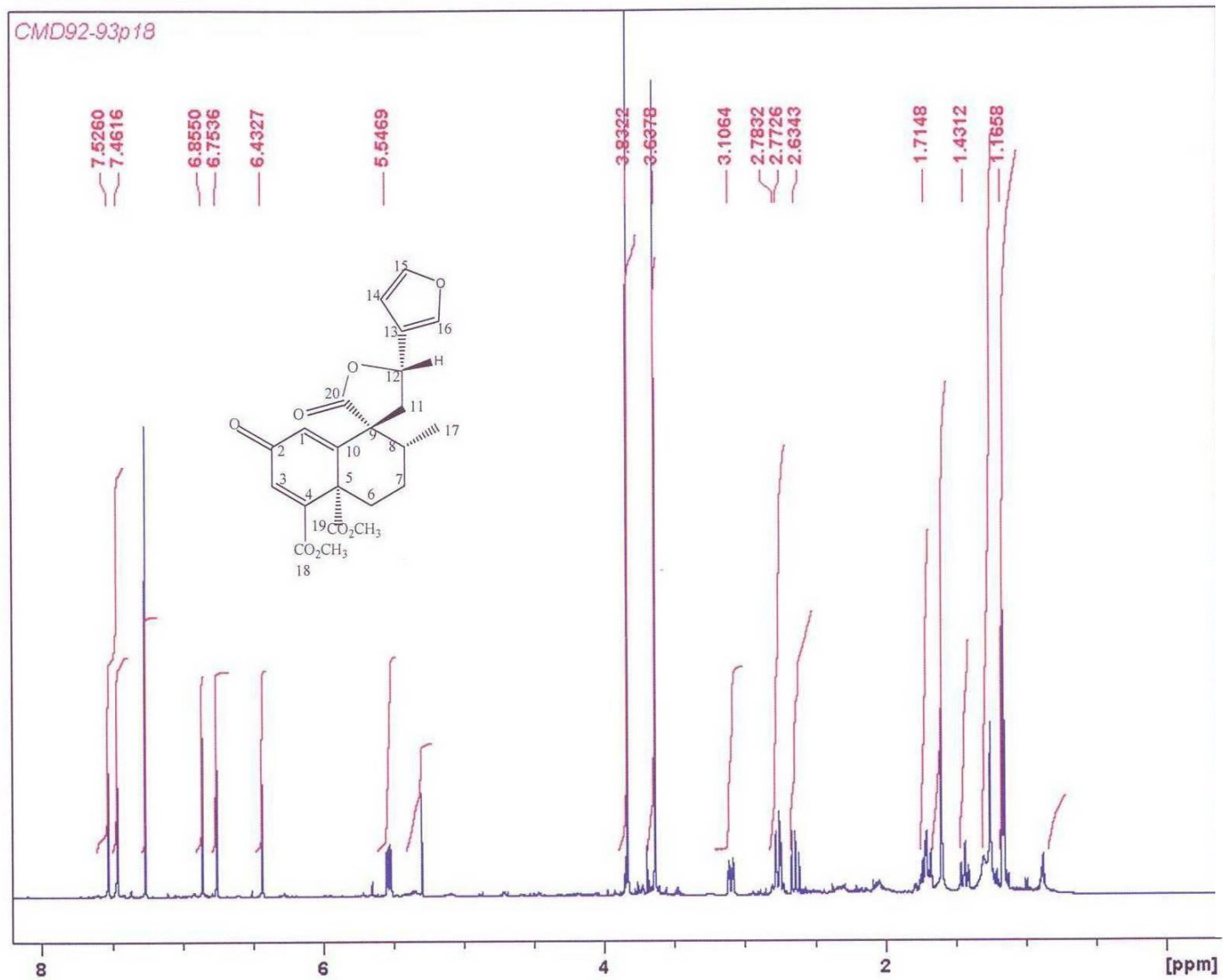
Appendix 23: HMBC spectrum of CMD-C in CDCl_3



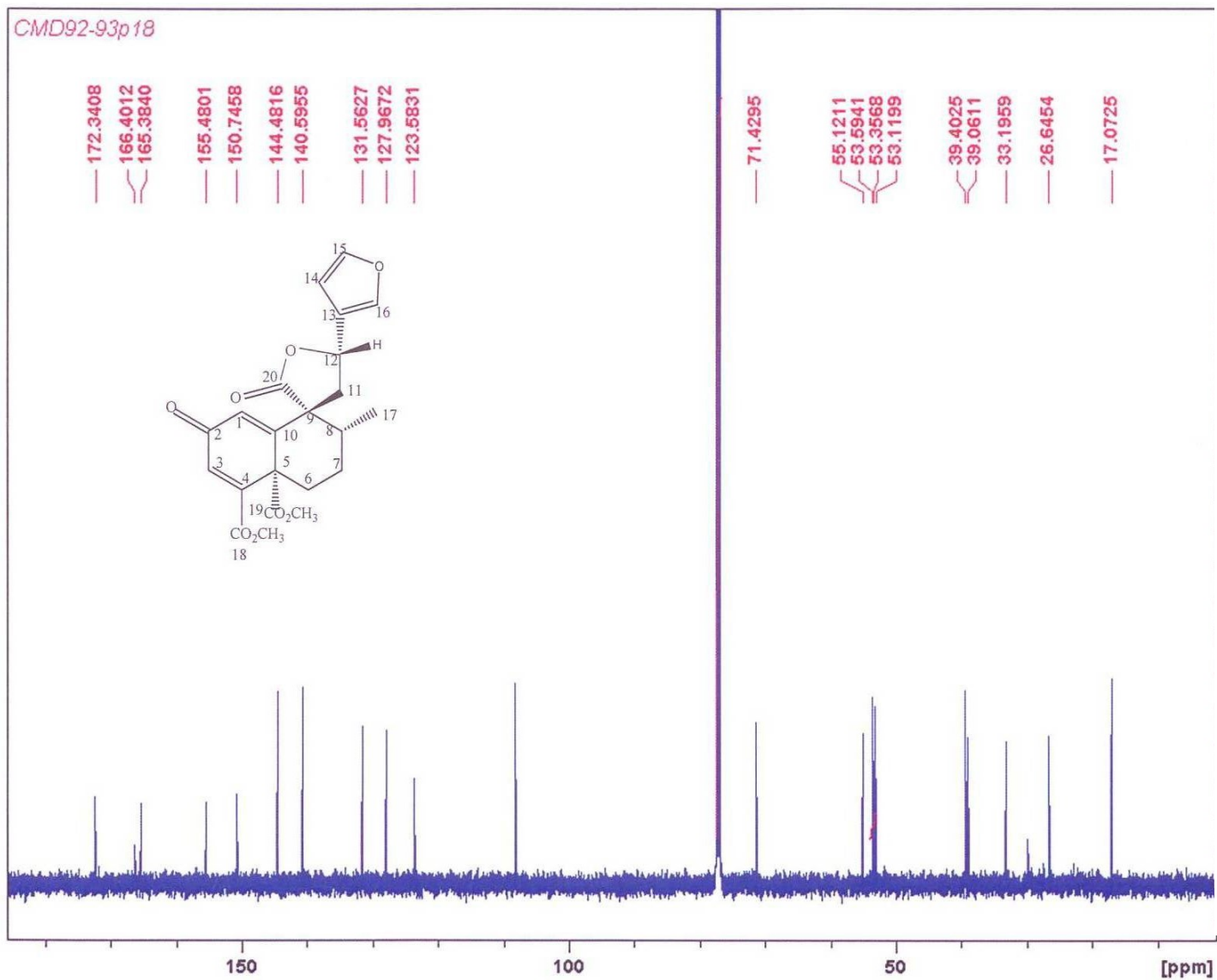
Appendix 24: COSY spectrum of CMD-C in CDCl_3



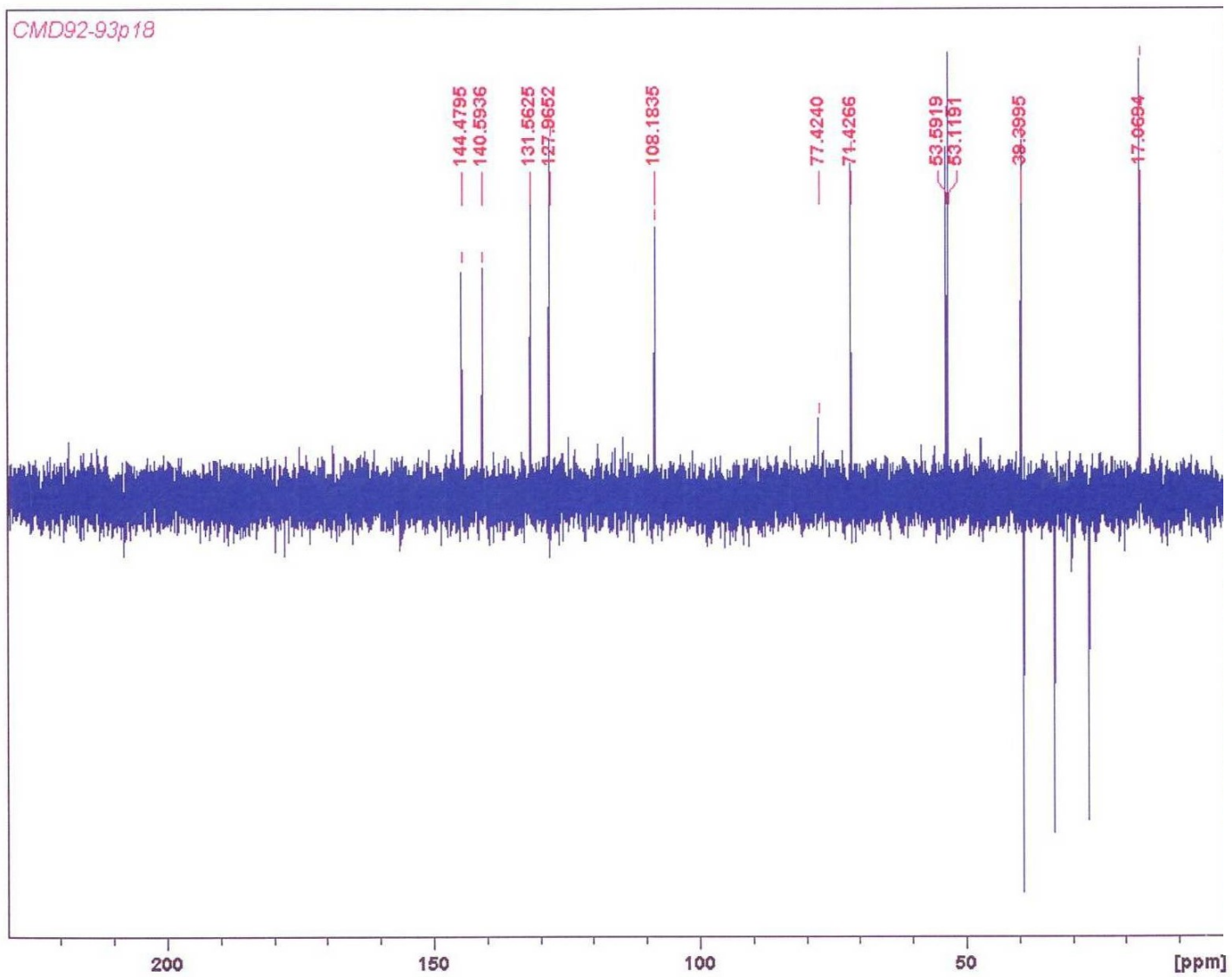
Appendix 25: NOESY spectrum of CMD-C in CDCl₃



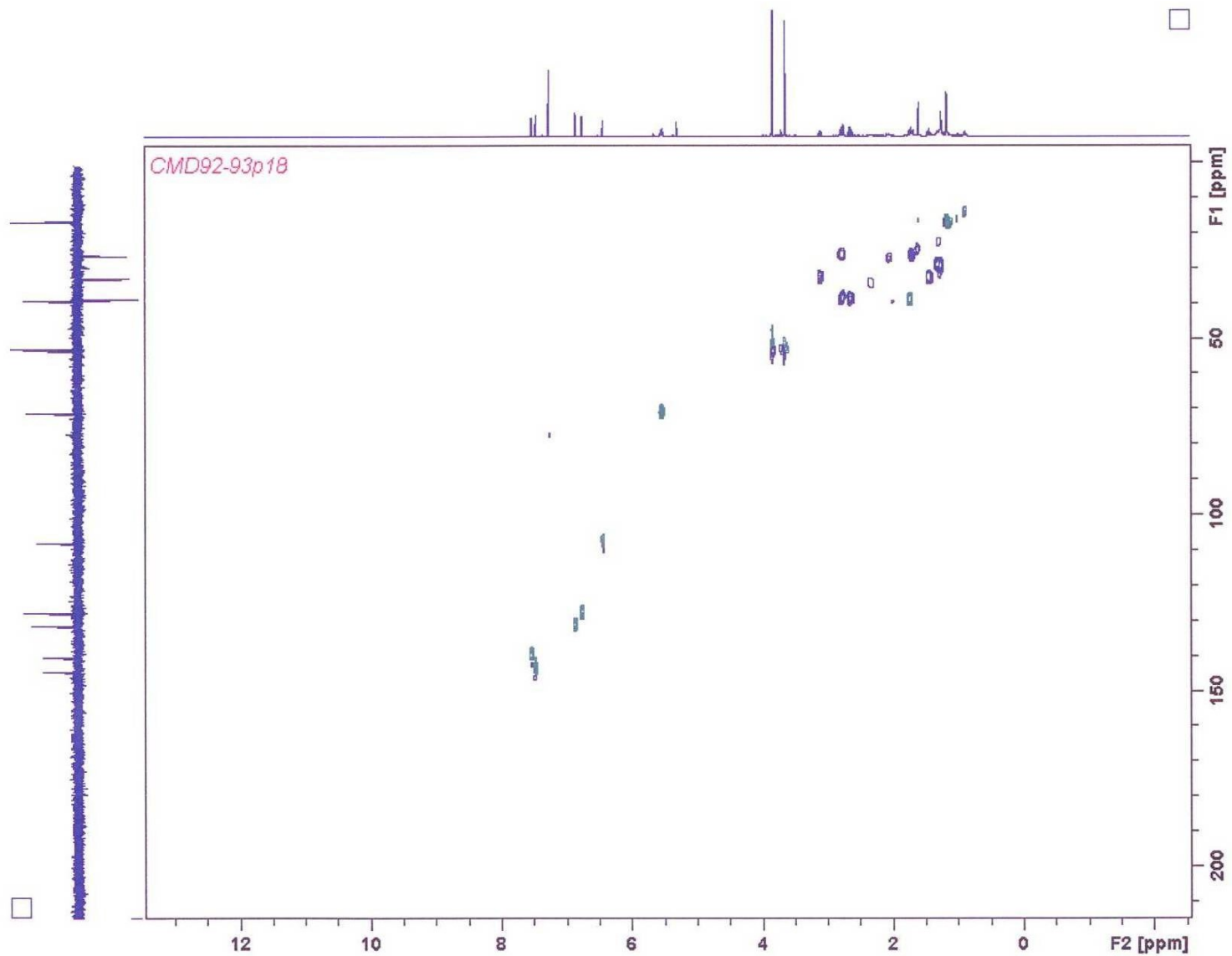
Appendix 26: ^1H NMR(500MHz) spectrum of CMD-D in CDCl_3



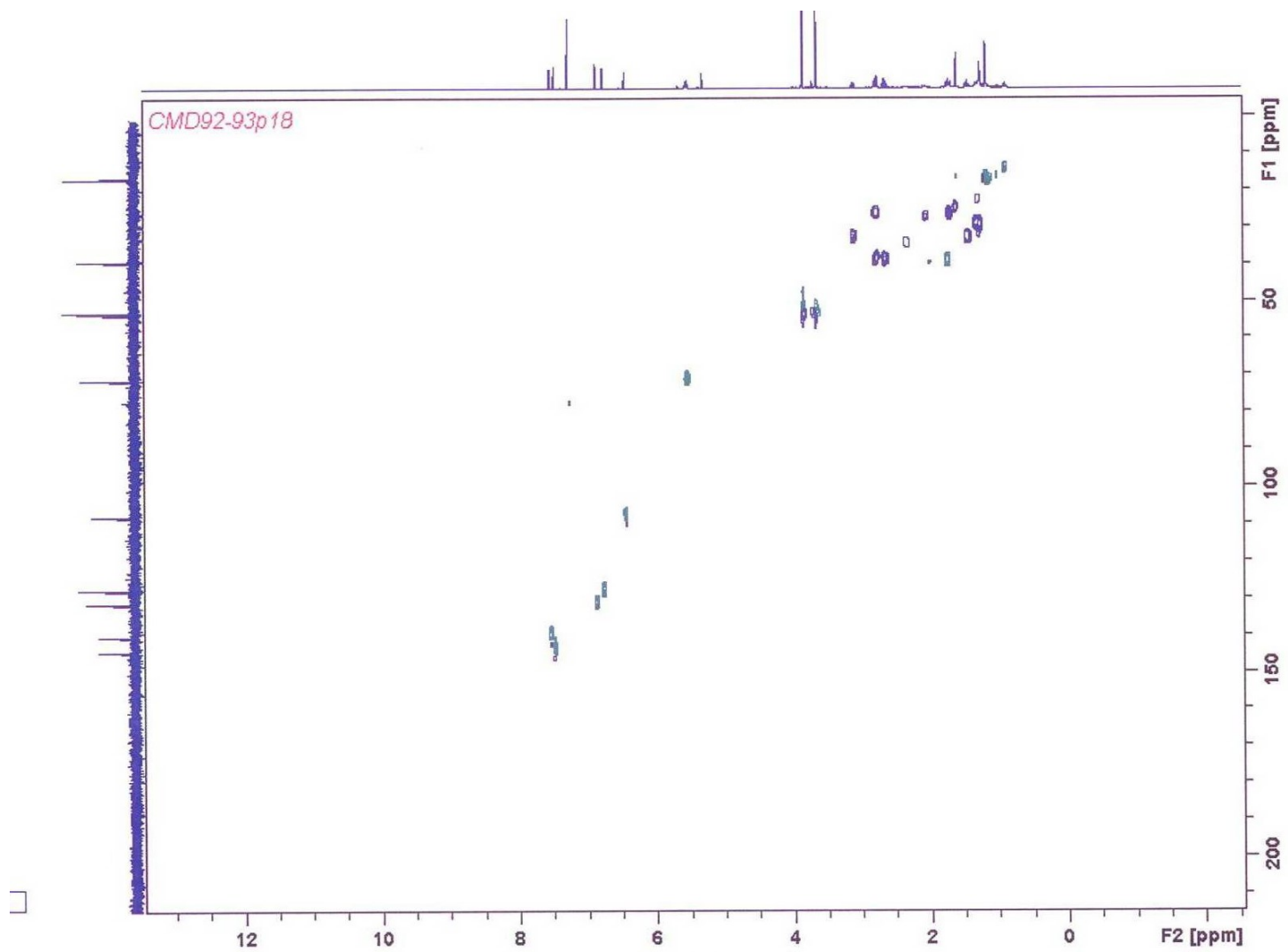
Appendix 27: ^{13}C NMR (125 MHz) spectrum of CMD-D in CDCl_3



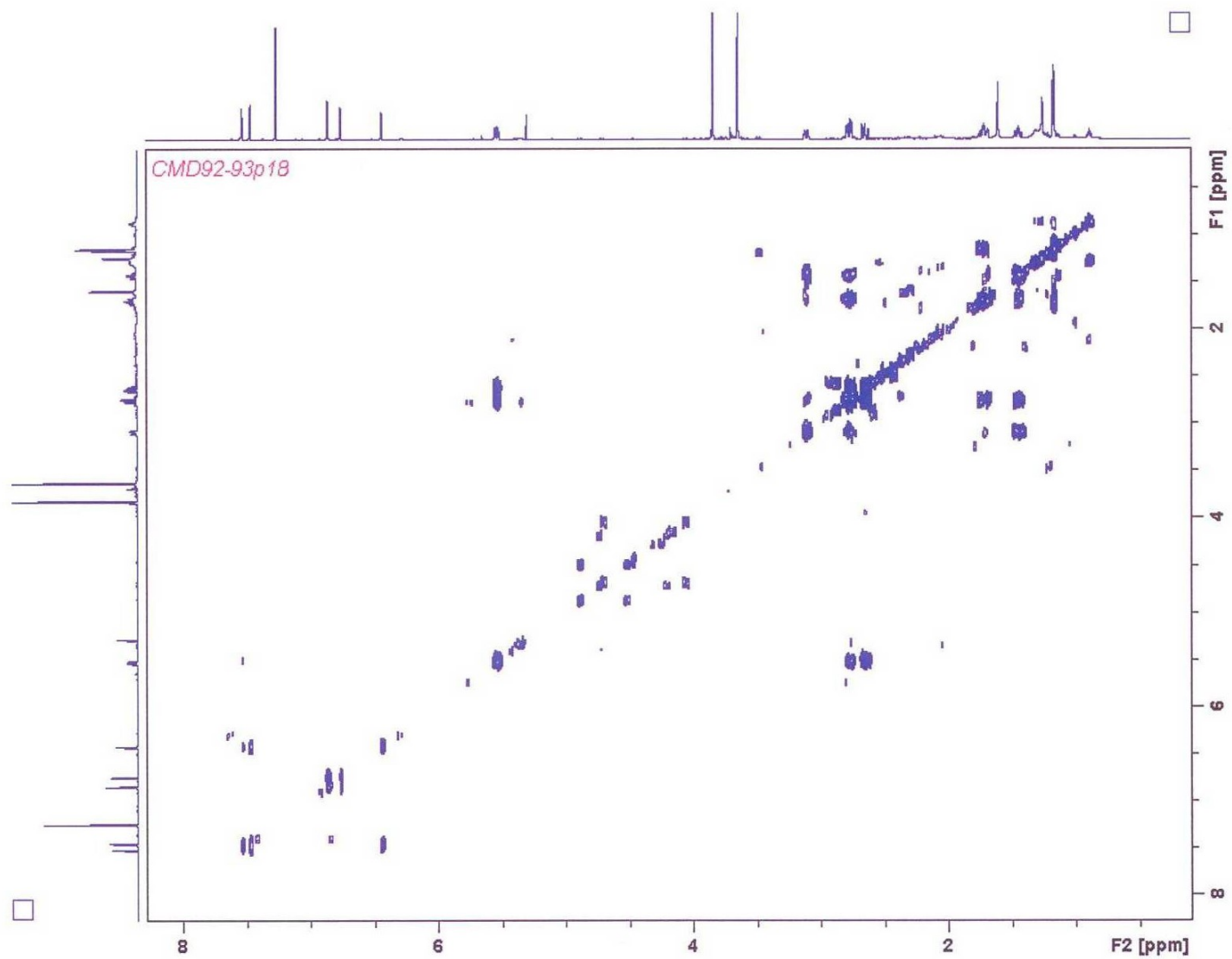
Appendix 28: DEPT spectrum of CMD-D in CDCl_3



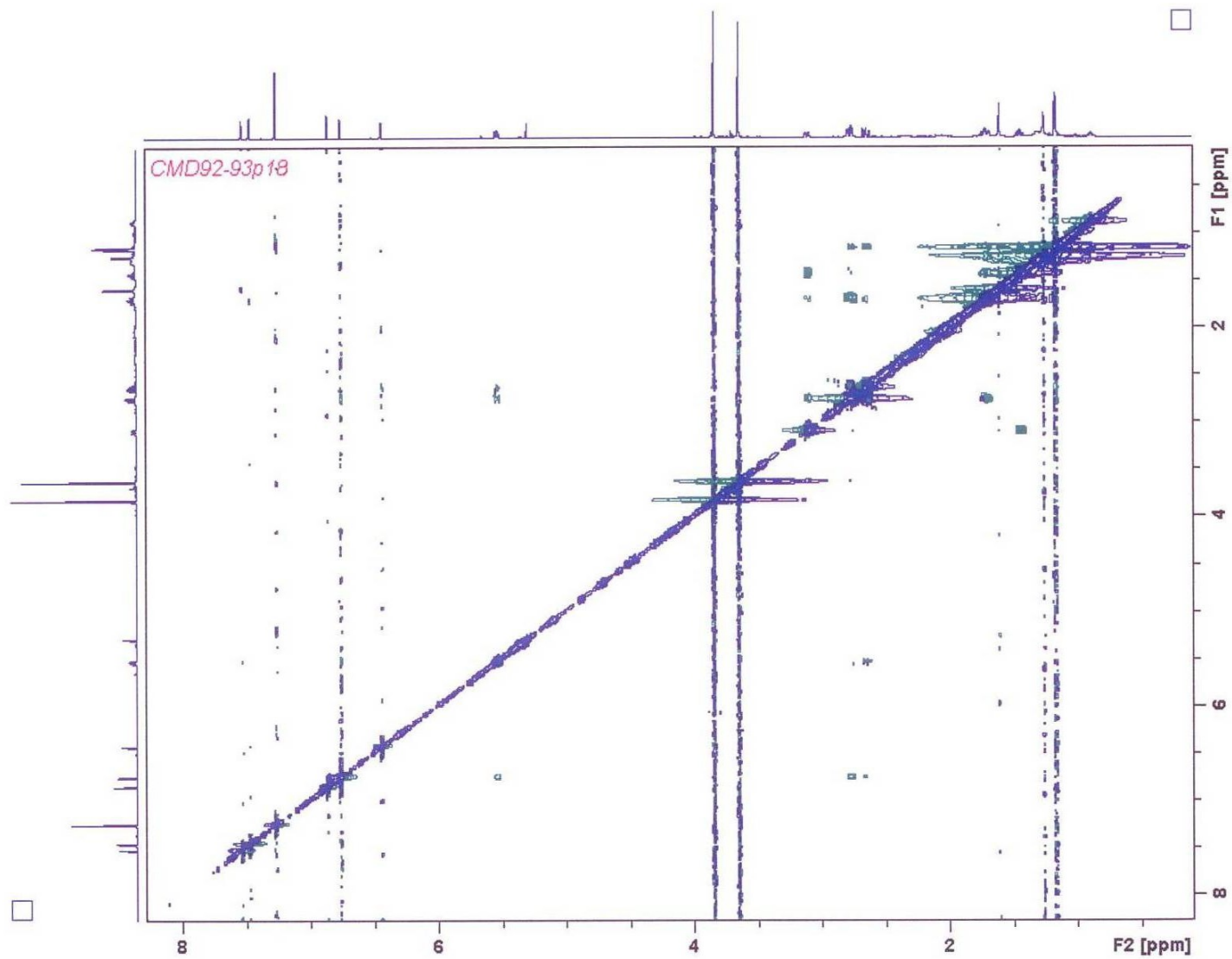
Appendix.29: HSQC DEPT spectrum of CMD-D in CDCl₃



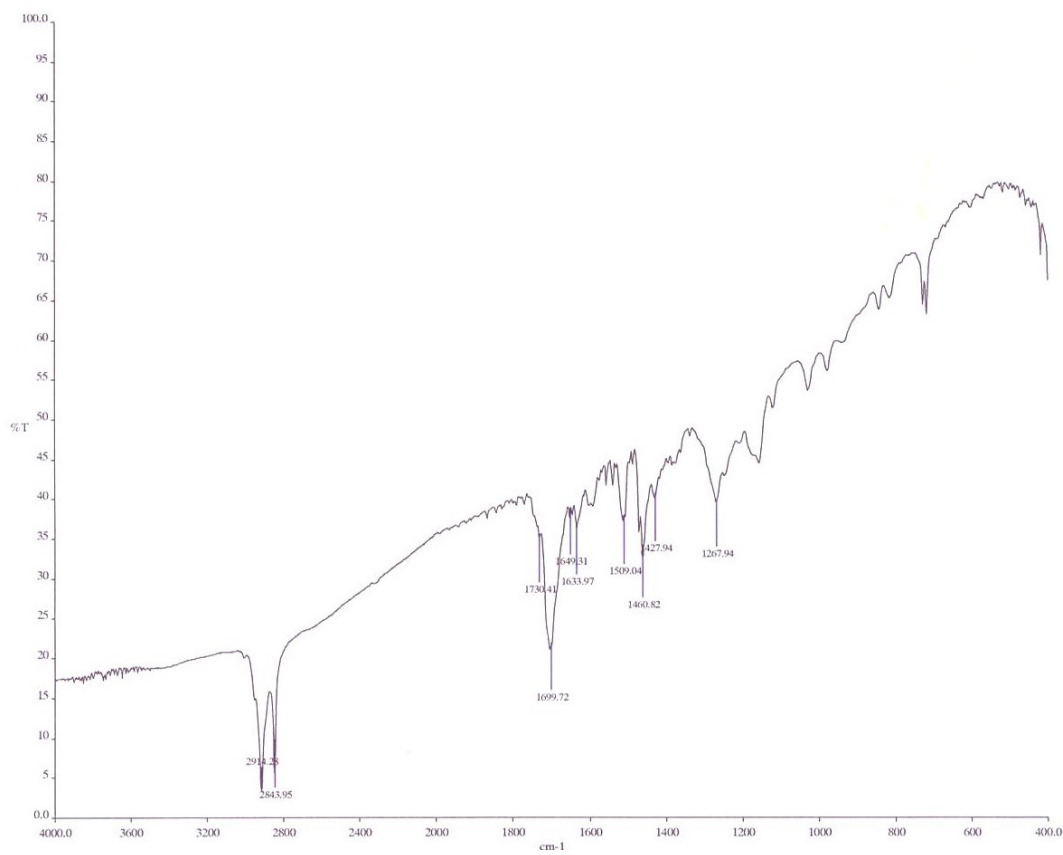
Appendix.30: HMBC spectrum of CMD-D in CDCl₃



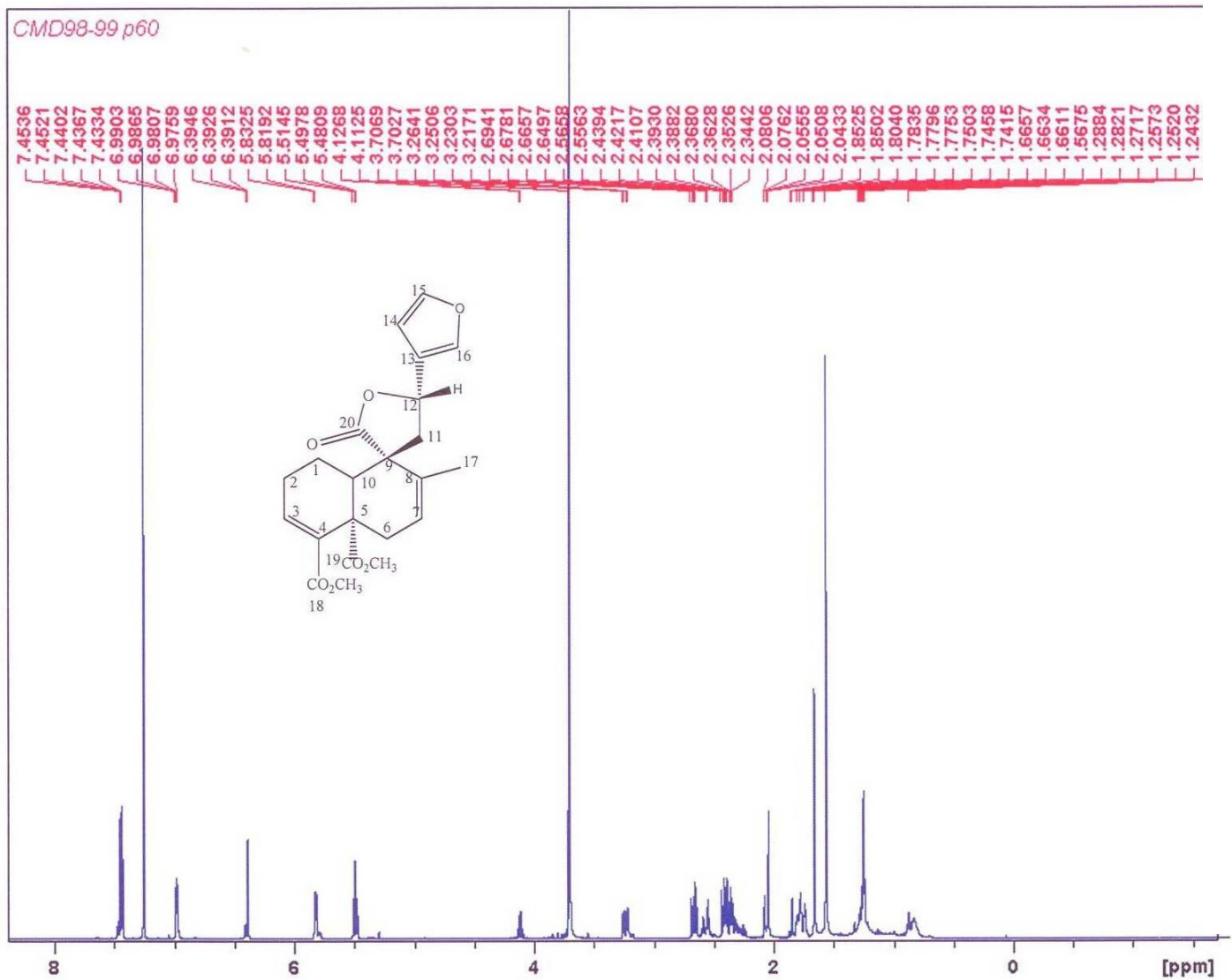
Appendix 31: COSY spectrum of CMD-D in CDCl_3



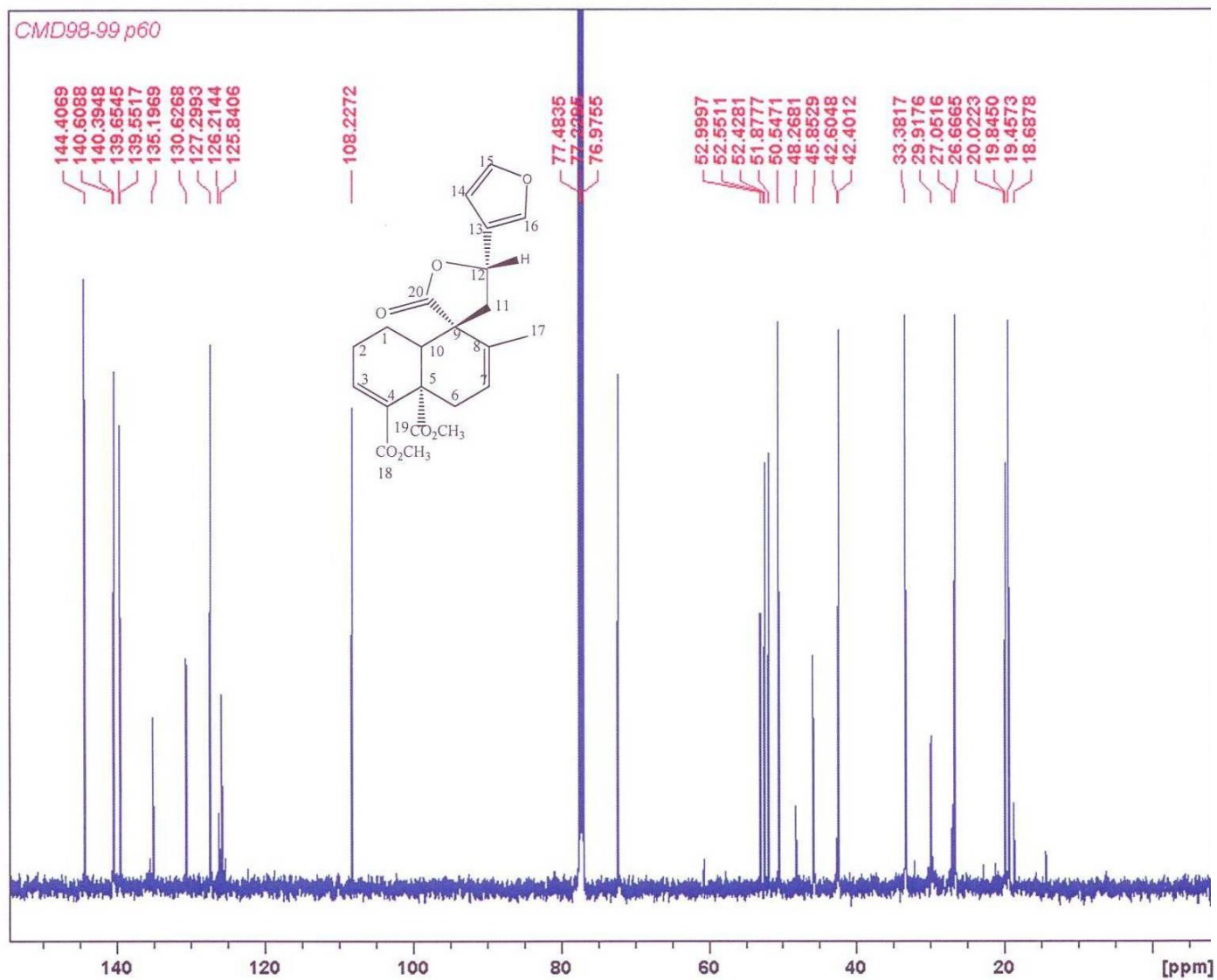
Appendix.32: NOESY spectrum of CMD-D in CDCl₃



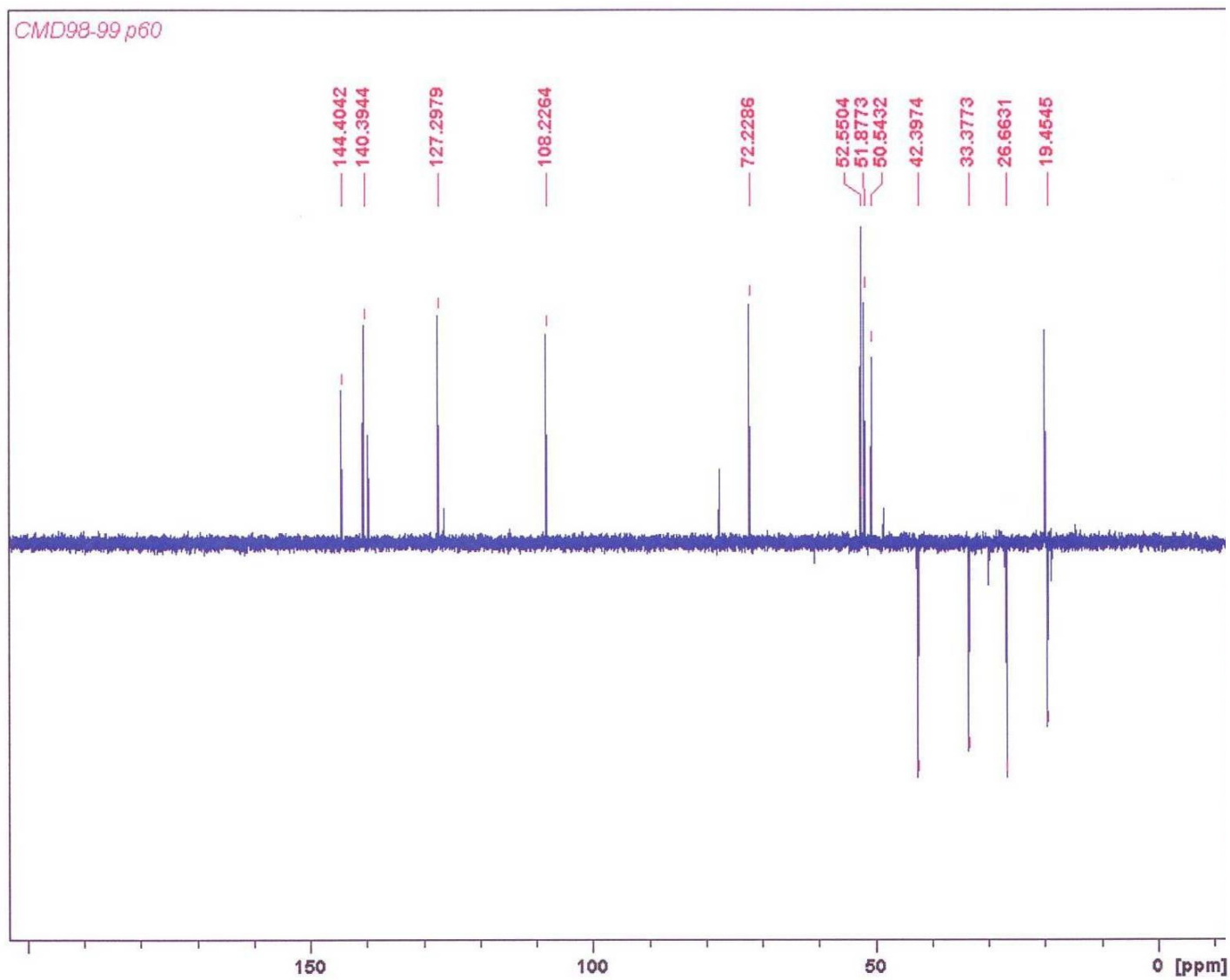
Appendix 33: IR spectrum of CMD-D in CDCl₃



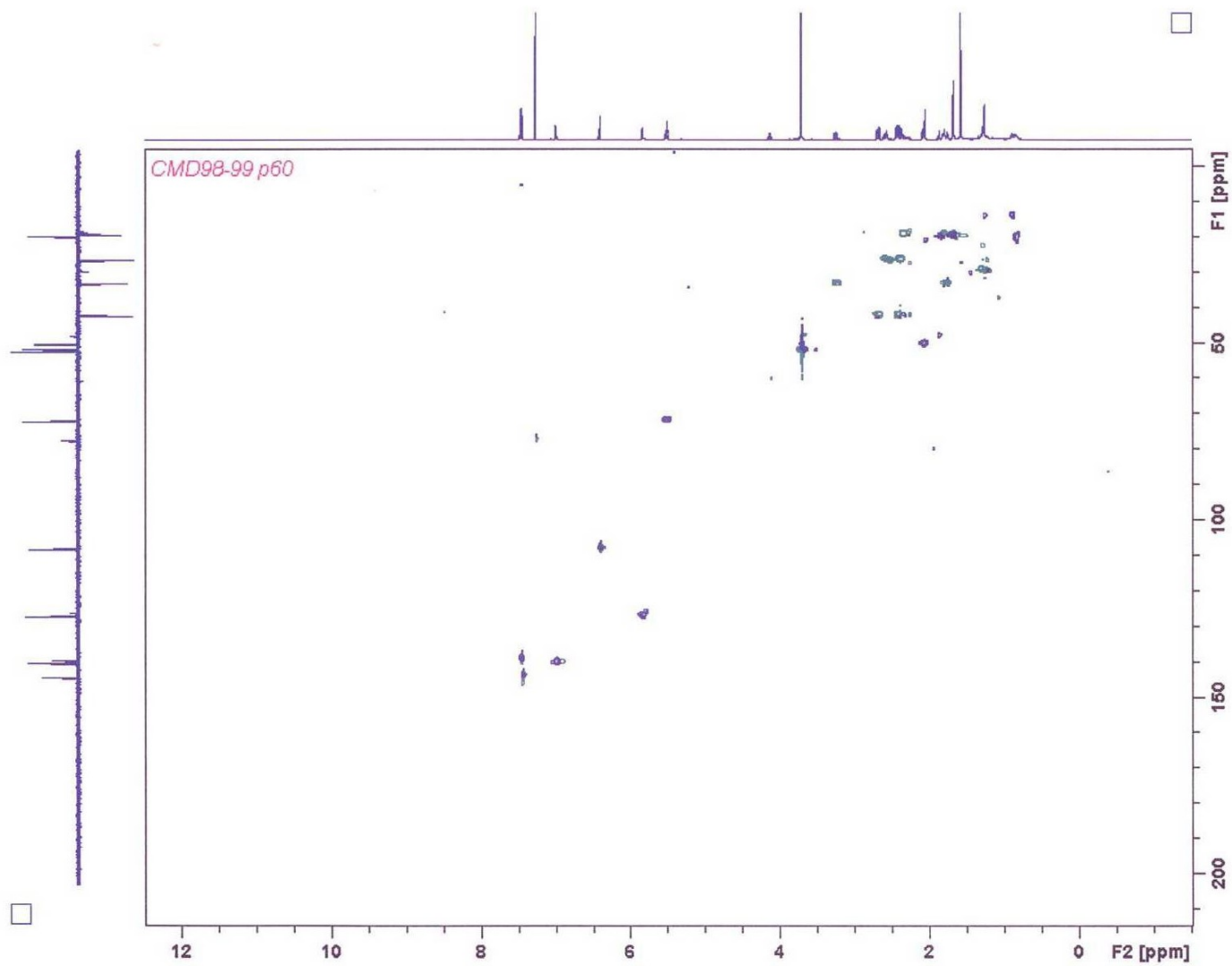
Appendix 34: ^1H NMR (500MHz) spectrum of CMD-E in CDCl_3



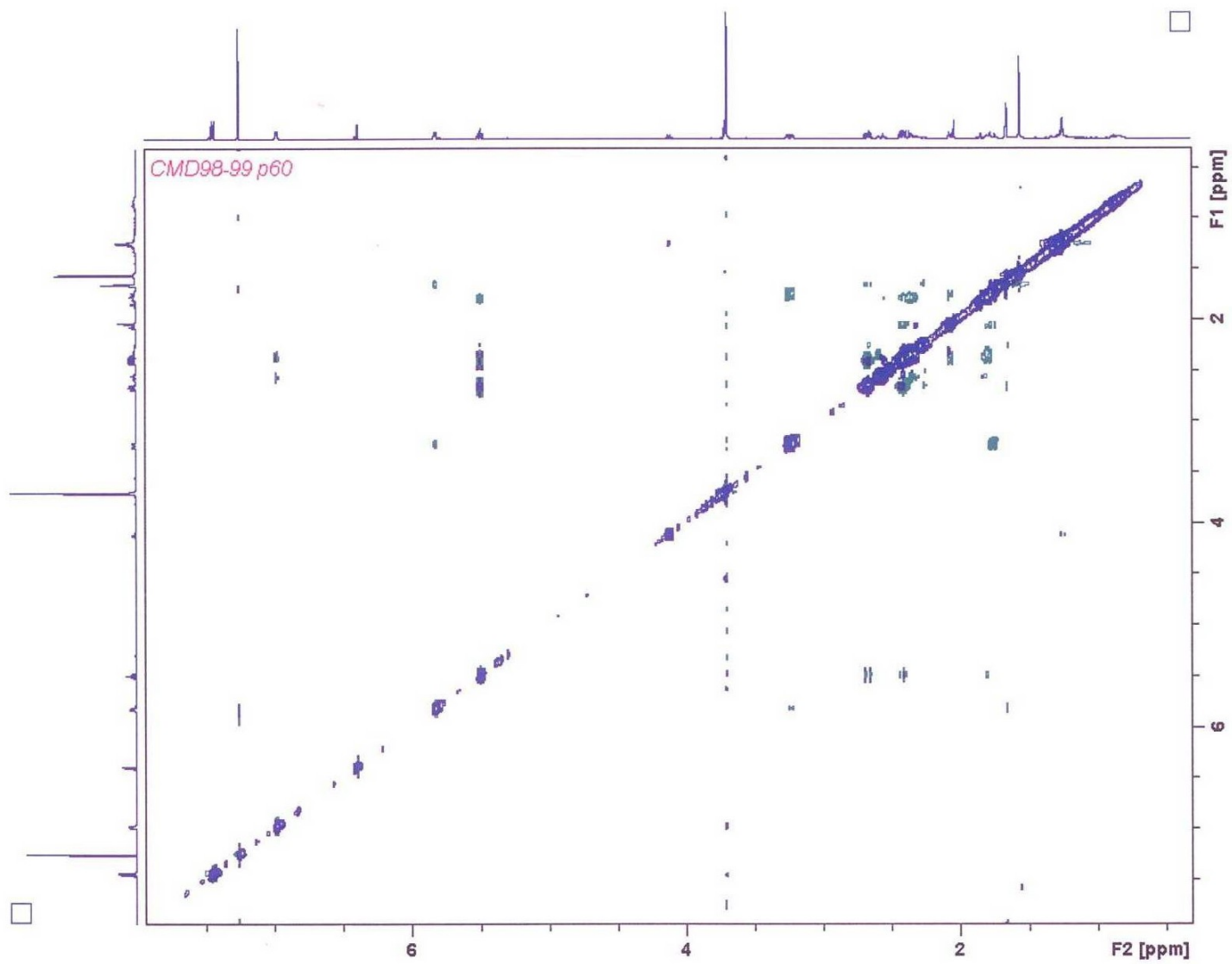
Appendix 35: ^{13}C NMR (125 MHz) spectrum of CMD-E in CDCl_3



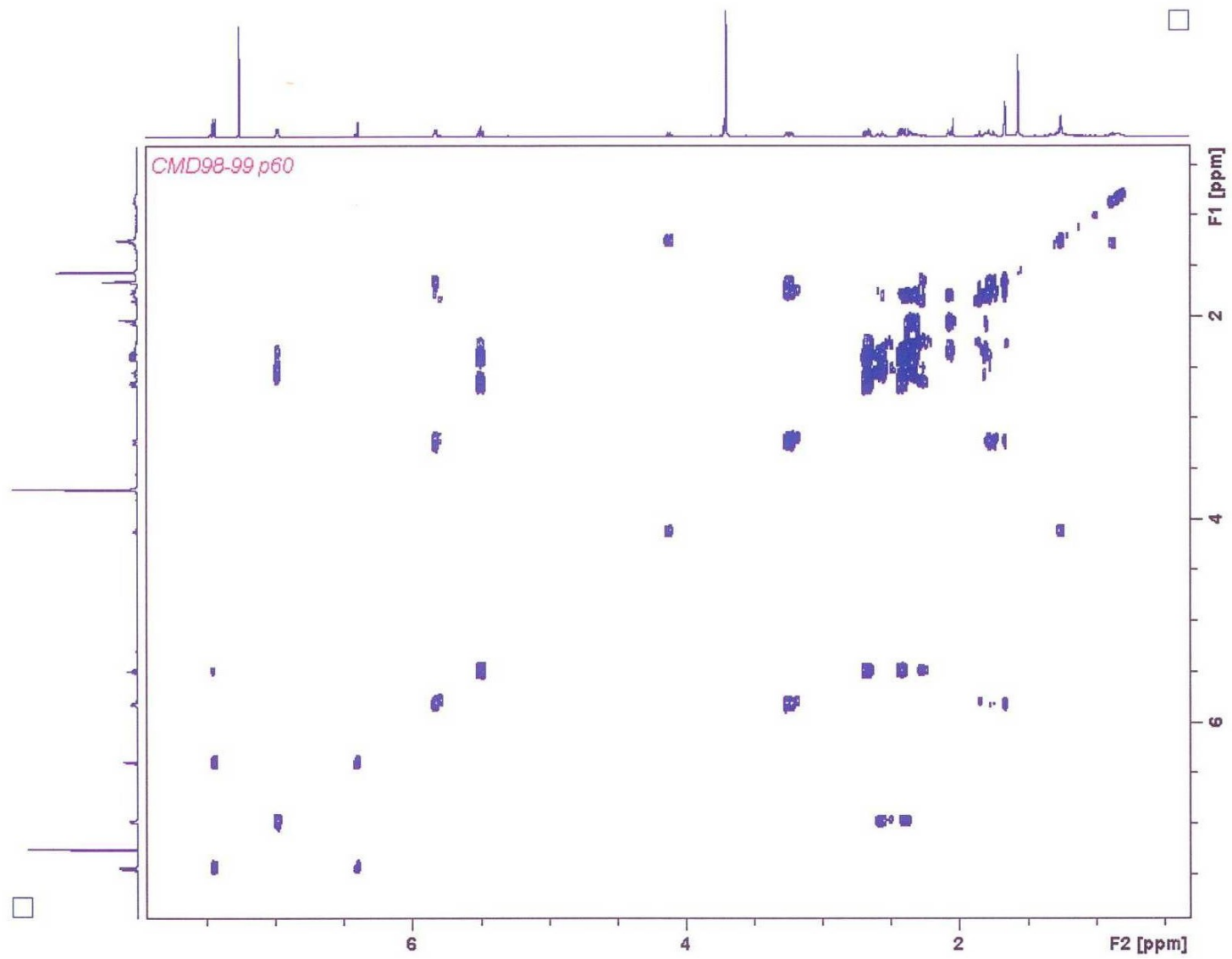
Appendix.36: DEPT spectrum of CMD-E in CDCl_3



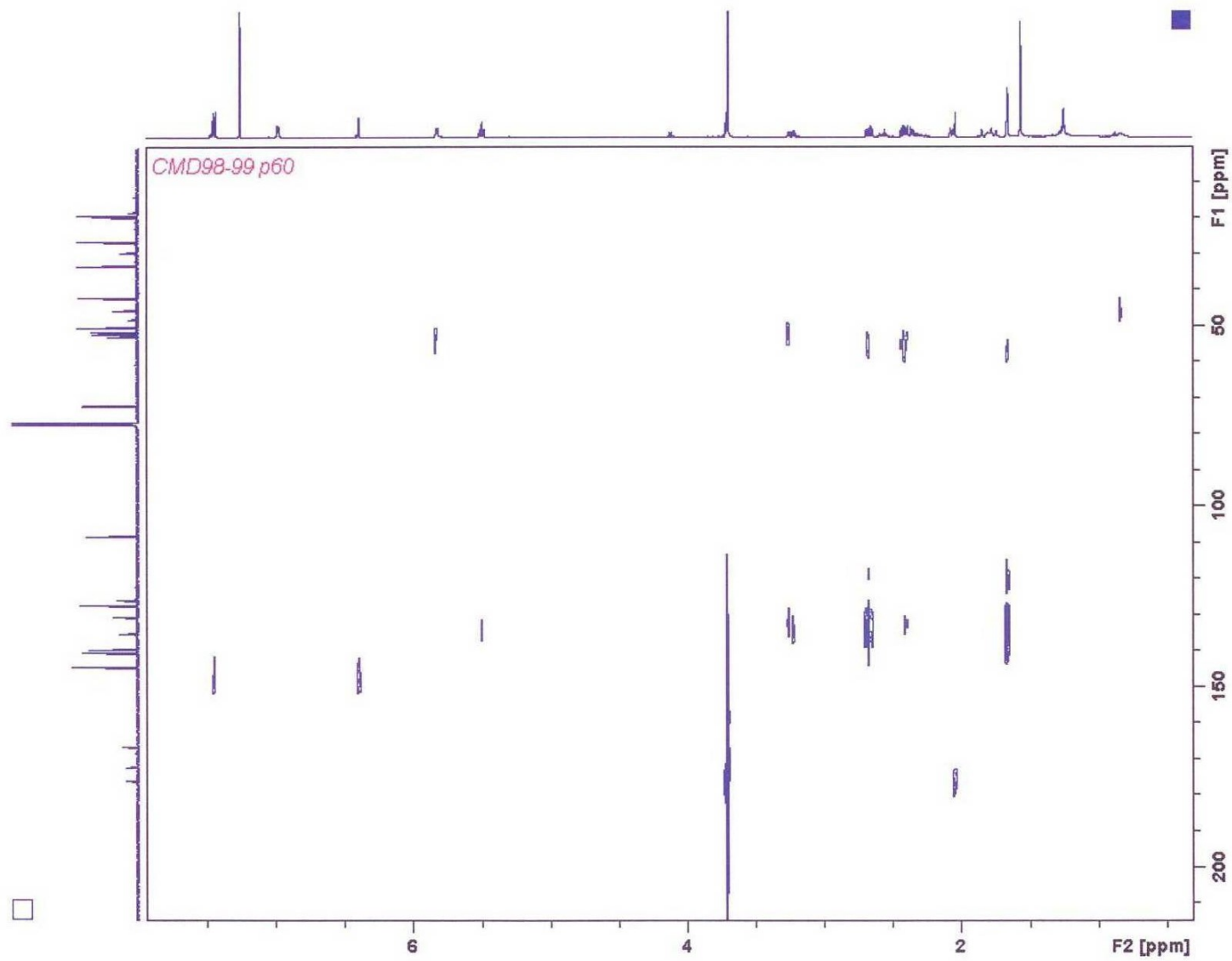
Appendix 37: HSQC DEPT spectrum of CMD-E in CDCl_3



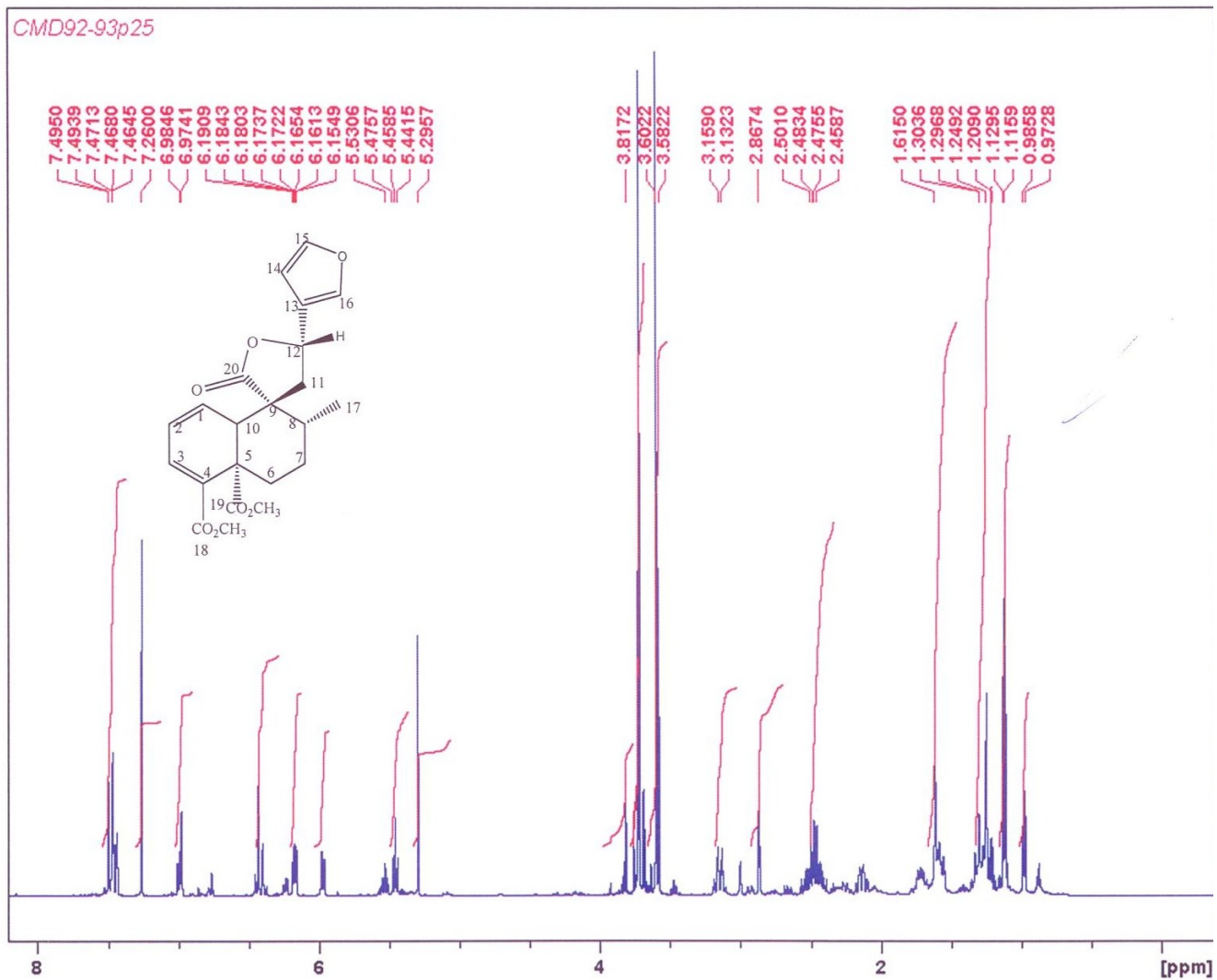
Appendix 38: HMBC spectrum of CMD-E in CDCl_3



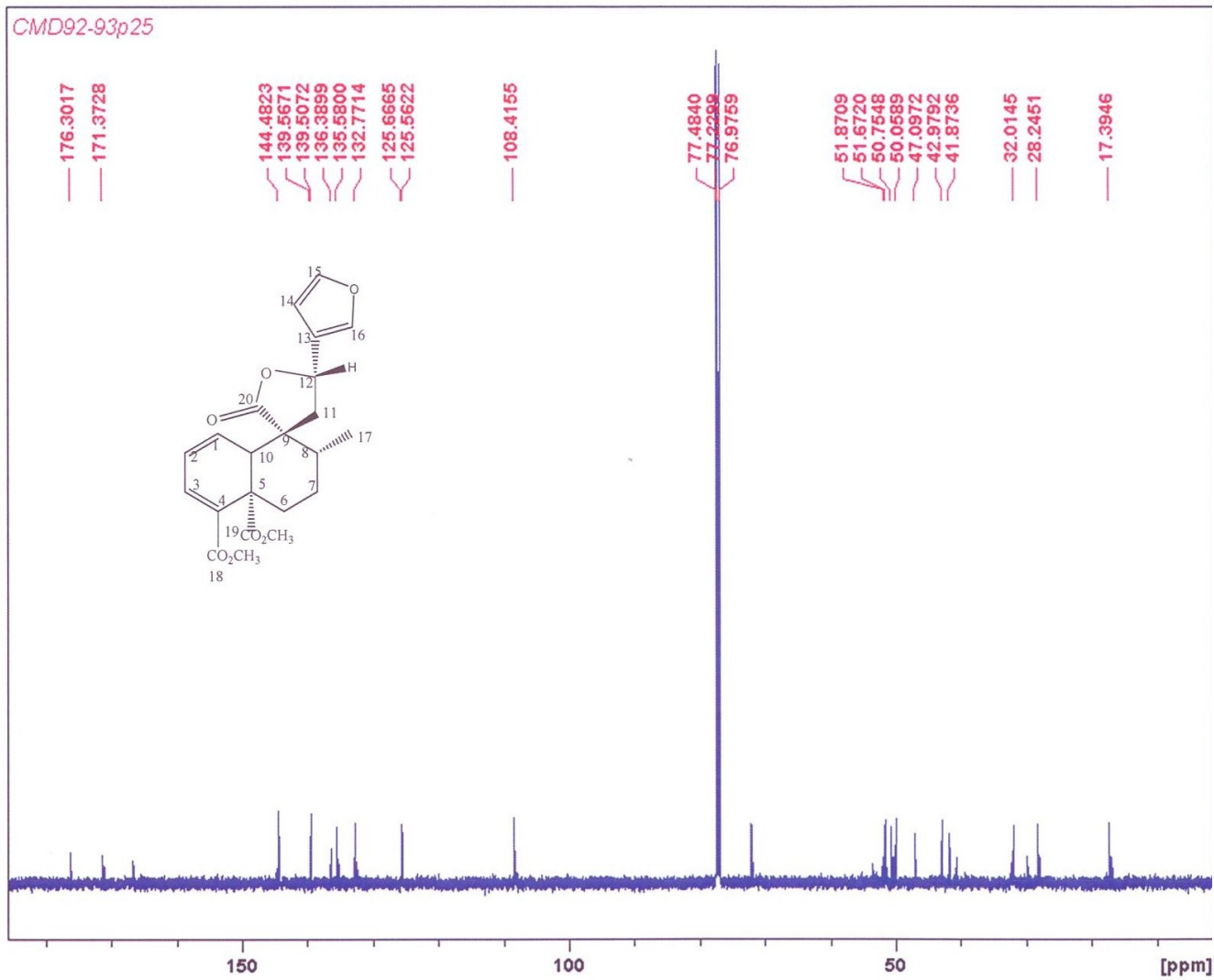
Appendix.39: COSY spectrum of CMD-E in CDCl₃



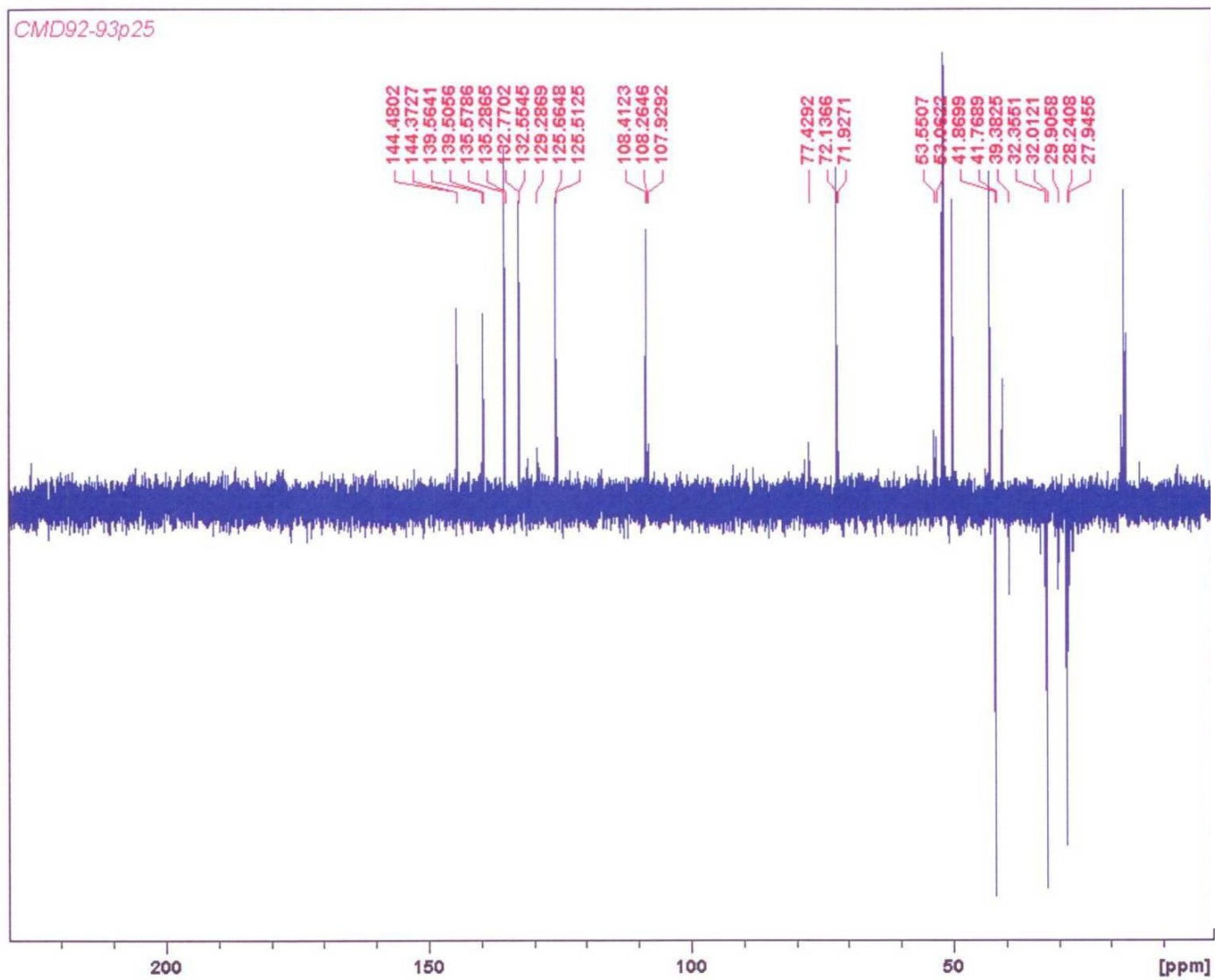
Appendix 40: NOESY spectrum of CMD-E in CDCl₃



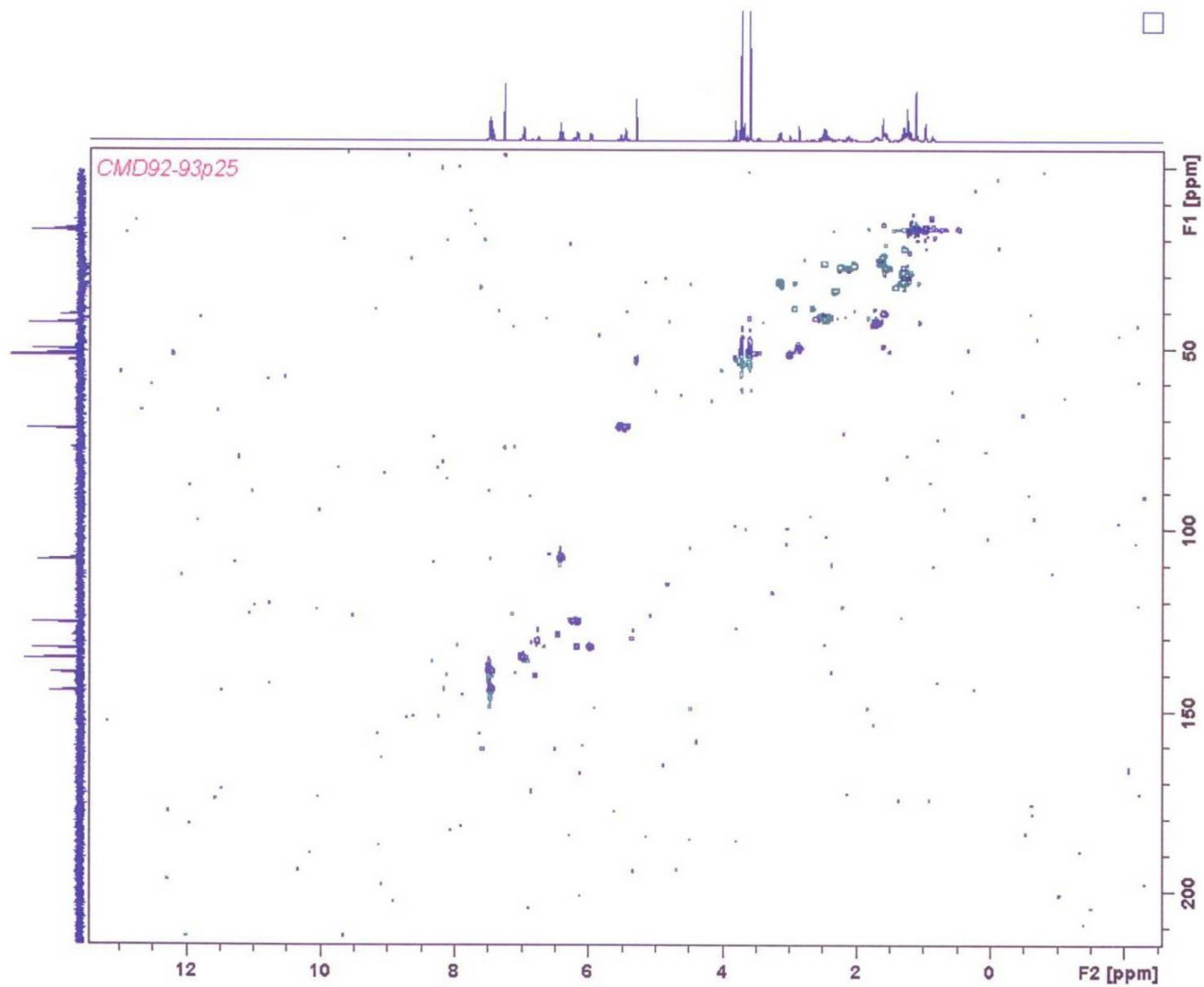
Appendix 41: ^1H NMR (500MHz) spectrum of CMD-F in CDCl_3



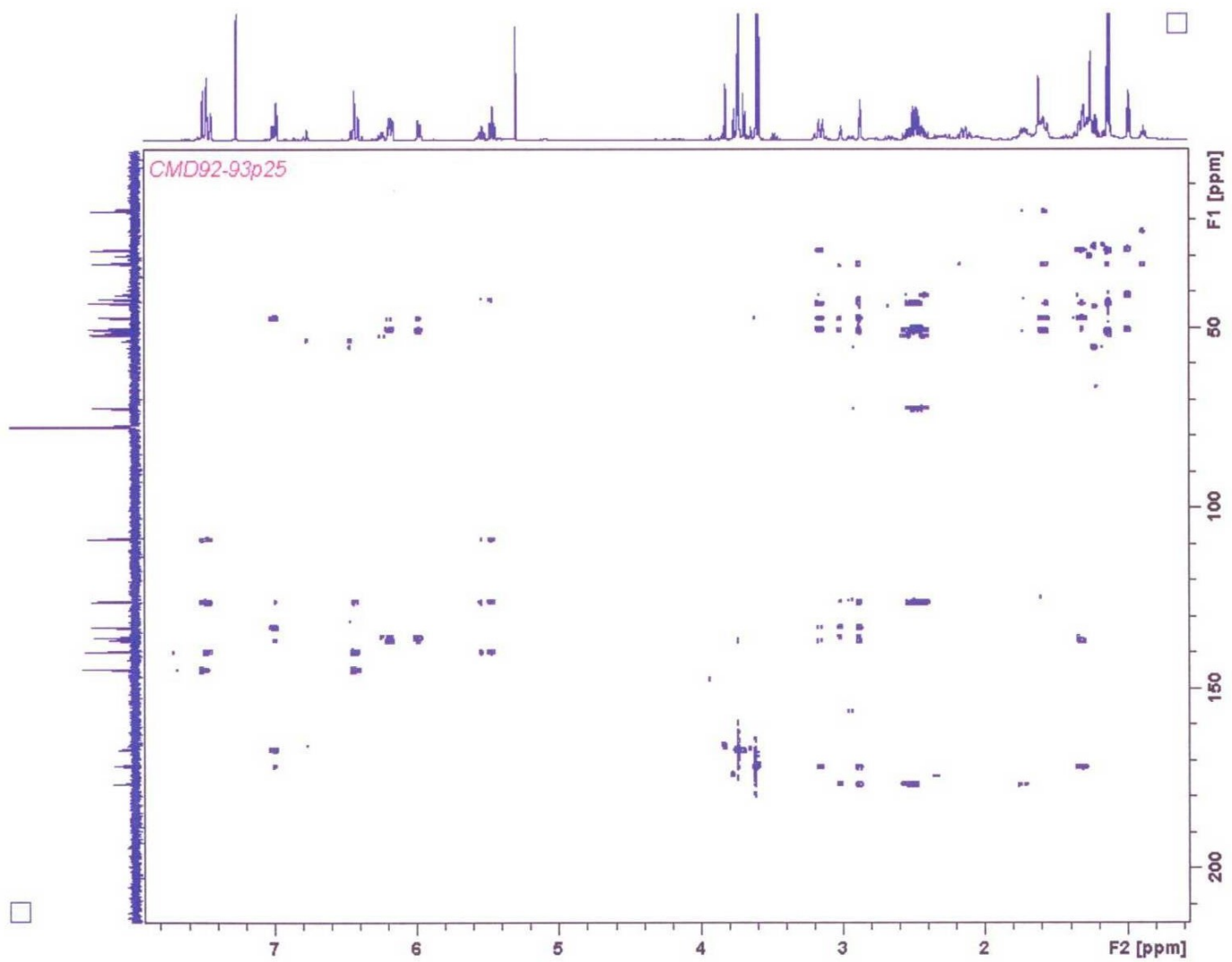
Appendix.42: ^{13}C NMR spectrum of CMD-F in CDCl_3



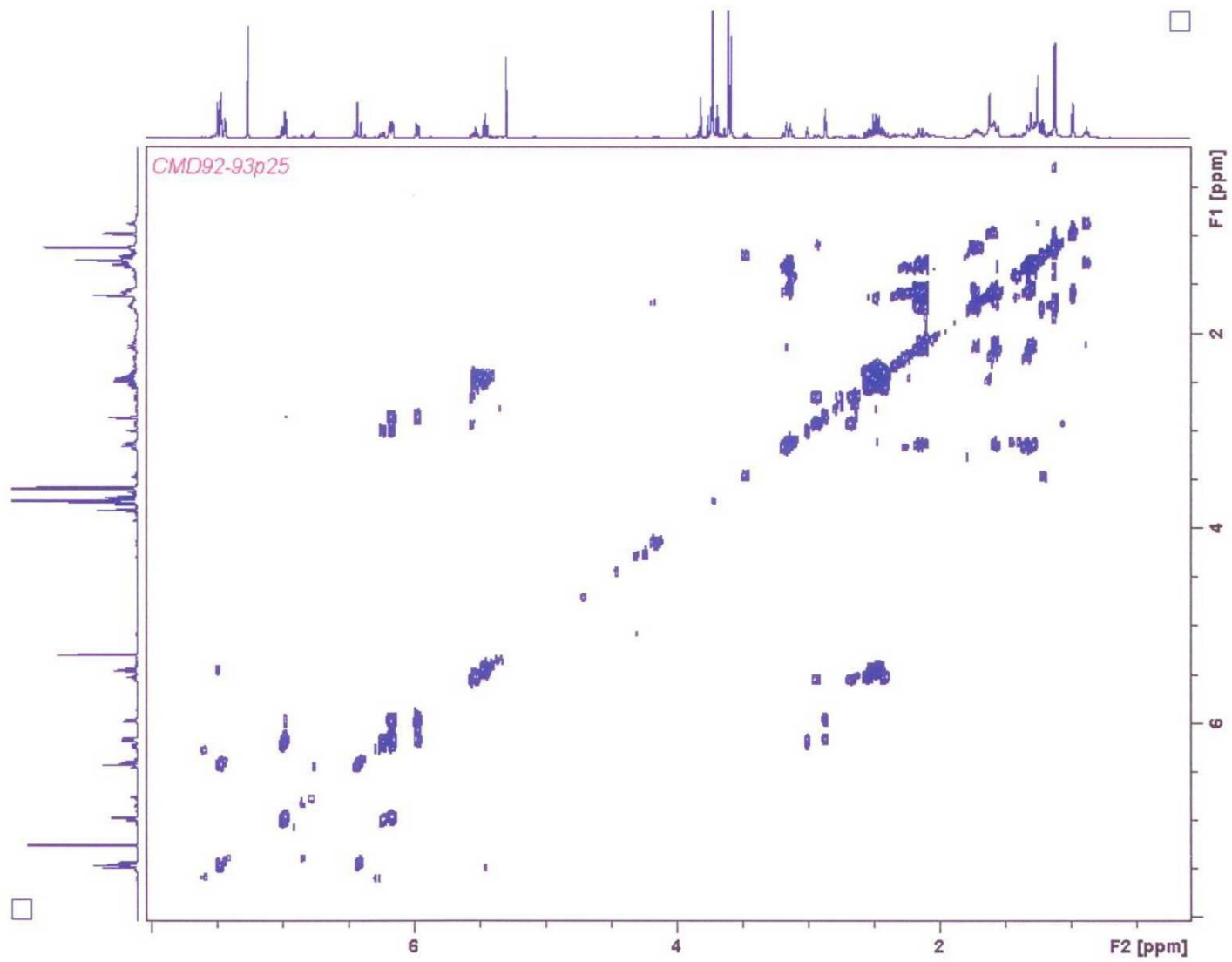
Appendix 43: DEPT spectrum of CMD-F in CDCl_3



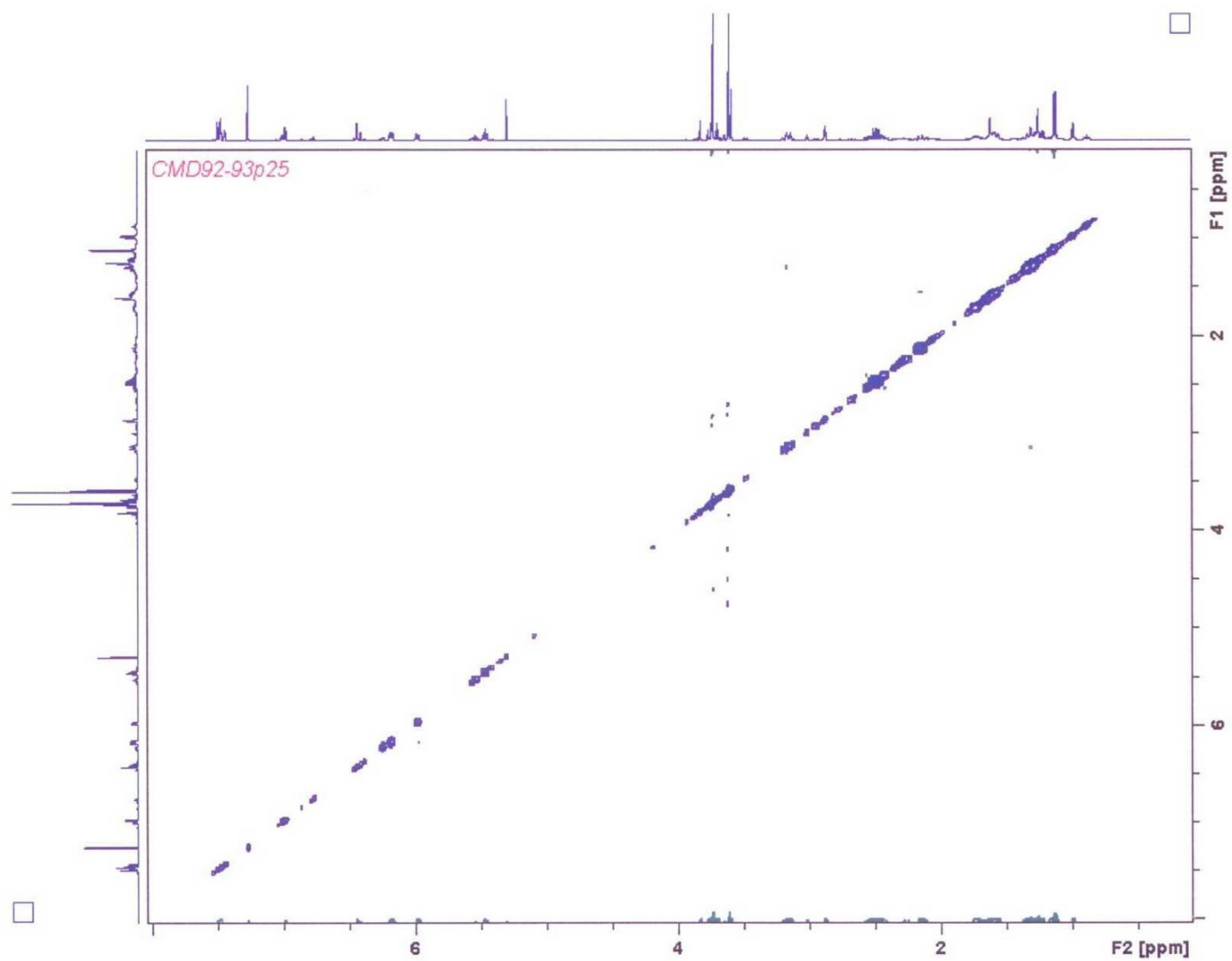
Appendix 44: HSQC DEPT spectrum of CMD-F in CDCl_3



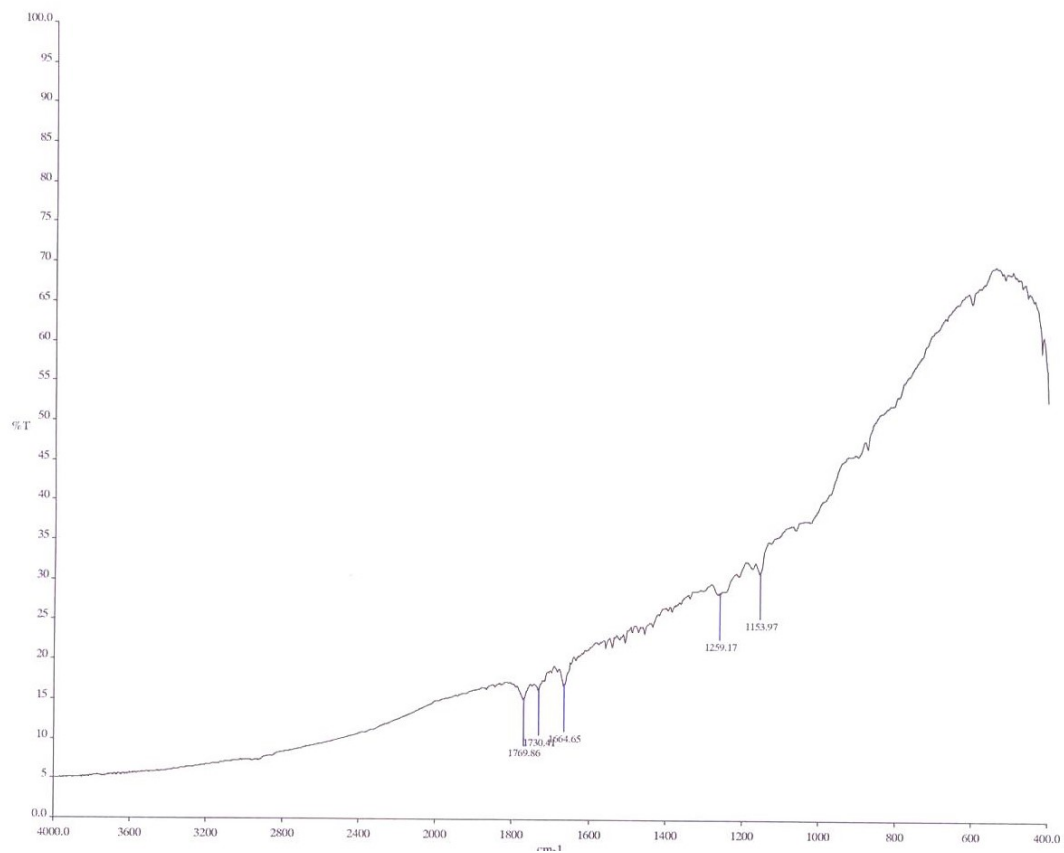
Appendix 45: HMBC spectrum of CMD-F in CDCl_3



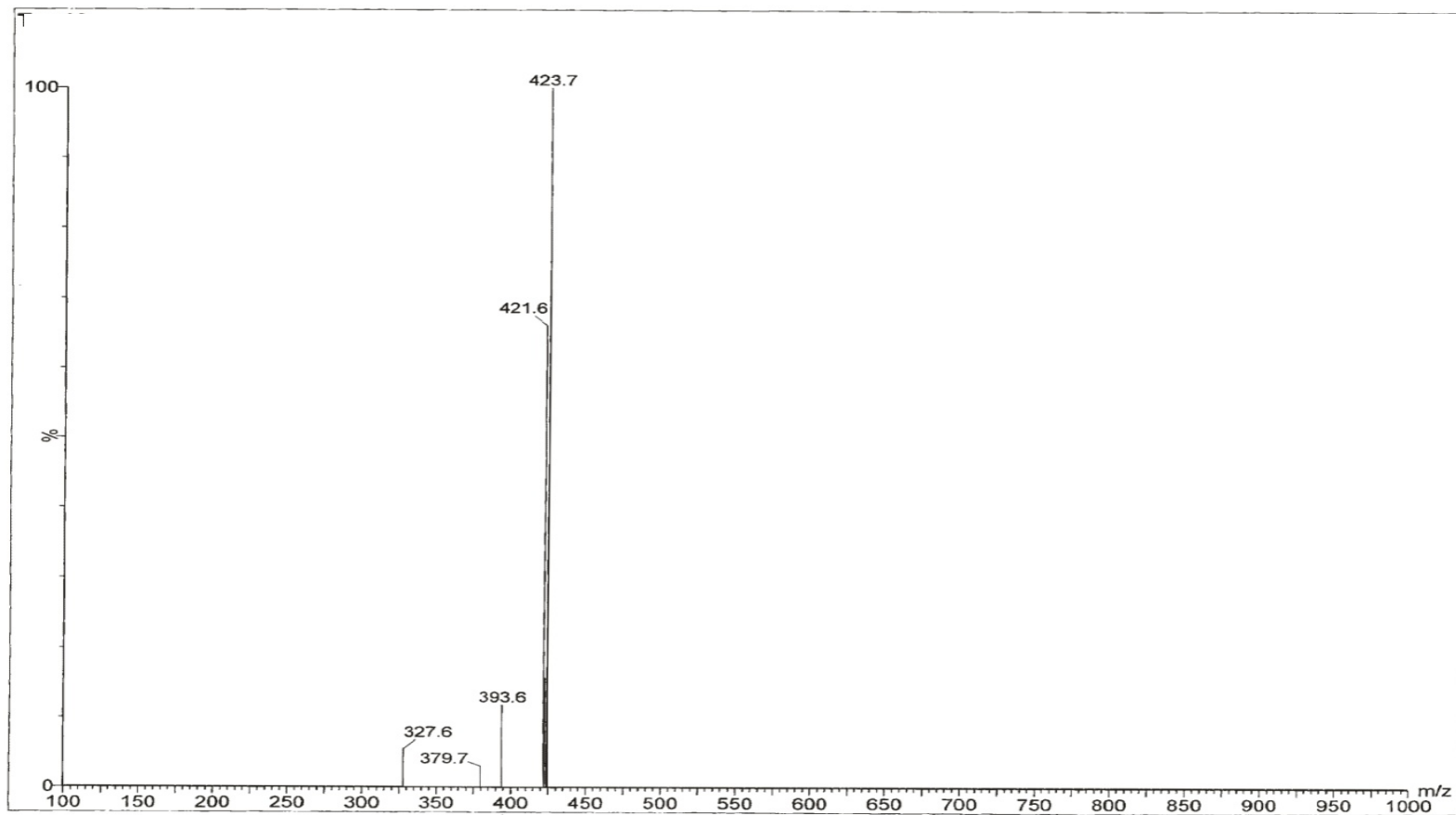
Appendix 46: COSY spectrum of CMD-F in CDCl₃



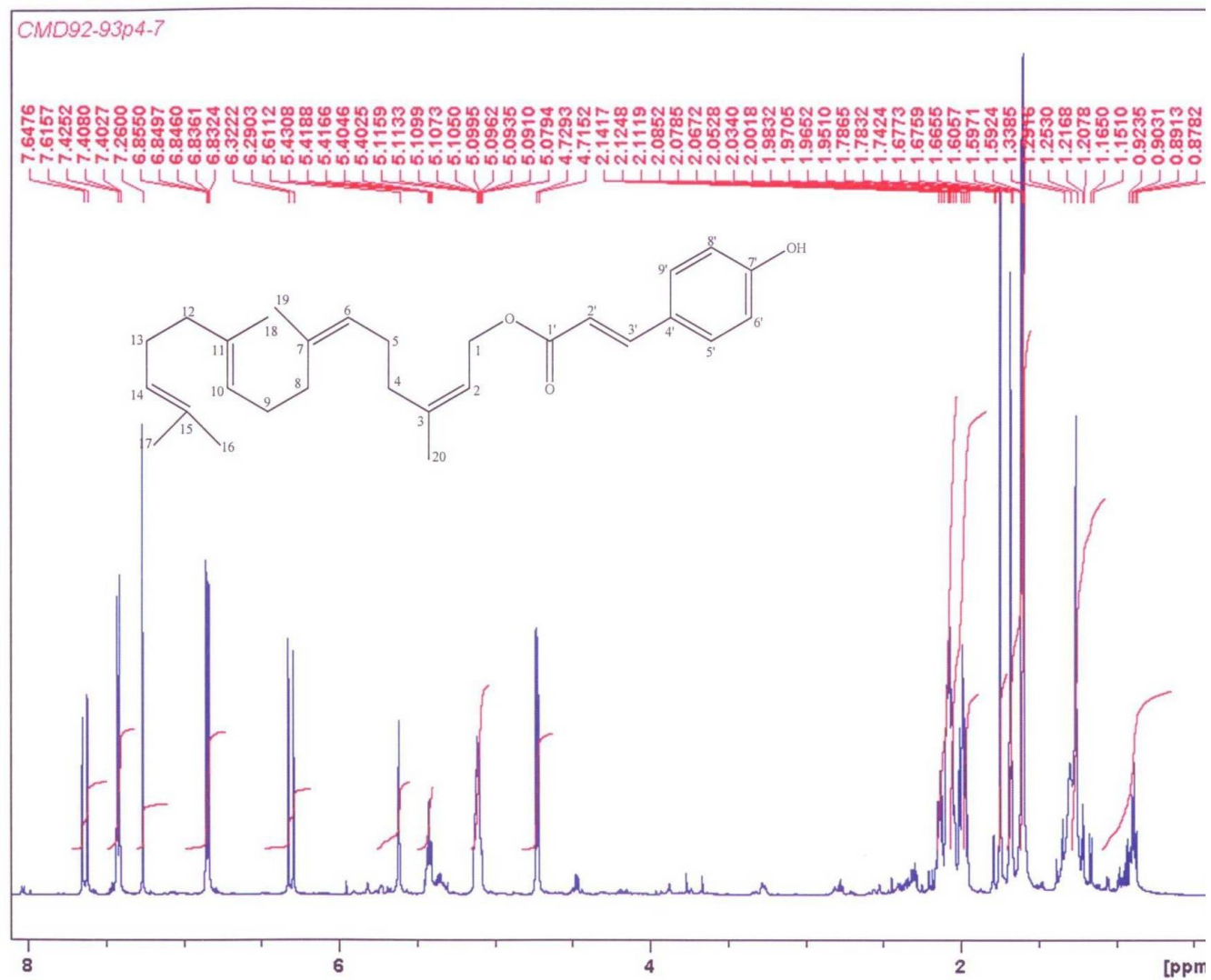
Appendix 47: NOESY spectrum of CMD-F in CDCl₃



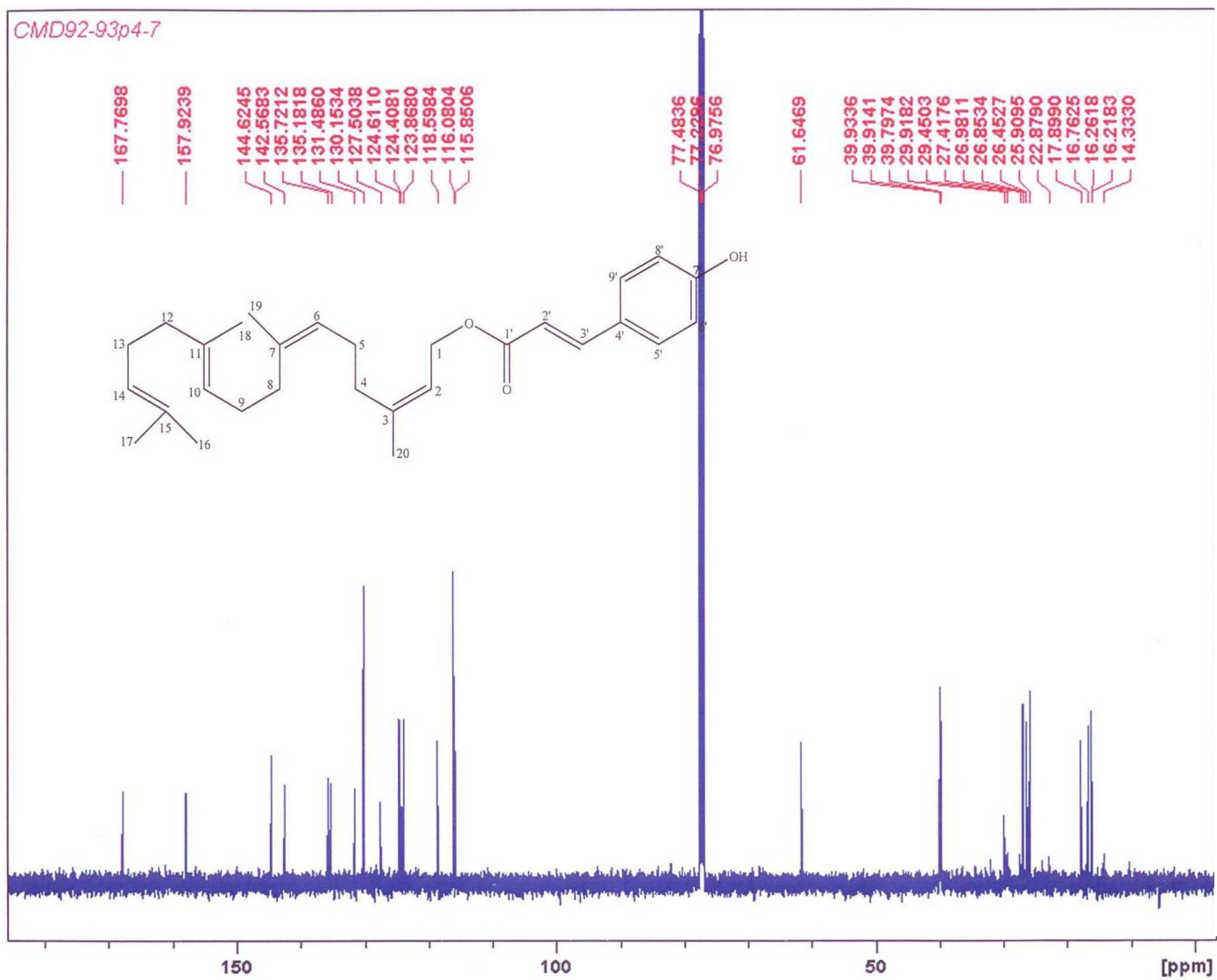
Appendix 48: IR spectrum of CMD-F in CDCl₃



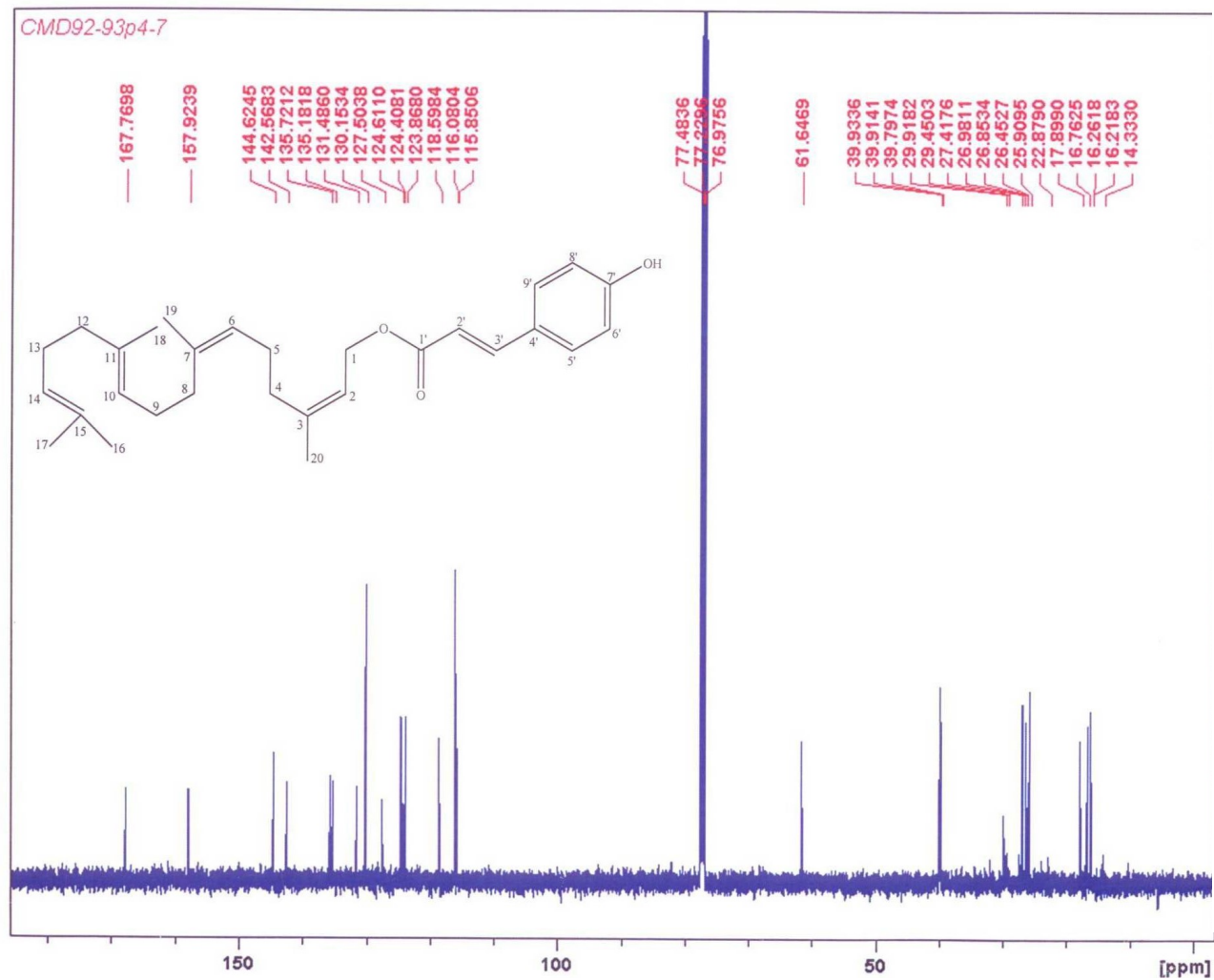
Appendix 49: MS spectrum of CMD-F



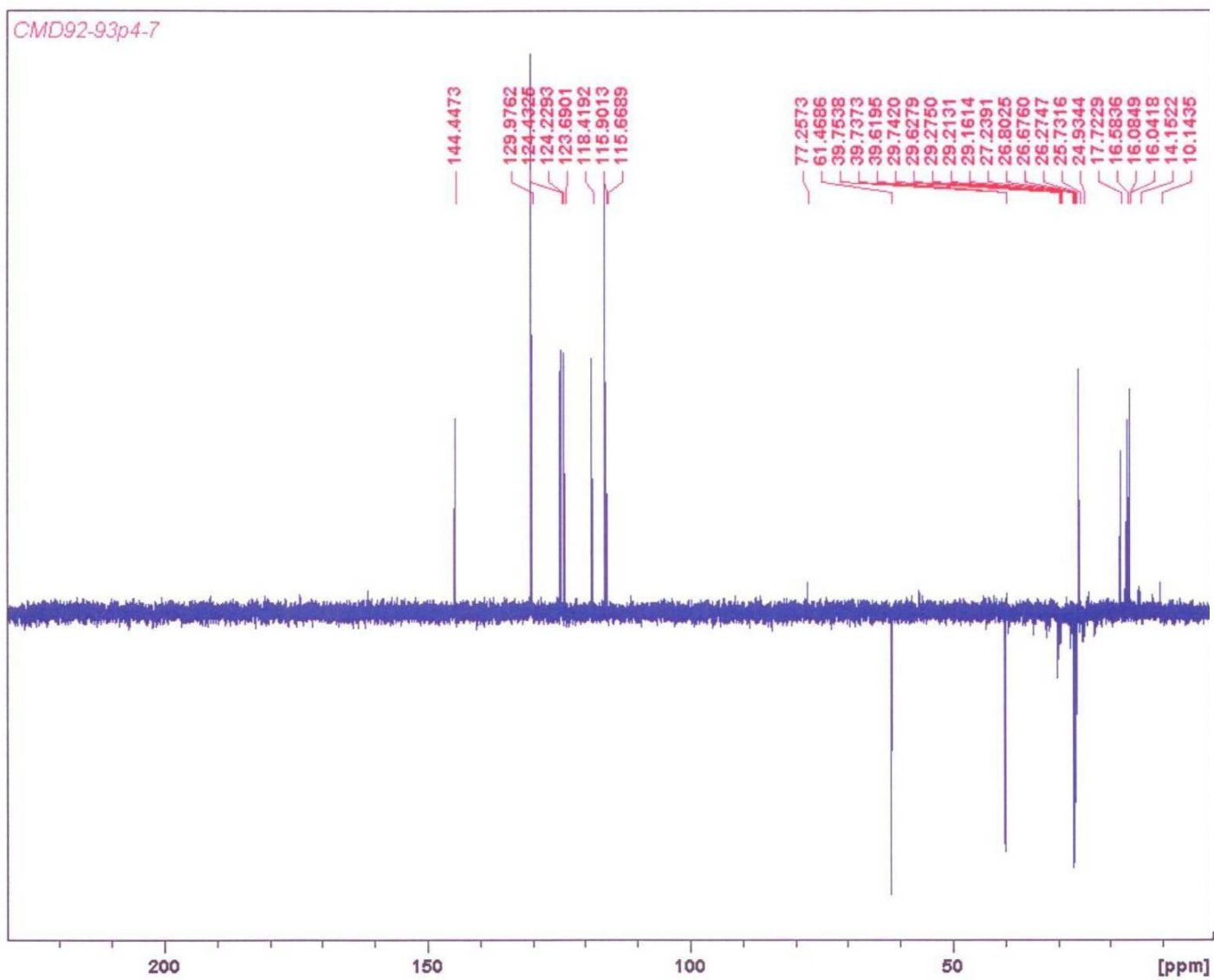
Appendix.50: ^1H NMR (500MHz) spectrum of CMD-G in CDCl_3



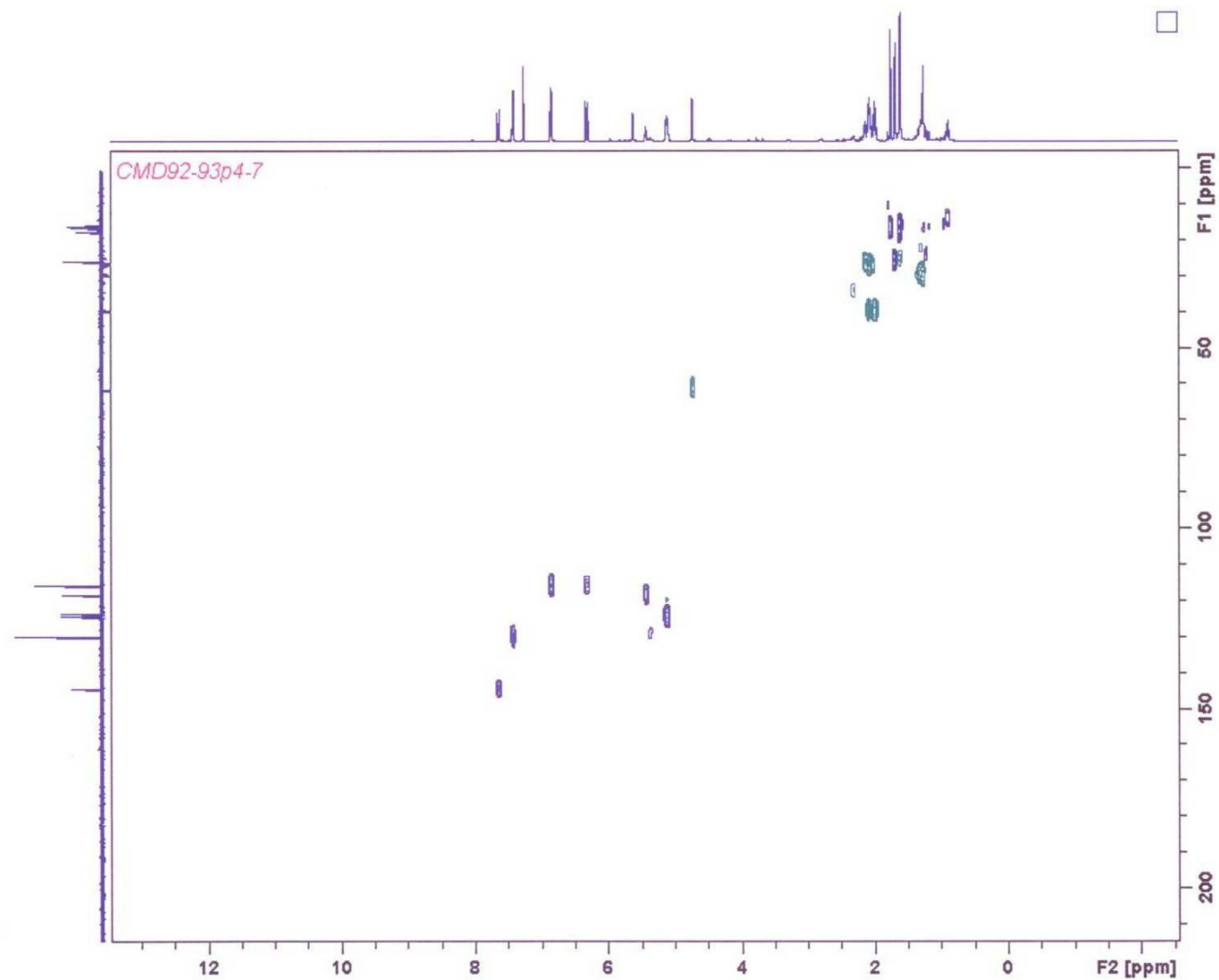
Appendix 51: ^{13}C NMR (125 MHz) spectrum of CMD-G in CDCl_3



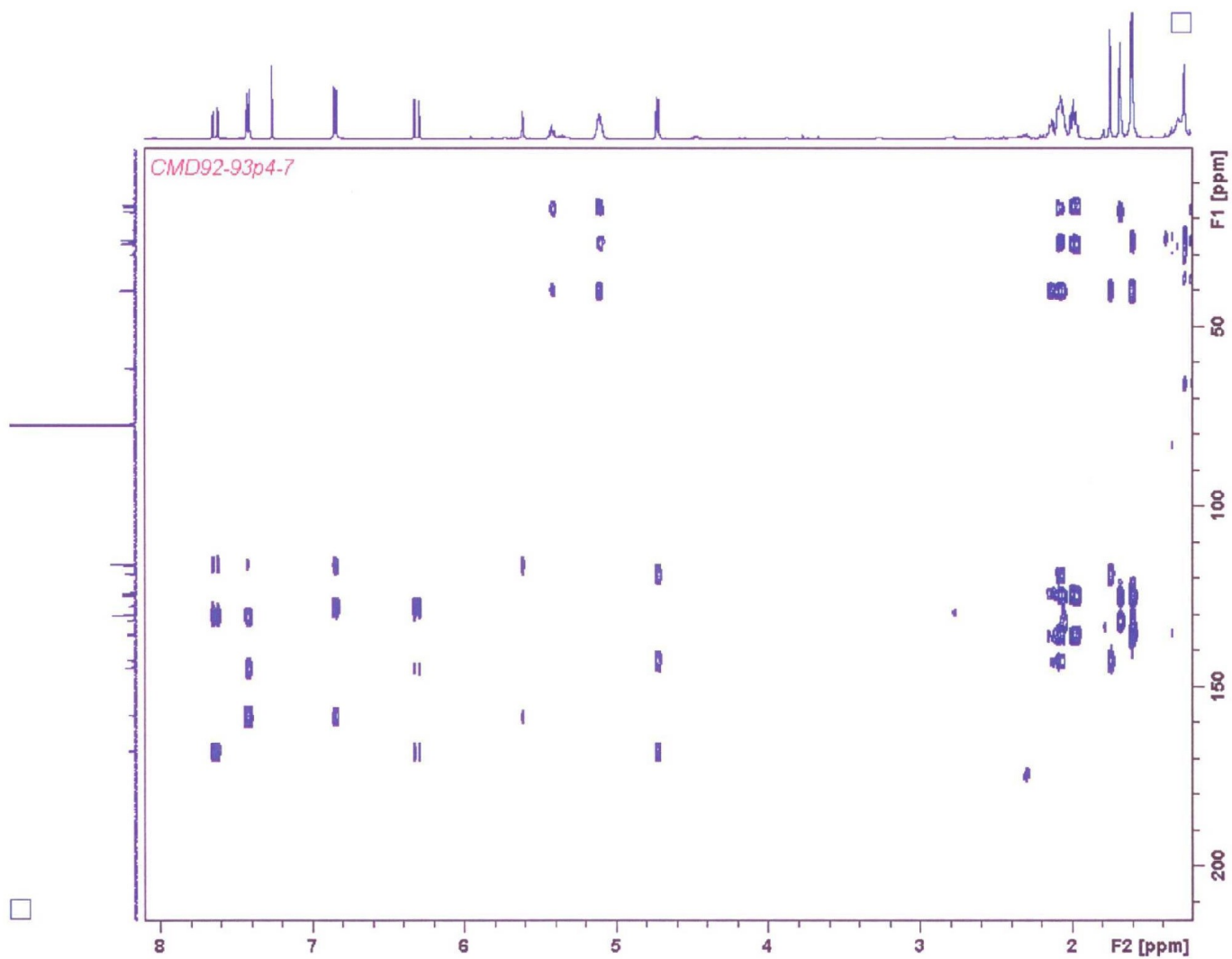
Appendix 52: ^{13}C NMR (125 MHz) spectrum of CMD-G in CDCl_3



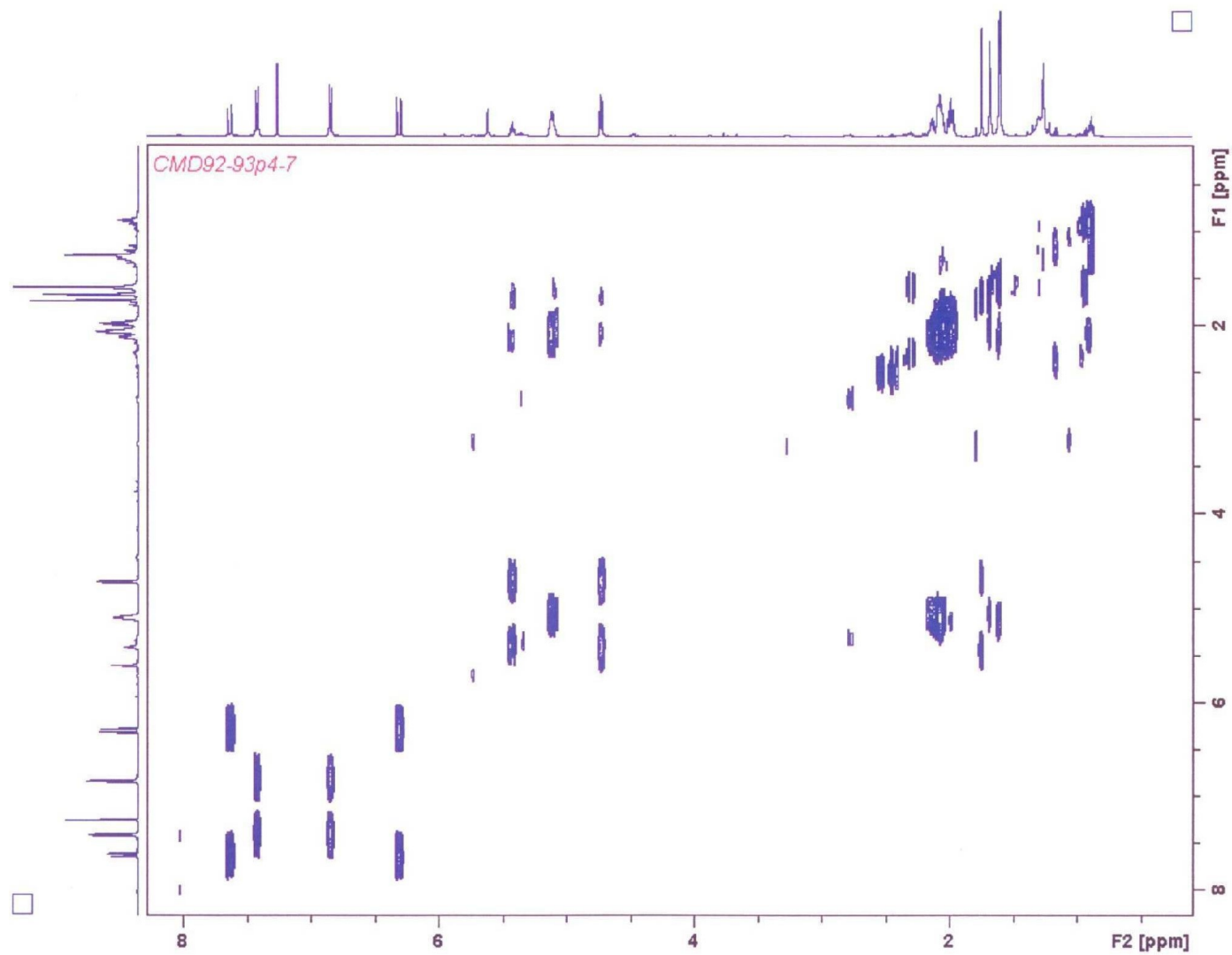
Appendix 53: DEPT spectrum of CMD-G in CDCl_3



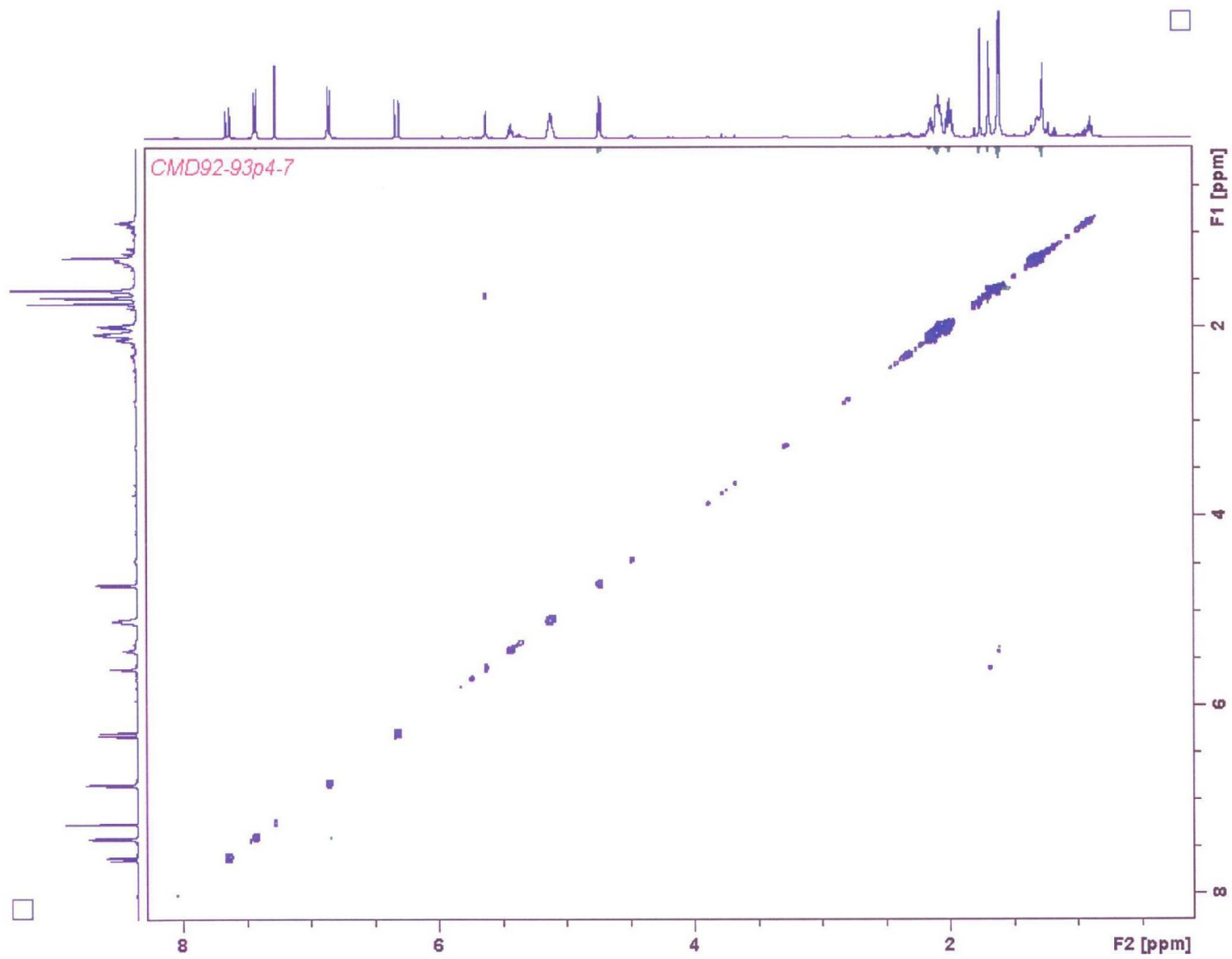
Appendix 54: HSQC DEPT spectrum of CMD-G in CDCl_3



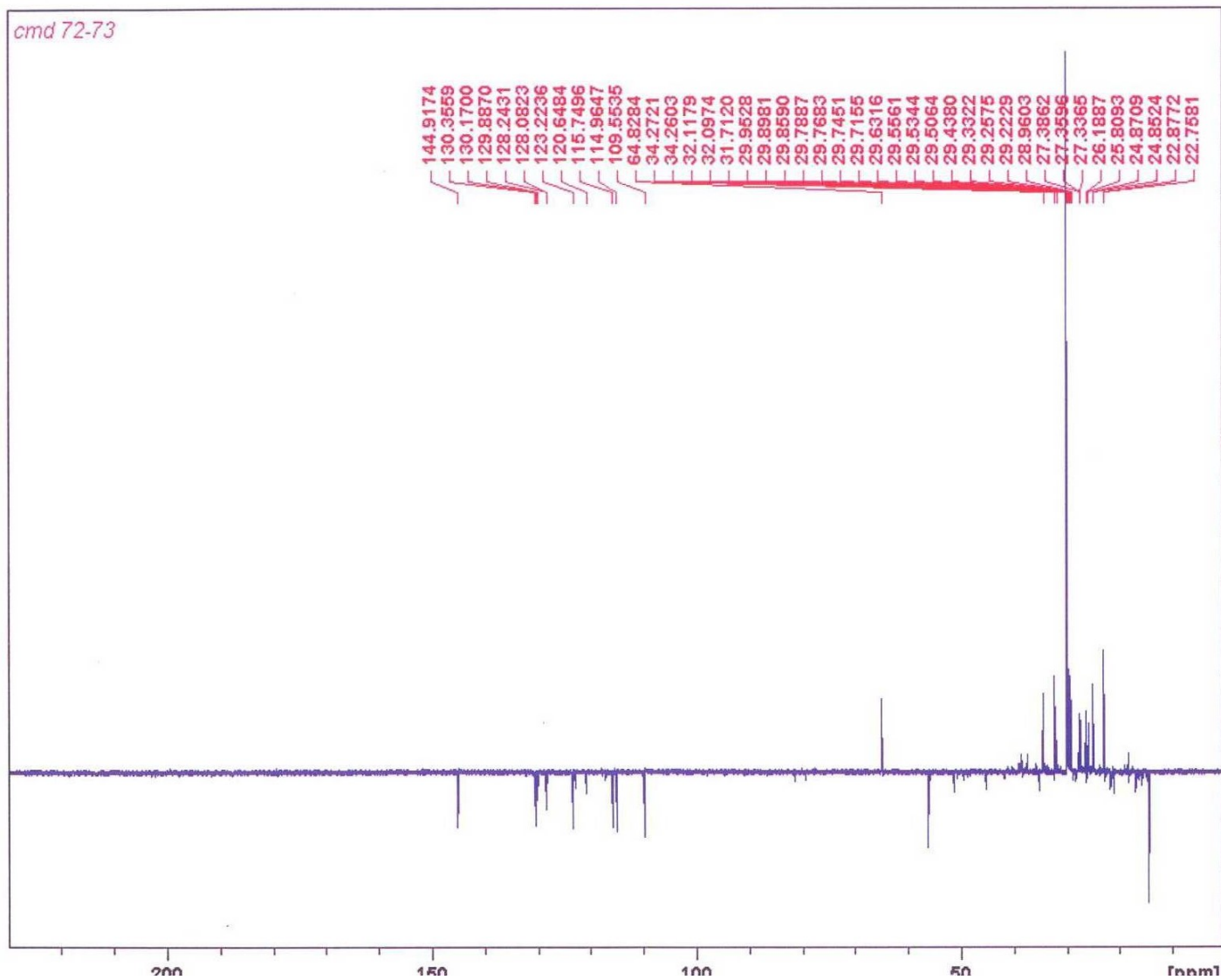
Appendix 55: HMBC spectrum of CMD-G in CDCl_3



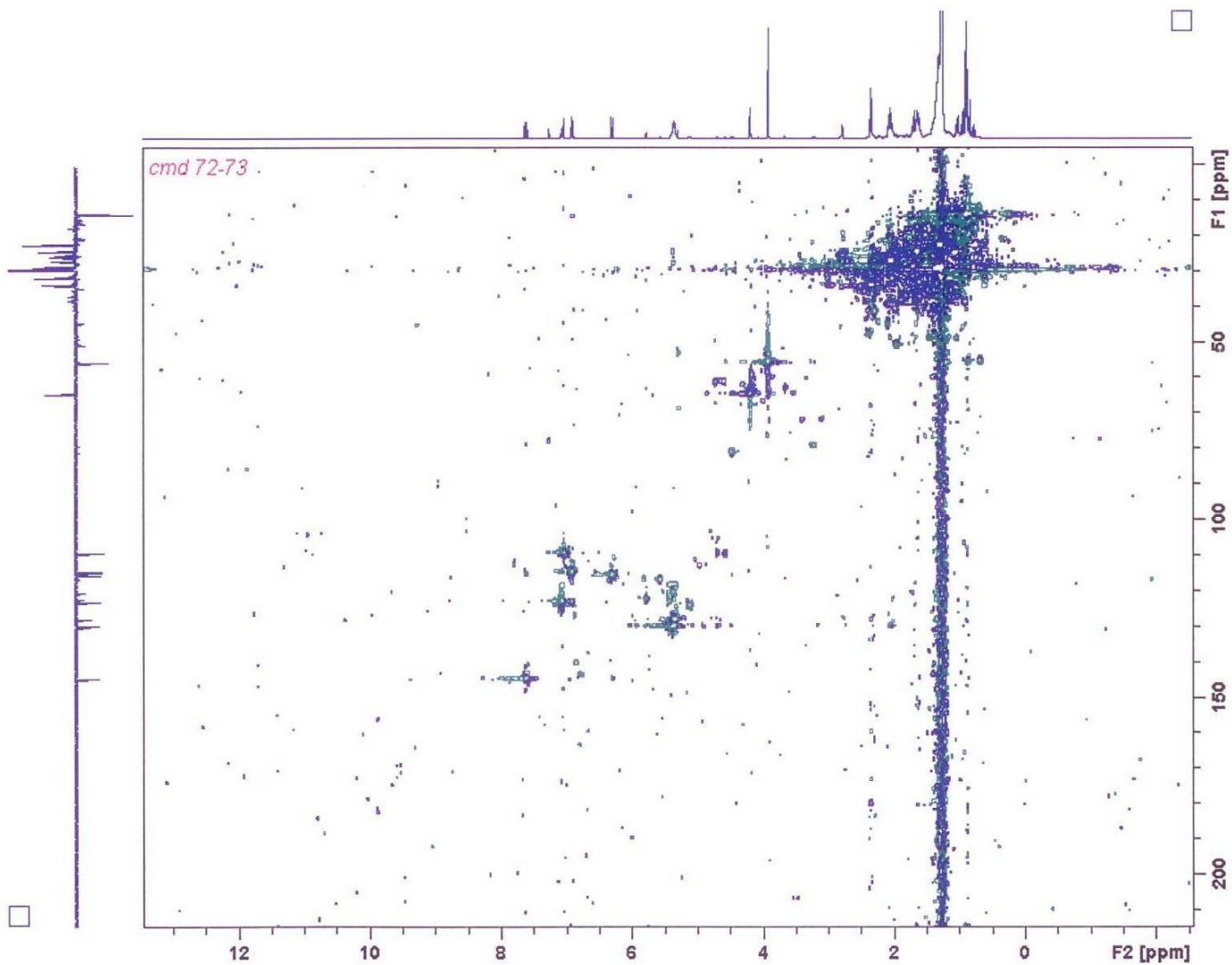
Appendix 56: COSY spectrum of CMD-G in CDCl_3



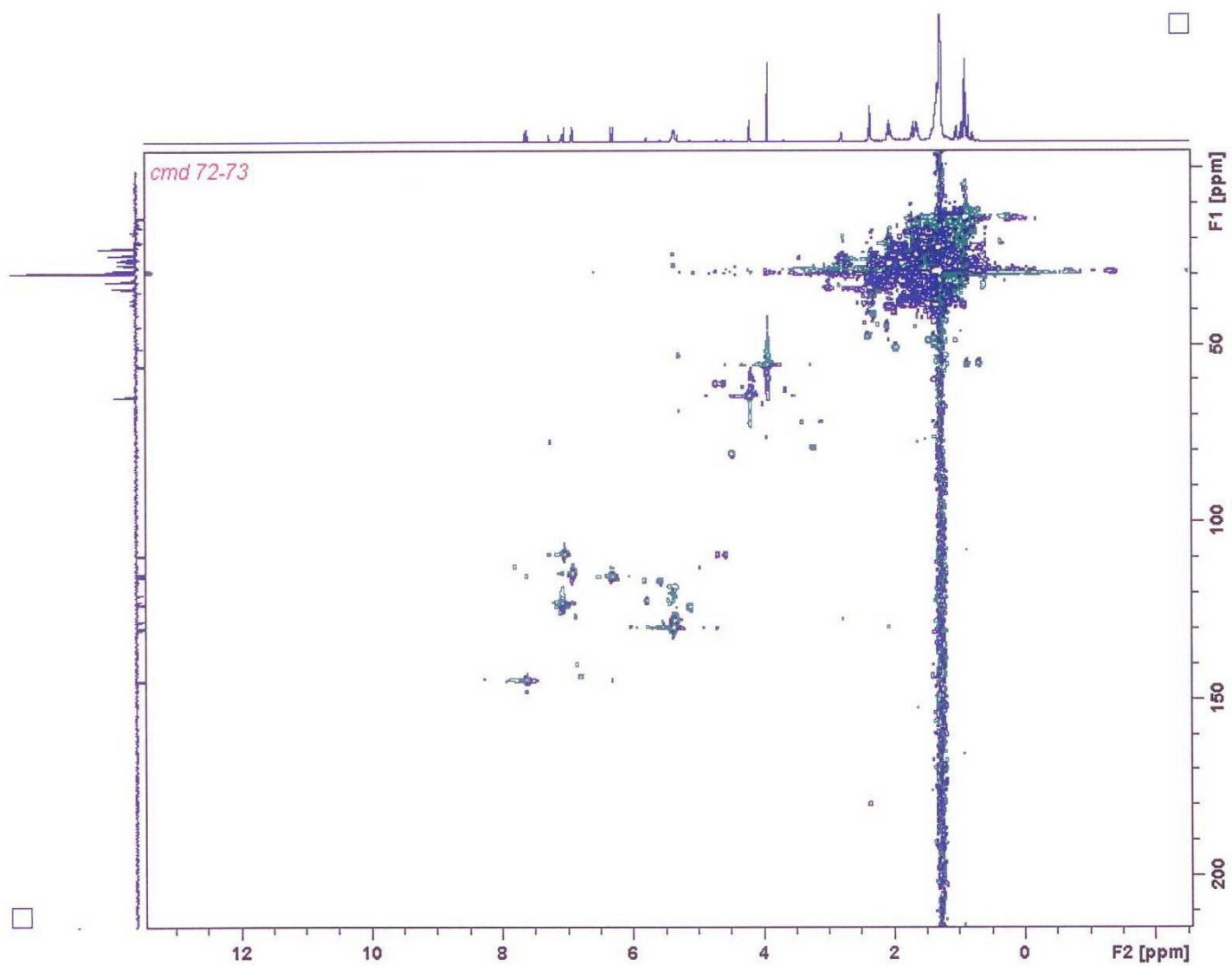
Appendix 57: NOESY spectrum of CMD-G in CDCl_3



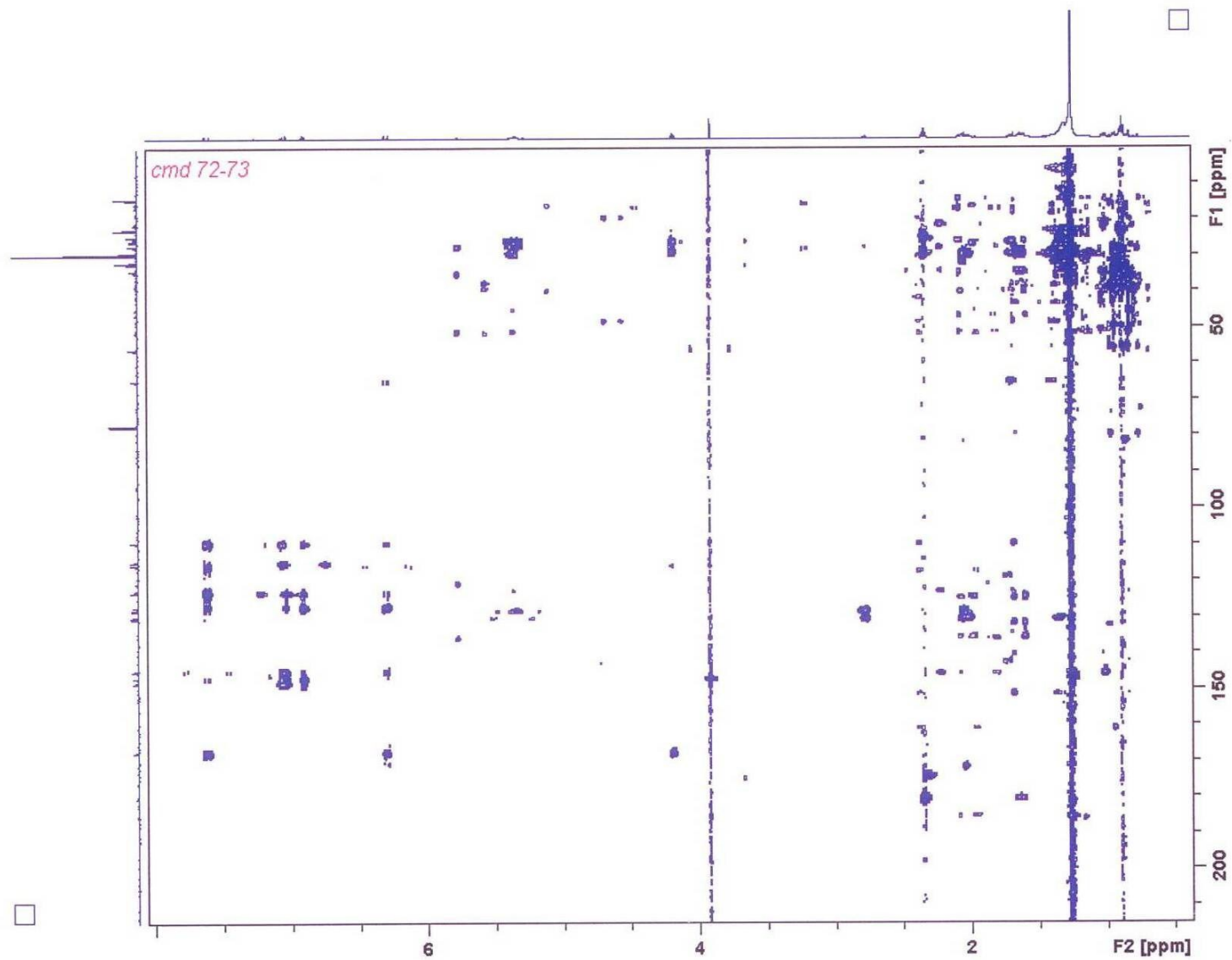
Appendix 60: DEPT spectrum of CMD-H in CDCl_3



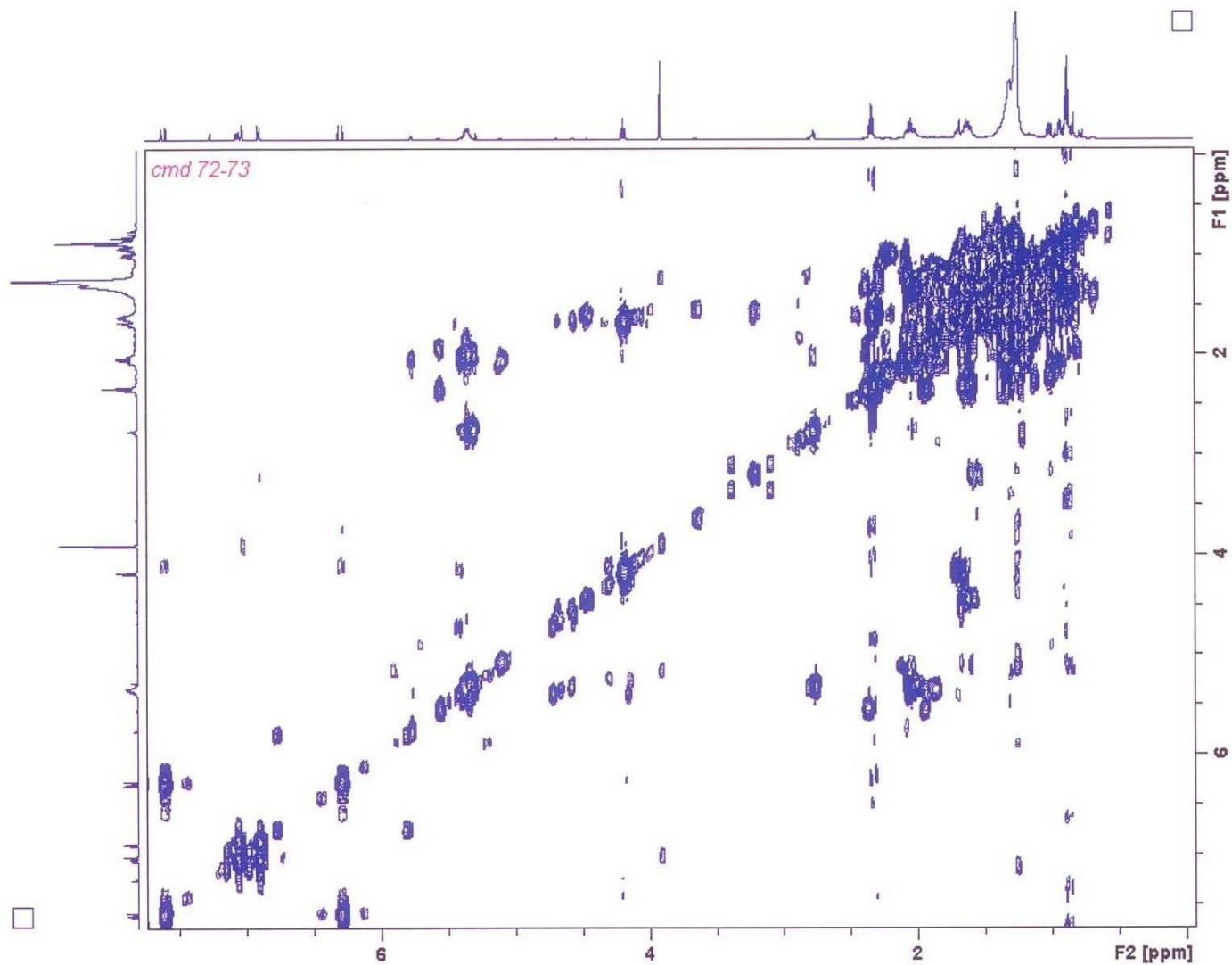
Appendix 61: HSQC DEPT spectrum of CMD-H in CDCl_3



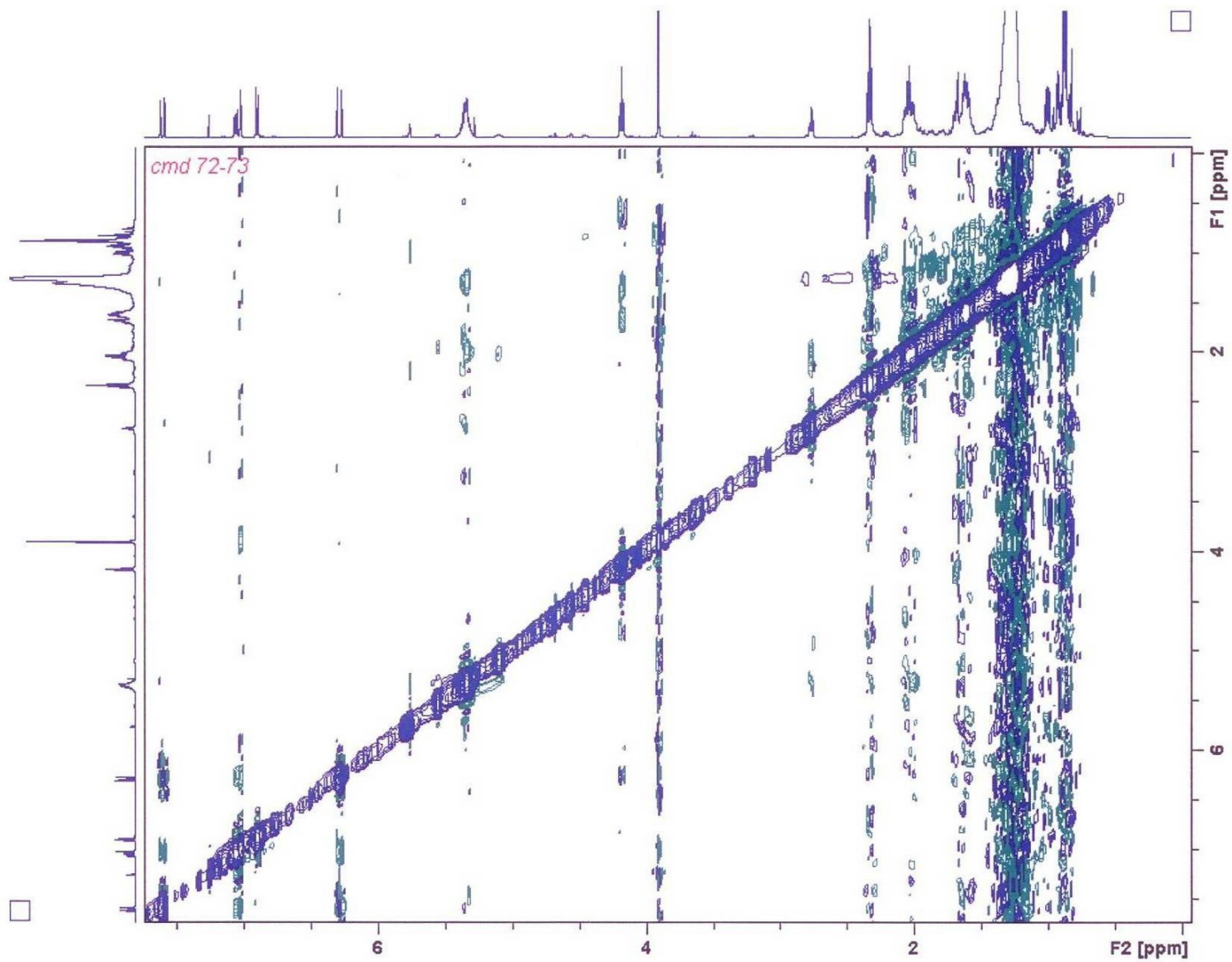
Appendix 62: HSQC DEPT spectrum of CMD-H in CDCl_3



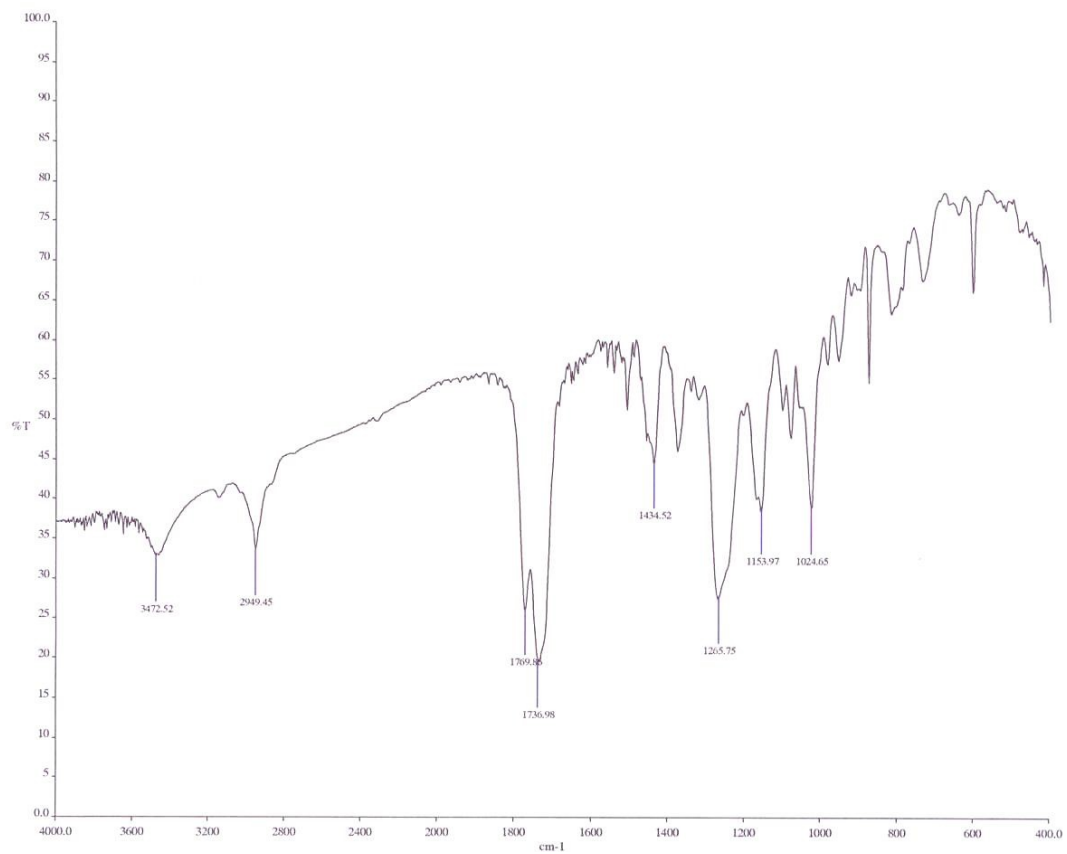
Appendix 63: HMBC spectrum of CMD-H in CDCl_3 (expanded)



Appendix 64: COSY spectrum of CMD-H in CDCl_3

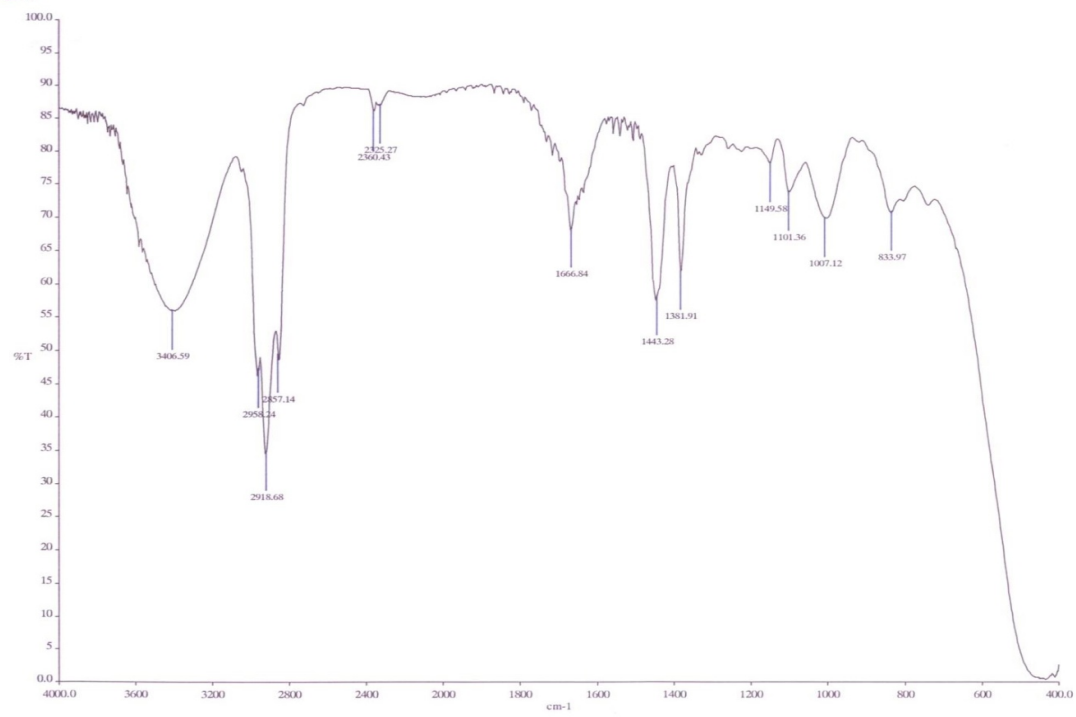


Appendix 65: NOESY spectrum of CMD-H in CDCl_3



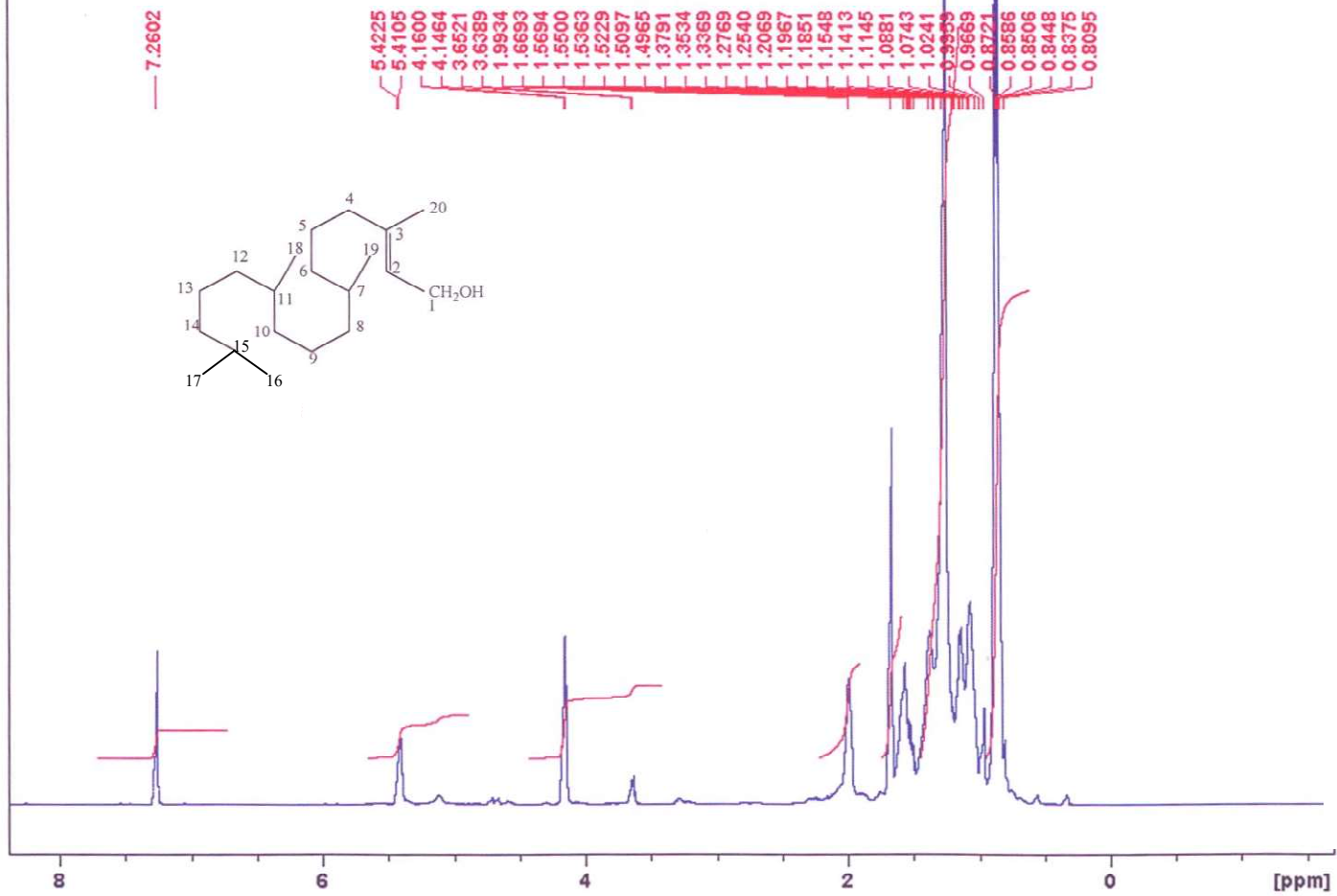
Appendix 66: IR spectrum of CMD-H in CDCl₃

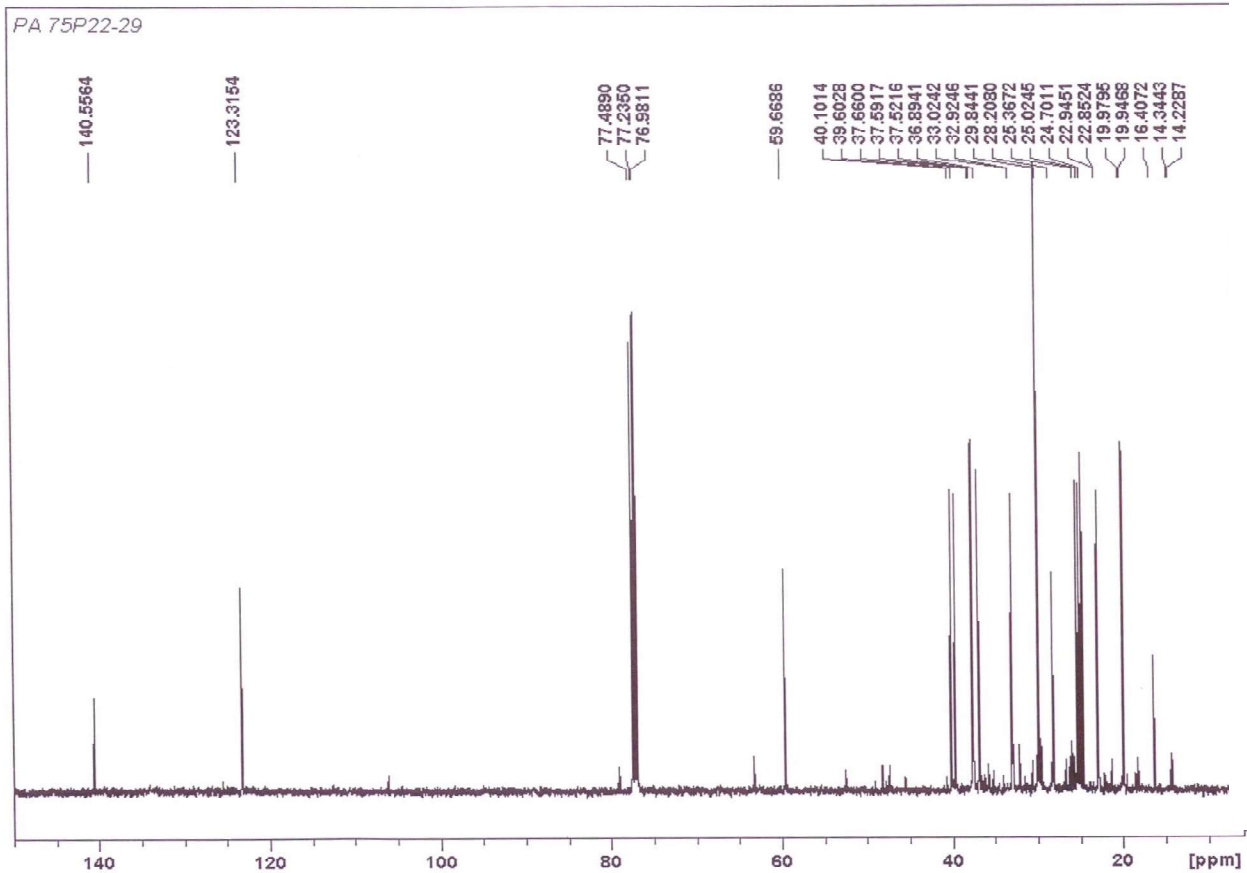
TOPE 9



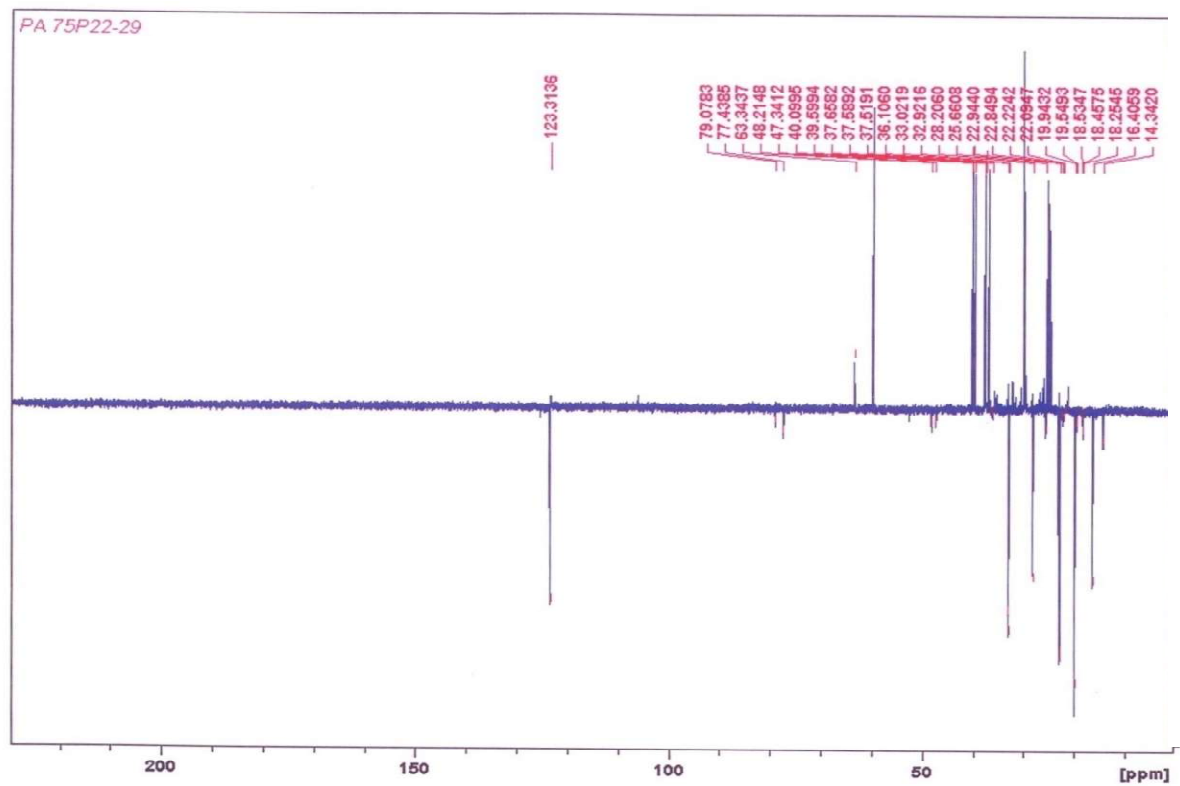
Appendix 67: IR spectrum of PA-A in CDCl₃

PA 75P22-29

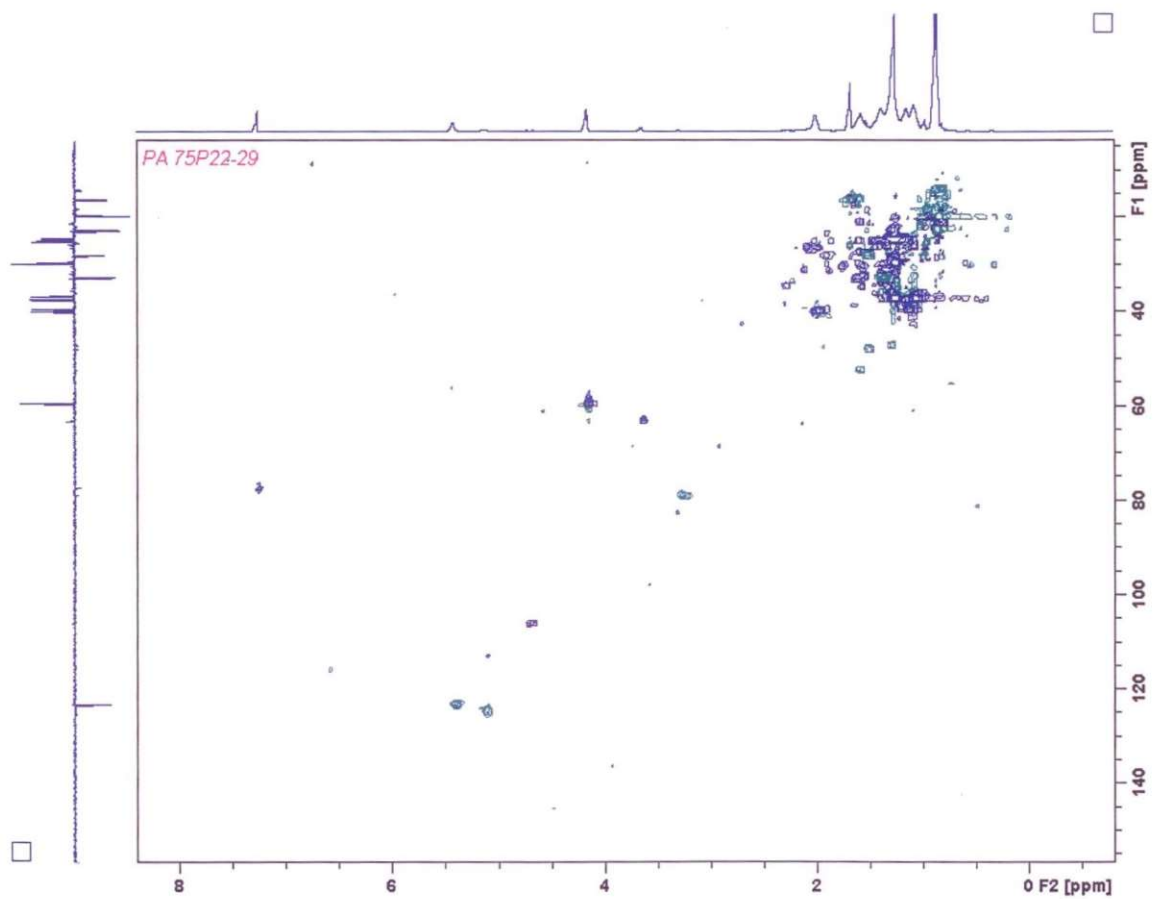




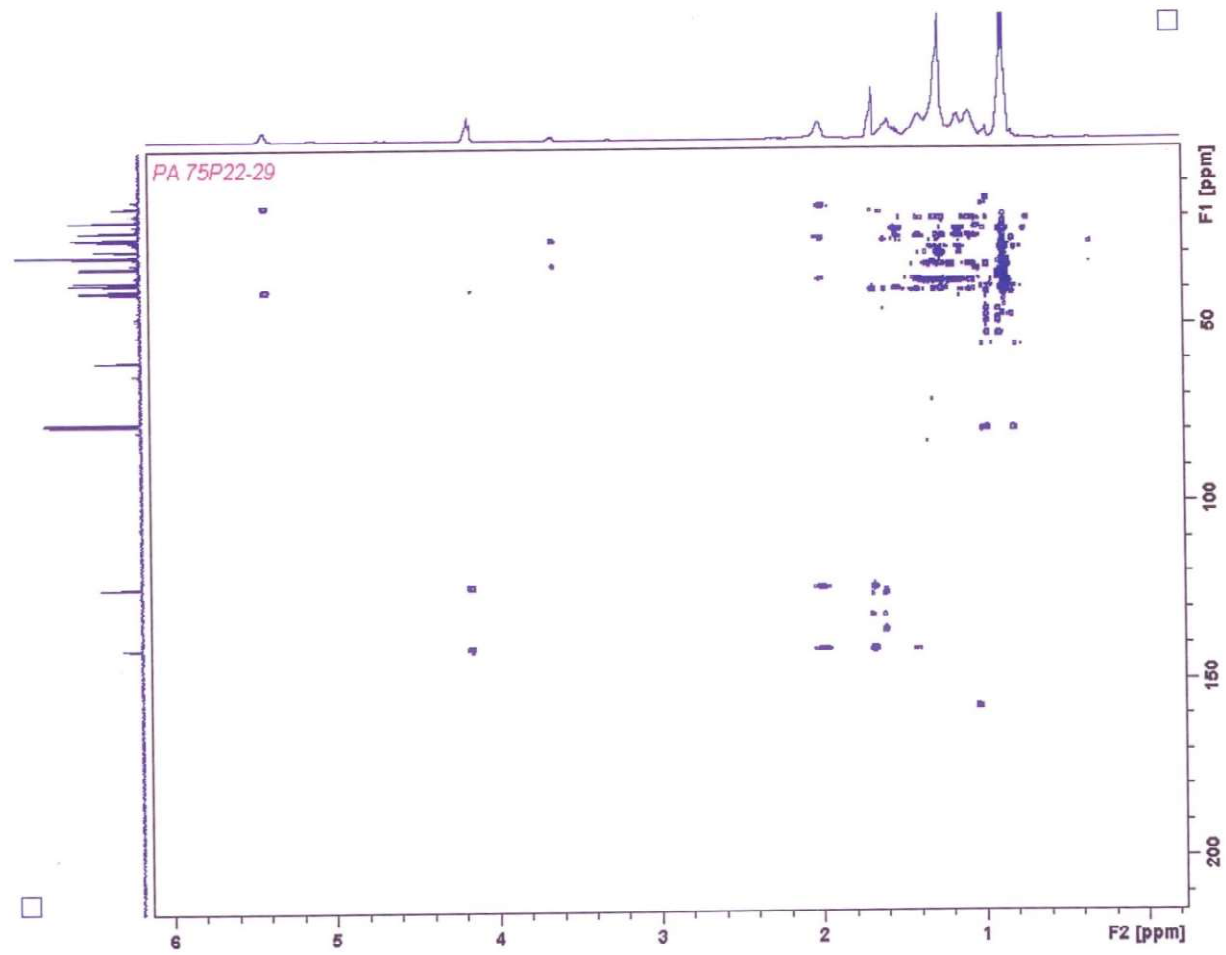
Appendix 70: ^{13}C -NMR (125 MHz) spectrum of PA-A in CDCl_3



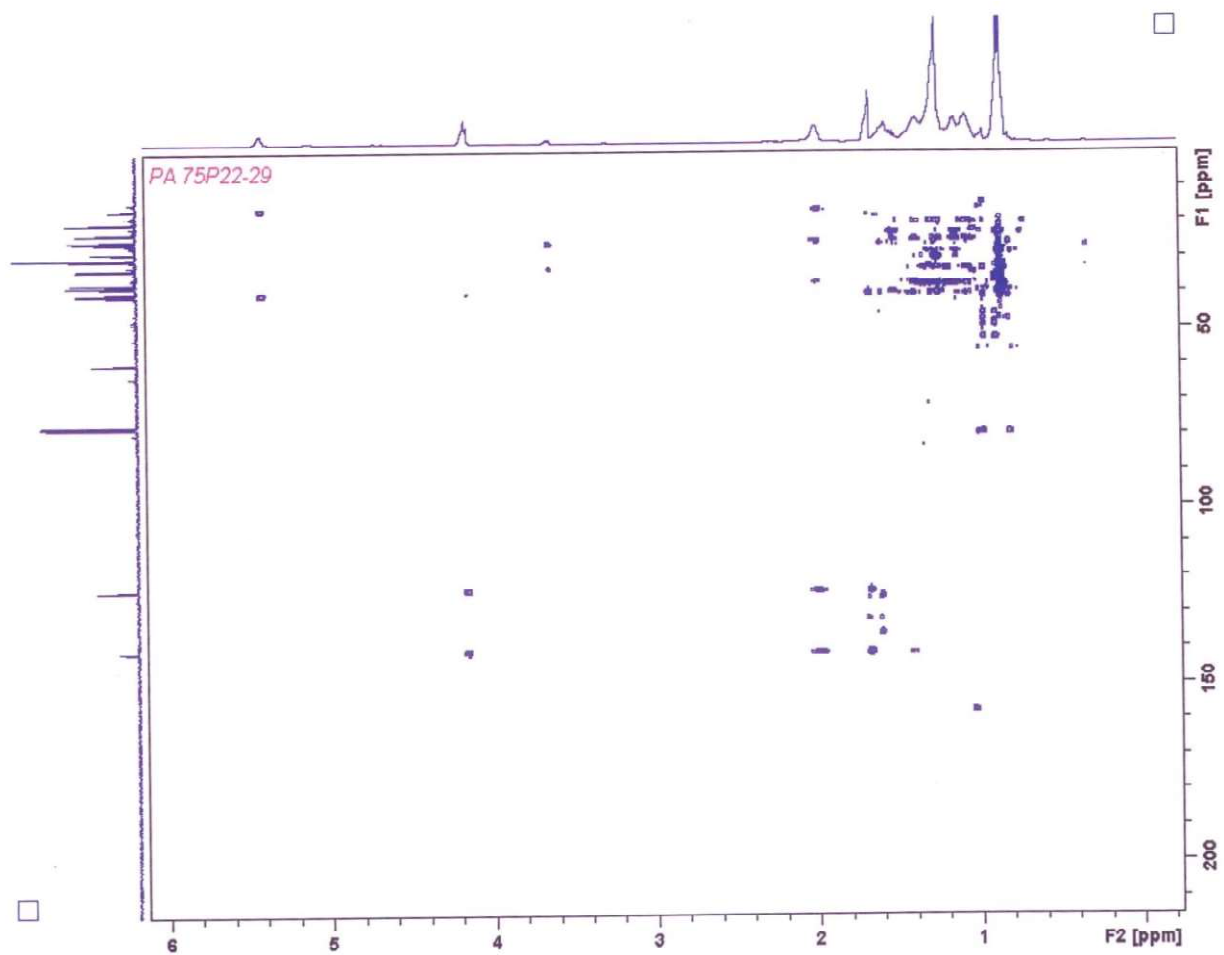
Appendix 71: DEPT spectrum of PA-A in CDCl_3



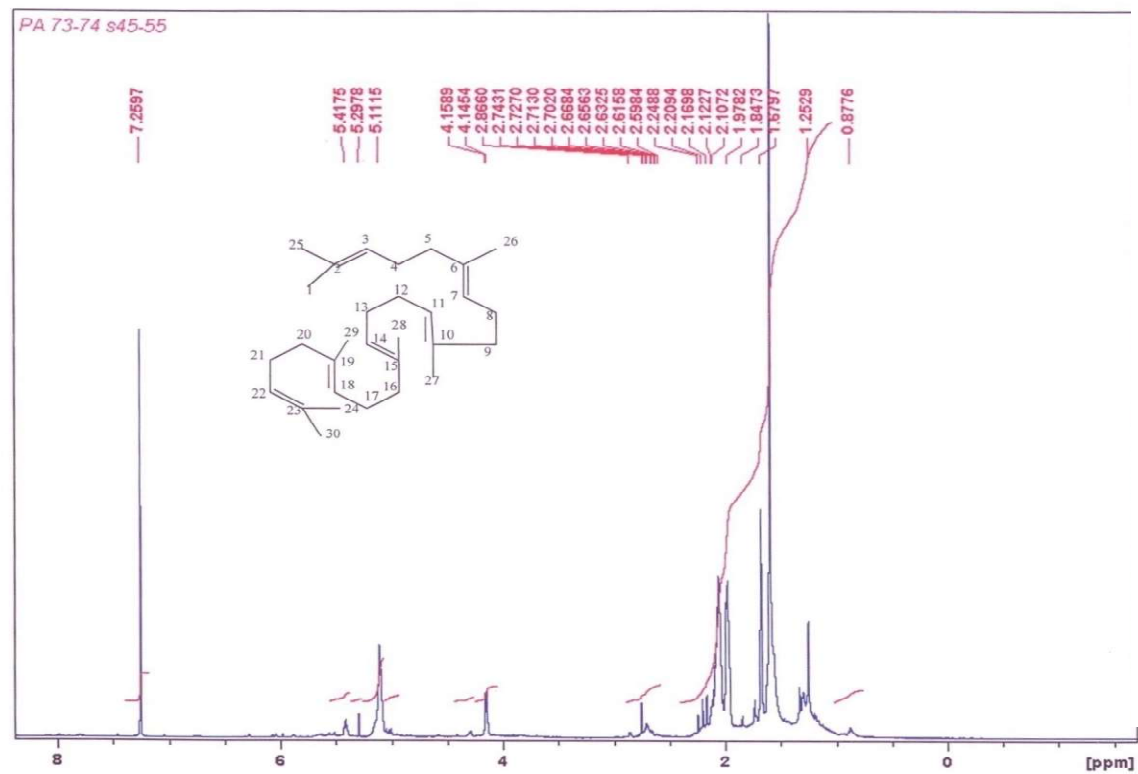
Appendix 72: HSQC DEPT spectrum of PA-A in CDCl_3



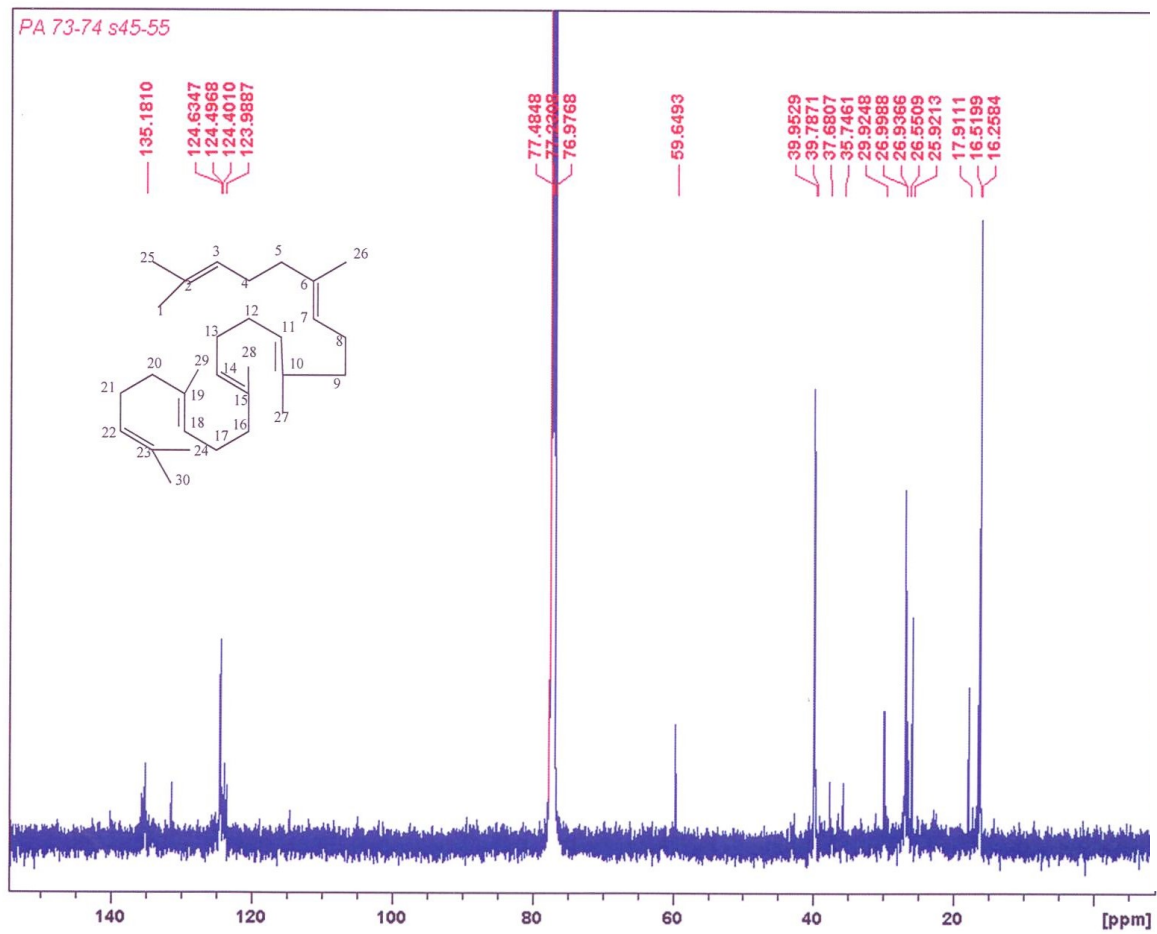
Appendix 73: HMBC spectrum of PA-A in CDCl₃



Appendix 74: HMBC spectrum of PA-A in CDCl₃ (expanded)

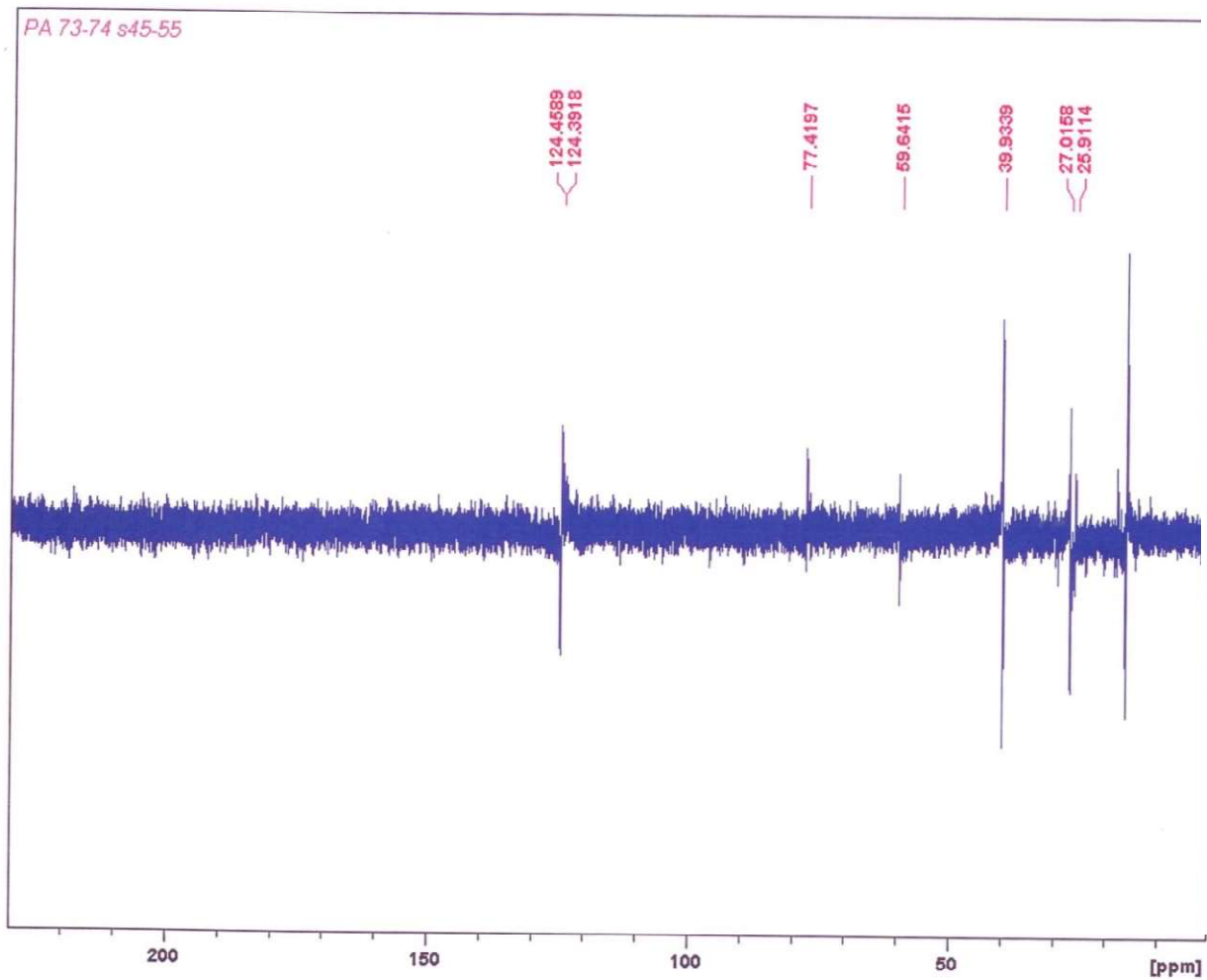


Appendix 75: $^1\text{H-NMR}$ (500MHz) spectrum of PA-B in CDCl_3

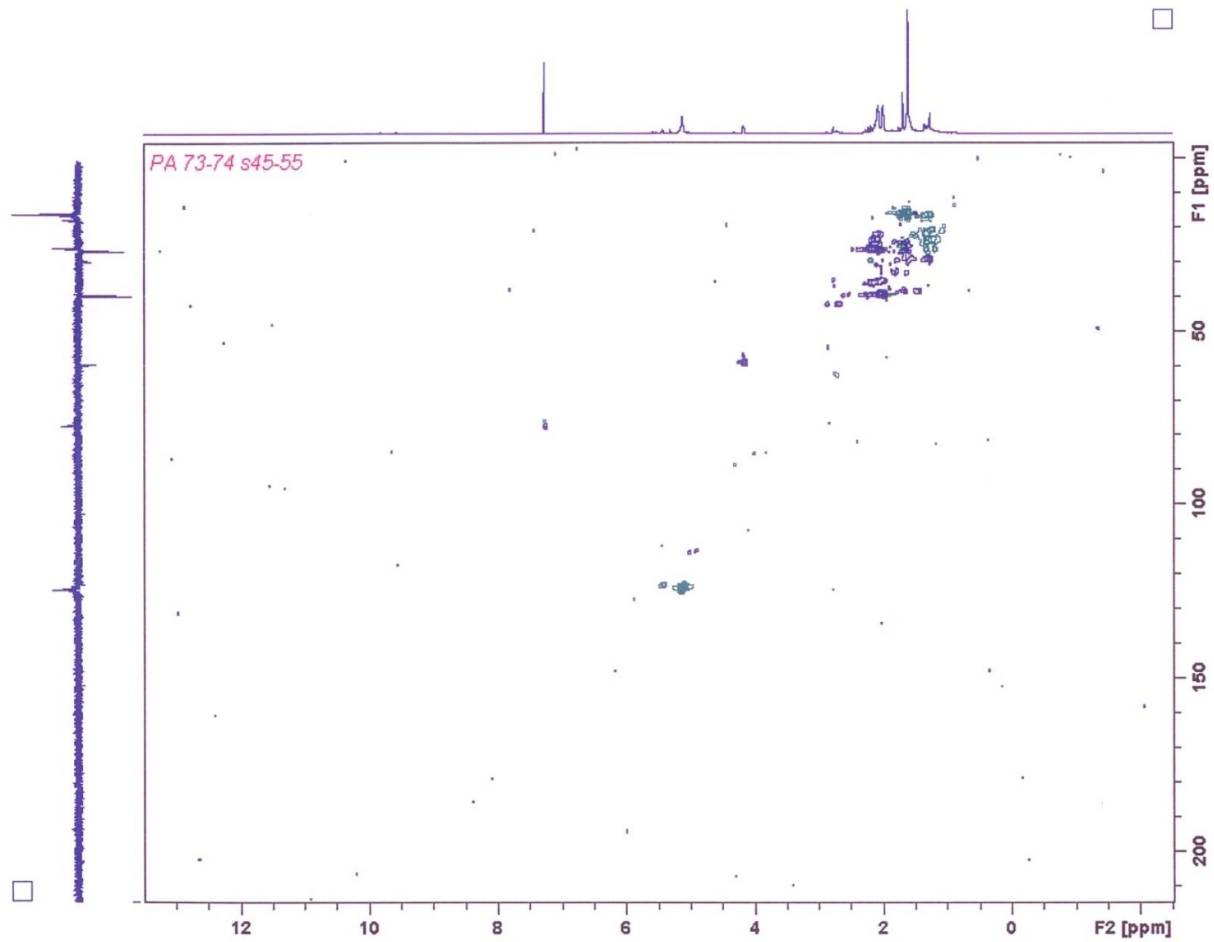


Appendix 76: ^{13}C -NMR (125 MHz) spectrum of PA-B in CDCl_3

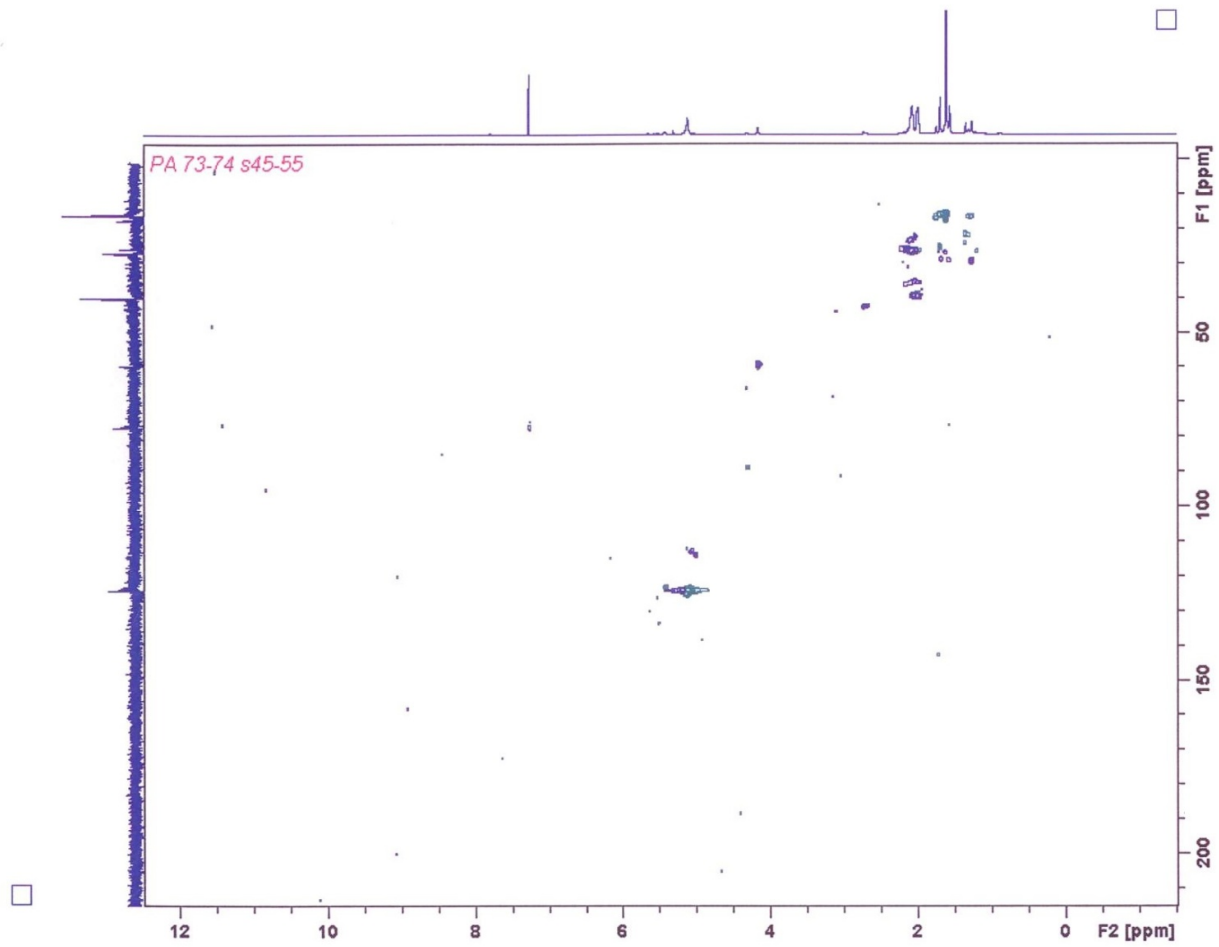
Fig. 39: ^{13}C -NMR (500MHz) spectrum of PA2 in CDCl_3



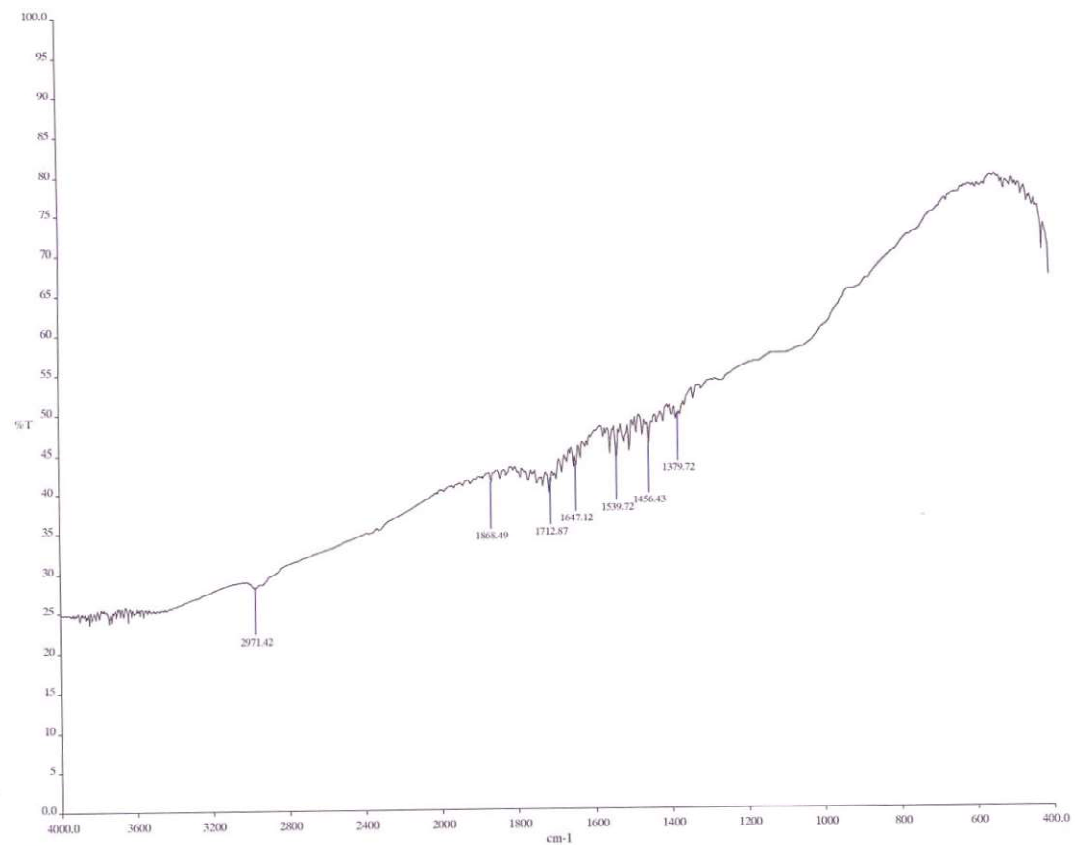
Appendix.77: DEPT spectrum of PA-B in CDCl_3



Appendix 78: HSQC DEPT spectrum of PA-B in CDCl_3

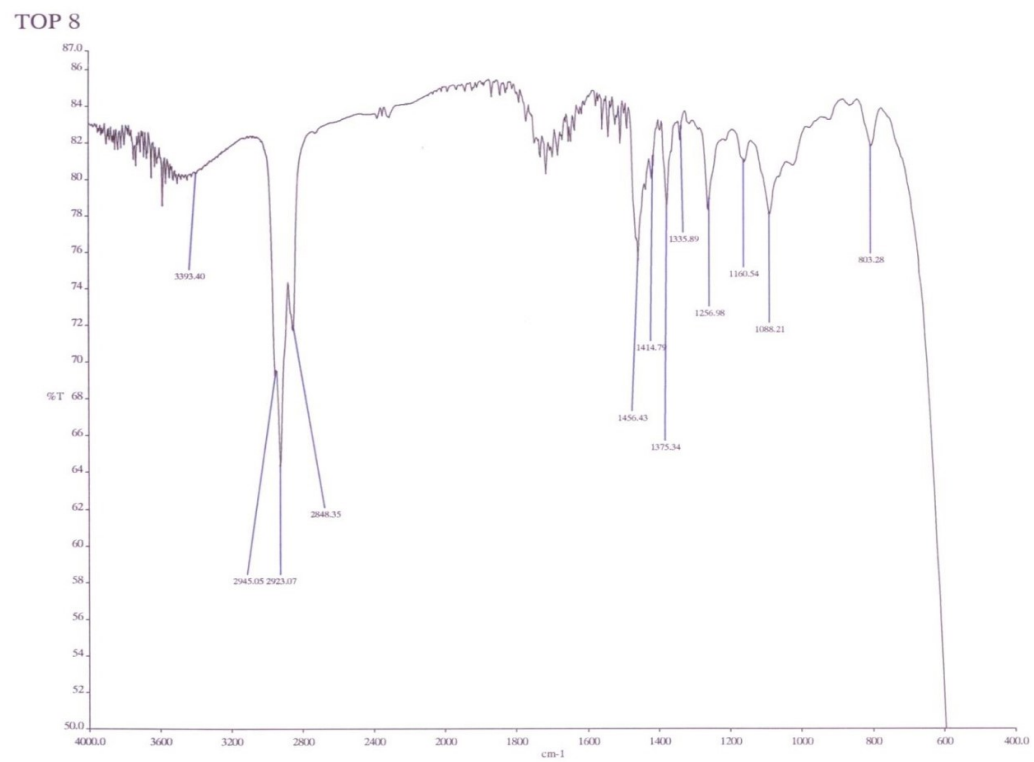


Appendix 79: HMBC spectrum of PA-B in CDCl₃

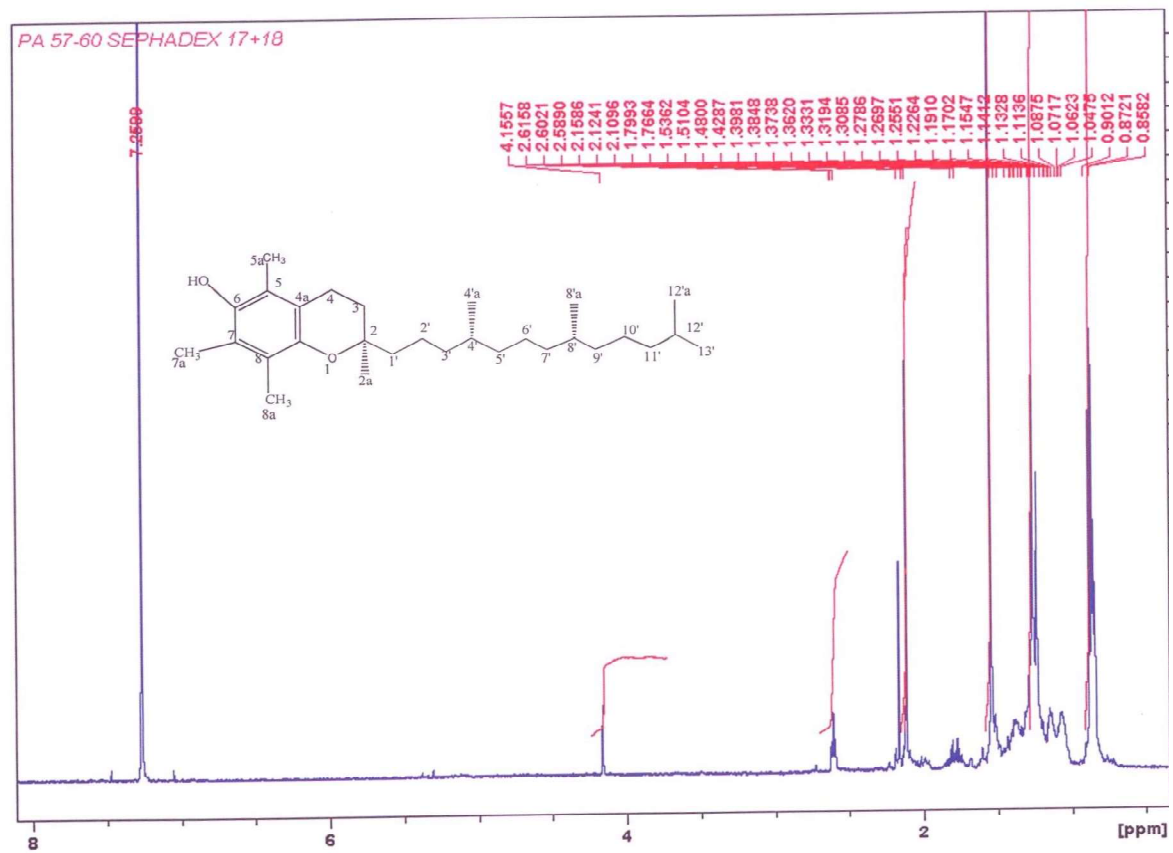


Top 10

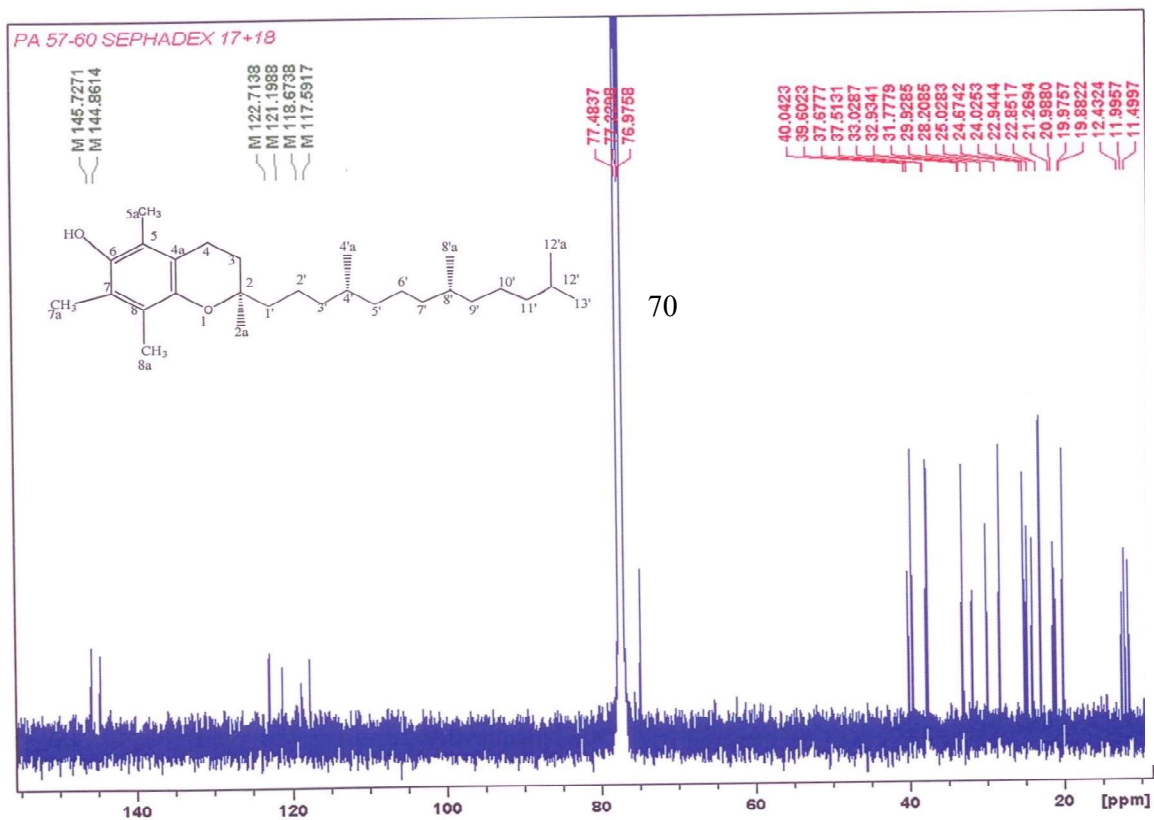
Appendix 80: IR spectrum of PA-B in CDCl₃



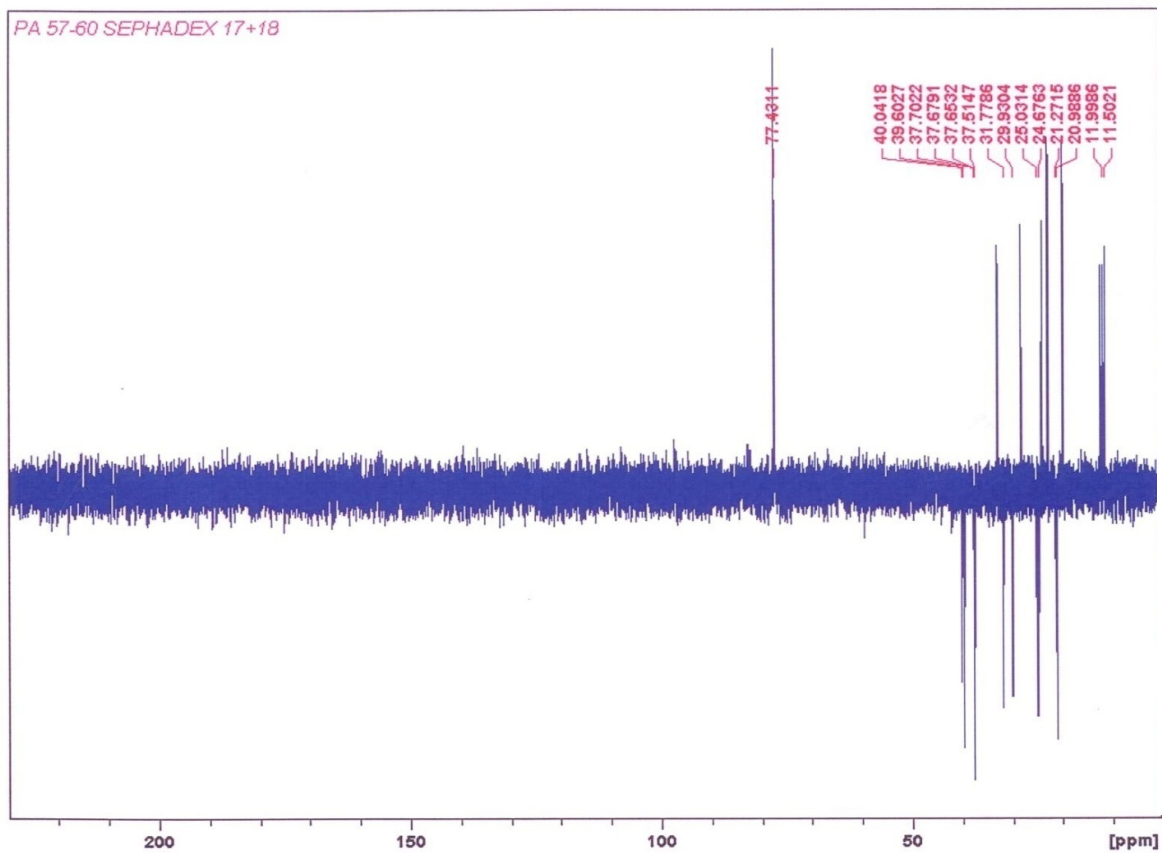
Appendix 81: IR spectrum of PA-B in CDCl₃



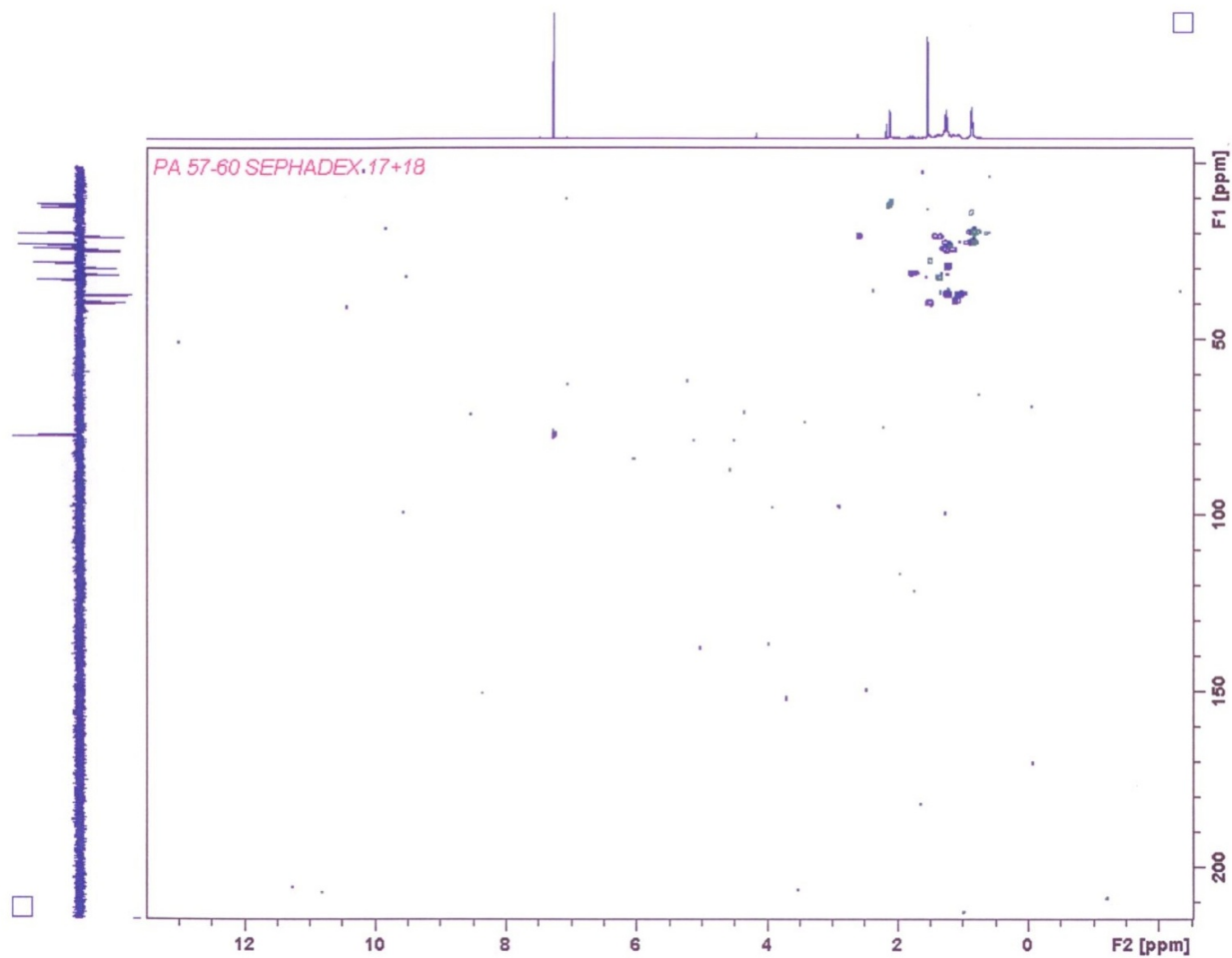
Appendix 82: ¹H NMR (500MHz) spectrum of PA-C in CDCl₃



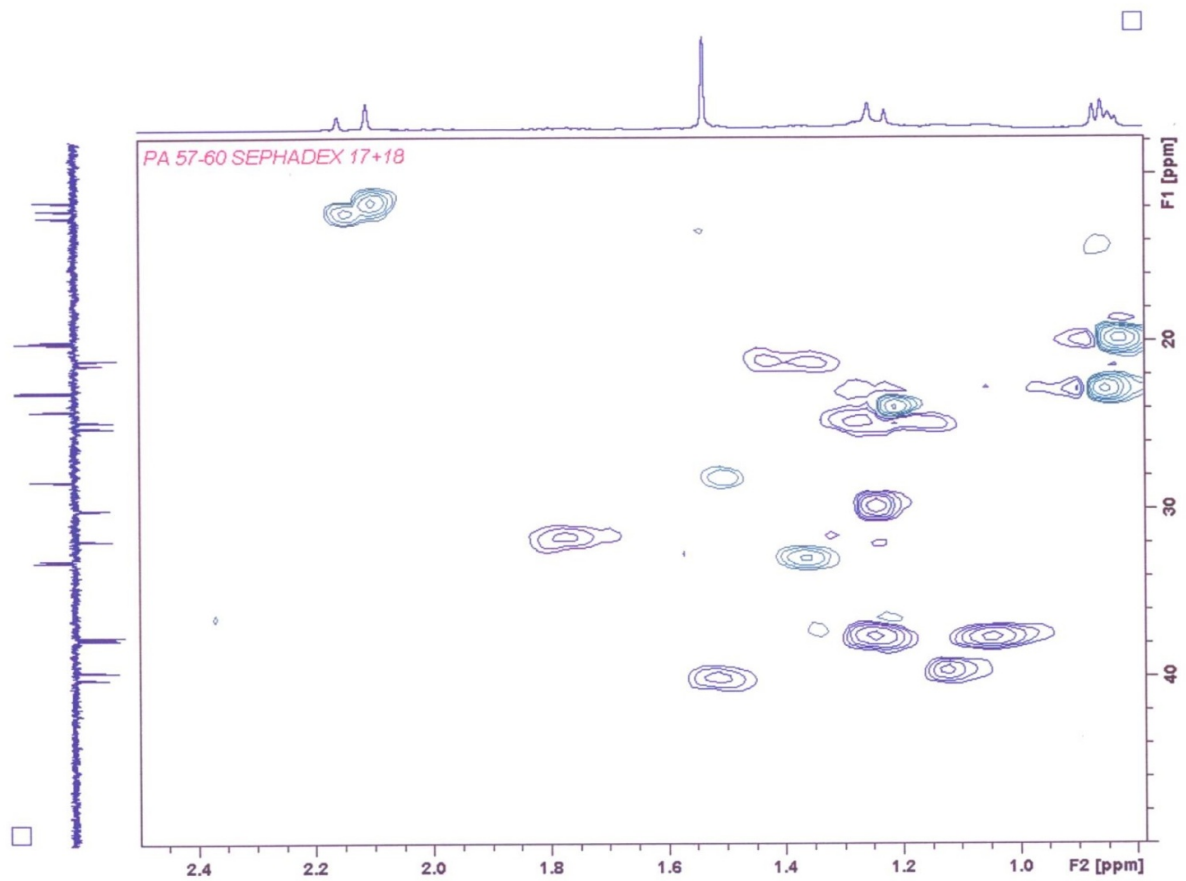
Appendix 83: ¹³C NMR (125 MHz) spectrum of PA-C in CDCl₃



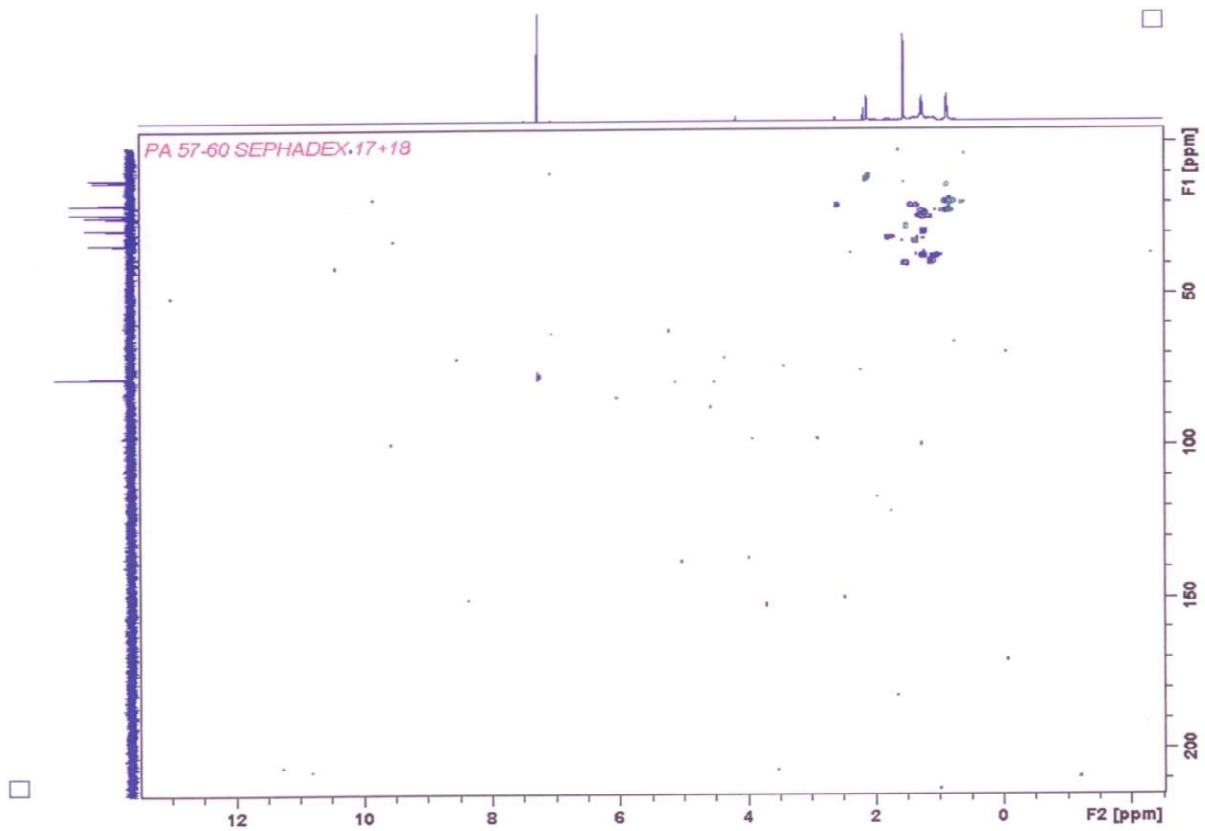
Appendix 84: DEPT spectrum of PA-C in CDCl_3



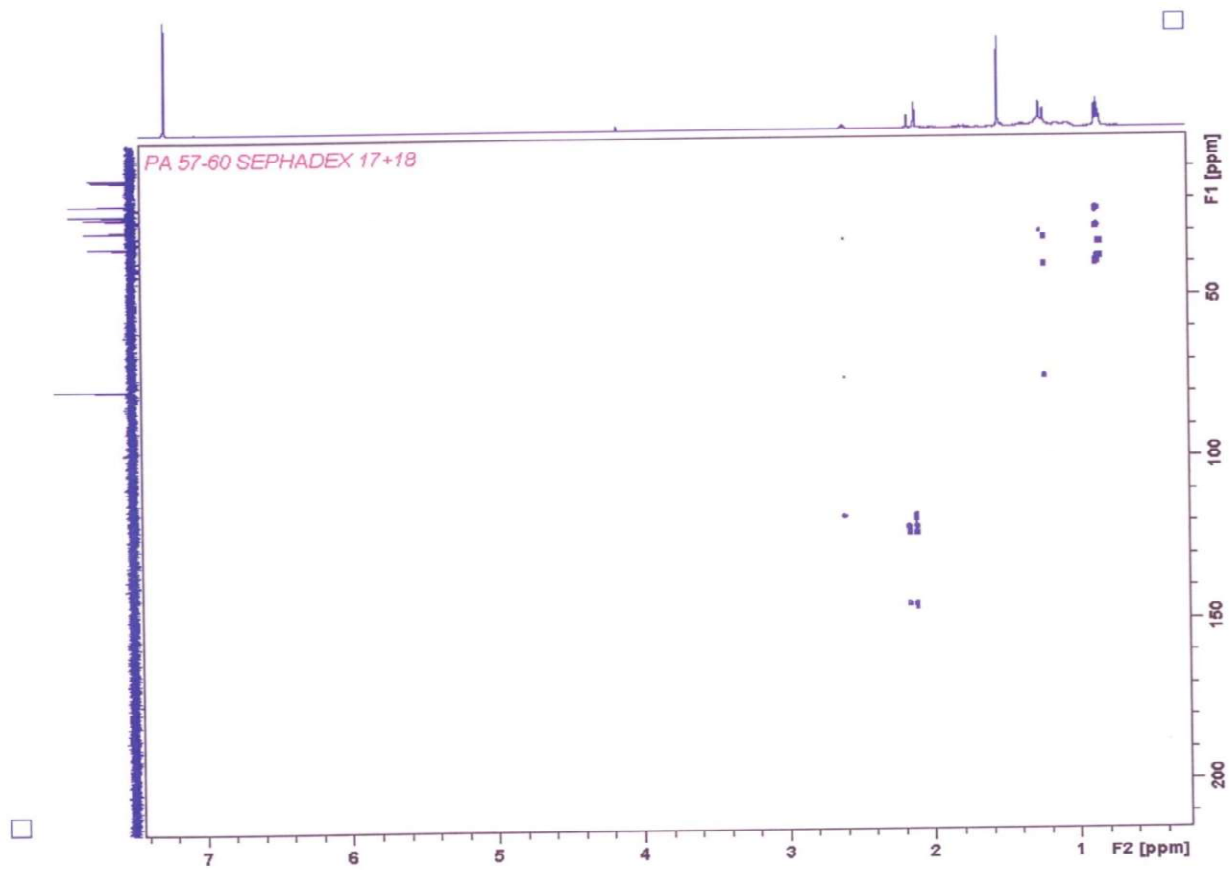
Appendix 85: HSQC DEPT spectrum of PA-C in CDCl_3



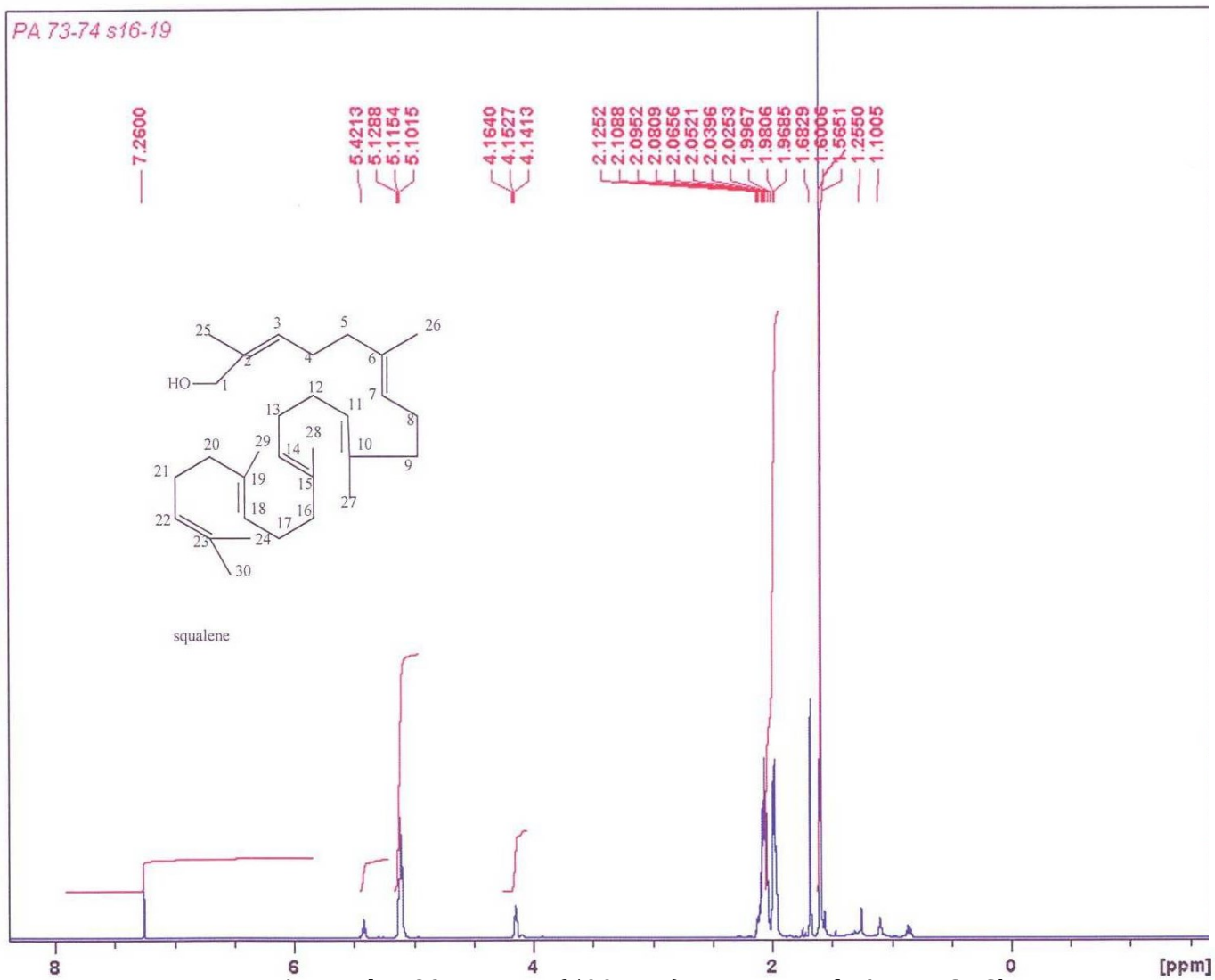
Appendix 86: HSQC DEPT spectrum of PA-C in CDCl_3 (expanded)

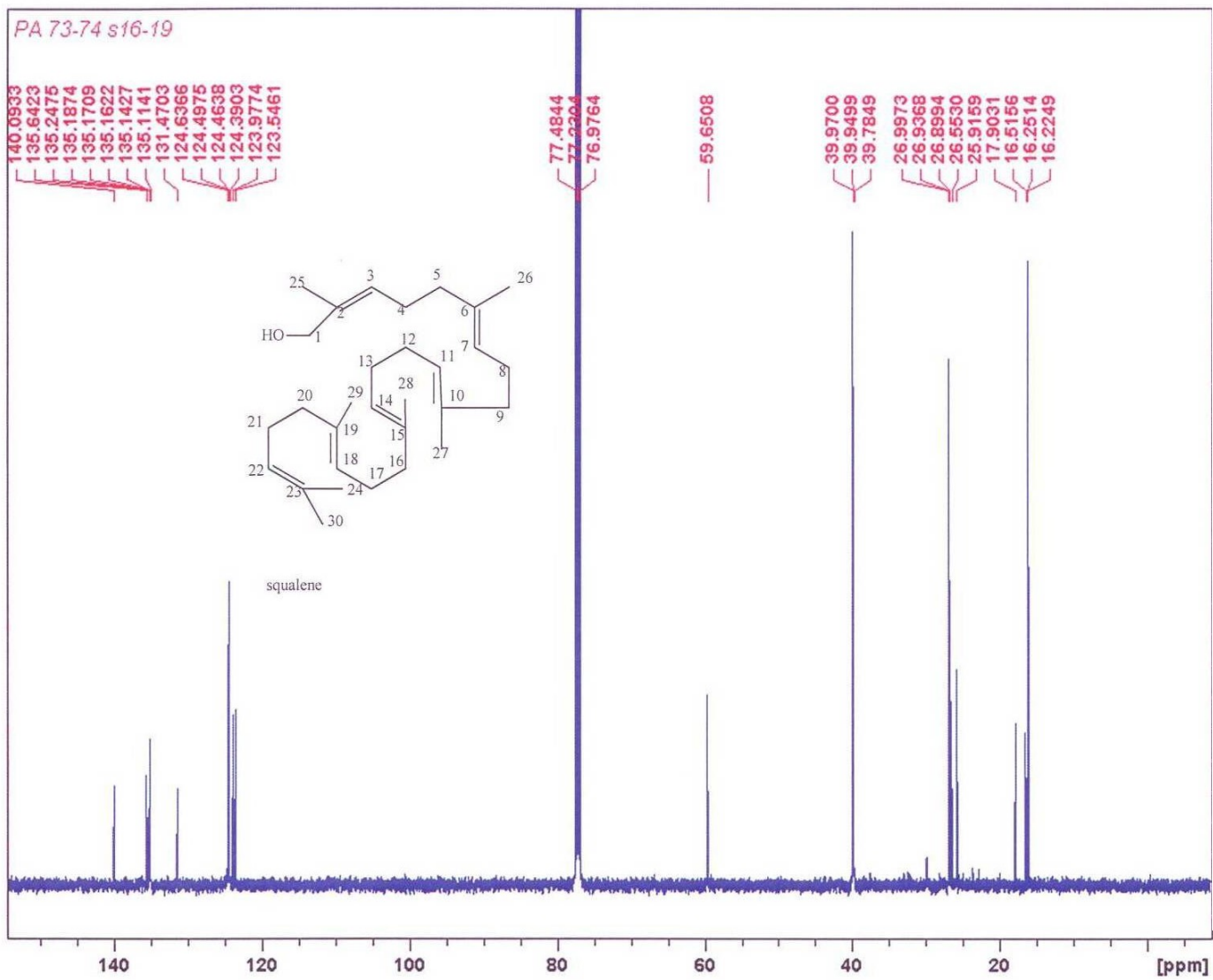


Appendix 87: HMBC spectrum of PA-C in CDCl_3

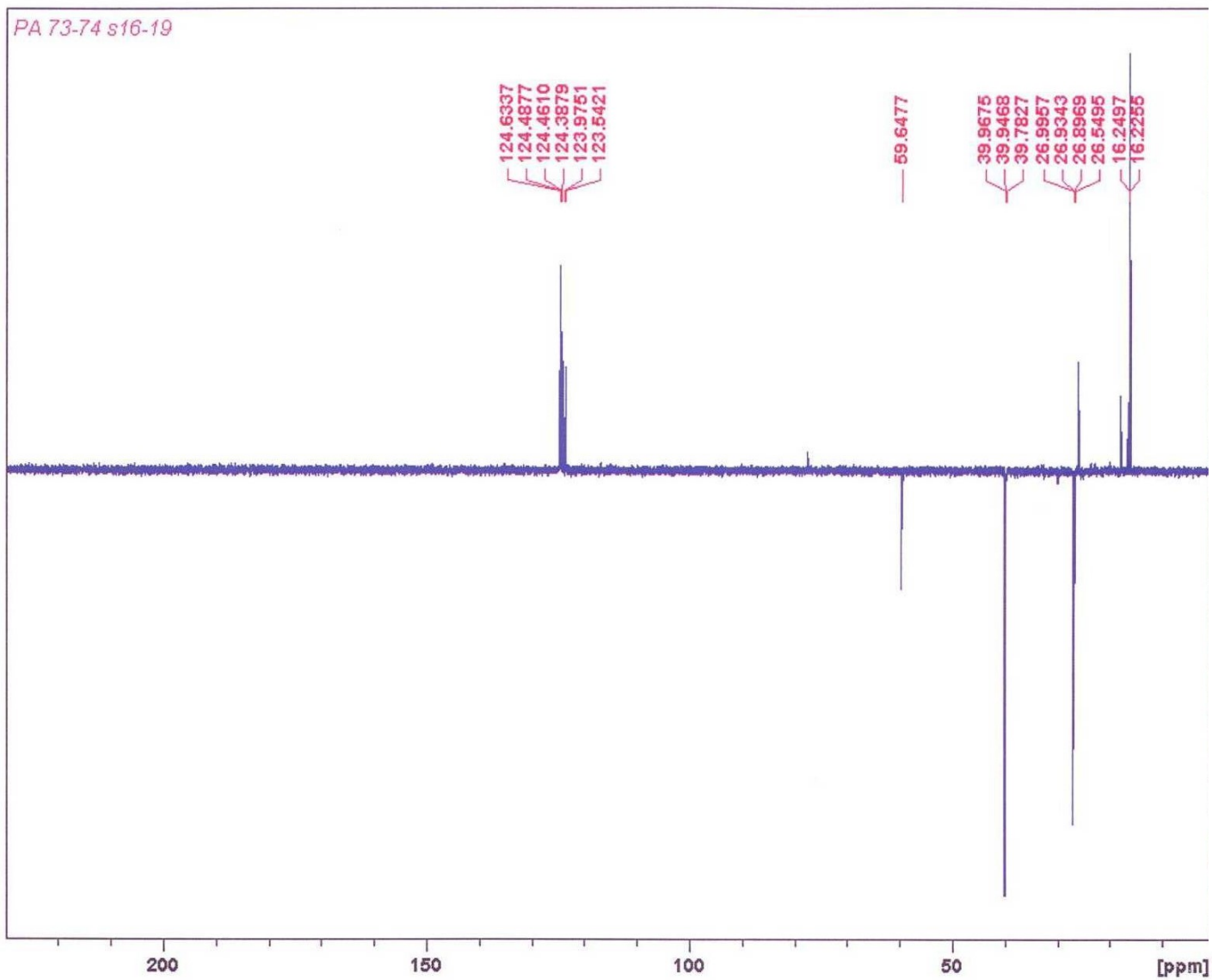


Appendix 88: HMBC spectrum of PA-C in CDCl₃ (expanded)

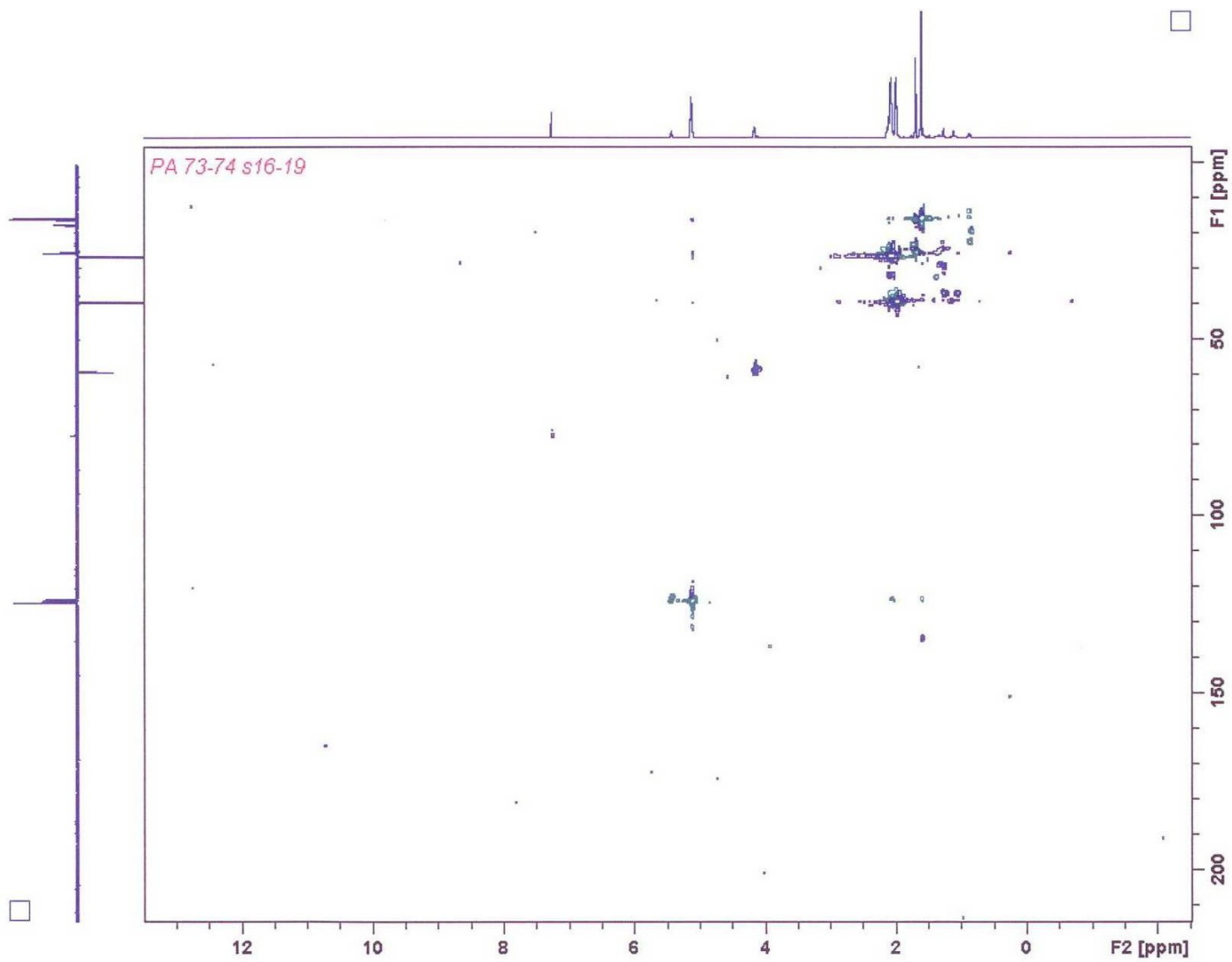




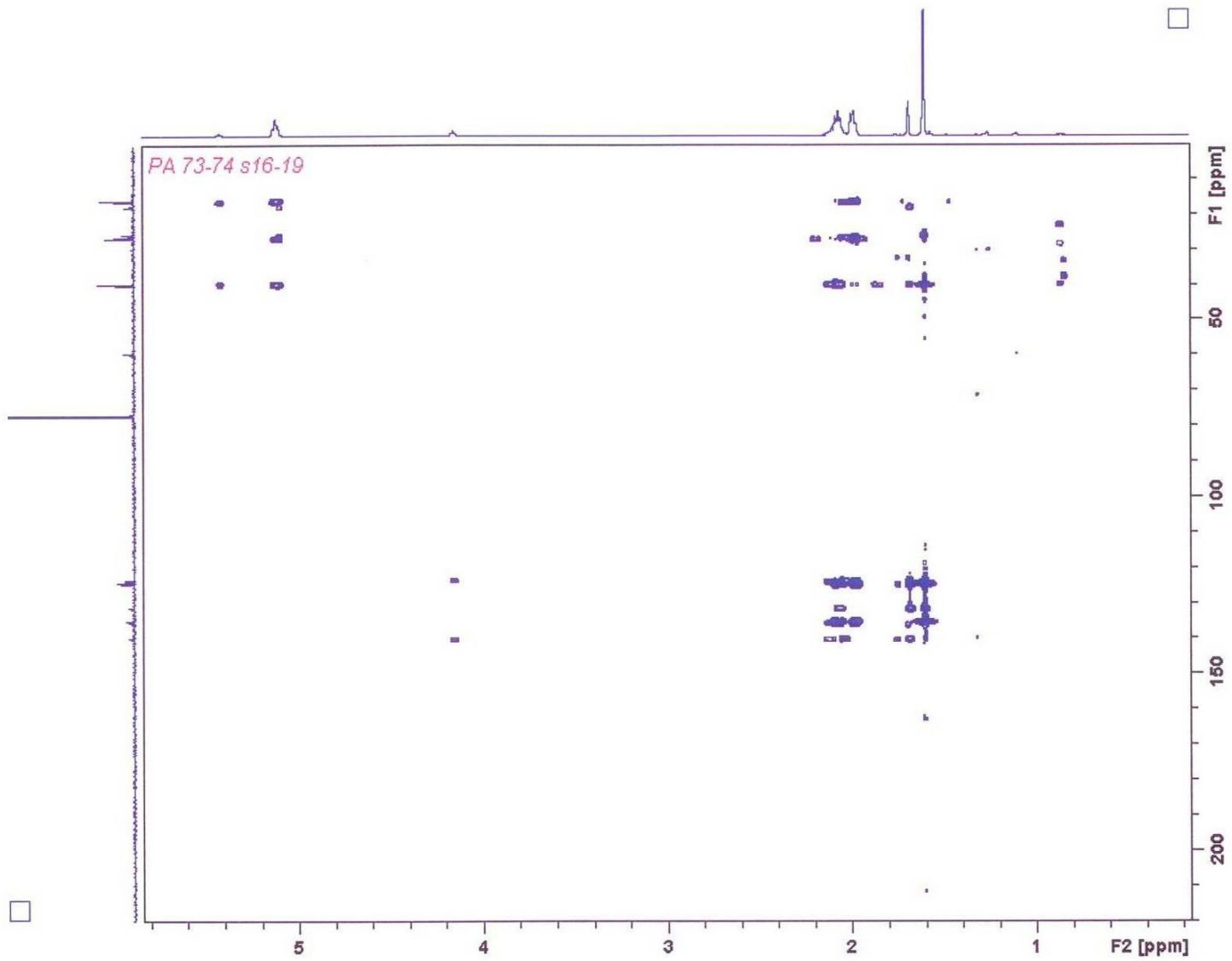
Appendix 90: ^{13}C NMR spectrum of PA-D in CDCl_3



Appendix 91: DEPT spectrum of PA-D in CDCl_3



Appendix 92: HSQC DEPT spectrum of PA-D in CDCl₃



Appendix 93: HMBC spectrum of PA-D in CDCl_3